

Cover Page



Universiteit Leiden



The handle <http://hdl.handle.net/1887/53237> holds various files of this Leiden University dissertation.

Author: Urem, M.

Title: Signalling pathways that control development and antibiotic production in streptomyces

Issue Date: 2017-10-10

**SIGNALLING PATHWAYS
THAT CONTROL DEVELOPMENT
AND ANTIBIOTIC PRODUCTION
IN *STREPTOMYCES***

PROEFSCHRIFT

ter verkrijging van
de graad van Doctor aan de Universiteit Leiden,
op gezag van Rector Magnificus prof.mr. C.J.J.M. Stolker,
volgens besluit van het College voor Promoties
te verdedigen op dinsdag 10 oktober 2017
klokke 13:45 uur

door
Mia Urem
geboren te Split, Kroatië
in 1986

PROMOTIECOMMISSIE

Promoter: Prof. dr. G.P. van Wezel

Overige leden: Prof. dr. H.P. Spaink
Prof. dr. A.H. Meijer
Prof. dr. M. Ubbink
Dr. S. Rigali (Universiteit van Luik, België)
Dr. K.J. McDowall (Universiteit van Leeds, Engeland)

Za moje roditelje

CONTENTS

CHAPTER I: General Introduction	P7
CHAPTER II: Intertwining Nutrient-sensory Networks and the Control of Antibiotic Production in <i>Streptomyces</i>	P11
CHAPTER III: OsdR of <i>Streptomyces coelicolor</i> and the Dormancy Regulator DevR of <i>Mycobacterium tuberculosis</i> Control Overlapping Regulons	P25
CHAPTER IV: SCO4393, a Novel Enzyme Involved in <i>N</i> -actetylglucosamine Metabolism	P47
CHAPTER V: Suppressor Mutants as a Tool to Identify GlcN Metabolic Genes in <i>S. coelicolor</i>	P65
CHAPTER VI: The ROK-family Regulator RokL6 (SCO1447) is Involved in the Control of Glucosamine-specific Metabolism in <i>S. coelicolor</i>	P77
CHAPTER VII: General Discussion & Nederlandse Samenvatting	P91
REFERENCES	P103
APPENDICES	P119
CURRICULUM VITAE	P144
LIST OF PUBLICATIONS	P145

CHAPTER I

GENERAL INTRODUCTION

Streptomyces are fascinating bacteria with a complex multicellular life cycle, which display beautifully diverse morphologies. Though predominantly considered to be soil dwellers, they are found in most environmental niches including aquatic habitats and in endophytic interactions (van der Meij *et al.*, 2017). Their life cycle begins with the germination of a single spore which expands into a scavenging network of vegetative hyphae. Stress conditions, such as nutrient depletion, initiate development; this morphological differentiation leads to the creation of aerial hyphae which ultimately form chains of spores that can then be dispersed to new habitats. The onset of development is closely linked to and coincides with the production of antibiotics and other bioactive molecules (Bibb, 2005; van Wezel & McDowall, 2011). Indeed, streptomycetes are avid producers of enzymes and secondary metabolites, including over 50% of all clinical antibiotics, which makes them highly interesting for medical, biotechnological and industrial purposes (Bérdy, 2005; Hopwood, 2007). However, a large portion of the biosynthetic gene clusters responsible for the production of antibiotics are poorly expressed under standard laboratory conditions.

A complicated and intertwining network of sensory and regulatory proteins is involved in the control of primary metabolism, development and antibiotic production in response to a multitude of stimuli and stressors occurring in the heterologous environments that streptomycetes live in. Identifying the triggers that activate secondary metabolism is of utmost importance for screening purposes. Thus we need to unravel the regulatory mechanisms that link biosynthesis of antibiotics, development and growth to the responses to biotic and abiotic changes in the environment. In this thesis, I have explored how the model organism *Streptomyces coelicolor* senses environmental signals and cues, and translates these into appropriate responses.

SENSING THE SURROUNDINGS

The aminosugar *N*-acetylglucosamine (GlcNAc) differentially regulates the growth, development and antibiotic production of *S. coelicolor* under different environmental conditions. The presence of this pleiotropic signal in a nutritionally poor environment, in contrast to a rich one, activates antibiotic production and development (Rigali *et al.*, 2008). Presumably, the presence of GlcNAc in a rich environment is interpreted as nutritional abundance, in the form of GlcNAc-polymer chitin, and in a nutrient-depleted environment it is perceived as a signal of development. Monomeric GlcNAc, from the cell wall's peptidoglycan, is released into the environment at the onset of development due to the autolytic degradation of part of the vegetative hyphae which provides the resources for the building of the aerial mycelium. GlcNAc is transported via the phosphoenolpyruvate-dependent phosphotransferase system (PTS) that simultaneously phosphorylates it to *N*-acetylglucosamine 6-phosphate (GlcNAc-6P), which is then deacetylated by NagA to form glucosamine-6P (GlcN-6P) (Nothaft *et al.*, 2010; Świątek *et al.*, 2012a). These phosphosugars are important in the GlcNAc activation of antibiotic production; both metabolic intermediates inhibit the ability of global pleiotropic regulator DasR from repressing antibiotic production (Tenconi *et al.*, 2015b; Rigali *et al.*, 2008; Rigali *et al.*, 2006).

The control of antibiotic production, development and other essential process is not limited to the regulatory power exerted by DasR. In addition to DasR, at least a handful of other regulatory proteins have been implicated in the control aminosugar utilisation, including AtrA and Rok7B7 (Nothaft *et al.*, 2010; Swiatek *et al.*, 2013; van Wezel & McDowall, 2011; Urem *et al.*, 2016a). In fact, the *Streptomyces coelicolor* genome alone encodes around 700 proteins with a predicted regulatory function (Bentley *et al.*, 2002), many of which regulate development and secondary metabolism in response to environmental conditions. Chapter

II reviews the global regulators that control antibiotic production and development, with emphasis on (amino)sugar-related nutrient sensory pathways, and explores the complexity of these regulatory networks given their antagonistic and/or cooperative behaviour and the extensive cross-talk amongst them.

RESPONDING TO STRESS

Streptomyces require quick sensing machinery and adaptive responses to survive the fluctuating landscape of their environments. Streptomyces may suffer from oxygen depletion as a result of environmental hypoxia or due to poor oxygen transfer within densely grown mycelia (van Dissel *et al.*, 2014). To survive in low oxygen conditions, the aerobic *Streptomyces* must activate its stress responses and anaerobic respiration pathways to survive (Fischer *et al.*, 2010; Fischer *et al.*, 2014; van Keulen *et al.*, 2007). Two-component systems (TCS) are important bacterial mechanisms for sensing and responding to environmental changes and stressors; a signal is detected by the sensory kinase (SK) which then phosphorylates its cognate response regulator (RR) to activate the appropriate response.

Chapter III describes the function of the novel TCS pair OsdRK (SCO0203-0204) that senses and responds to oxygen stress, and links this to the control of development. The depletion of oxygen is likely sensed by OsdK, which shares high similarity with the signal recognition domains of the sensory kinases DosT/DevS, responsible for the sensing of oxygen depletion in *Mycobacterium tuberculosis* (Honaker *et al.*, 2009; Sousa *et al.*, 2007). The response regulator OsdR recognises and binds targets of the *M. tuberculosis* dormancy regulator DevR, which recognises a binding site very similar to that of OsdR (Chauhan *et al.*, 2011). OsdR is phosphorylated by OsdK and in response positively regulates genes involved in stress response, anaerobic respiration and development. The regulon of OsdR is described in detail in this Chapter.

NEW PROTEINS IN AMINOSUGAR METABOLISM

With improved understanding of the regulatory networks controlling antibiotic production and development, it becomes possible to genetically manipulate strains. To exploit the inhibitory effect of GlcNAc metabolic intermediates on the DasR repression of antibiotic production, metabolic engineering efforts involved the creation of metabolic mutants that accumulate GlcN-6P and/or GlcNAc-6P. The *S. coelicolor nagA* deletion mutant, that accumulates GlcNAc-6P, had increased antibiotic production when grown on GlcNAc (Świątek *et al.*, 2012a; Świątek *et al.*, 2012b). The *nagB* deletion mutant accumulates GlcN-6P when grown in the presence of either GlcNAc or its deacetylated form glucosamine (GlcN), and as a consequence fails to grow. Selecting for suppressor mutants of the *nagB* deletion mutant, that relieve the aminosugar sensitivity, previously identified novel enzymes and regulators of aminosugar metabolism (Swiatek, 2012).

PHOSPHO(AMINO)SUGAR ISOMERASE SCO4393

The suppressor mutant analysis lead to the discovery of SCO4393, a phosphosugar isomerase not previously associated with aminosugar metabolism. Mutation of SCO4393 in *S. coelicolor* relieved the toxicity of both GlcN and GlcNAc to *nagB* mutants. This strongly suggests that SCO4393 plays a role in synthesizing the toxic intermediate that accumulates in *nagB* mutants when grown on GlcN or GlcNAc. Functional and structural studies of SCO4393 are described in Chapter IV. The crystal structure of SCO4393 was resolved and strongly suggests that the substrate is a phosphoaminosugar. Binding studies

identified GlcNAc-6P as a substrate, in contrast to related sugars GlcNAc, GlcN-6P, Fru-6P or GlcNAc-1P.

UNDERSTANDING GLCN METABOLISM

A suppressor mutant screen, specifically aimed at identifying novel components of GlcN metabolism, is described in Chapter V. The surprising role of GlcNAc metabolic genes in GlcN metabolism is explored further and also shown is how the toxicity of only GlcN but not GlcNAc to *nagB* mutants is alleviated by disruption of SCO1447, which encodes ROK-family regulator RokL6. The chapter also highlights how the selection and analysis of suppressor mutants that relieve the aminosugar sensitivity proved an indispensable tool for identifying novel proteins involved in aminosugar metabolism.

RokL6 is likely involved in the regulation of the response to GlcN and its transport and/or metabolism. In Chapter VI, proteomic analysis of the *rokL6* mutant of *S. coelicolor* suggested that GlcN sensing is independent of RokL6 function and that RokL6 regulates development and antibiotic production. Resistance of the *rokL6-nagB* mutant to the anticancer drug 2-deoxyglucose may provide new insights into the connection between glucose and aminosugar metabolism.

Finally, all data and new insights are discussed and summarized in Chapter VII.

CHAPTER II

INTERTWINING NUTRIENT-SENSORY NETWORKS AND THE CONTROL OF ANTIBIOTIC PRODUCTION IN *STREPTOMYCES*

Mia Urem, Magdalena A. Świątek-Połatyńska,
Sébastien Rigali and Gilles P. van Wezel

ABSTRACT

Actinobacteria are producers of a plethora of natural products of agricultural, biotechnological and clinical importance. In an era where mankind has to deal with rapidly spreading antimicrobial resistance, streptomycetes are of particular importance as producers of half of all antibiotics used in the clinic. Genome sequencing efforts revealed that their capacity as antibiotic producers has been underestimated, in particular as many biosynthetic pathways are silent under standard laboratory conditions. Here we review the global regulatory networks that control antibiotic production in streptomycetes, with emphasis on carbon- and aminosugar-related nutrient sensory pathways. Recent research has revealed intriguing connections between these regulons, and overlap and antagonism between the activities of among others the global regulatory proteins AtrA, DasR and Rok7B7 as well as GlnR (nitrogen control) and PhoP (phosphate control), are discussed. Finally, we provide ideas as to how these novel insights might help us to find ways to activate the transcription of silent biosynthetic gene clusters.

INTRODUCTION

Streptomycetes are filamentous soil bacteria that produce around 50% of all antibiotics in clinical use as well as a wide range of other natural products of medical, biotechnological or agricultural importance, including anti-cancer, anti-inflammatory and anti-fungal agents (Bérdy, 2005; Hopwood, 2007). The streptomycetes belong to the family *Streptomycetaceae* that are characterized by mycelial growth, with large GC-rich chromosomes that reflect the complexity of both their life cycle and rapidly changing environmental conditions (Labeda *et al.*, 2012; Ludwig *et al.*, 2012; Barka *et al.*, 2016). Like other filamentous actinobacteria, streptomycetes are found in terrestrial and marine environments, where nutrient supplies are often heterogeneous or fluctuating rapidly. To meet such diverse challenges, they metabolize a wide range of carbon, nitrogen, phosphate and sulphur sources using extensive sensing and transport systems that monitor the nutritional status of the environment and assist in scavenging of a wide range of nutrients. Streptomycetes possess a large number of genes for polysaccharide hydrolases (Hodgson, 2000) which facilitate the degradation and subsequent metabolism of complex polysaccharides, a large number of carbohydrate transport systems, the majority of which are ATP-binding cassette (ABC) transporters (Bertram *et al.*, 2004), and a staggering 700 regulatory proteins are encoded by the genome of the model actinomycete *Streptomyces coelicolor* (Bentley *et al.*, 2002).

Under conditions of stress, such as nutrient depletion, streptomycetes enter a complex life cycle, resulting in sporulation (Fig. 1). Once dispersed, spores germinate and grow as a branched, vegetative mycelium that consists of long multinucleoid hyphae. These hyphae are compartmentalized into large segments by cross-walls, making streptomycetes a model system for bacterial multicellularity (Elliot *et al.*, 2008; Claessen *et al.*, 2014). When streptomycetes enter the developmental program, the vegetative mycelium is degraded and a programmed cell death (PCD) process (Migueluez *et al.*, 1999, 2000; Manteca *et al.*, 2005a) provides the nutrients for the newly formed aerial mycelium, which eventually produces chains of unigenomic spores (Flårdh and Buttner, 2009). Sporulation is a highly complex process of coordinated cell division and DNA segregation, involving actinomycete-specific regulatory proteins (Traag and van Wezel, 2008; Jakimowicz and van Wezel, 2012; McCormick and Flårdh, 2012).

The onset of morphological differentiation roughly coincides with that of chemical differentiation, i.e. the production of secondary metabolites, also referred to as specialized metabolites or natural products (Fig. 1) (Bibb, 2005; van Wezel and McDowall, 2011). The model organism *S. coelicolor* produces a variety of antibiotics, including the red-pigmented prodiginines (Red) and the blue-pigmented actinorhodin (Act), the calcium-dependent antibiotic (Cda) and the plasmid-encoded methylenomycin (Mmy) (Bentley *et al.*, 2002; Hopwood, 2006). Besides Act, Cda, Mmy and Red, the genome of *S. coelicolor* encodes the Cpk (cryptic polyketide) proteins for the biosynthesis of yet another antibiotic, recently elucidated as coelimycin P1 (Gomez-Escribano *et al.*, 2012). Located within the biosynthetic gene clusters lie genes for pathway-specific transcriptional regulators, which then activate the production of the biosynthetic pathways. The extensively studied pathway-specific activators ActII-ORF4 (activates Act biosynthesis), CdaR (for Cda) and RedD (for Red) all belong to the SARP family of *Streptomyces* antibiotic regulatory proteins (Wietzorrek and Bibb, 1997). Once the pathway-specific activators are expressed, the biosynthetic gene clusters are activated with little downstream control (Bibb, 2005; van Wezel and McDowall, 2011). Indeed, when the *redD* transcriptional activator gene is put under the control of a different promoter, timing and/or localization of Red production is altered

accordingly (van Wezel *et al.*, 2000a). However, intricate regulatory networks are present to govern the timing of antibiotic production and its linkage to cell growth, nutrient selection, development and environmental stresses. Here, we review the intertwining global regulatory networks that translate environmental signals and the bacterium's metabolic status to the control of the specialized metabolism of streptomycetes, using the well-studied *S. coelicolor* as the model organism, and with special attention to the complex role of aminosugars.

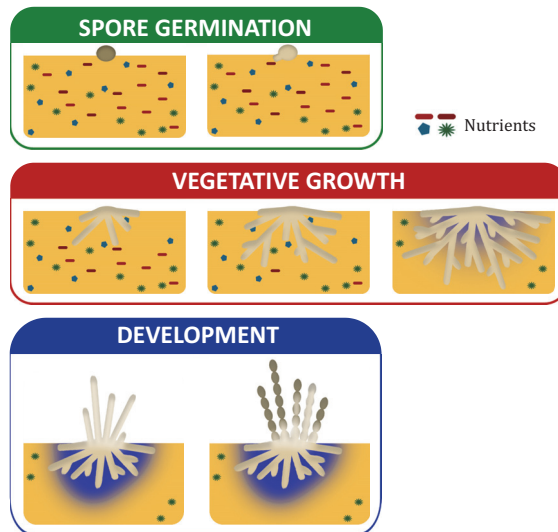


FIGURE 1. The *Streptomyces* life cycle.

Streptomyces form a branched mycelium that grows into the soil/media to scavenge nutrients. When nutrients become depleted, complex sensory and regulatory networks relay the environmental cues into responses. This leads to the production of antibiotics and other secondary metabolites as well as the development of aerial mycelia which eventually form spores as a means of escape from unfavourable conditions through dispersal. (Top) Germination: a spore germinates once favourable (nutrient-rich) conditions are sensed; (Middle) Vegetative growth: when nutritional content of the media is high, growth is promoted through branching and elongation of the hyphae via apical growth. Favourable nutrients (red) are depleted, and once other nutrients are also depleted, the developmental program is initiated which is accompanied by the production of antibiotics (blue, last panel); (Bottom) Development: to escape the nutrient-depleted environment, streptomycetes form erected aerial hyphae at the expense of the underlying substrate mycelium. At this time antibiotics (blue) are also produced. The aerial hyphae septate and are ultimately converted into chains of spores.

CARBON CATABOLITE REPRESSION AND THE CONTROL OF ANTIBIOTIC PRODUCTION

The most extensively studied nutrient sensory and control system in bacteria is without any doubt carbon catabolite repression (CCR), also known as glucose repression. Efficient carbon source utilisation is critical from the perspective of competition in the natural habitat. CCR of catabolic genes is often achieved by the combined activities of global and operon-specific regulatory mechanisms, including inducer exclusion (Gorke and Stülke, 2008). The phosphoenolpyruvate-dependent phosphotransferase system (PTS) plays a major role in the regulation of CCR in many microorganisms (Gunnewijk *et al.*, 2001; Brückner and Titgemeyer, 2002; Gorke and Stülke, 2008). The PTS transport system is specific to prokaryotes and uses a protein phosphoryl transfer chain, with phosphoenolpyruvate (PEP) as phosphoryl donor, to transport and phosphorylate specific carbohydrates. The system consists of the general energy-coupling phosphotransferase Enzyme I (EI) and phosphocarrier protein HPr in combination with diverse, carbohydrate-specific transport complexes called Enzyme II (EII) (Saier and Reizer, 1992; Postma *et al.*, 1993). In *Streptomyces*, deletion of the general *pts* genes (*ptsH*, *ptsI* and *crr* which encode HPr, EI

and EIIA, respectively), leads to vegetative arrest and consequently mutants have a non-sporulating (bald) phenotype (Nothaft *et al.*, 2003a; Rigali *et al.*, 2006). This phenomenon is most likely associated with altered production of the siderophore desferrioxamine, which is essential for proper development on especially glucose-containing media (Yamanaka *et al.*, 2005; Traxler *et al.*, 2012; Lambert *et al.*, 2014). This observation reveals a direct link between carbon utilization, iron homeostasis and the control of development, but it is currently unknown how this is mediated.

In both *Escherichia coli* and *Bacillus subtilis*, the PTS is critical for the regulation of CCR, however, the mode of regulation differs greatly. In *E. coli*, CCR is controlled via modulation of the phosphorylation state of the glucose transporter (EIIA^{Glc}). EIIA^{Glc} exists primarily in its non-phosphorylated state during active PTS-mediated glucose transport and inhibits the transport of non-PTS sugars (e.g. lactose, maltose, melibiose, raffinose), resulting in inducer exclusion for many sugar operons (Hogema *et al.*, 1998; Brückner and Titgemeyer, 2002). Conversely, in the absence of glucose, EIIA^{Glc} remains phosphorylated and activates the membrane-bound adenylate cyclase, leading to the accumulation of cyclic AMP (cAMP). This then forms a complex with its receptor protein CRP, which activates the transcription of many catabolic genes and operons (Gorke and Stülke, 2008). In *B. subtilis*, the phosphocarrier protein HPr plays the central role in the regulation of CCR. HPr is phosphorylated by the HPr kinase/phosphorylase (HprK/P), with HprK/P kinase activity stimulated by fructose-1,6-bisphosphate, while HprK/P phosphorylase activity is triggered by the accumulation of inorganic phosphate (Jault *et al.*, 2000; Mijakovic *et al.*, 2002). Phosphorylation of HPr triggers its interaction with the pleiotropic transcription factor CcpA (catabolite control protein A), which then exerts global repression of sugar catabolic operons (Deutscher *et al.*, 1995; Jones *et al.*, 1997).

In contrast to most bacteria, deletion of the general *pts* genes has no effect on glucose repression in *Streptomyces* (Butler *et al.*, 1999; Nothaft *et al.*, 2003b) and the cAMP-CRP complex, though globally impacting antibiotic production, has no role in CCR (Derouaux *et al.*, 2004a; Derouaux *et al.*, 2004b; Gao *et al.*, 2012). Surprisingly, in streptomycetes, glucose is not transported via the PTS but via the Major Facilitator Superfamily (MFS) permease GlcP (van Wezel *et al.*, 2005; Perez-Redondo *et al.*, 2010; Romero *et al.*, 2015) (see Fig. 2). This may have been an evolutionary adaptation to facilitate the key role of glucose kinase (also known as glucokinase) in CCR in these bacteria and at the same time prioritize mixed C- and N-sources. Indeed, *N*-acetylglucosamine (GlcNAc) and glutamate are highly preferred substrates for streptomycetes; in cultures with both glucose and glutamate, *S. coelicolor* consumes all the glutamate before glucose is metabolized (van Wezel *et al.*, 2006a; Romero-Rodríguez *et al.*, 2016). The surprising observation that the PTS does not play a general role in CCR may be due to the critical role GlcNAc plays in central metabolism and the control of development and antibiotic production (Nothaft *et al.*, 2003a; Rigali *et al.*, 2006), as discussed in the next section, and therefore alternative systems have been put in place to take over the control of carbon source regulation. Still, like in other bacteria, glucose exhibits CCR over other the utilisation of other carbon sources, such as glycerol, arabinose, fructose and galactose.

Glucose kinase (Glc, encoded by the *glkA* gene) performs the first step in glycolysis by phosphorylating glucose to glucose-6P (Fig. 2). A member of the ROK family of proteins (Repressors, ORFs and Kinases [Titgemeyer *et al.*, 1994]), Glc also plays a predominant role in CCR in *S. coelicolor* (Angell *et al.*, 1992; Angell *et al.*, 1994) and probably also in *Streptomyces peucetius* (Guzman *et al.*, 2005). While genome sequence comparison suggests that it is very likely that Glc also fulfils a dominant role in CCR in other streptomycetes, this concept awaits

experimental analysis. Deletion or mutation of *glkA* results in loss of glucose utilization as well as glucose repression of catabolite-controlled genes, including those for the utilization of agar (*dagA*), glycerol (*gylCABX*), galactose (*galP*), maltose (*malEFG*) and chitin (*chi*) (Angell *et al.*, 1992; Angell *et al.*, 1994; Hindle and Smith, 1994; van Wezel *et al.*, 1997; Saito *et al.*, 2000). The enzymatic activity of Glk strongly depends on the carbon source and growth phase, with high activity of Glk in glucose-grown cultures and low activity in cultures grown on the non-repressing carbon source mannitol, whereby Glk activity is likely modulated through metabolite-dependent activation and/or post-translational modification of the enzyme (van Wezel *et al.*, 2007). CCR also represses the production of antibiotics (Sanchez *et al.*, 2010). In the soil, sugars are closely monitored and the presence of high-energy nutrients promotes growth and suppresses developmental processes as well as antibiotic production, therefore many antibiotics are subject to CCR (Hostalek, 1980; Sanchez *et al.*, 2010). Examples include the production of chloramphenicol by *Streptomyces venezuelae* (Bhatnagar *et al.*, 1988), cephamycin by *Streptomyces clavuligerus* (Cortes *et al.*, 1986), erythromycin by *Saccharopolyspora erythraea* (Escalante *et al.*, 1982) and streptomycin by *Streptomyces griseus* (Demain and Inamine, 1970).

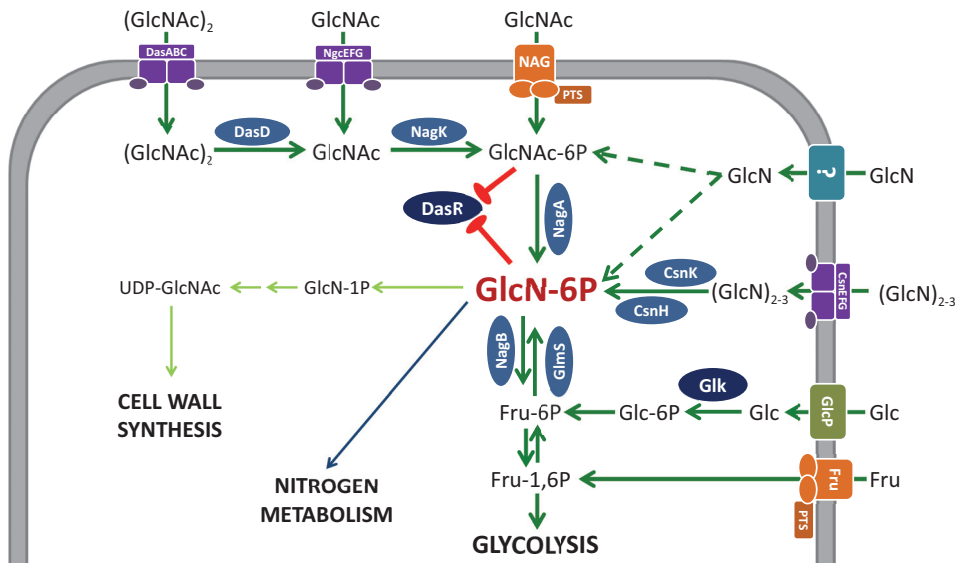


FIGURE 2. Carbohydrate metabolic pathways in *S. coelicolor*.

The primary metabolism of *S. coelicolor* is shown for *N*-acetylglucosamine (GlcNAc), *N,N'*-diacetylchitobiose (GlcNAc)₂, chitosan-derived oligosaccharides (GlcN)_{2,3}, glucose (Glc) and fructose (Fru) in addition to proposed pathway(s) for glucosamine (GlcN). Glucosamine 6-phosphate (GlcN-6P, red) is a central metabolite that stands at the crossroads of aminosugar metabolism, glycolysis, nitrogen metabolism and cell-wall synthesis. It also plays an important role in signalling of antibiotic production and development by modulating the activity of the global repressor DasR. GlcN-6P is obtained from internalization of monomers or oligomers of GlcN or GlcNAc and metabolism via CsnK and CsnH and via Naga, or in a reverse reaction by GlmS from glycolytic precursors. (GlcNAc)₂ is hydrolysed by DasD to GlcNAc and subsequently phosphorylated by NagK to GlcNAc-6P. A hypothetical metabolic route for GlcN via the GlcNAc pathway is presented, though no transporter or metabolic enzymes have so far been identified (Świątek *et al.*, 2012a; Viens *et al.*, 2015). Internalized glucose is phosphorylated by glucose kinase (Glk), which is key to carbon catabolite repression in *S. coelicolor*. ABC transporters are presented in purple, PTS transporters in orange, putative GlcN transporter in turquoise and the glucose MFS permease GlcP in green. Primary metabolic routes are represented by green arrows, with unknown routes indicated by dotted arrows. The cell-wall biosynthetic reactions are shown as light green arrows and nitrogen metabolism by a blue arrow.

In *Streptomyces lividans*, glucose inhibits actinorhodin production by repressing the *afsR2* gene, which encodes a global regulatory protein involved in the activation of specialized metabolite biosynthesis in diverse *Streptomyces* species (Kim *et al.*, 2001). In *S. coelicolor*, the homologue of AfsR2, AfsS, binds to a putative secreted solute binding protein encoded by SCO6569. Overexpression of this newly characterized protein significantly reduced actinorhodin production, while gene disruption led to accelerated antibiotic production (Lee *et al.*, 2009). This suggests that SCO6569 is an AfsS-dependent down-regulator of actinorhodin production in *S. coelicolor*. The flux of carbon through glycolysis also influences antibiotic production. Deletion of *pfkA2*, encoding one of the three phosphofructokinases in *S. coelicolor*, leads to enhanced production of the pigmented antibiotics actinorhodin and undecylprodigiosin (Borodina *et al.*, 2008). Genome-scale metabolic simulations suggested that decreased phosphofructokinase activity leads to an increase in the flux through the pentose phosphate pathway, which then stimulates the flux towards pigmented antibiotics (Borodina *et al.*, 2008).

AMINOSUGAR METABOLISM IN STREPTOMYCETES

Aminosugars are not only important nutrients but also play a key role as signalling molecules in streptomycetes, with *N*-acetylglucosamine (GlcNAc) involved in the activation of the onset of development and antibiotic production under poor nutritional conditions (Rigali *et al.*, 2008). A metabolic intermediate of aminosugar metabolism, glucosamine-6-phosphate (GlcN-6P) is a central molecule that stands at the cross-roads of many metabolic pathways, including glycolysis, cell-wall synthesis, glutamine and glutamate metabolism (Durand *et al.*, 2008). After the internalization and phosphorylation of GlcNAc, *N*-acetylglucosamine-6-phosphate (GlcNAc-6P) is deacetylated to GlcN-6P by the *N*-acetylglucosamine-6-phosphate deacetylase NagA. The resulting GlcN-6P can then be deaminated to fructose-6P by GlcN-6P deaminase NagB or go to other metabolic routes (Bates and Pasternak, 1965; Midelfort and Rose, 1977; Plumbridge, 2015). See Fig. 2 for an overview.

GlcNAc is the monomer of chitin, which is one of the most abundant polysaccharides on earth and a preferred substrate for streptomycetes, acting as both a source of carbon and nitrogen. Together with *N*-acetylmuramic acid, GlcNAc also forms the strands of peptidoglycan (PG), which make up the bacterial cell wall (Terrak *et al.*, 1999). Transport and subsequent internalization of GlcNAc has been studied in many bacteria and in most, uptake of GlcNAc occurs via the PTS (Bouma and Roseman, 1996; Reizer *et al.*, 1999; Alice *et al.*, 2003; Komatsuzawa *et al.*, 2004; Nothaft *et al.*, 2010; Liao *et al.*, 2014b; Plumbridge, 2015), but alternative uptake systems have been described (Xiao *et al.*, 2002; Saito *et al.*, 2007; Eisenbeis *et al.*, 2008; Boulanger *et al.*, 2010; Liao *et al.*, 2014b). In *E. coli*, GlcNAc is transported by NagE, while the related aminosugar glucosamine (GlcN) is transported via the non-specific hexose transporter ManXYZ (Jones-Mortimer and Kornberg, 1980; Postma *et al.*, 1996). *B. subtilis* transports GlcNAc via NagP, while GamP and the glucose transporter PtsG both transport GlcN (Reizer *et al.*, 1999; Bertram *et al.*, 2011; Gaugué *et al.*, 2013). Similar systems also exist in streptomycetes (Titgemeyer *et al.*, 1995; Wang *et al.*, 2002). As mentioned above, glucose is not transported by the PTS in streptomycetes, but instead the PTS is biased for GlcNAc and fructose utilization (Kamionka *et al.*, 2002; Nothaft *et al.*, 2003a; Nothaft *et al.*, 2003b; Nothaft *et al.*, 2010). GlcNAc is imported via the EIIABC complex, consisting of EIIA^{Crr} (Crr), EIIB^{GlcNAc} (NagF) and EIIC^{GlcNAc} (NagE2), while it is unclear how monomeric GlcN is internalized (Fig. 2). The utilization of GlcN, which originates from chitosan (an *N*-deacetylated derivative of chitin), appears equally complex as that of GlcNAc, involving multiple (unidentified) uptake and regulatory systems, in

addition to the *csnR-K* operon responsible for the import and utilization of GlcN dimers and chito-oligosaccharides (Dubeau *et al.*, 2011; Viens *et al.*, 2015). A suppressor screen, making use of the lethality of GlcN and GlcNAc to *S. coelicolor nagB* mutants, directly or indirectly due to the accumulation of GlcN-6P, showed that a lot of questions remain on how GlcN(Ac) is metabolized in streptomycetes (Świątek *et al.*, 2012a; Świątek *et al.*, 2012b). As expected, spontaneous suppressor mutants that survive on GlcNAc include those mutated in *nagA*, which is required for the formation of GlcN-6P. Surprisingly, GlcN toxicity is also relieved by mutations in *nagA*. This suggests that GlcN may be exclusively metabolized via the GlcNAc metabolic route (Świątek *et al.*, 2012b) (Fig. 2). Indeed, deletion of *nagK*, which encodes GlcNAc kinase that phosphorylates intracellular GlcNAc, also relieves GlcN toxicity to *nagB* mutants. Importantly, suppressor mutants were identified that could not be correlated to any of the known *nag* (GlcNAc metabolic pathway) genes and these are currently being elucidated by genome sequencing. Furthermore, deleting the *nag* metabolic genes has significant and growth medium-dependent effects on antibiotic production by *S. coelicolor*, with some mutants overproducing the pigmented antibiotic actinorhodin (Świątek *et al.*, 2012a; Świątek *et al.*, 2012b). For one, DNA binding activity of the pleiotropic antibiotic repressor DasR (which is discussed in detail below) is likely influenced by binding of various (amino-)sugars, including GlcN-6P and GlcNAc-6P (Rigali *et al.*, 2006; Rigali *et al.*, 2008; Liao *et al.*, 2015b; Fillenberg *et al.*, 2016) and different phosphorylated C6-sugars generated during glycolysis (Świątek-Połatyńska *et al.*, 2015; Tenconi *et al.*, 2015). Control of antibiotic production may therefore be influenced by the metabolic balance of these molecules. Approaches for rational strain engineering based on interference of the metabolic flux of amino sugars may, therefore, be a useful strategy. This concept awaits further experimental testing.

GLcN-6P STANDS AT THE CROSSROADS OF C- AND N- METABOLISM AND DEVELOPMENTAL PATHWAYS

In streptomycetes, GlcN-6P plays many key roles including a central role in the control of antibiotic production, thereby directly connecting the control of primary metabolism to that of secondary metabolism. GlcN-6P, together with GlcNAc-6P, acts as an allosteric effector of the nutrient sensory regulator DasR (Figs 2 and 3). The crystal structure of DasR in *S. coelicolor* and its distant orthologue NagR of *Bacillus subtilis* in complex with GlcN(Ac)-6P have been elucidated (Fillenberg *et al.*, 2015; Fillenberg *et al.*, 2016). DasR derives its name from the adjacent *dasABC* operon involved in *N-N'*-diacetylchitobiose [(GlcNAc)₂] metabolism but is also important for development, with *das* standing for deficient in aerial mycelium and spore formation (Seo *et al.*, 2002; Colson *et al.*, 2008). DasR is a GntR-family repressor with a pleiotropic role in the regulation of primary metabolism, development and antibiotic production. Extensive analysis of the DasR regulon showed that DasR directly controls the *pts*, *nag* and *chi* genes (for the chitinolytic system) and represses antibiotic production by direct binding to the promoter regions of the pathway-specific regulatory genes for all antibiotic biosynthetic gene clusters in *S. coelicolor* (Rigali *et al.*, 2006; Rigali *et al.*, 2008; Nazari *et al.*, 2012; Świątek-Połatyńska *et al.*, 2015). A similar pleiotropic role of DasR has also been reported in the erythromycin producer *Saccharopolyspora erythraea* (Liao *et al.*, 2014b; Liao *et al.*, 2015b). Recently, it was also shown that DasR indirectly represses the biosynthesis of iron-chelating siderophores through the direct control of the iron-homeostasis regulator *dmdR1* in *S. coelicolor* (Craig *et al.*, 2012; Lambert *et al.*, 2014).

The activity of DasR and its response to GlcN-6P and GlcNAc-6P levels depends on environmental conditions; growth on high concentrations of GlcNAc under famine

conditions (i.e. on minimal media) results in the global de-repression of its targets and enhanced antibiotic production and development while on rich media, GlcNAc represses antibiotic and development (Rigali *et al.*, 2006; Rigali *et al.*, 2008; van Wezel *et al.*, 2009). This phenomenon reflects conditions of *feast* or *famine*: under rich growth conditions (feast) streptomycetes likely interpret GlcNAc as derived from chitin and hence abundance of nutrients, while under poor growth conditions (famine) it would be seen as a by-product of hydrolysis of peptidoglycan and hence its own cell death. Abundance of nutrients will promote growth and postpone development, while the initiation of cell death requires sporulation and antibiotic production (Fig. 1).

Key in the sensing system is probably that chitin is metabolized and internalized as (GlcNAc)₂, which is imported via the ABC-transporter system DasABC-MsiK, while GlcNAc is imported via the PTS (Nothaft *et al.*, 2003a; Saito *et al.*, 2007; Saito *et al.*, 2008; Nothaft *et al.*, 2010). This GlcNAc disaccharide, (GlcNAc)₂, hydrolysed from chitin, induces the expression of chitinase genes as well as DasABC transporter of chitobiose in *S. coelicolor* (Saito *et al.*, 2007). In *Streptomyces olivaceoviridis*, the *ngcEFG* operon encodes an ABC transporter that imports *N*-acetylglucosamine and (GlcNAc)₂ with similar affinities (Xiao *et al.*, 2002; Saito and Schrepf, 2004). A homologue of this system exists in *S. coelicolor*, which might also import monomers and/or dimers of GlcNAc under certain conditions. After uptake, (GlcNAc)₂ is cleaved by the *N*-acetyl-β-d-glucosaminidase DasD into monomers of GlcNAc (Saito *et al.*, 2013) which are then phosphorylated by the NagK kinase and GlcNAc-6P is fed into the GlcNAc pathway described above (Fig. 2). The precise role of these transporters in nutrient sensing is not yet well understood, such as why deletion of either any of the *pts* genes or of *dasA* (but not *dasBC*) blocks development, even in the absence of the molecules they transport (Seo *et al.*, 2002; Rigali *et al.*, 2006; Colson *et al.*, 2008). In addition to GlcN-6P and GlcNAc-6P, other metabolites also modulate the DasR response regulon, including high concentrations of phosphate (organic or inorganic) which enhance binding of DasR to its recognition site *in vitro* (Świątek-Połatyńska *et al.*, 2015; Tenconi *et al.*, 2015). This suggests that the metabolic status of the cell determines the selectivity of DasR for its recognition site and thus the expression of its regulon.

CROSS-TALK BETWEEN ATR A, DASR AND ROK7B7

Regulatory complexity in *S. coelicolor* is governed by the cooperative or antagonistic action of various global regulators such as AtrA, DasR and Rok7B7 (Fig. 3), which are controlled in a growth phase-dependent manner and by the nutritional status of the cell. Like DasR, the TetR-family transcriptional regulator AtrA is highly conserved in streptomycetes, and AtrA is required for actinorhodin production in *S. coelicolor* and streptomycin production in *Streptomyces griseus*, by directly controlling the pathway-specific activator genes *actII-ORF4* and *strR*, respectively (Uguru *et al.*, 2005; Hong *et al.*, 2007). AtrA affects multiple regulatory pathways, including those that control sporulation (Nothaft *et al.*, 2010; Kim *et al.*, 2015). Interestingly, AtrA controls both the initial and final steps of the proposed DasR-mediated signalling pathway, namely the internalization of the signal (GlcNAc) via the activation of the transporter gene *nagE2*, and activation of the biosynthetic cluster for actinorhodin production via the transcriptional activation of *actII-ORF4* (Nothaft *et al.*, 2010). In this way, AtrA and DasR have antagonizing activities in *S. coelicolor* (Fig. 3).

The ROK-family protein Rok7B7 takes up an interesting position in the regulatory network as it connects the control of antibiotic production and CCR. Rok7B7 shares 48% amino acid identity to a protein encoded by *rep*, a gene isolated from a metagenomic library that accelerates sporulation and antibiotic production in *Streptomyces lividans* (Martinez *et*

al., 2005). Rok7B7 controls the expression of the adjacent xylose transport operon *xylFGH* and in the absence of Rok7B7, *S. coelicolor* grows very well on xylose, which normally is not used efficiently as a carbon source (Świątek *et al.*, 2013). Mutants lacking *rok7B7* also show delayed development and deregulated antibiotic production, as well as altered CCR. Indeed, Rok7B7 activates Act production but represses the biosynthesis of Red and Cda (Park *et al.*, 2009). A DNA affinity capture assay suggested that Rok7B7 can bind directly to promoters of *actII-ORF4* and *redD* (Park *et al.*, 2009), but a binding site has so far not been identified and it is therefore still a mystery how Rok7B7 controls its regulon (Park *et al.*, 2009; Świątek *et al.*, 2013). Like AtrA, Rok7B7 also activates primary and secondary metabolism through control of the GlcNAc *pts* (specifically *nagE2*) and *actII-ORF4* (Fig. 3) (Park *et al.*, 2009; van Wezel and McDowall, 2011). It thus appears that there is direct competition between DasR-mediated repression and activation by Rok7B7 (and AtrA) of key metabolic and antibiotic regulatory genes (Fig. 3).

Proteomic analysis of *S. coelicolor* and the *S. coelicolor glkA* deletion mutant revealed that glucose activates Rok7B7 and XylFGH in a Glk- and CCR-independent manner (Gubbens *et al.*, 2012) and this was also observed in a recent transcriptomic analysis (Romero-Rodríguez *et al.*, 2016). Interestingly, DasR and Rok7B7 both repress the expression of Glk (Świątek *et al.*, 2013; Świątek-Połatyńska *et al.*, 2015), while Glk represses Rok7B7 (Fig. 3) (Gubbens *et al.*, 2012). Conversely, deletion of *rok7B7* results in a loss of CCR, which directly implicates Rok7B7 in CCR (Gubbens *et al.*, 2012; Romero-Rodríguez *et al.*, 2016). The upregulation of Rok7B7 in glucose-grown cultures may be explained as feedback control to try to achieve CCR in the absence of Glk activity. Since Glk expression is constitutive and Glk is activated posttranslationally (van Wezel *et al.*, 2007; Romero-Rodríguez *et al.*, 2016), direct transcriptional control of *glkA* by Rok7B7 is unlikely. The ligand for Rok7B7 is unknown, although its phylogenetic linkage to xylose utilization suggests that it is mediated by a C5 carbon.

LINKING NITROGEN AND PHOSPHATE CONTROL: GLNR AND PHOP

A novel linkage between C- and N-metabolism was established recently, when it was shown that GlnR not only controls nitrogen metabolism but also the uptake and metabolism of carbon (Liao *et al.*, 2015a). *S. coelicolor* can use a wide range of nitrogen sources, including ammonia, nitrate (Wang and Zhao, 2009), nitrite, urea (Tiffert *et al.*, 2008), amino sugars and amino acids (Reuther and Wohlleben, 2007). Utilization of different nitrogen sources is controlled by the orphan response regulator GlnR (Fig. 3), whose gene expression is nitrogen dependent (Tiffert *et al.*, 2008). In *Saccharopolyspora erythraea*, most ABC transporters are under control of GlnR and its disruption lead to impaired growth on sugars including maltose, mannitol, mannose, sorbitol and trehalose (Liao *et al.*, 2015a) and in their transcriptional analysis of CCR in *S. coelicolor*, Romero-Rodríguez and colleagues also observed upregulation of GlnR by glucose (Romero-Rodríguez *et al.*, 2016). Under control of GlnR, actinomycetes are able to induce carbohydrate uptake and metabolism when nitrogen, which is essential for the synthesis of proteins, co-factors and specialized metabolites, is limited. Interestingly, it was shown that the three genes for citrate synthase are all controlled by several global nutrient sensory regulators including GlnR and DasR, but also the cAMP receptor protein, CRP (Liao *et al.*, 2014a). CRP controls early processes during growth in *Streptomyces* (Derouaux *et al.*, 2004b; Piette *et al.*, 2005) and acts as a global regulator of Act, Cda and Red production and it was suggested that it coordinates precursor flux from primary to secondary metabolism (Gao *et al.*, 2012).

Besides the linkage with CRP and DasR, there is also significant cross-talk between

GlnR and the global phosphate regulator PhoP (Fig. 3), which is part of a two-component system. Phosphate plays an important role in the control of antibiotic production, with many antibiotics repressed by phosphate (reviewed in [Martin, 2004; Martin and Liras, 2010]). PhoP and GlnR together control antibiotic production by monitoring the metabolic status of phosphate and nitrogen in *Streptomyces* (Santos-Beneit *et al.*, 2009; Santos-Beneit *et al.*, 2012). Transcriptomic and biochemical data show that PhoP also controls expression of *glnR*, though it is unlikely that GlnR controls *phoP* directly. PhoP also competes with GlnR for the promoter regions of genes for nitrogen metabolism and this PhoP-mediated control of nitrogen metabolism may help balancing the cellular P/N equilibrium (Sola-Landa *et al.*, 2013). Expression of antibiotic biosynthetic gene clusters is upregulated in response to low phosphate (Rodríguez-García *et al.*, 2007; Nieselt *et al.*, 2010; Allenby *et al.*, 2012), as well as by ammonium limitation (Fink *et al.*, 2002; Reuther and Wohlleben, 2007; Lewis *et al.*, 2011), though ChIP-on-chip studies indicated that this is not through direct binding of pathway-specific antibiotic activators promoters. Instead, PhoP binds upstream of genes which encode for other regulatory proteins that control antibiotic gene clusters, including *afsS* and *atrA* (Allenby *et al.*, 2012). The *afsS* gene encodes a small protein which activates antibiotic production in various streptomycetes, in a yet unknown manner (Martin *et al.*, 2011; Santos-Beneit *et al.*, 2011).

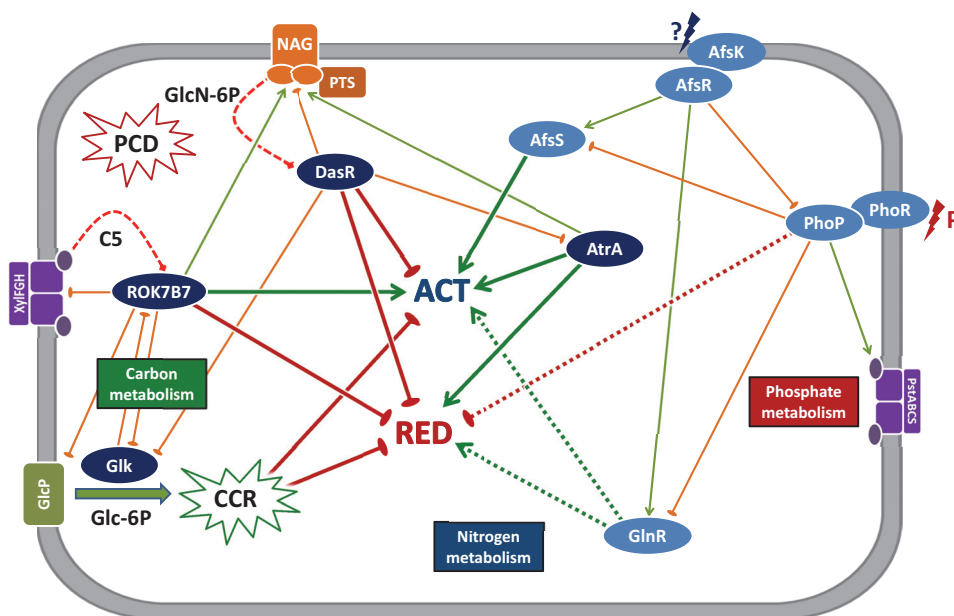


FIGURE 3. Intertwining nutrient regulatory networks that control antibiotic production in *S. coelicolor*.

Global regulatory networks translate environmental signals and the cell's metabolic status to secondary metabolic responses. Only regulatory networks controlling the biosynthetic genes for actinorhodin (Act) and prodiginines (Red) are shown. The biosynthesis of antibiotics is under the control of specific transcriptional regulators, situated within the biosynthetic clusters, which in turn are under global control. Carbon control proteins central to this review presented as dark blue ovals, other regulators light blue. Dotted lines indicate uncertainty of control (direct or indirect). Activation of antibiotic production is shown as thick green arrows and repression by thick red lines with an ellipse. In addition to regulatory control of antibiotic production, global transcriptional regulators also control enzymes involved in metabolic pathways as well as other global transcriptional regulator. This is represented by thin lines; positive control by green arrows, negative control by orange lines with an ellipse. CCR, carbon catabolite repression; PCD, programmed cell death. Dashed red lines indicate inhibition by ligands (Rok7B7 by C5 sugars (C5); DasR by GlcN-6P). For transporters see Fig. 2.

The AfsK serine/threonine kinase and its cognate response regulator AfsR also control antibiotic production via modulation of *afsS* (Lee *et al.*, 2002). In addition to competition for the *afsS* promoter, PhoP and AfsR also cross-regulate expression of *glnR*, the phosphate transporter gene *pstS* and *phoPR*, which encodes response regulator PhoP and its cognate sensory kinase, the phosphate limitation sensor PhoR (Santos-Beneit *et al.*, 2009; Santos-Beneit *et al.*, 2012). The response regulator AfsQ1 and cognate sensory kinase AfsQ2 act as conditional (positive) pleiotropic regulators of phosphate transporter PtsS as well as development and antibiotic production (Wang *et al.*, 2013), whereby the AfsQ1 binding site upstream of the Red biosynthetic genes overlaps with the site recognized by DasR.

The role of inorganic phosphate (Pi) in antibiotic production involves another direct target gene of PhoP, *ppk*, which encodes an enzyme that acts as an adenosyl diphosphate kinase (ADPK), regenerating ATP under conditions of Pi limitation (Chouayekh and Virolle, 2002; Ghorbel *et al.*, 2006a; Ghorbel *et al.*, 2006b). By regenerating ATP from ADP and polyphosphates, *ppk* plays a key role in maintaining the energetic homeostasis of the cell. Its deletion in *S. lividans* results in enhanced actinorhodin production in the glucose-rich and Pi limited medium R2YE (Chouayekh and Virolle, 2002). The increased Act production is attributed to increased degradation of lipid storage vesicles, containing mainly triacylglycerols (TAG), in order to restore the energetic balance caused by the ATP deficiency in the *ppk* mutant (Le Marechal *et al.*, 2013). TAG degradation generates fatty acids and thus ultimately acetyl-CoA, which is among others a precursor for polyketide biosynthesis. The total TAG content in *S. coelicolor* and the amount of lipid vesicles are much lower than in *S. lividans*, suggesting higher degradation of storage lipids and thus higher accumulation of the precursor acetyl-CoA in this strong Act producer (Le Marechal *et al.*, 2013).

Finally, phosphorylated sugars also inhibit antibiotic production in streptomycetes. This effect is mediated by the phosphate moiety rather than the sugar moiety of the extracellular phosphor-sugars as the inactivation of *phoP* and *ppk* prevents and enhances, respectively, their utilization as nutrient sources and their inhibitory effect on antibiotic production (Tenconi *et al.*, 2012).

PERSPECTIVE: APPLICATION FOR ANTIBIOTIC DISCOVERY

Despite the phenomenal potential of actinomycetes as antibiotic producers, the antibiotic pipelines have nearly dried out. This is particularly due to replication, in other words, high-throughput screening efforts result in finding the same molecules over and over again, rather than identifying compounds with novel chemical structures and bioactivities (Payne *et al.*, 2007; Cooper and Shlaes, 2011; Lewis, 2013; Kolter and van Wezel, 2016). However, genome sequencing established that even widely studied species are relatively untapped sources of natural products (Bentley *et al.*, 2002; Ikeda *et al.*, 2003; Ohnishi *et al.*, 2008; Cruz-Morales *et al.*, 2013) and the wealth of genome sequence information that is currently being fed into the databases will reveal tens to hundreds of thousands of biosynthetic gene clusters. Undoubtedly, only a fraction of these have successfully been induced under laboratory conditions and a critical step is to identify the nutritional and ecological triggers and cues that allow the activation of these silent biosynthetic gene clusters (Zhu *et al.*, 2014a; Rutledge and Challis, 2015).

Understanding the regulatory networks that control biosynthetic gene clusters is of critical importance, with the induction by GlcNAc of the DasR-repressed *cpk* operon, which specifies the cryptic polyketide antibiotic Cpk, as an example of how such information can be harnessed to directly activate silent gene clusters (Rigali *et al.*, 2008). Similarly, knowledge

gained from unravelling the cellobiose utilization regulon controlled by CebR in *Streptomyces scabies* was recently applied to induce the expression of the biosynthetic gene cluster for the herbicide thaxtomin (Francis *et al.*, 2015). Scanning the genomes of actinomycetes for sites matching the consensus binding site for DasR revealed many putative target genes that relate to secondary metabolism, suggesting that DasR may control the production of a wide variety of specialized metabolites, including clinical drugs such as clavulanic acid, chloramphenicol, daptomycin and teichoplanin (van Wezel *et al.*, 2006b). Indeed, the addition of GlcNAc to minimal media often elicits the production of antibiotics, identifying novel compounds (Zhu *et al.*, 2014b). Bettering our understanding of the nutrient sensory regulatory networks and the way they are controlled by the metabolic status of the cell will also improve our fundamental understanding of the control of antibiotic production. Once more regulatory networks are unravelled, and the corresponding regulatory elements are mapped to the biosynthetic gene clusters, specific nutrient-mediated activation of natural products will become more and more routine, thereby providing new impetus to drug-discovery efforts.

ACKNOWLEDGEMENTS

The work was supported in part by the Belgian program of Interuniversity Attraction Poles initiated by the Federal Office for Scientific Technical and Cultural Affairs (PAI no. P7/44); and by a VICI grant 10379 from the Netherlands Technology Foundation STW.

CHAPTER III

OSDR OF *STREPTOMYCES COELICOLOR* AND THE DORMANCY REGULATOR DEVR OF *MYCOBACTERIUM TUBERCULOSIS* CONTROL OVERLAPPING REGULONS

Mia Urem, Teunke van Rossum, Giselda Bucca, Geri F. Moolenaar,
Emma Laing, Magda A. Świątek-Połatyńska, Joost Willemse,
Elodie Tenconi, Sébastien Rigali, Nora Goosen,
Colin P. Smith and Gilles P. van Wezel

ABSTRACT

Two-component regulatory systems allow bacteria to respond adequately to changes in their environment. In response to a given stimulus, a sensory kinase activates its cognate response regulator via reversible phosphorylation. The response regulator DevR activates a state of dormancy under hypoxia in *Mycobacterium tuberculosis*, allowing this pathogen to escape the host defense system. Here, we show that OsdR (SCO0204) of the soil bacterium *Streptomyces coelicolor* is a functional orthologue of DevR. OsdR, when activated by the sensory kinase OsdK (SCO0203), binds upstream of the DevR-controlled dormancy genes *devR*, *hspX*, and *Rv3134c* of *M. tuberculosis*. *In silico* analysis of the *S. coelicolor* genome combined with *in vitro* DNA binding studies identified many binding sites in the genomic region around *osdR* itself and upstream of stress-related genes. This binding correlated well with transcriptomic responses, with deregulation of developmental genes and genes related to stress and hypoxia in the *osdR* mutant. A peak in *osdR* transcription in the wild-type strain at the onset of aerial growth correlated with major changes in global gene expression. Taken together, our data reveal the existence of a dormancy-related regulon in streptomycetes which plays an important role in the transcriptional control of stress- and development-related genes.

Introduction

Complex natural habitats of bacteria call for rapid response systems to ensure adaption to often-changing environmental conditions. One prevalent mechanism that bacteria such as streptomycetes use to couple environmental stimuli to adaptive responses consists of a sensor kinase (SK) and a cognate response regulator (RR), which act as a two-component signal transduction system (TCS) (Fig. 1) (Stock *et al.*, 2000; Whitworth, 2012). Upon stimulation of the sensory domain of the SK by an external signal, the SK autophosphorylates itself prior to the transfer of the phosphate to a conserved His residue in the RR (Stock *et al.*, 2000). Typically, the activity of the RR is mediated through DNA binding, although RNA and protein binding activities as well as catalytic activities have also been reported (Stock *et al.*, 2000; Whitworth, 2012).

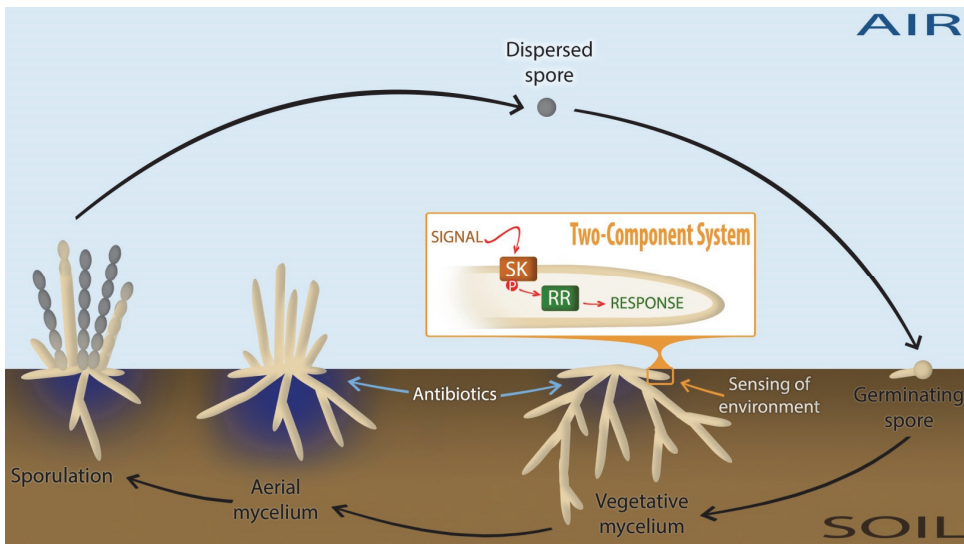


FIGURE 1. Life cycle of *Streptomyces* and environmental sensing of nutrients.

The *Streptomyces*' life cycle begins when, under favourable conditions, a dispersed spore begins to germinate. This leads to the production of branched network of vegetative hyphae. Under environmentally adverse conditions, such as nutrient depletion, streptomycetes initiate a complex developmental program whereby the vegetative mycelium serves as a substrate for a new so-called aerial mycelium. This stage of development usually corresponds with the production of secondary metabolites, such as antibiotics (as highlighted). Eventually the outer part of the aerial hyphae develops into chains of spores and which will be dispersed, so as to escape the unfavourable conditions, until the cycle begins again.

Numerous regulatory networks exist in order to accurately sense and respond to the changing environmental conditions. Two-component systems (TCS) couple the environmental stimulus (signal) of a sensor kinase (SK) to an adaptive response through phosphorylation of a cognate response regulator (RR) which exerts a regulatory response (usually through DNA binding), as illustrated in the orange box.

Soil-borne bacteria, such as streptomycetes, have developed intricate sensory systems to detect nutrient availability and to initiate appropriate response mechanisms. *Streptomyces* are industrially important organisms and produce a wide range of natural products, including over 50% of all known antibiotics (Barka *et al.*, 2016; Hopwood, 2007). The bacteria have a complex mycelial lifestyle (Fig. 1) and produce a branching network of vegetative hyphae, which are compartmentalized by cross-walls, making *Streptomyces* a rare example of a multicellular prokaryote (Claessen *et al.*, 2014). Under environmentally adverse conditions, such as nutrient depletion, streptomycetes initiate a complex developmental program whereby the vegetative mycelium serves as a substrate for a new

so-called aerial mycelium. Eventually, the outer part of the aerial hyphae develops into chains of spores (Flardh and Buttner, 2009). In turn, the spores are able to survive periods of unfavorable conditions, such as anaerobiosis (for example, as a result of heavy rainfall). Though the model organism *Streptomyces coelicolor* is able to survive anaerobic conditions, anaerobic growth has not been reported for this microorganism (Van Keulen *et al.*, 2007).

The environmental conditions of a streptomycete's natural habitat are ever-changing, and the complexity of the signals that are received and of the responses that are transmitted is reflected in the large number of TCSs, with the genome of *S. coelicolor* encoding 85 sensory kinases and 79 response regulators, with 67 known sensor-regulator pairs (Hutchings *et al.*, 2004). One such pair is made up of the SK SCO0203 and the RR SCO0204. Unusually, SCO0203 has a second cognate RR in addition to SCO0204, namely, the orphan response regulator SCO3818 (Wang *et al.*, 2009). The deletion of either RR gene was shown to enhance the production of actinorhodin, the blue-pigmented antibiotic of *Streptomyces coelicolor*. Although no biochemical evidence was provided, it was previously suggested that sensory kinase SCO0203 may be a direct orthologue of DosT, an SK from a well-studied TCS from the pathogenic obligate aerobe *Mycobacterium tuberculosis* (Daigle *et al.*, 2015).

In *M. tuberculosis*, gradual oxygen depletion is sensed by two SKs (DosT and DevS [alternatively known as DosS]) and induces a regulon controlled by the response regulator DevR (alternatively known as DosR), which consists of some 50 genes, including universal stress proteins (USPs), nitroreductases (which allow anaerobic nitrate respiration), redox proteins, and heat shock proteins (Gerasimova *et al.*, 2011). It is thought that this TCS regulates the escape from the host defense system by promoting dormancy to survive anaerobic conditions, and it is likely that this nonreplicating state plays a major role in the resistance of the bacilli to antibiotics (Chao and Rubin, 2010; Martínez and Rojo, 2011). An orthologous oxygen-sensing mechanism in streptomycetes may be essential for the sensing of oxygen levels in soil; under conditions of oxygen depletion, the appropriate response needs to be activated to ensure survival. Alternatively, under nutrient availability (and sufficient oxygen), vegetative hyphae form a very dense mycelium, where oxygen is locally depleted, and this depletion might be regulated via SCO0203/SCO0204.

In this work, we suggest that the TCS pair SCO0203/SCO0204 regulates a dormancy-related response in *S. coelicolor*. Major changes are seen in the global transcription patterns of genes related to stress and development in SCO0204 null mutants. The predicted core regulon of SCO0204, which revolves around the region from SCO0167 to SCO0219 in the *S. coelicolor* genome, contains many dormancy regulon-related genes and is conserved between SCO0204 and the dormancy regulator, DevR, of *M. tuberculosis*. We show binding of SCO0204 upstream of *M. tuberculosis* genes that are part of the DevR regulon as well as binding to the predicted binding site in *S. coelicolor*, including direct binding to developmental genes (which lack a predicted binding site). The locus tags SCO0203 and SCO0204 were named *osdK* and *osdR*, respectively, to highlight their function in response to oxxygen availability, stress, and development.

MATERIALS AND METHODS

BACTERIAL STRAINS AND MEDIA.

The bacterial strains described in this work are listed in Table S1 in the supplemental material. *E. coli* strains JM109 and ET12567 were grown and transformed by standard procedures (Sambrook *et al.*, 1989). *S. coelicolor* A3(2) M145 was the parent for the *osdK* (GSTC1), *osdR* (GSTC2 and GSTC3), and *osdRK* (GSTC4) null mutants. *S. coelicolor* M512 (M145 $\Delta redD \Delta actII$ -ORF4 [Floriano and Bibb., 1996]) was the parent strain for the *osdR* null mutant GSTC6, and M512 and GSTC6 were the hosts for promoter probing experiments (Van Wezel *et al.*, 2000a). Preparation of protoplasts, transformations, and conjugations were performed according to routine procedures (Kieser *et al.*, 2000). R5 medium was used for regeneration of protoplasts and MS medium (Kieser *et al.*, 2000) for the selection of mutants, for the preparation of spores, and for phenotypic characterization of mutants. To obtain mycelia for transcript analysis, strains were grown on minimal medium (agar plates with mannitol [1%, wt/vol] [Kieser *et al.*, 2000]).

PREPARATION OF GENE KNOCKOUT CONSTRUCTS.

Details for all plasmids and mutants are presented in Table S1 in the supplemental material. The gene replacement strategy was as described previously (Świątek *et al.*, 2012) and used the highly unstable vector pWHM3 (Vara *et al.*, 1989), harboring around 1,500 bp of flanking region on either side of the gene targeted for deletion, and the genes of interest were replaced by the apramycin resistance cassette *aacC4* (Blondelet-Rouault *et al.*, 1997). PCRs were performed as previously described (Colson *et al.*, 2007) with the oligonucleotides listed in Table S2. Plasmids pGWS378 and pGWS376 allowed gene replacement of *osdK* and *osdR*, respectively. To create an in-frame *osdR* deletion mutant (designated GSTC3), construct pGWS377, which carries only the flanking regions, was used for homologous recombination. Construct pGWS380 was designed for the construction of an in-frame *osdRK* double mutant (called GSTC4) by combining the upstream region of *osdR* (obtained from pGWS377) and the downstream region of *osdK* (obtained from pGWS378). GSTC6 (M512 $\Delta osdR$) was created for promoter probing purposes using the same approach as for the *S. coelicolor* M145 *osdR* mutant.

PROTEIN ISOLATION, PHOSPHORYLATION OF OSDR, AND ELECTROPHORETIC MOBILITY SHIFT ASSAYS.

His₆-tagged OsdR and OsdK were overexpressed from plasmids pET0203 and pET0204 in *E. coli* BL21(DE3) (Wang *et al.*, 2009). The plasmids were a kind gift from Weihong Jiang (Shanghai Institutes for Biological Sciences, Chinese Academy of Sciences, Shanghai, China). Proteins were isolated using Ni-nitrilotriacetic acid (NTA) chromatography as described previously (Mahr *et al.*, 2000).

In vitro autophosphorylation of 30 pmol of OsdK was performed with ³²P-radiolabeled ATP as described previously (Wang *et al.*, 2009). For transphosphorylation of OsdR, 30 pmol of OsdK was autophosphorylated in 10 μ l and incubated for 20 min at 30°C. Following a chill on ice, 80 pmol of OsdR was added. *In vitro* phosphorylation of OsdR for electrophoretic mobility shift assays (EMSAs) was achieved using the phosphor donor acetyl phosphate (AcP) as described previously (Chauhan and Tyagi, 2008). EMSAs with ³²P-radiolabeled probes were performed as previously described (Rigali *et al.*, 2006).

The OsdR binding site was predicted and used to scan the *S. coelicolor* genome by PREDetector (Hiard *et al.*, 2007). This binding sequence was investigated by binding assay experiments with wild-type and mutated 50-mers of the predicted binding site upstream of

SCO0200. The most-conserved nucleotides in the predicted binding sites (Table 1 and Fig. 2B) were identified, and single (50a, 50b), double (50ab), and quintuple (50x) substitutions were introduced (for 50-mer oligomers, see Table S2 in the supplemental material).

PROMOTER PROBING.

Promoter probing experiments were performed using the *redD* system as described previously (Van Wezel *et al.*, 2000a). The nonpigmented mutant *S. coelicolor* M512 lacks the pathway-specific activator genes *actII-ORF4* and *redD* (Floriano and Bibb., 1996). When *redD* is transcribed from a promoter element cloned into the promoter-probe vector pIJ2587 (Van Wezel *et al.*, 2000a), the RED biosynthetic pathway is activated, which can be monitored as a nondiffusible red pigment. Constructs for the *redD* promoter-probe system were created for the promoters of SCO0200, *osdR*, and SCO0207, using the *whiG* promoter as the control (Table S1). The promoter fragments were amplified by PCR, and EcoRI/BamHI-digested fragments were cloned into pIJ2587, resulting in the constructs pGWS345, pGWS1058, pGWS1059, pGWS1060 (for probing of *whiG*), SCO0200, *osdR*, and SCO0207.

TRANSCRIPT ANALYSIS.

RNA was isolated from *S. coelicolor* M145 (wild-type strain) and its *osdR* mutant GSTC2 by harvesting biomass from cellophane disks on MM with 1% mannitol after 24, 30, 36, 42, and 54 h of growth. Total RNA was isolated as described previously (Rigali *et al.*, 2006).

MICROARRAY ANALYSIS.

The quality and integrity of the RNA was tested with the Agilent 2100 Bioanalyzer (Agilent Technologies). The RNA was reverse transcribed into cDNA using Cy3-dCTP (<http://www.surrey.ac.uk/fhms/microarrays/Downloads/Protocols/index.htm>). Together with Cy5-dCTP-labeled *S. coelicolor* M145 genomic DNA as the common reference, the samples were hybridized onto 44,000 60-mer oligonucleotide microarray slides (Bucca *et al.*, 2009). The fluorescent signals on the slides were captured by an Agilent microarray scanner with Feature Extraction software (Agilent Technologies). Within-array normalization (global median) followed by cross-array normalization was performed in R (<http://www.r-project.org>) using Limma (version 2.5.0) (Gentleman *et al.*, 2004; Smyth and Speed, 2003). Rank product analysis by means of the R packages RankProd (Hong *et al.*, 2006) and RankProdIt (Laing and Smith, 2010) was applied to identify significantly differentially expressed genes (for which the probability of false prediction [PFP] value was <0.01) between the wild type and mutant at each time point.

RT-qPCR ANALYSIS.

For RT-qPCR analysis, cDNA was generated using the iScript Advanced cDNA synthesis kit (Bio-Rad Laboratories). RT-qPCRs were performed on 200 ng RNA with the iTaq universal SYBR green supermix (Bio-Rad Laboratories), using *rpsI* (SCO4735) as an internal control. Each reaction mixture was tested in triplicate and for normalization between different plates, with the 24 h wild-type sample as the reference. An average of all three measurements was used to calculate normalized expression.

MICROSCOPY.

Cryo-scanning electron microscopy was performed as described previously (Colson *et al.*, 2008) with a JEOL JSM6700F microscope. Stereomicroscopy was done using a Zeiss Lumar.V12 stereomicroscope. Confocal laser-scanning microscopy was performed

with a Leica TCS-SP2 microscope and Leica confocal software. Staining of dead and viable *Streptomyces* filaments and spores was performed as described previously (Tenconi *et al.*, 2012) using the cell-impermeable nucleic acid stain propidium iodide (for dead cells) and the green fluorescent nucleic acid stain SYTO 9 (for live cells). Samples were examined at wavelengths of 488 and 568 nm for excitation and 530 nm (green) and 630 nm (red) for emission.

BIOINFORMATICS ANALYSIS.

Motif searching was performed with InterProScan (Zdobnov and Apweiler, 2001) and Pfam 24.0 (Finn *et al.*, 2008). Protein homology searches were performed using BLASTp (Altschul *et al.*, 2005). The comparative analysis of the upstream regions of OsdR orthologues was performed with MEME (Bailey *et al.*, 2009), using orthologues from *S. coelicolor*, *S. clavuligerus*, *S. scabies*, *S. ghanaensis*, *S. bingchengensis*, *S. cattleya*, *S. sviveus*, *S. viridochromogenes*, *S. griseoaurentiacus*, *Streptococcus* sp. E14, *Streptococcus* sp. TRS4, and *S. hygrosopicus*. The *S. coelicolor* genome was scanned for possible similar *cis*-acting regulatory elements using PREDetector (Hiard *et al.*, 2007). The consensus sequence for the predicted binding site of OsdR was visualized using WebLogo (Crooks *et al.*, 2004). The *M. tuberculosis* DevR binding site logo was created based on the primary DevR binding sites identified in reference Chauhan *et al.*, 2011.

ACCESSION NUMBERS.

The microarray expression data have been deposited in ArrayExpress (with the accession number E-MTAB-4597). The GenBank nucleotide sequence accession number of *M. tuberculosis* DosT is P9WVGK0, and that of DevS it is NP_217648.

RESULTS

ANALYSIS OF THE TWO-COMPONENT REGULATORY SYSTEM OSDKR.

SCO0203 (OsdK) and SCO0204 (OsdR) form a two-component regulatory system (Wang *et al.*, 2009) and are encoded by the *osdR-osdK* operon. OsdK has 41% and 42% amino acid identity (57% amino acid similarity) with DevS and DosT, respectively (see Fig. S1 in the supplemental material), and it was postulated as a possible ortholog of the dormancy sensory kinases of *M. tuberculosis* (Selvaraj *et al.*, 2012). Indeed, of the 18 amino acid residues required for oxygen sensing (Cho *et al.*, 2009; Podust *et al.*, 2008), 15/18 residues of DosT and 12/18 residues of DevS are conserved in OsdK (Fig. S1). The interaction between the RR DevR and its target site is known in structural detail (Wisedchaisri *et al.*, 2005). OsdR and DevR share 61% amino acid identity (79% amino acid similarity) (Fig. S1 and S2), and comparison of the residues in the DevR and OsdR proteins revealed that 11 of the 13 residues implicated in DNA binding are conserved between DevR and OsdR (Fig. S2).

To test whether *S. coelicolor* OsdR could bind to the recognition site of *M. tuberculosis* DevR, electrophoretic mobility shift assays (EMSAs) were performed. His₆-tagged OsdK and OsdR were purified, and the sensory kinase OsdK was autophosphorylated using ³²P-radiolabeled ATP and then used to transphosphorylate OsdR (Fig. S3). OsdR transphosphorylation could be achieved with autophosphorylated OsdK. However, OsdR readily lost its phosphosignal in the presence of OsdK, as previously observed for DevRS/DosT. Therefore, acetyl phosphate (AcP) was used as phosphor donor (Chauhan and Tyagi, 2008). As probes for EMSAs we used three mycobacterial promoters that are known targets of DevR (Chauhan and Tyagi, 2008), namely, the promoters for *devR*, Rv3134c (which is located upstream of *devR* and encodes a universal stress domain protein), and *hspX*, which encodes a latency-related heat shock protein. As negative controls, DNA fragments of the upstream region of *dasR* of *S. coelicolor* and AT-rich DNA from *Escherichia coli* were used. OsdR bound with low affinity to the DNA fragment encompassing the *dasR* promoter region, while no binding was seen when AT-rich *E. coli* control DNA was used (Fig. 2A). Interestingly, OsdR bound well to all probes for the mycobacterial target genes (Fig. 2A). Furthermore, similar differential affinities for the three fragments were observed as described previously for DevR in *M. tuberculosis* (Chauhan and Tyagi, 2008), with stronger binding upstream of Rv3134c and *hspX* than to the autoregulatory site of *devR*. Nonphosphorylated OsdR bound significantly less efficiently to the probes. Taken together, these data strongly suggest that OsdR and the dormancy regulator DevR recognize the same upstream regulatory elements, with phosphorylation by OsdK required to enhance DNA binding.

IN SILICO PREDICTION OF THE OSDR REGULON OF *S. COELICOLOR*.

The OsdR consensus sequence was deduced by searching the upstream regions of *osdR* orthologues from 12 *Streptomyces* species for possible similar *cis*-acting regulatory elements using MEME (Bailey *et al.*, 2009). This identified a 16-nucleotide palindromic consensus sequence, 5'-AGGGCCGATCGGCCCT, which conforms well to the consensus sequence found in *M. tuberculosis* (Fig. 2B). The *S. coelicolor* genome was then scanned by PREDetector (Hiard *et al.*, 2007), using a position weight matrix (see Table S3 in the supplemental material) based on 12 predicted upstream elements as inputs. With a cutoff score of 8.0 for medium reliability (Rigali *et al.*, 2015), PREDetector identified putative binding sites for OsdR upstream of 27 transcription units. There was a total of 43 binding sites that may affect the transcription of 85 genes, which therefore may qualify as the direct OsdR response regulon (Table 1).

TABLE 1. Predicted binding sites for SCO0204 (OsdR) in *Streptomyces coelicolor*.

Locus tag ^a	Function	Sequence	Position ^b	Score ^c	Cotranscribed gene(s) ^d	Function(s)
SCO0204c	OsdR, two-component response regulator	AGGGCCGGTCCGGCCCC	-81	13.74		
SCO0200c	Universal stress protein	GGGGCCGACCGTCCT	-100	12.49	SCO0199c/ SCO0198c	Zinc-deprived alcohol dehydrogenase, universal stress protein
SCO0215c	Nitroreductase family protein	AGGGCCGTCCGGCCCC	-99	12.24		
SCO0208	Pyruvate phosphate dikinase	CGGGCCGACCGGCCCT	-102	12.19		
			-158			
			-144	10.08		
SCO0207c	Universal stress protein		-88			
SCO5979	Enoyl-CoA hydratase	CGGGACCTTCGGCCCT	-80	11.62	SCO5980	Bifunctional hydroxylase, oxidoreductase
SCO5978c	Hypothetical protein		-68			
SCO2637	Secreted serine protease	AGGGCCGGTCCGGCCT	-53	11.27		
SCO7188c	Subtilisin-like secreted peptidase	GGGGACGATCGTCCCC	-47	11.2		
SCO0039	Hypothetical protein	AGGGCCGTTCGGCCCT	-132	10.86	SCO0040/ SCO0041/ SCO0042	Glycosyl transferase, integral membrane protein, hypothetical protein
SCO0038c	Sigma factor		-130		SCO0037c/ SCO0036c	Sigma factor, hypothetical protein
SCO0168	Crp-like regulatory protein	GAGGCCGGTCCGGCCCT	-284	10.75		
		GGGGCCGACCGTCCT	-36	9.21		
SCO0167c	Universal stress protein	AGGGACCTTCGGCCCC	-391	10.75		
			-114	10.73		
SCO0216	Nitrate reductase alpha chain NarG2	AGGGACCTTCGGCCCC	-53	10.73	SCO0217/ SCO0218/ SCO0219	Nitrate reductase beta chain NarH2, nitrate reductase delta chain NarJ2, nitrate reductase delta chain NarI2
SCO5410	Hypothetical protein	AGGGCAGGACGGCCCT	+36	10.6		
SCO6041	Protoporphyrinogen oxidase	GGGGCCGTCCGGCCCC	-51	10.57	SCO6042	Chlorite dismutase (oxygen-generating enzyme)
SCO6040c	Lipoprotein		-246		SCO6039c	Flavoprotein oxidoreductase, CoA disulfide reductase
SCO3431	EmrB/QacA subfamily transporter	GGGGCCGAACGGCCGT	+13	10.52		
SCO6164	Hypothetical protein with DksA/TraR family C4 zinc finger domain	GGGTCCGATCGGCCCG	-62	10.5		
SCO6163c	Sensor kinase		-334		SCO6162c	Two-component system response regulator
SCO0517	Possible Crp-like regulatory protein	GGGACCGACCGGCCCT	-248	10.49		
		AGGGCCGGCCGGCCCG	-268	10.46		
SCO3857	Nosiheptide resistance regulator	GGGGCCGTTCGGGGCT	-271	10.34		
SCO3856c	Peptidyl-prolyl <i>cis-trans</i> isomerase		-66			
SCO5251	Puromycin <i>N</i> -acetyltransferase	AGGGCCGTACGGCACC	-243	10.31		
SCO2347	Integral membrane protein	AGGGCCGAAAGTCCCG	-295	10.3		
SCO2348	Secreted protein		-221			
SCO0214	Pyridoxamine 5'-phosphate oxidase	GGGGCCATCCGGCCCT	-50	10.18		
SCO0213c	Nitrate-nitrite transporter protein		-252		SCO0212c	Hemerythrin cation binding domain-containing protein (oxygen transporting protein)
SCO0179c	Zinc-containing dehydrogenase	TGGGCCGGTCCGGCCCC	-152	9.46		
SCO7021	Secreted protein	AGGGCCGAACGGCCCA	-94	9.4	SCO7022	Hypothetical protein SC1H10.11.
SCO4412	Regulatory protein	AGGGCCGAACGGCCGT	-261	9.34		
SCO0355	Conserved hypothetical protein	AGGGGTGACCGGCCCG	-81	9.2	SCO0356	Probable oxidoreductase

^a SCO numbers in boldface were tested by EMSA.

^b Position relative to the start of the gene.

^c The cutoff score calculated using the PREDetector algorithm and based on the position weight matrix in Table S3 in the supplemental material.

^d Genes known or predicted to be cotranscribed with the gene and therefore likely influenced by the regulatory element.

Eight binding sites were identified upstream of genes/operons in the vicinity of *osdR*, including *osdR* itself, controlling 20 of the 22 genes in the region between SCO0198 and SCO0219 (Fig. 2C). Comparison with the genomic region around *M. tuberculosis devR* revealed significant gene synteny (Fig. 2C). Of the 11 *S. coelicolor* genes for USP domain proteins, 8 are found in the genomic region between SCO0167 and SCO0021, and in *M. tuberculosis*, *usp* genes are part of the DevR regulon. SCO0213 to SCO0219 encode a nitrate transporter and nitrate reductase, which also prominently feature in the DevR regulon. When a lower cutoff score of 6.0 was used, PREDetector predicted a possible 27 elements in the regions SCO0167 to SCO0181 and SCO0198 to SCO0219.

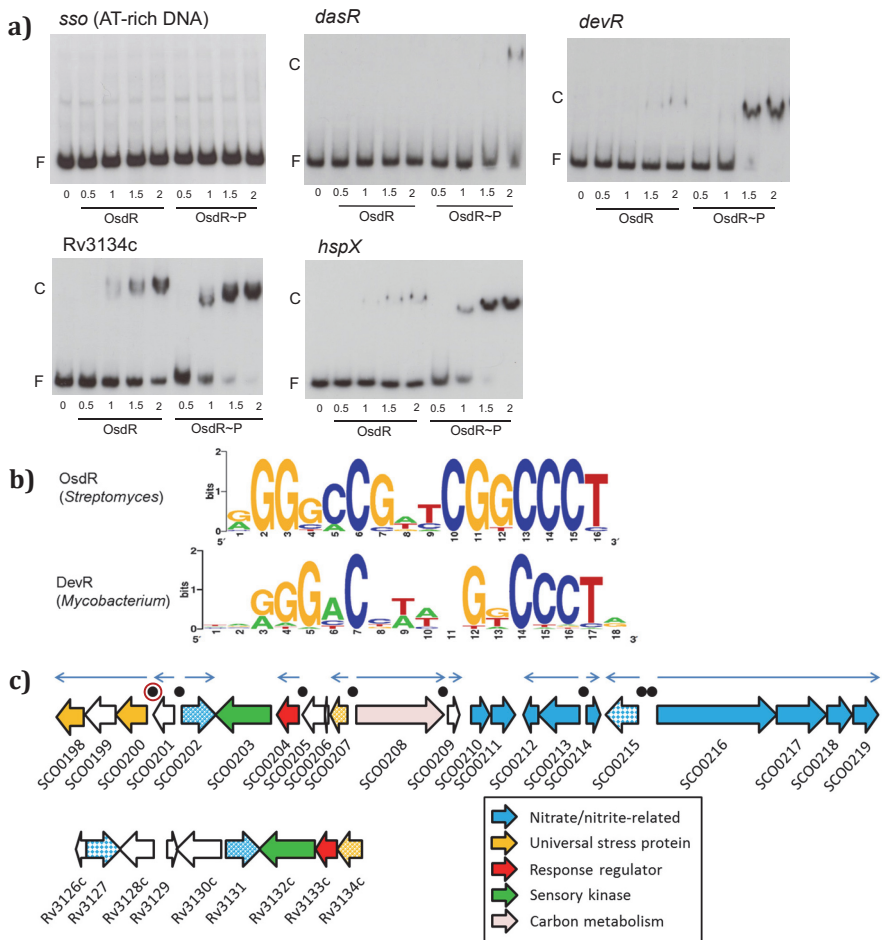


FIGURE 2. Determination of the binding site of OsdR (SCO0204) and comparison to DevR.

- EMSAs with purified His6-tagged OsdR on known targets of *devR* in *M. tuberculosis*. Both phosphorylated (OsdR~P) and non-phosphorylated (OsdR) were used in the assays. OsdR~P was obtained after AcP-phosphorylation *in vitro*. Numbers on the horizontal axis refer to concentrations in μM. F: free DNA fragment; C: complexes of DNA and protein.
- Sequence Logo representation of a cis-regulatory element identified upstream of *osdR*. As input for MEME the upstream region of *osdR* orthologues of *S. coelicolor*, *S. scabiei*, *S. griseoaurantiacus*, *Streptomyces species e14* and *S. clavuligerus* were used. For comparison, the upstream regulatory element recognized by DevR (Crooks *et al.*, 2004) is presented.
- Gene synteny between the loci around *osdR* in *S. coelicolor* (top) and *devR* in *M. tuberculosis* (bottom). Functional categories are given in the figure and black dots indicate predicted OsdR binding sites, with that of *upsA* (SCO0200) highlighted with a red ring. Orthologues are presented in the same colors and when multiple genes with similar function are present, then in patterns.

SPECIFICITY ANALYSIS OF OSDR BINDING TO THE PREDICTED REGULATORY ELEMENT OF *USPA*.

To investigate whether OsdR binds specifically to the predicted nucleotide sequence, a 50-mer probe of the upstream region of *uspA* (SCO0200), centered on the predicted binding site, was used as a probe (see Table S2 in the supplemental material). Indeed, AcP-phosphorylated OsdR (OsdR~P) bound well to the DNA fragment (Fig. 3A). Some retarded DNA remained in the wells of the gel, likely due to bridging, whereas each of the monomers of the OsdR dimer bound to a different probe rather than to the same site, which can result in long concatemers, as was observed for, e.g., NagR in *Bacillus subtilis* (Fillenberg *et al.*, 2015) and DasR in *S. coelicolor* (Tenconi *et al.*, 2015).

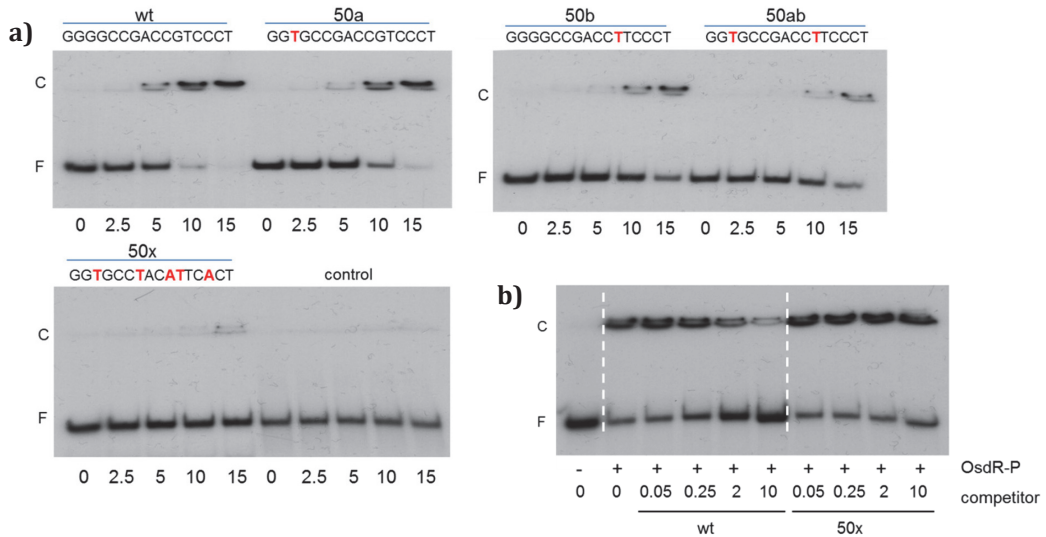


FIGURE 3. EMSAs with OsdR on a predicted *S. coelicolor* binding site.

- a) Analysis of the OsdR binding site by mutation of highly conserved nucleotides in the *uspA* (SCO0200) binding site. 20 fmol of 50mer DNA was incubated with increasing concentrations of OsdR-P (in μM). Substitutions to the *uspA* binding site are indicated in red in the sequences; 50mer *dasR* fragment was used as control.
- b) Competition assays using 10 μM of protein and 20 fmol of labeled 50mers centered on the *uspA* binding site. Increasing concentrations of unlabeled competitor 50mer is added, either wild type *uspA* 50mer or mutated *uspA* 50mer with 5 substituted highly conserved nucleotides (50x). -/+ refer to the presence of phosphorylated OsdR. Competitor DNA in μM. F: free DNA fragment; C: complexes of DNA and protein.

We then designed four mutant 50-mer probes containing single mutations (designated 50a and 50b), a double mutation (50ab), or a quintuple mutation (50x) of the most conserved nucleotides of the binding site. In line with the predicted importance of the conserved nucleotide positions in the consensus sequence (Fig. 2B), nucleotide permutations significantly decreased the binding of OsdR to the probes, such that the single G→T substitution at position 3 (50a) and the G→T substitution at position 11 (50b) lowered binding efficiency by around 50%, which was further reduced by mutating both positions (Fig. 3A). Binding was abolished when five of the conserved nucleotides were mutated (50x). We also performed a competition assay with unlabeled DNA on the radiolabeled wild-type 50-mer *uspA* probe. Increasing the amount of the unlabeled wild-type *uspA* probe strongly inhibited binding by OsdR, while addition of unlabeled competitor DNA with 5 permutations in the binding site (50x) had no effect on OsdR binding (Fig. 3B). Taken together, these experiments provide conclusive evidence that OsdR specifically recognizes the predicted regulatory element.

VERIFICATION OF THE REGULON PREDICTIONS BY EMSAS.

Next we tested DNA binding by OsdR to predicted targets using EMSAs of PCR-amplified DNA probes (Table S2). These were *uspA*, *osdR*, SCO2637 (for a serine protease), and SCO2967 (for a carboxypeptidase), and the intergenic regions between the divergent genes SCO0207 and SCO0208 (for another USP domain protein and pyruvate phosphate dikinase), SCO5978 and SCO5979 (for a hypothetical protein and an enoyl coenzyme A [enoyl-CoA] hydratase), and SCO6040 and SCO6041 (for a lipoprotein and a protoporphyrinogen oxidase). All the predicted binding sites were bound by OsdR, with most probes fully bound by OsdR~P (at 1 μM), except SCO2637, which was bound with 2-fold-lower affinity (Fig. 4A). This suggests that phosphorylation (by OsdK) leads to enhanced binding of OsdR

to its binding sites. The combined predictions and EMSA data reveal some 50 likely OsdR target genes or gene clusters, of which at least 13 have orthologues that are controlled by DevR in *M. tuberculosis* (*osdR*, SCO0167, SCO0198, *uspA* [SCO0200], and SCO0207 and genes for nitrate reductase subunits).

TRANSCRIPTIONAL ANALYSIS OF OSDR TARGETS.

To analyze the transcriptional control by OsdR, promoter probing was performed using the Red promoter probing system (see Materials and Methods) in the nonpigmented *S. coelicolor* strain M512 and the M512 *osdR* mutant derivative GSTC6. Promoter-probe vectors harboring the upstream regions of *uspA* (SCO0200), *osdR*, and SCO0207 were introduced into *S. coelicolor* M512 and the mutant GSTC6, and the promoter activity was analyzed, with as a control the empty vector or the vector with the *whiG* promoter, which is transcribed constitutively (the developmental control of the gene product σ^{WhiG} is governed primarily at the posttranslational level). While the empty vector did not show activity and *whiG* transcription was not affected by the deletion of *osdR*, P_{SCO0200}, P_{SCO0204} and P_{SCO0207} were all active in M512 but poorly or not expressed in the mutant (Fig. 5), strongly suggesting that the genes are transcriptionally activated by OsdR.

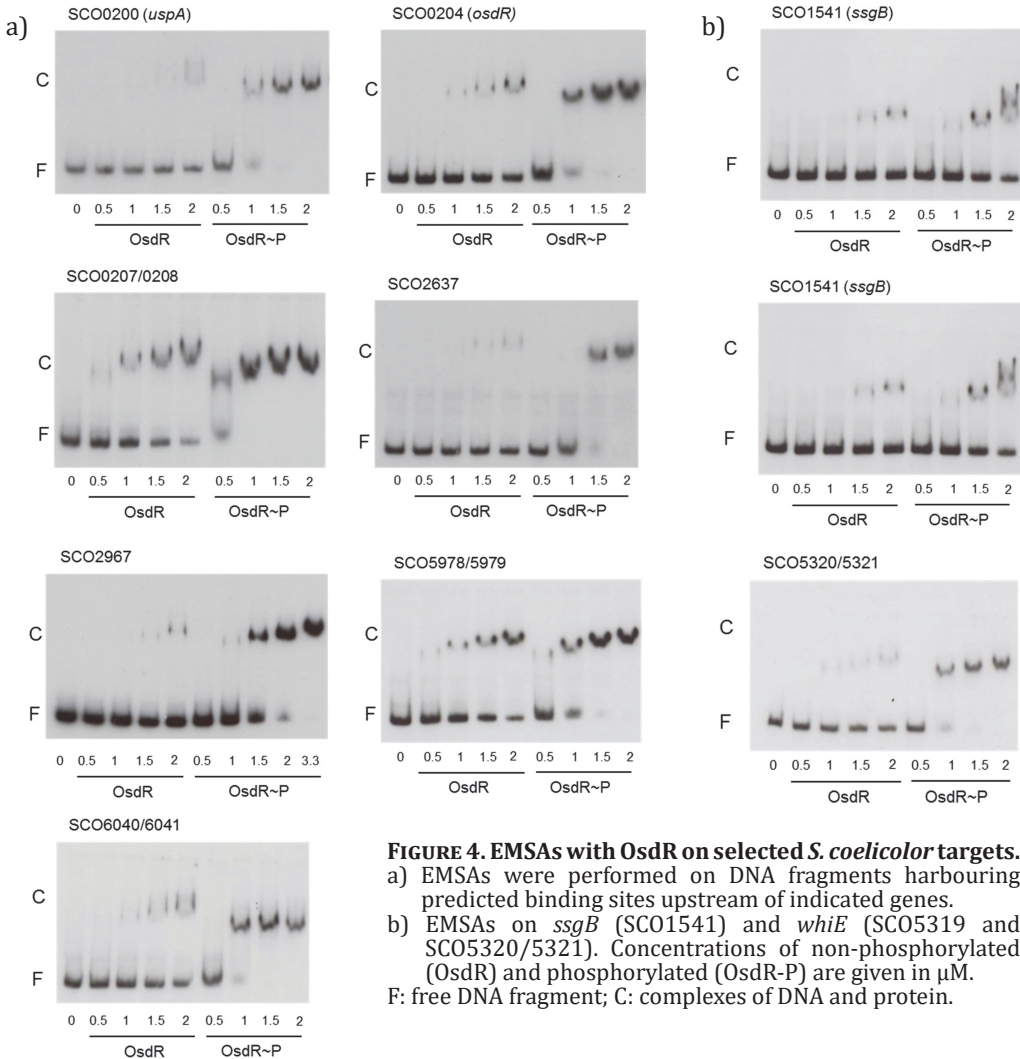


FIGURE 4. EMSAs with OsdR on selected *S. coelicolor* targets.
 a) EMSAs were performed on DNA fragments harbouring predicted binding sites upstream of indicated genes.
 b) EMSAs on *ssgB* (SCO1541) and *whiE* (SCO5319 and SCO5320/5321). Concentrations of non-phosphorylated (OsdR) and phosphorylated (OsdR-P) are given in μ M. F: free DNA fragment; C: complexes of DNA and protein.

GLOBAL TRANSCRIPTION PROFILING OF THE *OSDR* NULL MUTANT BY DNA MICROARRAY ANALYSIS.

Phenotypic analysis of the M145 *osdR* null mutants GSTC2 and GSTC3 as well as M145 Δ *osdK* (GSTC1) and M145 Δ *osdRK* (GSTC4) on MS medium indicated earlier formation of mycelial hyphae in the *osdR* mutants and accelerated sporulation and enhanced production of the grey spore pigment (Fig. 6A). In the absence of both OsdR and OsdK, this phenotype was not observed. High-resolution imaging by cryo-scanning electron microscopy revealed that the spores had a normal morphology (Fig. 6B). Observation of the spores with laser confocal microscopy indicated a strong delay in the germination of spores of the *osdR* null mutant compared to that of spores of the parental strain (Fig. 6C). Staining of dead and viable spores showed that this delay in germination in the GSTC2 mutant was not due to extensive accumulation of dead spores, as the proportions of viable/dying spores were comparable between *S. coelicolor* M145 and its *osdR* mutant derivative GSTC2.

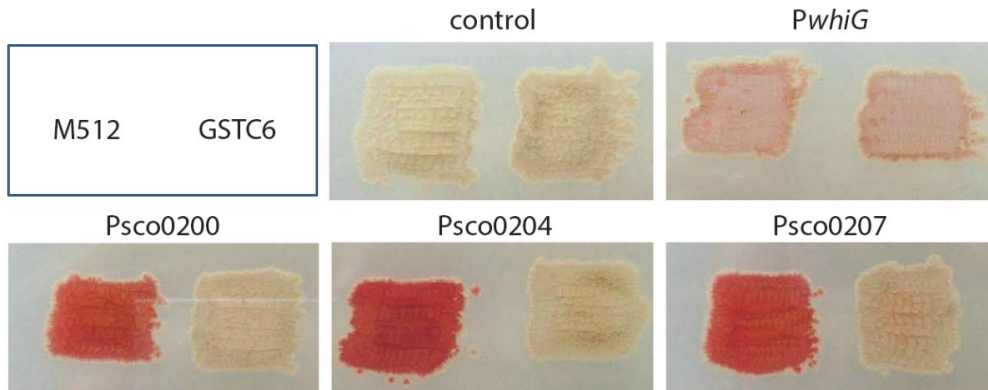


FIGURE 5. *In vivo* transcriptional analysis of OsdR targets.

Promoter probing assays for the analysis of transcription of the promoters of *uspA* (SCO0200), *osdR* (SCO0204) and SCO0207 in the M512 *osdR* null mutant (GSTC6). As controls empty vector pIJ2587 and the *whiG* promoter were used.

To obtain a global overview of the effect of the deletion of *osdR* on transcription, microarray analysis was performed using RNA extracted from *S. coelicolor* M145 and its *osdR* null mutant GSTC2 grown on minimal medium (MM) agar plates overlaid with cellophane discs. Biomass was harvested at time points corresponding to vegetative growth (24 h), the onset of aerial growth (30 h), aerial growth (36 h), early sporulation (42 h), and sporulation (54 h) in the parental *S. coelicolor* M145. RNA from two independent biological replicate experiments was subsequently used as a template for cDNA synthesis/Cy3-dCTP labeling and subsequently hybridized onto oligonucleotide-based *S. coelicolor* whole-genome DNA microarrays (see Materials and Methods). By rank product analysis, a list of genes whose levels of expression were statistically significantly different was obtained at a percentage of false positives (PFP) of <0.01. With the additional cutoff of a minimum 2-fold change in the levels of transcription between the wild type and mutant, a list of over 800 genes whose transcription was significantly altered in the *osdR* null mutant was obtained (see Table S4 in the supplemental material). Classes of genes that were overrepresented were related to stress, anaerobic growth, and development. Notably, and as detailed further below, many of the genes that were differentially expressed between the wild type and *osdR* mutant had particularly strongly altered mRNA levels at 36 h. Suggestively, transcription of OsdR itself peaks at 36 h in wild-type cells, as shown in the present study and as established previously (see, e.g., reference Świątek et al., 2013).

STRESS-RELATED GENES AND THE CHROMOSOMAL REGION AROUND *OSDRK*.

The majority of the genes encoding universal stress proteins are located in the vicinity of *osdK* and *osdR*, and several are predicted or proven members of the direct OsdR regulon (see above). Of these, SCO0167, SCO0172, SCO0181, and SCO0200 (*uspA*) were all downregulated at one or more time points in the mutant (Fig. 7A). The same was observed for the genes for the nitrate reductase system Nar2 (SCO0216 to SCO0219) at 36 h (Fig. 7C). *S. coelicolor* has three different nitrate reductases (Nar1 to -3) for anaerobic respiration, each active at different stages of development (Fischer et al., 2010; Fischer et al., 2014). Genes for the two other nitrate reductase systems were not affected (see Table S4 in the supplemental material).

Deletion of *osdR* had a major effect on the transcription of many of the genes that were previously shown to be involved in stress management (Facey et al., 2011; Kim et al., 2015; Pagels et al., 2010; Bueno et al., 2012; Shin et al., 2011), such as the response to redox and (thiol) oxidative, osmotic, and temperature stress (Fig. 7B; see also Table S4 in the supplemental material). The σ factor gene *sigL*, which is involved in osmoprotection and oxidative stress (Lee et al., 2005), was upregulated, as was *catB*, but most of the stress-related genes were significantly downregulated. This included genes that in *B. subtilis* are part of the oxidative-stress response regulon (Zuber, 2009), namely, *kataA*, *trxA*, *trxB*, *msrA*, a *catR/perR*-like gene, and the genes for the oxidative-stress-related σ factor/anti- σ factor pair SigR/RsrA (Jung et al., 2011; Kang et al., 1999; Kim et al., 2012), as well as genes involved in protein degradation and folding, such as *clpP1* to *clpP2* (SCO2618 to SCO2619), *dnaK*, *hspR*, *groEL1*, *groEL2*, *groES*, genes encoding the proteasome (SCO1643 to SCO1644), and several cold shock genes. Zinc-related genes like those of the gene cluster for the zincophore coelibactin, were downregulated at all time points except 36 h, at which time levels of transcription were comparable between wild-type and *osdR* mutant cells (Fig. S4). Sufficient zinc is necessary for processes related to protein folding, redox balance, and oxygen stress (Kallifidas et al., 2010; Li et al., 2003; Shin et al., 2011). Similar changes in expression were observed for genes related to sulfur, cysteine synthesis, and thiol homeostasis (Fig. S4), which are involved in the management of (thiol) oxidative, redox, or osmotic stress (Dai and Outten., 2012; Paget et al., 2001).

DEVELOPMENTAL CONTROL.

Major changes were observed in the global transcription profile of developmental genes, with a very distinctive pattern of upregulation of many sporulation genes in the absence of *osdR* at most time points, while early-developmental (*bld*) genes were downregulated at the same time points (Fig. 7D). Transcription of other genes, namely, *ssgB*, *ssgG*, *smeA-ssfA*, *chpADFG*, *rdlAB*, and *sapB*, all followed the same pattern, with a sharp peak at the onset of sporulation in wild-type cells and, instead, a steady increase in the mutant (see Table S5 in the supplemental material). SsgB and SsgG are members of the actinomycete-specific family of SsgA-like proteins (SALPs) (Jakimowicz and van Wezel., 2012) and determine the positions of septum sites during sporulation-specific cell division (Keijser et al., 2003; Willemse et al., 2011). SmeA and SsfA are also involved in the control of septation as well as DNA segregation (Ausmees et al., 2007), and the *rdl* and *chp* genes encode the rodlin and chaplin proteins, respectively, which form amyloid-like structures to create a water-repellent hydrophobic sheath around aerial hyphae and spores (Claessen et al., 2003; Claessen et al., 2002; Elliot et al., 2003). SapB is a lanthipeptide that acts as a signaling molecule for the onset of development (Kodani et al., 2004; Willey et al., 1991). The same transcriptional upregulation was observed for the *whiE* gene cluster for the spore

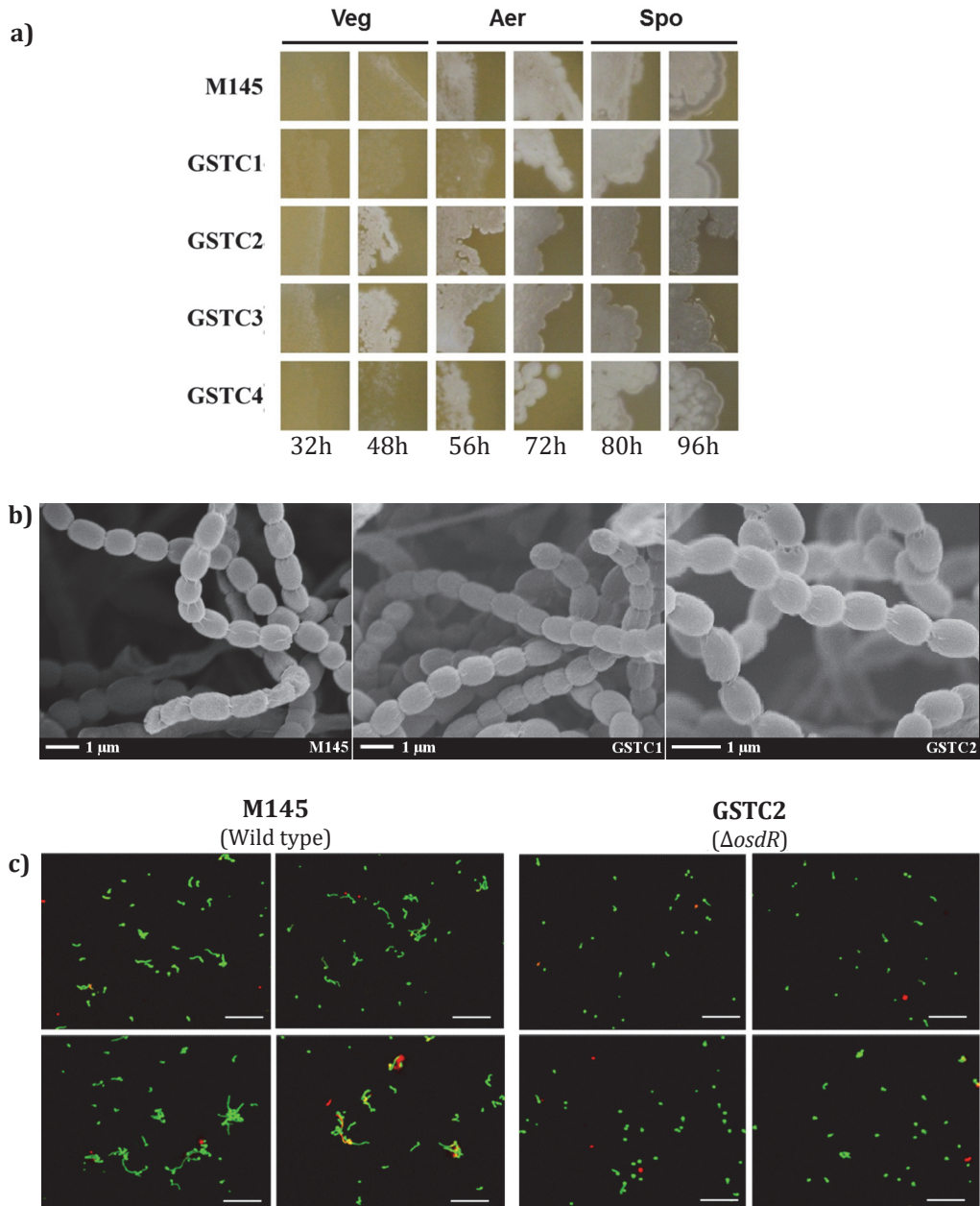


FIGURE 6. Phenotypic analysis of M145 *OsdK* and *OsdR* null mutants.

a) The different *osdK* and *osdR* mutants and their parent *S. coelicolor* A3(2) M145 were grown on MS agar plates and monitored in time (hours given below). Veg, vegetative growth; Aer, aerial growth; Spo, sporulation.

b) Phenotypic characterization of the *osdK* and *osdR* mutants and their parent *S. coelicolor* M145 by cryo-scanning electron microscopy. Samples were prepared after 5 days of growth on MS.

c) Confocal fluorescence micrographs of germinating spores of *S. coelicolor* M145 and its *osdR* mutant GSTC2. Spores were inoculated onto MM agar and imaged after 7 h. Cells were stained with propidium iodide (PI) to identify dead cells (red) and with SYTO 9 green to identify living cells.

Strains: GSTC1, M145 $\Delta osdK$; GSTC2, M145 $\Delta osdR$; GSTC3, M145 *osdR* in-frame deletion mutant; GSTC4, M145 *osdRK* double mutant.

pigment *WhiE* (Kelemen *et al.*, 1998) and for the *whiE*-like gene cluster from SCO7449 to SCO7453, which also produces a spore pigment (Salerno *et al.*, 2013) (Fig. 7D; Table S4). The upregulation of sporulation genes correlates well to the accelerated development and enhanced pigmentation of *osdR* mutants (Fig. 6A).

Conversely, the early-developmental genes were downregulated in the *osdR* null mutant, including *bldC*, *bldG*, *bldM*, *bldN*, and *crp*, as well as *chpCEH*. The *crp* gene encodes the cAMP receptor protein that controls spore germination and early development (Piette *et al.*, 2005; Derouaux *et al.*, 2004). The reduced expression of *crp* correlates with the observed strong delay in the germination of spores of the *osdR* null mutant (Fig. 6C). *bldG* encodes a developmental anti- σ factor antagonist that controls the activity of the stress σ factor σ^H , *bldM* and *whiI* encode orphan response regulators that control complex developmental pathways (Al-Bassam *et al.*, 2014), and *bldN* encodes a σ factor that is required for the transcription of, among other genes, the *chp* and *rdl* genes (Bibb *et al.*, 2012; Bibb *et al.*, 2000). The downregulation of *chpCEH* contrasts with the upregulation of the other *chp* genes, which is the first time that such differential regulation has been observed. Interestingly, the *chpCEH* genes have been shown to belong to the early *chp* genes and are sufficient to support aerial development, while the other *chp* genes as well as *rdlAB* are produced significantly later during development (Di *et al.*, 2008). This is again consistent with the concept that OsdR represses sporulation and activates early-development processes.

DIFFERENTIAL EXPRESSION AT 36 h.

Interestingly, some 200 genes showed deregulated expression at the 36 h time point. These genes include 22 genes in the genomic region between SCO160 and SCO0220, as well as other members of the direct or indirect OsdR regulon that are involved in nitrogen metabolism and anaerobic respiration genes (e.g., *nar2*, *ureAB*, *nirB*, *glnD*, *glnII*, *glnK*, and *draK*), development (*whiE* and *whiE*-like genes, *ssgB*, *chp*, and *rdl*), stress management, etc. (see Table S5 in the supplemental material). These genes all showed a sharp rise or drop of transcription at 36 h in wild-type cells, with transcription recovering at 42 h, while such a sharp change in transcript levels was not seen in the *osdR* null mutant. The deregulated transcription of these genes in wild-type cells corresponds to a peak in *osdR* transcription at 36 h. A sharp peak in the expression of *osdR* toward the end of exponential growth in liquid cultures was observed by others, both in shake flasks (Huang *et al.*, 2001) and in a fermentor (Nieselt *et al.*, 2010). The transition from exponential to stationary phase roughly corresponds to the onset of aerial growth in surface-grown cultures. Interestingly, another peak in transcription was observed around 5 h after spore germination (Strakova *et al.*, 2013), which may correspond to OsdR's control of early events.

VERIFICATION BY RT-QPCR AND EMSAS.

To corroborate the microarray data, reverse transcription-quantitative PCR (qPCR) analysis was performed on independent RNA samples isolated from the mycelia of *S. coelicolor* M145 and its *osdR* null mutant GSTC2 grown under the same conditions as those used to prepare RNA samples for microarray analysis. The results were normalized using *rpsI* (SCO4735) as the internal standard, and RNA obtained from mycelia of M145 grown for 24 h was used to normalize the results between the different qPCR runs. Similar trends in expression profiles were observed in both sets of transcript analyses (Fig. 8; see also Fig. S5 in the supplemental material). Expectedly, no *osdR* transcripts were detected in the *osdR* null mutant. The peak in the transcription of *osdR* after 36 h in wild-type cells, both in the microarray and in the qPCR data, again suggests that *osdR* plays an important regulatory role

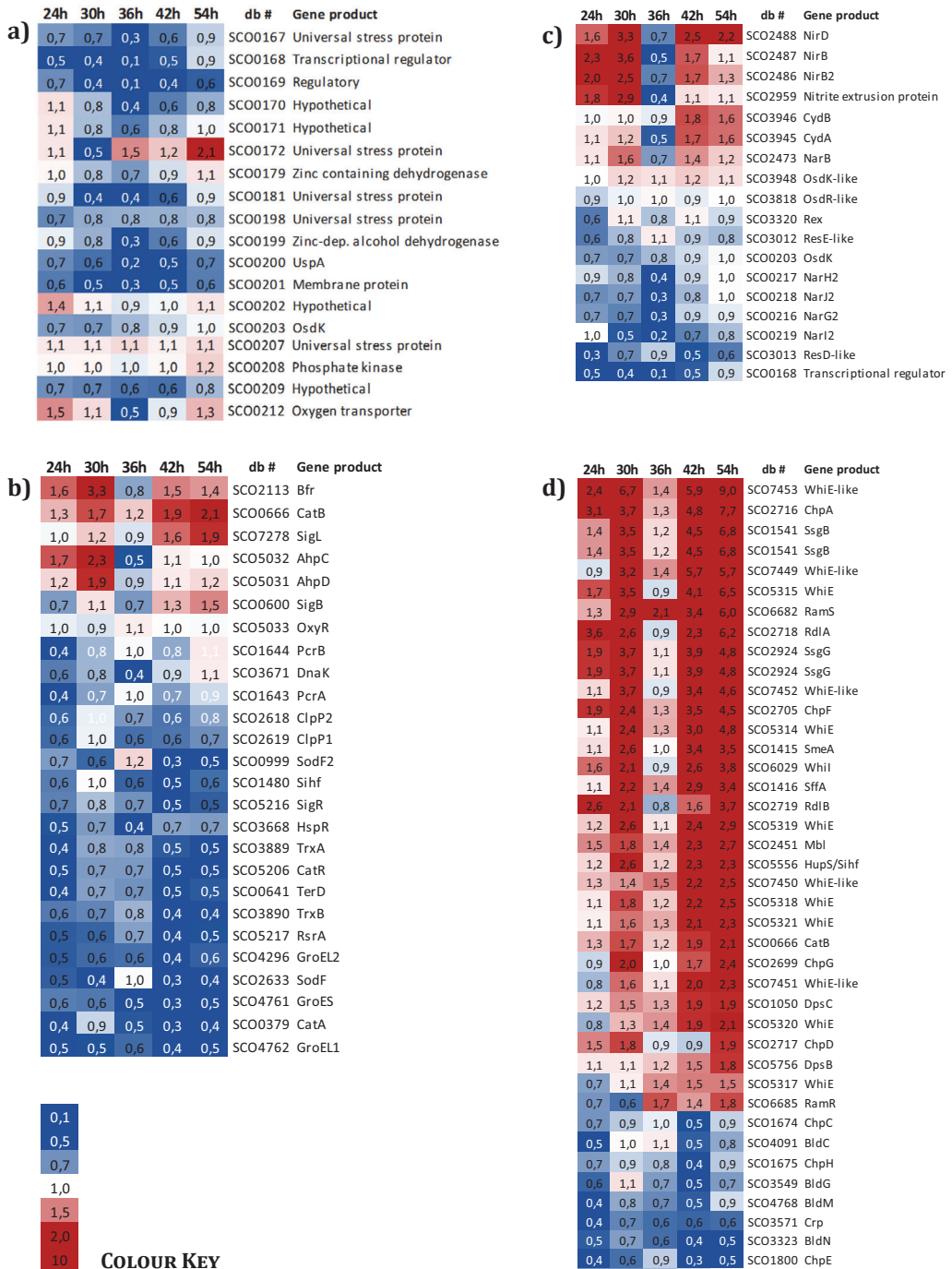


FIGURE 7. Heat maps of stress and development-related genes differentially expressed between the *osdR* mutant and its parent *S. coelicolor* M145.

Transcription patterns (expressed as fold changes *osdR* mutant/wild-type) are presented for (A) genes close to *osdRK*; (b) stress-related genes; (c) anaerobic growth-related genes; (d) developmental genes. RNA was isolated from MM agar during vegetative growth (24 h), vegetative/aerial growth (30 h), aerial growth (36 h), aerial growth/early sporulation (42 h) and sporulation (54 h). Only genes with a pfp value less than 0.010 are shown. Blue, downregulated (<0.5) and red, upregulated (>2.0) in the mutant; intermediate fold changes represented in white. See Table S4. db #, database gene number.

at this stage of the life cycle (Fig. 8). Downregulation of *upsA* (SCO0200) in the *osdR* mutant together with the binding of OsdR to the upstream regulatory element strongly suggests that *uspA* transcription is transactivated by OsdR. *sfgB* (SCO1541) transcription was higher in the mutant, which corresponds well with the accelerated development and enhanced spore pigmentation of GSTC2 (Fig. 6). The transcription of SCO5320 and SCO5321, which are part of the *whiE* gene cluster for the grey spore pigment, was increased at several time points (though *whiE* transcription also characteristically peaked at 36 h in the wild-type strain).

While no regulatory elements were predicted upstream of *sfgB* or within the *whiE* cluster, EMSAs showed specific binding by phosphorylated OsdR to *sfgB* and to the intergenic region between genes SCO5320 and SCO5321 (Fig. 4B), while the promoters of SCO5319 and SCO5316 (the latter is not shown) were only weakly bound by OsdR *in vitro*. Considering the lack of binding of nonphosphorylated OsdR to the upstream regions of SCO5316 and SCO5319 and the weak binding of OsdR~P, it is unclear whether these two genes are directly controlled by OsdR *in vivo*.

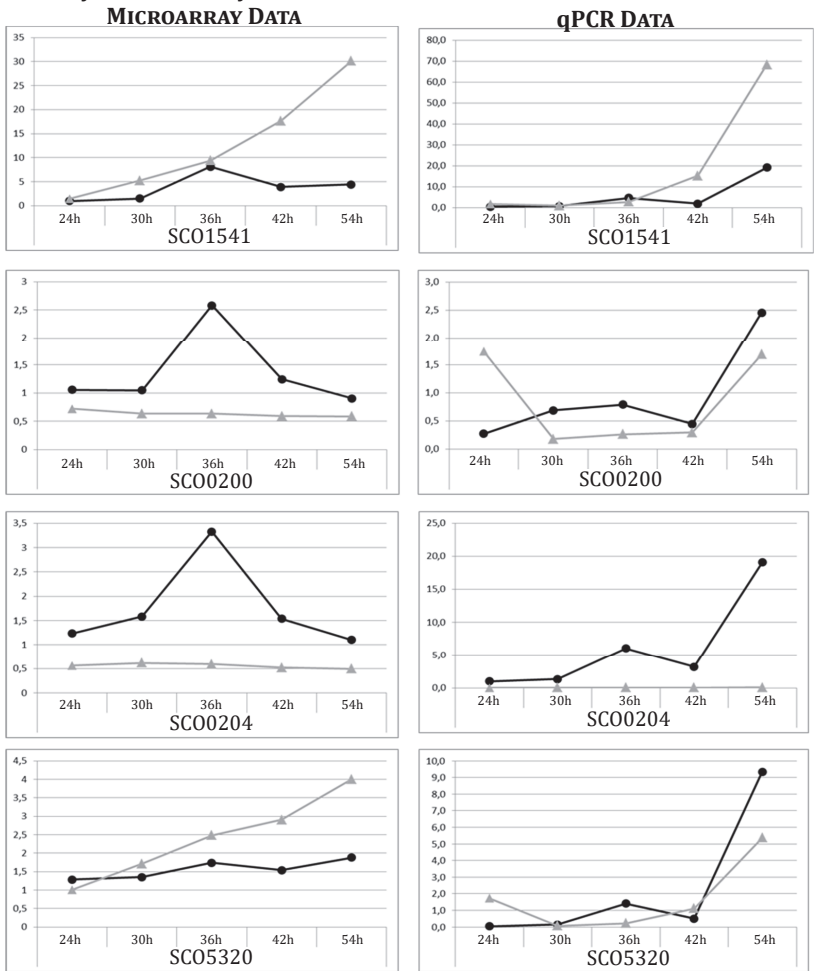


FIGURE 8. Microarray and RT-qPCR expression profiles of genes deregulated in the *osdR* mutant.

RNA for microarray analysis (left) and RT-qPCR (right) profiling was prepared from independent cultures. For time points see Figure 7. The expression profiles in wild type (black, ●) and the *osdR* mutant (grey, ▲) were compared between the microarray data (left) and RT-qPCR (right). Genes of interest tested: SCO0200 (*uspA*), SCO0204 (*osdR*), SCO1541 (*sfgB*) and SCO5320 (*whiE*). See also Fig. S4. Note that the graphs are at the same scale.

DISCUSSION

The two-component regulatory system (TCS) formed by OsdK (SCO0203) and OsdR (SCO0204) shows significant sequence similarity to the dormancy TCS in *Mycobacterium tuberculosis* (Podust *et al.*, 2008). In this work, we show not only that the OsdR binding site conforms very well to the binding site for DevR in *M. tuberculosis* but also that OsdR recognizes the regulatory elements upstream of key genes of the *M. tuberculosis* dormancy regulon and with affinities similar to those of DevR. EMSAs established OsdR binding to short, 50-bp DNA sequences containing the predicted recognition site, and the specificity was validated by the decrease in binding upon changing of one or more nucleotides of the consensus sequence. Thus, the TCS formed by OsdK and OsdR is most likely orthologous to the dormancy control system DosT/DevS/DevR in *M. tuberculosis*. This is further supported by gene synteny, as many genes for USP domain proteins are in the vicinity of the TCSs in the respective organisms. Despite hundreds of millions of years of evolution, some 15 targets are conserved between the DevR-controlled dormancy regulon of *M. tuberculosis* and the regulon predicted to be controlled by OsdR in *S. coelicolor*. Most of these lie in the region around *osdR*, namely, SCO0167, *uspA*, *osdR*, SCO0207, SCO0215, and SCO0216 to SCO0219 (*narG2-narJ2*).

The sensory kinase OsdK activates its cognate response regulator, OsdR, by phosphorylation and enhances its DNA binding capability, as shown by the enhanced binding of OsdR~P in the EMSAs. Combined, the *in silico* predictions and *in vitro* validation by EMSAs indicate that around 50 genes or gene clusters are controlled directly by OsdR. Analysis of the transcriptional changes in the *osdR* null mutant by global transcription profiling revealed the deregulation of numerous stress-related genes, including numerous stress-related genes in the region around *osdR*. A distinctive pattern of deregulation of developmental genes was evident, with upregulation of sporulation genes (including *whiE*, *whiI*, *smeA-ssfA*, *rdlAB*, *ssgBG*, *ramS*, and the late *chp* genes) and downregulation of genes involved in early development (*bldC*, *bldG*, *bldM*, *bldN*, *crp*, and the early *chp* genes), which corresponds well to the observed accelerated development of *osdR* mutants. The transcriptional data suggest that OsdR controls a hinge point in development. This is perhaps best illustrated by the divergent transcription of the *chp* genes in the *osdR* mutant. It has previously been shown that the *chpCEH* genes are expressed earlier than the other *chp* genes and also that the ChpCEH proteins are sufficient to form the characteristic chaplin layer on the outside the aerial hyphae and spores and to support aerial growth. BldN was previously shown to control all of the *chp* genes (Elliot *et al.*, 2003; Bibb *et al.*, 2012), which does not explain the difference in *chp* gene expression profiles. Our data show that in the *osdR* null mutant, transcription of *bldN* and *chpCEH* is reduced, while the other *chp* genes as well as *rdlAB* are upregulated. Therefore, we propose that fine-tuning of *chp* and *rdl* gene expression is maintained by OsdR.

Some of the differentially expressed genes that lack an obvious consensus sequence, in particular the *ssgB* and genes of the *whiE* gene cluster, were bound by OsdR *in vitro*. This indicates that the OsdR regulon may be larger than anticipated, and some members of the regulon may be controlled by so-called class II binding sites, in other words, sites that do not conform to the predicted consensus sequence site. Similar duality has been shown for many other functionally diverse global regulatory networks in bacteria, including those controlled by LexA (Wade *et al.*, 2005) and Crp (Gao *et al.*, 2012) in *E. coli*, Spo0A in *B. subtilis* (Molle *et al.*, 2003), CtrA in *Caulobacter crescentus* (Laub *et al.*, 2002), and Crp (Gao *et al.*, 2012), GlnR (Pullan *et al.*, 2011), PhoP (Allenby *et al.*, 2012), and DasR (Świątek-Połątyńska *et al.*, 2015) in *Streptomyces*. For *B. subtilis* Spo0A, some 15% of the total binding sites were not

bound *in vitro* (Molle *et al.*, 2003).

Extensive studies of the DosT and DevS signaling systems have indicated that, during hypoxia, the dissociation of oxygen from the SKs results in the transition from the inactive to the active states of these proteins. With the initial DevR hypoxic response mediated by DosT, which has a higher dissociation constant than DevS, the response is then maintained through DevS. Differences in the local structures surrounding a heme in either SK result in different oxygen affinities (Cho *et al.*, 2009; Podust *et al.*, 2008). Additionally, ascorbic acid, nitric oxide, and carbon monoxide also induce the DevR regulon (Taneja *et al.*, 2010). NO has been shown to activate DosT under aerobic conditions by displacement of oxygen (Sousa *et al.*, 2007), while DevS acts as a redox sensor of the electron transport system and a decrease activates the SK under aerobic conditions (Honaker *et al.*, 2010). The similarity of the amino acid residues involved in signal recognition by DosT/DevS and OsdK suggests that oxygen is the major candidate as a sensory signal. Indeed, Daigle and colleagues showed that *osdR*, as well as many genes in the genomic region around *osdR*, were strongly upregulated in wild-type cells under both low-oxygen conditions and when cells were grown with sodium nitroprusside, an NO donor (Daigle *et al.*, 2015). Additional evidence for the oxygen stress-related function of OsdR was provided by a study of the proteomes of large versus small pellets (Van Veluw *et al.*, 2012), in which oxygen depletion within large pellets—which created local anaerobic conditions—resulted in the upregulation of various proteins expressed from the OsdR-controlled SCO0168-SCO0208 genomic region (Fischer *et al.*, 2014).

In liquid-grown cultures, where *S. coelicolor* forms large mycelial pellets (causing oxygen transfer problems toward the center of the clump [Van Dissel *et al.*, 2014]), and on solid-grown cultures (Van Keulen *et al.*, 2007), local oxygen depletion occurs. OsdKR-mediated oxygen sensing may well be responsible for the response to microaerobic conditions, during which the bacterium switches metabolism to meet the challenge of low oxygen. Still, streptomycetes cannot grow anaerobically, despite the presence of an arsenal of genes for enzymes associated with anaerobic metabolism (Borodina *et al.*, 2005). This has previously been referred to as the “anaerobic paradox.” This is exemplified by the surprising presence of three nitrate reductases in *S. coelicolor*, and our work shows that one of these is directly controlled by OsdR. Alternatively, *S. coelicolor* may undergo a state of dormancy as a means of survival. Indeed, while *S. coelicolor* cannot grow in oxygen-deprived soil, it is able to survive periods of anaerobiosis in which it remains dormant (Van Keulen *et al.*, 2007). Sporulation is a state of dormancy, and the fact that spore germination is significantly delayed in *osdR* null mutants without affecting spore viability (Fig. 6C) supports the notion that *osdR* controls this dormancy state. This delay was corroborated independently by imaging the germination of 500 spores of the wild type and the *osdR* mutant using light microscopy (not shown).

The transcriptional changes at 36 h of growth in the *osdR* null mutant are noteworthy, and while the results need to be worked out further, they may have major implications for the control of the switch from early- to late-developmental growth. Interestingly, such a clear transition in the global transcriptional profile of *S. coelicolor* has been reported previously, during growth in a fermentor. Distinctive sharp increases and decreases in the transcription of many genes were observed at this time point, and importantly, this includes several genes of the OsdR regulon, namely, genes in the nitrate reductase cluster adjacent to *osdR* (SCO0212-SCO0220), *bldN*, the *bldN*-controlled *chp* genes, and several other developmental genes (Nieselt *et al.*, 2010). We observed a similar distinctive change in gene expression at 36 h in surface-grown cultures of wild-type cells, with many of the genes of

the OsdR regulon, as well as *osdR* itself, showing expression in the wild-type strain different from that in the *osdR* null mutant. To some extent, the data from surface- and liquid-grown cultures can be compared, with many developmental genes upregulated in liquid-grown cultures at the time corresponding to the transition from exponential to stationary growth, suggesting that the phase of growth cessation in submerged culture is comparable to the onset of development (Huang *et al.*, 2001). Our data provide a first indication that OsdR may play a major role in mediating a switch in gene expression during the transition from normal to developmental growth. The transcription of *osdR* also shows a peak almost immediately after germination (Strakova *et al.*, 2013), which suggests that OsdR may play a similar role during the transition from dormancy to early growth. Such a role of OsdR in mediating a rapid and global change in gene expression requires further investigation.

In summary, the TCS OsdKR of *S. coelicolor* is orthologous to the dormancy TCS system of *M. tuberculosis*, with OsdR regulating development and stress management in *S. coelicolor*. The signal activating this response system is likely related to stress, such as nutrient deprivation or hypoxic stress; however, this remains to be confirmed. OsdK also partners with SCO3818 (Wang *et al.*, 2009), which adds an extra level of complexity. This also means that deletion of *osdR* may not completely inactivate the OsdK-based sensory system in *S. coelicolor*. The system may be even more complicated, as sensory kinase SCO3948 has a higher amino acid identity to OsdK than any other SK encoded by the *S. coelicolor* genome. Mutational and functional analysis followed by a system-wide analysis of the effects of all possible members of the control system on global gene expression should establish the level of cross talk between the two sensory systems and how they control the stress response of the complex soil bacterium *Streptomyces*.

ACKNOWLEDGMENTS

We are grateful to Weihong Jiang for providing plasmids pET0203 and pET0204 and to Tom Ottenhoff for providing genomic DNA of *M. tuberculosis* Rv37.

CHAPTER IV

SCO4393, A NOVEL ENZYME INVOLVED IN *N*-ACETYLGLUCOSAMINE METABOLISM

Mia Urem, Magda A. Świątek-Połatyńska, Patrick Voskamp,
Navraj S. Pannu and Gilles P. van Wezel

ABSTRACT

Streptomyces bacteria are a bountiful source of diverse secondary metabolites, including the majority of clinical antibiotics. However, many of the biosynthetic gene clusters (BGCs) for natural products are silent under laboratory conditions. Better understanding of the connection between primary and secondary metabolic pathways, and the regulatory networks controlling them is required to activate the expression of these cryptic BGCs. A well-studied example is the activation of antibiotic production by metabolites derived from *N*-acetylglucosamine (GlcNAc), which modulate the activity of the global antibiotic repressor DasR inside the cell. Here, we present the phosphosugar isomerase SCO4393 as a novel member of the GlcNAc metabolic pathway. Deletion of SCO4393 relieves toxicity of both glucosamine (GlcN) and GlcNAc to *S. coelicolor nagB* mutants. Crystal structures of SCO4393 and SCO4393 in complex with GlcNAc-6P and with a culture-derived ligand, have been determined. The structures revealed that SCO4393 is a dimer with two active sites located at the interface of the monomers. The ligand-bound structure along with the ligand-free structure showed tightening of the active site upon binding. ITC binding studies strongly suggest that GlcNAc-6P is a major candidate substrate. Since accumulation of GlcNAc-6P is not toxic to *S. coelicolor* cells, we propose that the substrate of SCO4393 is a related aminosugar.

INTRODUCTION

With the rise of multidrug resistance in pathogenic bacteria, it is becoming increasingly critical to find novel drug therapies (O'Neill, 2014; WHO, 2014). The soil-dwelling, mycelial bacteria of the *Streptomycetaceae* family are prolific producers of diverse secondary metabolites that include some two third of all known antibiotics as well as immunosuppressant and anticancer drugs (Barka *et al.*, 2016; Bérdy, 2005, Hopwood, 2007). Despite the large number of antibiotics known to be produced by these bacteria, genome sequencing revealed that they likely have a greater capacity for the production of secondary metabolites than previously believed (Bentley *et al.*, 2002; Ikeda *et al.*, 2003; Ohnishi *et al.*, 2008; Cruz-Morales *et al.*, 2013). Streptomyces have the biosynthetic potential to produce dozens of secondary metabolites but the biosynthetic gene clusters (BGC) that specify many of these molecules remain poorly expressed under routine growth conditions (Medema *et al.*, 2015; Nett *et al.*, 2009). Current strategies for the activation of BGCs include the exploitation of bacterial responses to environmental triggers, the manipulation of metabolic pathways and regulatory networks, as well as the application of elicitors, identified from the ecological backgrounds of streptomyces, during screenings (Okada & Seyedsayamdost, 2016; Rutledge & Challis, 2015; van der Meij *et al.*, 2017; Zhu *et al.*, 2014a).

In the model organism *Streptomyces coelicolor*, *N*-acetylglucosamine (GlcNAc) is a preferred source of carbon and nitrogen (Nothaft *et al.*, 2003a; Nothaft *et al.*, 2010). GlcNAc is abundantly available in its dimeric form, *N*-*N'*-diacetylchitobiose [(GlcNAc)₂], as a component of chitin. GlcNAc is also found in cell wall peptidoglycan (PG), the chains of which consist of alternating GlcNAc and *N*-acetylmuramic acid (MurNAc) residues cross-linked via peptide bridges. Under rich nutritional conditions (feast), GlcNAc activates growth and represses development and antibiotic production (Rigali *et al.*, 2006; Rigali *et al.*, 2008). Under poor growth conditions (famine), GlcNAc instead activates development and antibiotic production. This phenomenon has been exploited to elicit secondary metabolites on minimal media during screens for novel antibiotics (Zhu *et al.*, 2014b).

The activation of antibiotic production and developmental onset by GlcNAc under poor growth conditions is mediated via the GntR-family repressor DasR (Rigali *et al.*, 2006; Rigali *et al.*, 2008). This global nutrient sensory regulator controls the uptake and metabolism of GlcNAc via direct binding to the promoter regions of the *chi*, *nag* and *pts* genes, encoding the enzymes of the chitinolytic system, GlcNAc metabolism and the phosphoenolpyruvate-dependent phosphotransferase system (PTS), respectively (Świątek-Połatyńska *et al.*, 2015; Świątek *et al.*, 2012a). In *Streptomyces coelicolor*, DasR also directly controls all the pathway-specific regulators for antibiotic production and the regulators for iron-chelating siderophore production (Świątek-Połatyńska *et al.*; 2015, Craig *et al.*, 2012; Lambert *et al.*, 2014). The DNA-binding activity of DasR is modulated by intracellular metabolites, whereby GlcNAc metabolic intermediates GlcNAc-6P and GlcN-6P allosterically induce the release of DasR from its recognition sites (Tenconi *et al.*, 2015; Rigali *et al.*, 2008; Fillenberg *et al.*, 2015; Świątek-Połatyńska *et al.*, 2015).

Monomeric GlcNAc, *e.g.* released during autolytic degradation of the cell wall, is taken up by *S. coelicolor* via the PTS, thereby phosphorylating the incoming GlcNAc to GlcNAc-6P (Nothaft *et al.*, 2003a; Nothaft *et al.*, 2010). To metabolise GlcNAc from chitin, chitinolytic enzymes are secreted which produce (GlcNAc and its oligomers for internalization of via ABC-transporter complex DasABC-MsiK (Colson *et al.*, 2008; Saito *et al.*, 2007; Schrempf, 2001). After the intracellular cleavage of (GlcNAc)₂, monomers of GlcNAc are phosphorylated by *N*-acetylglucosamine kinase NagK (Świątek *et al.*, 2012a). Following

from GlcNAc-6P, deacetylation by NagA forms glucosamine 6-phosphate (GlcN-6P) which is a central molecule at the intersection of multiple metabolic pathways, including glycolysis via conversion to fructose 6-phosphate (Fru-6P) by glucosamine-6-phosphate deaminase NagB (Świątek *et al.*, 2012a).

GlcNAc and its deacetylated derivative glucosamine (GlcN), are toxic to *S. coelicolor* *nagB* mutants, presumably due to the accumulation of GlcN-6P or a derivative thereof (Świątek *et al.*, 2012b). Spontaneous suppressor mutations were obtained for *S. coelicolor* *nagB* mutants that circumvented the toxicity of GlcNAc and/or GlcN. Mutation of *nagA* surprisingly restored growth of *nagB* mutants on both GlcNAc and GlcN, which suggests that GlcN may be metabolised via the GlcNAc pathway (Świątek *et al.*, 2012b). Two novel aminosugar-related genes were discovered in this screen (Świątek, 2012; this thesis), namely the ROK-family regulatory gene SCO1447 (*rokL6*), mutation of which exclusively relieves toxicity of GlcN to *nagB* mutants, and SCO4393, which encodes a putative phosphosugar isomerase. Deletion of the latter restores the ability of *nagB* mutants to grow in the presence of either GlcN or GlcNAc.

SCO4393 is a highly-conserved protein among streptomycetes and is also found in various other bacteria. In this work, we provide a functional and structural analysis of SCO4393 of *S. coelicolor* and analyse its role in the metabolism of aminosugars GlcN and GlcNAc. Structural studies supported by *in vitro* binding assays provide the first hints into the potential ligand of this novel primary metabolic enzyme.

MATERIAL AND METHODS

BACTERIAL STRAINS, CULTURE CONDITIONS, PLASMIDS AND OLIGONUCLEOTIDES

All strains described in this work are listed in Table S1. *Escherichia coli* was grown and transformed according to standard procedures (Sambrook *et al.*, 1989) with *E. coli* JM109 serving as the host for routine cloning, and *E. coli* ET12567 (MacNeil *et al.*, 1992) for the isolation of non-methylated DNA for transformation into *Streptomyces* (Kieser *et al.*, 2000). For heterologous protein expression, *E. coli* Rosetta™(DE3)pLysS from Novagen was used. *E. coli* was grown in Luria-Bertani (LB) media in the presence of selective antibiotics as required, with the following final concentrations; ampicillin (100 µg/ml) and chloramphenicol (25 µg/ml).

Streptomyces coelicolor A(3)2 M145 was obtained from the John Innes Centre strain collection and was the parent of all mutants. *S. coelicolor* *nagA*, *nagB* and *nagK* mutants (Świątek *et al.*, 2012a) and *nagB* suppressor mutants (Świątek, 2012), have been described previously. All *Streptomyces* media and routine techniques, including transformation via protoplast regeneration, are described in the *Streptomyces* manual (Kieser *et al.*, 2000). A mixture of 1:1 yeast-extract malt extract (YEME) and tryptic soy broth (TSB) liquid media was used to cultivate mycelia for protoplast preparation, and glucose-containing R5 agar media, with appropriate selective antibiotics, was used for protoplast regeneration after transformation. SFM (soy flour mannitol) agar was used for the cultivation of spores. Phenotypic characterization was done on R5 and minimal media (MM) agar supplemented with sugars as stated and where appropriate with the antibiotics apramycin (50 µg/ml) and/or thiostrepton (20 µg/ml) as selective markers.

All plasmids and oligonucleotides described in this work are summarised in Tables S1 and S2 of the supplemental material, respectively. The shuttle vector pHJL401 was used as a low-copy plasmid in *Streptomyces* (Larson & Hershberger, 1986), which is very well suited for genetic complementation experiments (van Wezel *et al.*, 2000a). The unstable multi-copy shuttle vector pWHM3 (Vara *et al.*, 1989) was exploited for gene replacement strategies (van Wezel *et al.*, 2005). Cre recombinase expressing plasmid, pUWLcre (Fedoryshyn *et al.*, 2008) was used for the creation of deletion mutants via genetic excision via *loxP* marked sites (see below for details). Expression vector pET-15b (Novagen), which introduces an N-terminal His-Tag, was used for heterologous expression of SCO4393. All DNA sequencing was performed by BaseClear BV (Leiden, The Netherlands).

GENETIC COMPLEMENTATION AND KNOCK-OUT MUTANTS

For genetic complementation of SCO4393, its coding region and 217 bp upstream region, likely encompassing the promoter region, was amplified from *S. coelicolor* M145 genomic DNA using primers compF-217 and compR+762 (Table S2), and cloned into pHJL401 to give plasmid pGWS1051.

The procedure for the creation of *S. coelicolor* gene replacement and deletion mutants is described in detail in (Świątek *et al.*, 2012a). Gene replacement mutants were generated via homologous recombination, with the gene of interest replaced by the apramycin resistance cassette *aac(C)IV*. For this, the upstream and downstream flanking regions of SCO4393 were PCR-amplified from genomic DNA using primer pairs LF-1438/LR+15 and RF+768/RR+2157 and cloned into pWHM3 using engineered EcoRI/XbaI and XbaI/HindIII restriction sites, respectively. The apramycin resistance cassette flanked by *loxP* sites was cloned in-between as an XbaI fragment. The resulting knock-out plasmid was designated pGWS1052 and introduced into *S. coelicolor* via protoplast transformation. Correct recombination events were checked by the appropriate antibiotics resistance

and confirmed by PCR. To obtain deletion mutants, the apramycin resistance cassette was excised by introduction of Cre recombinase expressing plasmid, pUWLcre (Fedoryshyn *et al.*, 2008), which allows for efficient removal of the cassette via the loxP recognition sites (Khodakaramian *et al.*, 2006). Deletion mutants were checked based for the appropriate antibiotic sensitivity (loss of apramycin resistance) and confirmed by PCR.

HETEROLOGOUS EXPRESSION AND PURIFICATION OF SCO4393

For *in vitro* experiments and structure elucidation via X-ray crystallography, N-terminally His₆-tagged SCO4393 was expressed in *E. coli* Rosetta™(DE3)pLysS. SCO4393 was PCR amplified from *S. coelicolor* genomic DNA using primers pETF-1and pETR-756 (Table S2), and cloned into pET15b. His₆-tagged SCO4393 was purified using a Ni-NTA column (GE Healthcare) with Isolation Buffer (500 mM NaCl, 5% glycerol, 50 mM HEPES, 10 mM β-mercaptoethanol, pH 8) containing 250 mM imidazole, as described (Mahr *et al.*, 2000). Fractions containing SCO4393 were pooled and concentrated before further purification by size exclusion chromatography (Superdex 200) with Isolation Buffer. Fractions containing SCO4393 were pooled and concentrated prior to use in crystallization trials and *in vitro* experiments. Protein was concentrated using 10 kDa molecular weight cut-off centrifugal filter units (Amicon) and samples were analysed by 15% SDS-PAGE and native PAGE electrophoresis.

PROTEIN CRYSTALLIZATION CONDITIONS

Purified SCO4393 at a concentration of 15-20 mg/ml was used to screen crystallization conditions by sitting-drop vapour-diffusion using the PGA Screen (Molecular Dimensions), Clear Strategy Screens CSS-I and CSS-II (Molecular Dimensions), JCSG+ (Qiagen/Molecular Dimensions) and the PACT screen (Molecular Dimensions) as well as optimization screens at 20°C. The 75 μL reservoir of 96-well Innovaplate SD-2 plates was pipetted by a Genesis RS200 robot (Tecan) and drops were made by an Oryx6 robot (Douglas Instruments). SCO4393 crystals with the open-ring intermediate were obtained in 0.2 M MgCl₂, 0.1 M TRIS (pH 8.5) and 25% (w/v) PEG MME 2000. All other crystals were obtained from JCSG number 83 (96-well G11) which consisted of 2.0 M Ammonium sulphate, 0.1 M BIS-Tris, pH 5.5. Crystals were soaked in cryoprotectant solution (mother liquor with 10-20% glycerol) in the presence or absence of 100mM ligand candidates, and flash-frozen in liquid nitrogen.

TABLE 1. Data collection and refinement statistics (molecular replacement).

	Ligand	GlcNAc-6P	GlcN-6P
Data collection			
Space group	P 1 2 1 1	P 6 5 2 2	P 6 5 2 2
Cell dimensions			
<i>a</i> , <i>b</i> , <i>c</i> (Å)	60.91, 99.03, 73.45	88.06, 88.06, 283.46	87.57, 87.57, 273.21
α, β, γ (°)	90, 106.07, 90	90, 90, 120	90, 90, 120
Resolution (Å)*	1.95 (1.95 – 1.99)	2.52 (2.52 – 2.61)	1.64 (1.64-1.74)
<i>R</i> _{meas}	0.167 (1.115)	0.256 (2.918)	0.202 (1.461)
<i>I</i> / σ <i>I</i>	8.8 (1.7)	9.7 (1.2)	4.3 (0.1)
CC(1/2)	0.993 (0.596)	0.998 (0.527)	0.986 (0.387)
Completeness (%)	98.3 (81.4)	100.0 (100.0)	81.7 (19.2)
Multiplicity	5.3 (5.1)	18.9 (19.5)	4.4 (1.2)
Refinement			
Resolution (Å)	1.95	2.52	1.64
No. reflections	57 318	21 792	59 305
<i>R</i> _{work} / <i>R</i> _{free}	0.196 (0.317)/	0.208 (0.348)/	0.267 (0.469)/
	0.241 (0.343)	0.250 (0.402)	0.301 (0.550)
No. atoms	7617	3681	3580
R.m.s. deviations			
Bond lengths (Å)	0.014	0.012	0.018
Bond angles (°)	1.56	1.744	1.851

*Values in parentheses are for highest-resolution shell.

STRUCTURAL DATA COLLECTION

X-ray data were collected at the European Synchrotron Radiation Facility (Grenoble, France) on beamline ID-23 for SCO4393 with the open-ring intermediate: 1410 images were collected on a Pilatus 6M detector at an X-ray wavelength of 0.9724 Angstroms, an exposure time of 0.037 seconds, transmission of 10% and an oscillation range of 0.2 degrees., while uncomplexed SCO4393 and SCO4393 in complex with GlcNAc-6P were collected on beamline ID-29 with a Pilatus 6M detector. For the native/uncomplexed crystal, 1020 images were collected at 1.2727 Å wavelength with an exposure time of 0.02 seconds, transmission of 100% and an oscillation range of 0.05 degrees. For SCO4393/GlcNAc-6P crystals, 680 images were collected at 0.976251 Angstroms wavelength with an exposure time of 0.02 seconds, transmission of 47.34% and an oscillation range of 0.1 degrees, XDS (Kabsch, 2010) was used to process all the data collected while aimless (Evans & Murshudov, 2013) was used for scaling and merging the integrated intensities. Table 1 shows the data collection and refinement statistics for all data sets obtained.

STRUCTURE DETERMINATION, REFINEMENT AND ANALYSIS

The structure of SCO4393 with the open-ring intermediate was solved by molecular replacement with Molrep (Vagin & Teplyakov, 2000) using the structure of a putative phosphoheptose isomerase from *Bacillus halodurans* C-125 determined at the Joint Center for Structural Genomics (PDB code 3CVJ) as a search model. The other structures were solved by molecular replacement with Molrep, but using the refined SCO4393 structure with the open-ring intermediate as the starting model. All structures were iteratively refined with REFMAC5 (Murshudov *et al.*, 2011) from the CCP4 package (Winn *et al.*, 2011) and manual model building and adjustments were done with Coot (Emsley *et al.*, 2010). The quality of the final models was validated with Molprobit (Chen *et al.*, 2010) and wwPDB Validation Service (Berman *et al.*, 2003). The ligand molecules were validated by Privateer (Agirre *et al.*, 2015). Final refinement statistics for all structures are given in Table 1. All figures showing structural representations were prepared with the program PyMOL (The PyMOL Molecular Graphics System, Version 1.8 Schrödinger, LLC).

ISOTHERMAL TITRATION CALORIMETRY

In vitro analysis of SCO4393 interaction with potential ligand candidates was examined thermodynamically by isothermal titration calorimetry (ITC) using a VP-ITC microcalorimeter (Microcal). To minimise interference of salts and other buffer components during ITC experiments, the buffer SCO4393 was taken up with was exchanged with ITC Buffer (50 mM HEPES, pH 8) using 10 kDa molecular weight cut-off centrifugal filter unit (Amicon) until the NaCl concentration was reduced below 50 µM. Following this, SCO4393 was dialysed overnight in 1L of ITC Buffer at 4°C to further reduce the concentration of salt and glycerol. The buffer from the dialysis was used to prepare the ligand samples (1 mM) to minimise discrepancies with the SCO4393 samples. Ligand was titrated at 6 or 8 µl injections into the sample cell containing 50 mM SCO4393 at 25°C. Data analysis and graphic representation were done using the program Origin (Microcal).

BIOINFORMATICS ANALYSIS

Motifs were predicted using InterProScan (Zdobnov & Apweiler, 2001) and Pfam 24.0 (Finn *et al.*, 2008) and protein homology searches were performed using BLASTp (Altschul *et al.*, 2005). Synttax used for gene synteny (Oberto, 2013). Protein alignments were visualised using Boxshade (www.ch.embnet.org/software/box_form.html).

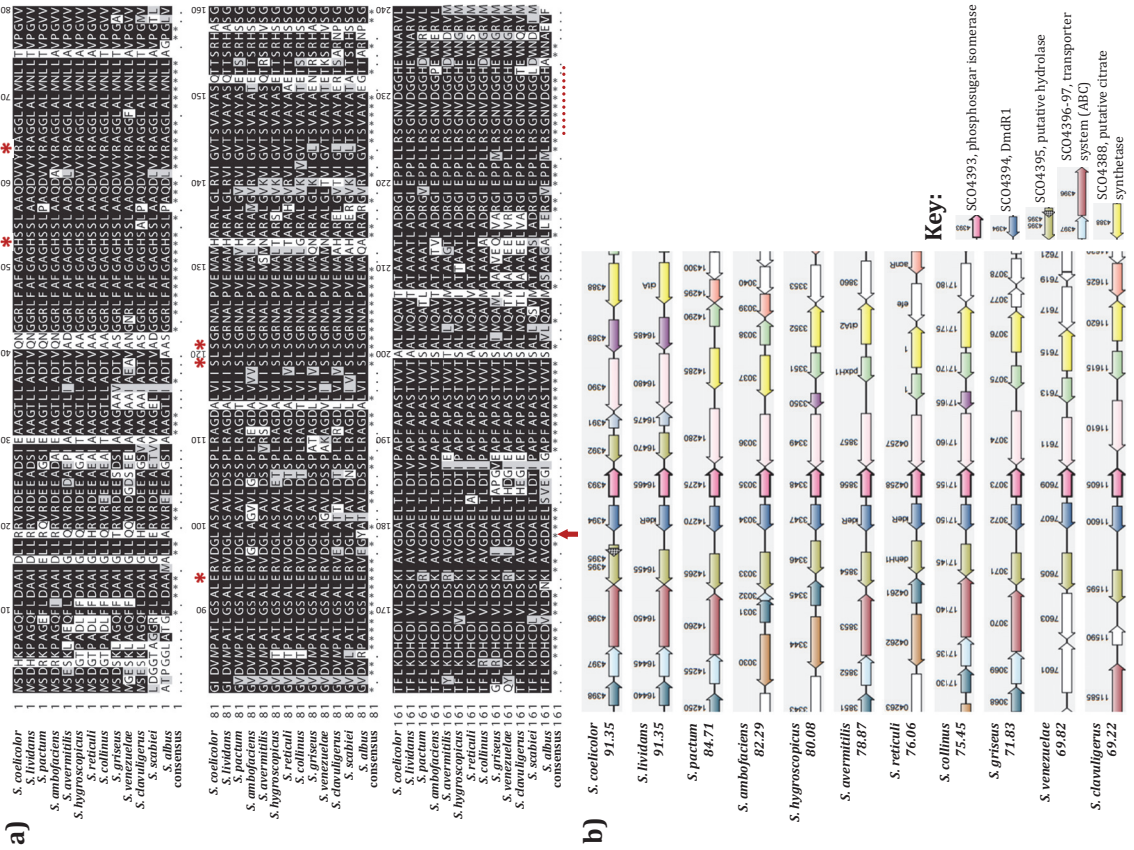
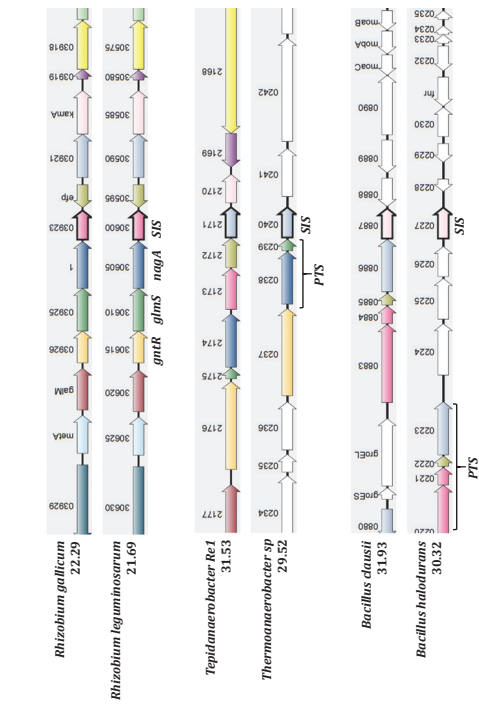


FIGURE 1. Sequence alignment and gene synteny for SCO4393.
 a) Alignment of the SCO4393 protein sequence with homologs from other *Streptomyces* species up to residue 240. Identical amino acids are shaded black, and amino acids with similar properties are in grey with a consensus of the alignment given below (*, identical; ·, similar). The D179N mutation identified in SMA11 is indicated with a red arrow (below). Residues likely to be important for ligand binding (see Fig. 4) are indicated with red stars (* above) and the loop that conformationally shifts during ligand binding (see Fig. 5) is underlined by a red dotted line (below). The image was generated using Boxshade.
 b) Gene synteny between SCO4393 in *S. coelicolor* and homologs in other *Streptomyces* species. Analysis was done using Syntax (scores are given).
 c) Gene synteny of SCO4393 homologs found in some species of firmicutes and proteobacteria done using Syntax (scores are given). SCO4393 orthologs in *Rhizobium* species are located close to *nagA*, *glnS* and a gene for a GntR transcriptional regulator. In *Bacilli* and *Thermoanaerobacteria*, SCO4393 orthologs are located in proximity to genes of PTS components and other PTS-related genes. Homologs are presented in the same colours and highlighted in the key for *S. coelicolor*. Genes of interest in other bacteria are annotated and SCO4393 homologs are labelled 'SIS'.

c)



RESULTS

MUTATIONS IN SCO4393 RELIEVE TOXICITY OF AMINOSUGARS TO *S. COELICOLOR* *nagB* MUTANTS

Genomic analysis of suppressor mutants of the *S. coelicolor nagB* deletion mutant previously identified novel candidates in the metabolic pathways of GlcNAc and GlcN as well as the regulation thereof (Świątek, 2012; this thesis). One such mutation was identified in SCO4393 in suppressor mutant SMA11, which harboured a single nucleotide permutations (SNP) at nucleotide position 535 (G to A substitution), leading to a non-silent change from aspartic acid to asparagine (Asp179Asn) in the sugar isomerase (SIS) domain of the predicted gene product (Świątek, 2012). Other suppressor mutants were also screened for possible mutations in SCO4393 by introducing construct pGWS1051, which expresses wild-type SCO4393. Transformants regaining aminosugar sensitivity, as a result of the presence of wildtype copies of SCO4393 expressed from the plasmid, were confirmed by sequencing the PCR-amplified SCO4393 gene from a number of mutants. Indeed, suppressor SMA13 harboured the same G to A substitution at position 535 as SMA11 as well as a frameshift as a result of an insertion at nucleotide position 561. Together, this indicates that mutations in SCO4393 are sufficient to suppress the toxicity of GlcNAc (and GlcN) to *nagB* deletion mutants. This suggests that a functional SCO4393 protein is necessary for the toxic effect of the aminosugars and that the sugar isomerase likely plays a currently undefined role in the formation of the toxic intermediate.

SCO4393 IS A HIGHLY CONSERVED SIS-DOMAIN PROTEIN IN *STREPTOMYCES*

SCO4393 is a conserved hypothetical protein with a sugar isomerase (SIS) domain (Bateman, 1999), predicted to span almost the entire length of the protein. SIS domains are typically found in phosphosugar-binding proteins, including some with transcriptional control over the biosynthetic genes of phosphosugars, and phosphosugar isomerases such as MurQ and GlmS (Jaeger & Mayer, 2008; Reith & Mayer, 2011; Kim *et al.*, 2009). The closest paralogue of SCO4393 is MurQ (SCO4307) but the proteins only share 31% amino acid identity (43% positives). MurQ contains a SIS-esterase domain that is responsible for the conversion of MurNAc-6P to GlcNAc-6P by cleavage of the lactyl ether bond. This, in combination with the relatively low sequence similarity, suggests that no functional homologue of SCO4393 exists in *S. coelicolor*.

There is high sequence similarity (at least 80% aa identity and 90% positives) between the SCO4393 orthologues in different *Streptomyces* species (Fig. 1A). Gene synteny analysis shows that also the genomic region around SCO4393 is highly conserved among streptomycetes (Fig. 1B). The regulatory gene *dmdR1* (SCO4394) is expressed divergently from SCO4393 in *S. coelicolor* and many, but not all, other streptomycetes. DmdR1, which is a repressor of iron utilization and also controls production of iron-chelating siderophores, is induced by GlcNAc in *Streptomyces* via repression of DasR (Craig *et al.*, 2012). A DasR-responsive element (*dre*) has been identified in the intergenic region of SCO4393 and *dmdR1*, 54 nt upstream of the translational start of SCO4393 (Craig *et al.*, 2012). Other genes in the genomic region of SCO4393 with high gene synteny include a putative hydrolase, components of an ABC transporter and a putative citrate synthetase.

Based on gene synteny analysis, homologs of SCO4393 with an amino acid similarity of 30-40% (45-60% positives) and containing a SIS-domain of unknown function are present in several other bacterial phyla, including firmicutes and proteobacteria. In Gram-negative soil-dwelling Rhizobia, the orthologous gene is suggestively located downstream of the aminosugar-related metabolic genes *glmS* and *nagA*, with a gene encoding a GntR regulator

in the same operon (Fig. 1C). In firmicutes, such as *Thermoanaerobacter* and *Bacillus* species, SCO4393 homologs lie in close proximity to genes encoding components of the PTS and related genes. This is strong supportive evidence for a role of SCO4393 in aminosugar metabolism.

GLCNAC SENSING IS AFFECTED IN *S. COELICOLOR* SCO4393 MUTANTS

To create an *S. coelicolor* SCO4393 deletion mutant and a SCO4393-*nagB* double mutant, first gene replacement mutants were created whereby the SCO4393 gene from nucleotides 15 to 768 (relative to the transcriptional start site) was substituted with an apramycin resistance cassette. Homologous recombination of the gene was achieved by transformation with plasmid pGWS1052, which was constructed by cloning the resistance cassette between the upstream and downstream flanking regions of SCO4393 in the unstable multi-copy vector pWHM3. Correct recombination events were confirmed by resistance to apramycin and sensitivity to thiostrepton (for loss of the vector sequences) and by PCR. To create deletion mutants, the apramycin resistance cassette was excised from genome by Cre recombinase, expressed from the introduced pUWLcre plasmid, via the *loxP* sites located on either end of the cassette. Mutants were screened for sensitivity to apramycin and confirmed by PCR.

The *S. coelicolor* SCO4393 single mutant had a phenotype similar to its parent M145 on MM with GlcN and GlcNAc (Fig.2). Though both sugars induced antibiotic production and development on MM, development was impaired when GlcN was added. On R5 agar plates, production of the blue-pigmented actinorhodin was blocked or delayed in the mutant compared to the parental strain, and reduced in the presence of GlcN. Interestingly, GlcNAc sensing on R5 agar was lost in the SCO4393 mutant; the mutant developed abundant aerial hyphae and produced pigmented antibiotics in the presence of the aminosugar, in contrast to the parent. This suggests that SCO4393 affects the levels of an intermediate metabolite or metabolites required for the regulation of the GlcNAc response under rich growth conditions (feast).

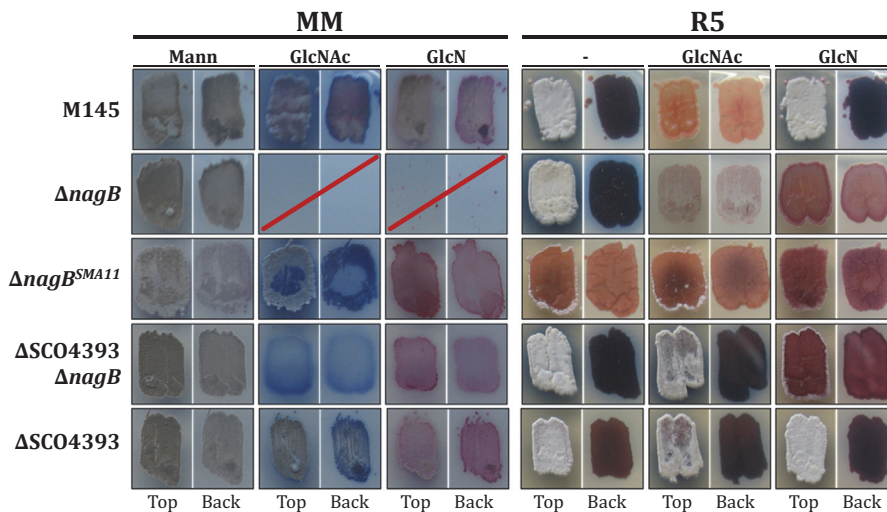


FIGURE 2. Phenotypic analysis of *S. coelicolor* SCO4393 mutants.

Spores of *S. coelicolor* M145, its *nagB* and SCO4393 deletion mutants, *nagB* suppressor mutant SMA11, and double mutants SCO4393-*nagB*, SCO4393-*nagA* and *nagA*-SCO4393 were plated onto minimal media (MM) or glucose-containing R5 agar plates, supplemented with 50 mM mannitol (Mann), glucosamine (GlcN) or *N*-acetylglucosamine (GlcNAc) as indicated. Mutants that failed to grow on GlcN or GlcNAc are indicated with a red line. The top view and bottom (back) view of the plates are indicated underneath.

Deletion of SCO4393 restored the ability of the *S. coelicolor nagB* mutant, which accumulates lethal levels of GlcN-6P or related metabolite(s), to grow on MM with GlcNAc and GlcN (Fig.2). The *nagB*-SCO4393 double mutant retained a phenotype similar to that of the parental strain and suppressor mutant SMA11 on MM with either aminosugar, though growth was less pronounced. The double mutant had a wild-type phenotype on R5 agar plates but failed to develop or produced blue-pigmented actinorhodin when GlcN was added, similar to *nagB* mutants. However, similarly as for the SCO4393 mutant, GlcNAc did not affect development or antibiotic production of the double mutant on R5 agar, suggesting that GlcNAc sensing had been lost. Thus, we present SCO4393 as a novel enzyme involved in aminosugar metabolism.

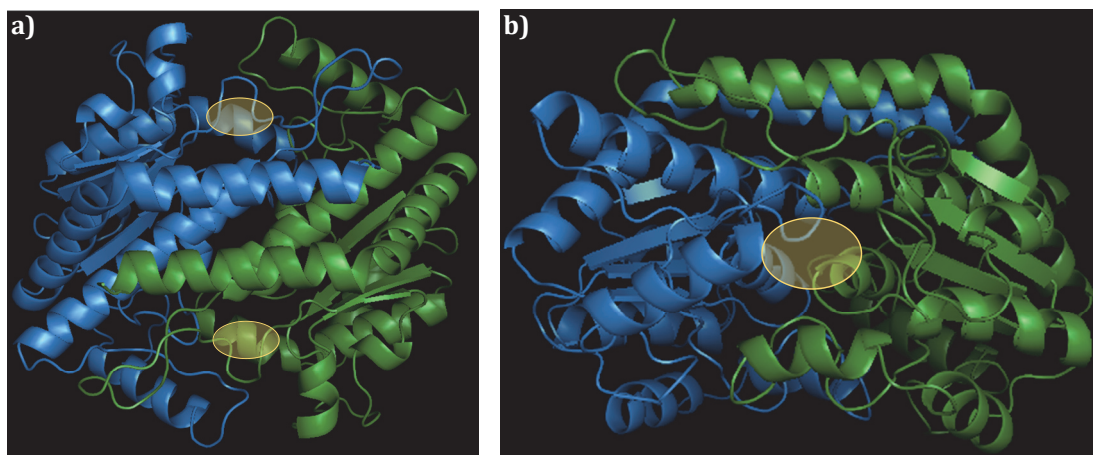


FIGURE 3. Crystal structure of SCO4393 dimer.

Image of the SCO4393 structure with determined by X-ray crystallography. The individual monomers (blue and green) of the dimer are shown with a view of both active sites (a), indicated in yellow, and a view into the active site (b), formed at the interface of the monomers.

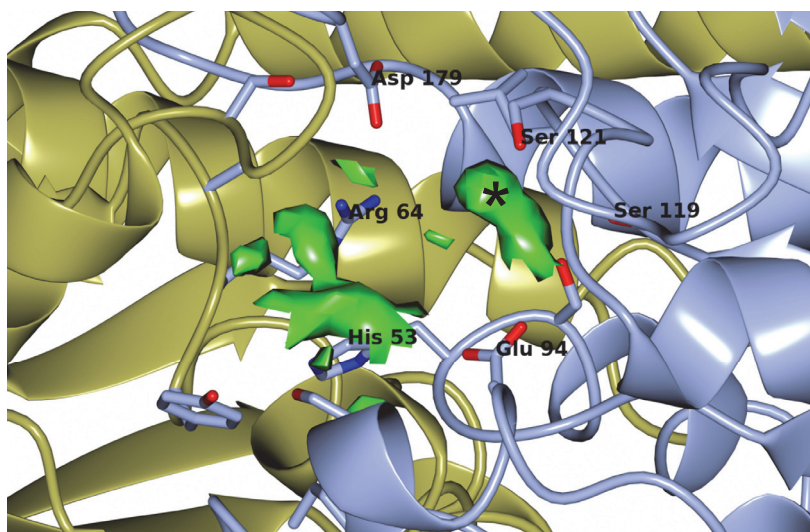


FIGURE 4. Trapped ligand intermediate in the active site of SCO4393.

Strong densities are shown in green within the active site of SCO4393. The density labelled with an asterisk (*) is proposed to be a phosphate group given its proximity and interactions with the serine residues. The monomers of SCO4393 shown in light blue and olive green.

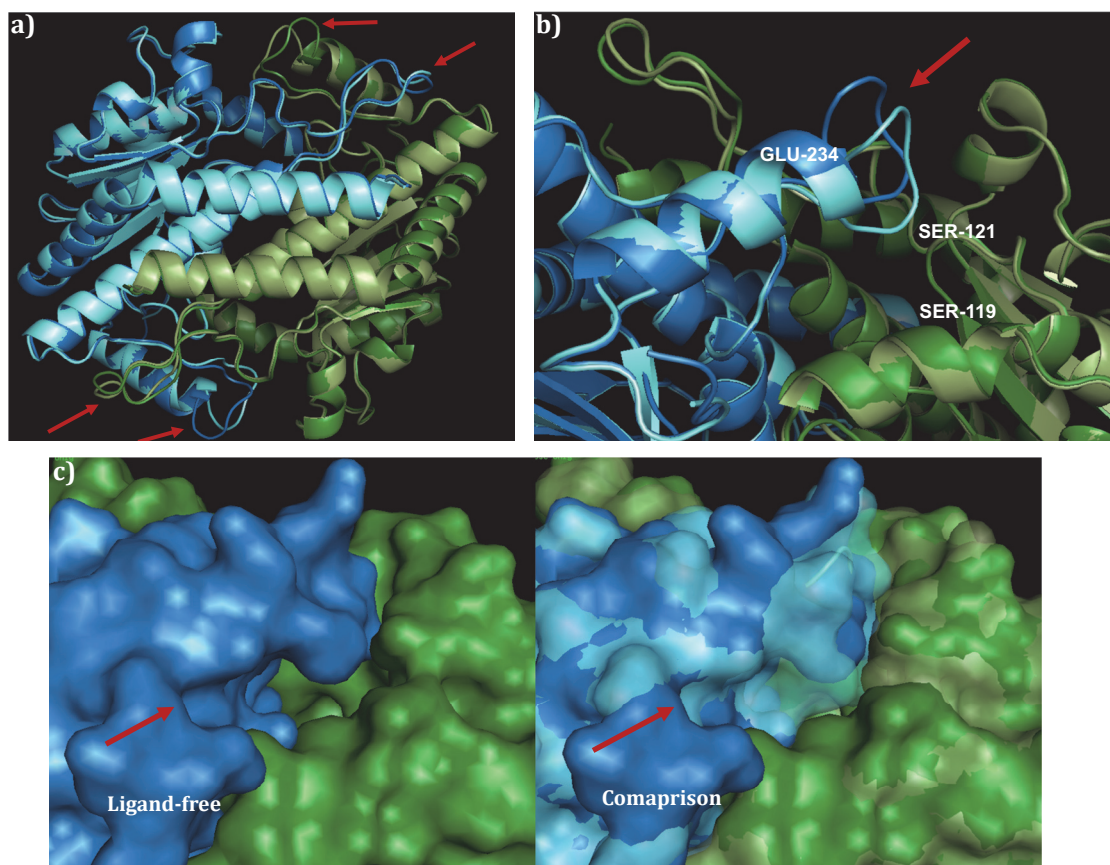


FIGURE 5. Comparison of SCO4393 with and without bound ligand.

Conformational shifts affecting access to the active site are indicated with red arrows. The subunits of ligand-bound SCO4393 are given in dark colours (blue and green) and the subunits of the ligand-free structure are given in light shades of blue and green.

- Global comparison of the ligand-free (light colours) and ligand-bound (dark colours) structure of SCO4393.
- Close up of conformational shift around the active site. Important residues relating to the position of the loop and for phosphate binding are labelled and the shift of the loop toward the active site is shown.
- Surface view of ligand-bound SCO4393 with open entry to the active site (dark colours) on the left and on the right, comparison with the ligand-free structure (light, transparent colours) with obscured entry. The surface view is in the same orientation as 5B.

STRUCTURAL INSIGHTS INTO SCO4393

N-terminally His₆-tagged SCO4393 was heterologously expressed in *E. coli* BL21 cells and purified to homogeneity (see Materials and Methods). The structure of SCO4393-His₆ was determined by X-ray crystallography. The refined 2.0 Å resolution model of SCO4393 consisted of residues 4-251 and positive electron density within the active site was noticed (described below). The refinement of the structure of the ligand-free enzyme, obtained by soaking the crystals in GlcN-6P, was determined to a resolution of 1.6 Å, using the 2.0 Å SCO4393 model as a template. *S. coelicolor* SCO4393 forms a dimer, with two active sites at the monomer interfaces on either side of the complex (Fig. 3). There is structural similarity between SCO4393 and other SIS-domain proteins, especially phosphoheptose isomerase BH3325 (3CVJ) of *Bacillus halodurans* and sedoheptulose-7-phosphate isomerase GmhA (2I2W), which is involved in lipopolysaccharide biosynthesis in *E. coli* (Taylor et al., 2008).

STRUCTURAL STUDIES OF SCO4393 LIGAND BINDING

Strong electron densities were observed within the SCO4393 active site, suggesting that the protein was isolated from *E. coli* with a bound ligand (Fig. 4). One density (labelled * in Fig. 4) is in close proximity to serine residues Ser54, Ser119 and Ser121, which have been implicated in phosphate binding. This suggests that the observed density relates to a phosphate group. Given the link to GlcNAc metabolism, the ligand could be GlcNAc-6P or a related phosphosugar. Interestingly, an Asp179Asn mutation is observed in suppressor mutants SMA11 and SMA13, which likely disrupts the catalytic activity of SCO4393 by destabilising the active site (Fig. 4), thus rendering it non-functional. Comparison of the structures of the substrate-free structure to that of the ligand-bound SCO4393 reveals minor changes in the structure of the protein with the exception of the conformational shifts of two loops (Fig. 5A). The loop formed between residues Ser226 and Glu234 is likely involved in keeping the ligand in position. In the substrate-free structure, the loops are shifted such that the binding pocket is largely obscured (Fig. 5B).

To investigate whether SCO4393 can bind GlcNAc-6P, crystals were soaked in 100 mM GlcNAc-6P for up to 5 min and the structures determined to a resolution of 2.5 Å. Crystals that had been soaked for less than five min retained an empty binding site. The active site of the crystal soaked for 5 min contained GlcNAc-6P but the enzyme was in ligand-free conformation, despite interactions with the *N*-acetyl-amine functional group and the phosphate moiety (Fig. 6). Indeed, the phosphate group was bound by the serine residues. However, the structure showed that GlcNAc-6P was in the alpha form, and NMR analysis of the ligand-soaking solution also determined it to be α -GlcNAc-6P (data not shown). Given that, to our knowledge, biological reactions of GlcNAc-6P require the β -form, we cannot rule out the consequences of soaking with α -GlcNAc-6P on binding and the potential enzymatic reaction.

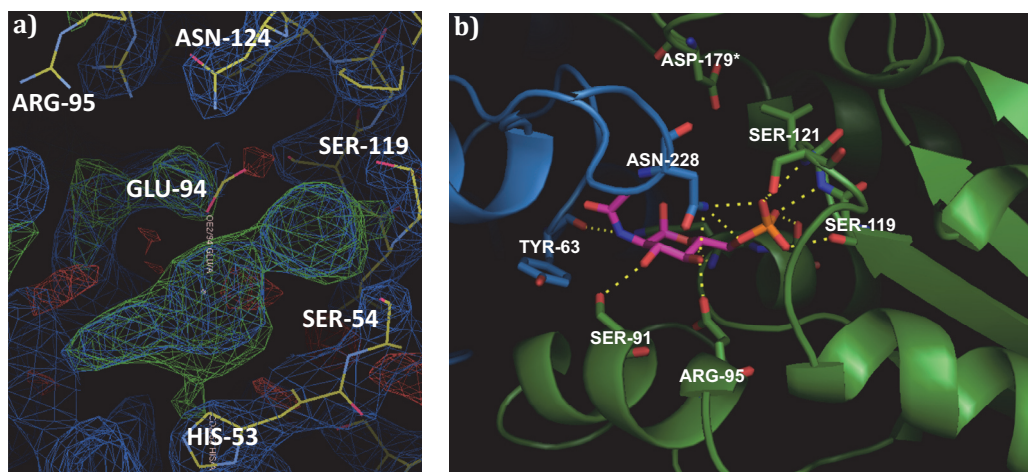


FIGURE 6. SCO4393 soak with GlcNAc-6P.

SCO4393 active site after soaking with 100 mM α -GlcNAc-6P for 5 minutes. SCO4393 remains in ligand-free conformation after soaking. The residues mutated in suppressor SMA11 (Asp179) is labelled by an *.

- View of the electron density of active site of SCO4393; mapped densities shown in dark blue, positive density differences in green and negative density differences in red. The large, positive density (green) in the centre shows the α -GlcNAc-6P with the phosphate group in the vicinity of the serine residues and the sugar moiety between GLU-94 and HIS-53.
- Close-up of the active site with the modelled GlcNAc-6P illustrating the interactions between the metabolite and residues of the SCO4393 active site. The subunits and residues of SCO4393 are shown in dark blue and green, GlcNAc-6P is shown in pink. Nitrogen is represented in blue, oxygen in red and phosphorus in orange.

SCO4393 LIGAND BINDING STUDIES

In addition to structural studies, SCO4393-ligand binding was also examined by isothermal titration calorimetry (ITC). Potential ligands were titrated at a concentration of 1 mM into 50 mM SCO4393 at 25°C. Of all the molecules tested, only α -GlcNAc-6P was bound by the protein, while no binding was seen for GlcNAc, GlcNAc-1P, Glc-6P or Fru-6P (Fig. 7). The importance of the *N*-acetyl group, given that GlcN-6P was unable to bind SCO4393, and the C6 phosphate group, given the complete lack of binding of GlcNAc and GlcNAc-1P, is highlighted.

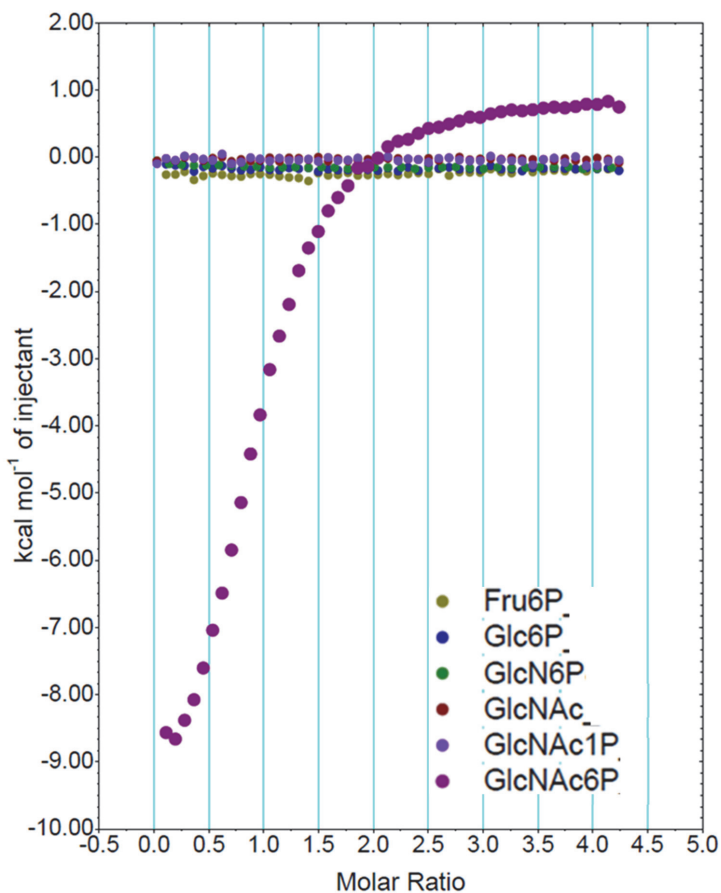


FIGURE 7. SCO4393 binding assays investigated by ITC.

For ITC binding studies, 1 mM ligand was titrated with 6 or 8 μ L injections into 50 mM purified SCO4393. Fru-6P (dark yellow), Glc-6P (blue), GlcN-6P (green), GlcNAc (dark red), GlcNAc-1P (bright purple) and α -GlcNAc-6P (aubergine) were tested. Note that SCO4393 was only able to bind α -GlcNAc-6P.

DISCUSSION

N-acetylglucosamine is a preferred carbon source for streptomycetes and stands at the cross-roads between aminosugar metabolism, glycolysis and cell-wall synthesis (Fig. 8). The molecule also plays a key role in nutrient sensing and the ultimate decision to initiate development and antibiotic production (Rigali *et al.*, 2008). Deletion of *nagA* or *nagB* results in altered antibiotic production, likely due to the accumulation of GlcNAc-6P or GlcN-6P, when grown in the presence of GlcNAc or GlcN, respectively (Świątek *et al.*, 2012a). This prompted further investigation into the possibility of altering the flux of GlcN(Ac) as a strategy to activate antibiotic production. In this work, we investigated a new enzyme involved in aminosugar metabolism that was discovered via a suppressor screen of *nagB* mutants, which fail to grow on GlcN or GlcNAc. Suppressor mutations that relieved aminosugar sensitivity of *nagB* mutants were found in SCO4393, which encodes a likely phosphosugar isomerase (Świątek, 2012).

The genetic environment around SCO4393 is highly conserved in streptomycetes. Homologs of SCO4393, with relatively low sequence similarity (around 30%), are also found in bacteria such as firmicutes and proteobacteria and in these bacteria, the gene is often found associated with *pts* transporter genes or adjacent to *nagA* and *glmS*. Both NagA and GlmS generate GlcN-6P, from GlcNAc-6P and Fru-6P, respectively (Fig. 8). Interestingly, divergently expressed from SCO4393 is the gene of iron-homeostasis regulator DmdR1 (SCO4394) in *S. coelicolor*, which is induced by GlcNAc (Craig *et al.*, 2012). Addition of iron to rich media with GlcNAc restores antibiotic production and development under feast conditions in *S. coelicolor* (Lambert *et al.*, 2014). These data suggest linkage between GlcNAc and iron homeostasis in *Streptomyces*.

The crystal structure of SCO4393 was resolved to a high resolution and showed that the entry of the SCO4393 active site is blocked in the substrate-free conformation, while it is opening the ligand-bound form. The ligand-bound structure showed densities of an unknown ligand trapped in the active site. Given the proximity of the observed densities to the serine residues, which are most likely involved in phosphate binding, we speculate that part of the observed density is that of the phosphate group of the ligand, kept in place by Ser54, Ser119 and Ser121. Indeed, the serine residues of SCO4393 bound the phosphate group of GlcNAc-6P (Fig. 6), after crystals were soaked in the compound. ITC binding studies demonstrated that SCO4393 binds α -GlcNAc-6P, while it failed to bind GlcNAc, GlcNAc-1P, Glc-6P or Fru-6P (Fig. 7). Though this suggests that the phosphate group and acetyl group may be essential, proteins from the crystal soaked in α -GlcNAc-6P for 5 min remained in ligand-free form, despite the interactions of the SCO4393 backbone with both the phosphate and acetyl groups of the ligand. The potential catalytic residues of the SCO4393 binding pocket are characteristic of sugar isomerases, such as glucose-6P isomerase (Solomons *et al.*, 2004), with His, Arg and Glu involved in the opening and closing of the ring, and stabilization of the intermediate. Preliminary modelling of GlcNAc-6P onto the density within the active site of ligand-bound SCO4393 suggests that the metabolite would have to be in an open-ring conformation, with the further density being an acetyl-amine group (NH-C=O-CH₃) (Fig. 4). It should be noted that experiments were performed with α -GlcNAc-6P, while β -GlcNAc-6P is thought to be biologically favoured. Taken together, the *in vitro* data suggest that the substrate is a phospho-aminosugar, and related to GlcNAc-6P.

The key question to address is, what is the toxic molecule that accumulates in *nagB* mutants grown on high concentrations of GlcN or GlcNAc? Mutants that lack a functional NagA enzyme accumulate high levels of GlcNAc-6P, which is lethal in *B. subtilis* and *E. coli* (Plumbridge, 2015). However, *S. coelicolor nagA* null mutants grow in the presence of

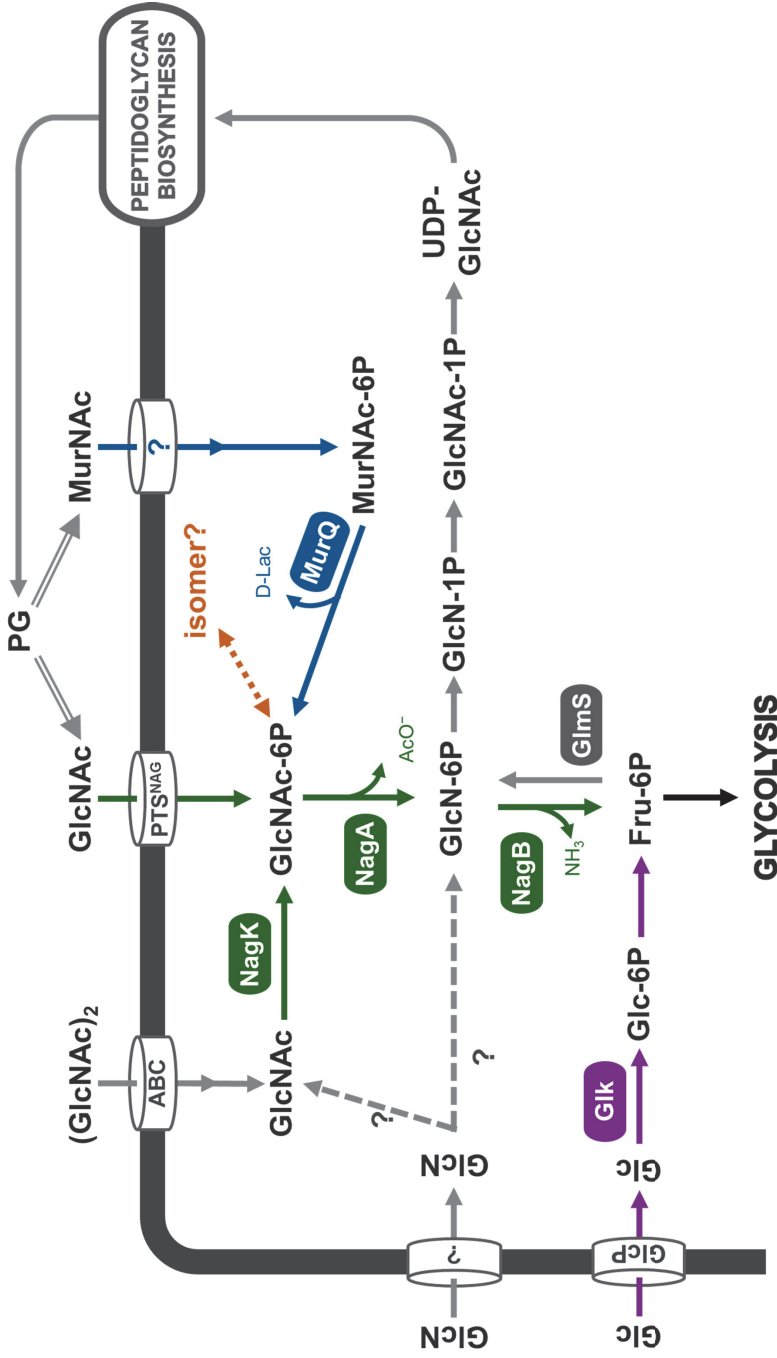


FIGURE 8. Schematic representation of GlcNAc and GlcN metabolism and peptidoglycan recycling in *S. coelicolor*. Peptidoglycan degradation releases monomers of GlcNAc and MurNAc, which are subsequently taken up by the cells for recycling. The PTS phosphorylates monomeric GlcNAc during transport into the cell while MurNAc metabolism involves transport and phosphorylation by unidentified proteins, followed by the conversion of MurNAc-6P to GlcNAc-6P by MurQ. Subsequently, GlcNAc-6P is deacetylated to GlcN-6P by NagA, and NagB is able to convert GlcN-6P to Fru-6P for glycolysis. Alternatively, GlcN-6P can be used for the biosynthesis of novel PG and, in the absence of aminosugars, GlcN-6P can also be synthesised via Glms from glycolytic products (Fru-6P). Chitin derived, dimeric (GlcNAc)₂ is imported via the ABC transporter system DasABC and cleaved to intracellular monomers of GlcNAc, which is phosphorylated by NagK. Limited information is available on GlcN transport and metabolism in *S. coelicolor* but GlcN metabolic pathway is proposed via acetylation to GlcNAc and NagK phosphorylation or GlcN could also be phosphorylated to GlcN-6P directly. Also shown is glucose (Glc) metabolism towards glycolysis. Glc is imported by MFS importer GlcP and then phosphorylated to Glc-6P by glucokinase (Glk). Metabolic routes are represented by arrows and proposed/unknown routes by dotted arrows, with central pathways and enzymes highlighted in green. D-Lac, D-lactate; AcO⁻, acetate; NH₃, ammonia. For details, refer to the text.

GlcNAc, strongly suggesting that toxicity is not caused by GlcNAc-6P or direct metabolic derivatives, and that instead the toxic compound is derived from GlcN-6P. Indeed, deletion of *nagA* is sufficient to restore growth of *nagB* mutants on aminosugars, even though preliminary metabolomic experiments revealed strong accumulation of GlcNAc-6P in these mutants (MU, GPvW and Christoph Müller, unpublished data). Zooming in on GlcN-6P, this is the starter molecule for cell-wall biosynthesis. We believe that the biosynthetic pathway of Lipid II may indeed play a major role in toxicity. For one, toxicity of GlcN(Ac) is relieved when cells are pre-grown to early exponential phase (Świątek *et al.*, 2012a). At this stage, peptidoglycan biosynthesis is maximal, and precursors are readily incorporated. This may not yet be the case for germinating spores. A second indication that cell-wall precursors play a role in toxicity comes from so-called L-forms. These are cells that lack a wall, enforced by growth in the presence of the cell-wall targeting antibiotic penicillin and the cell wall hydrolase lysozyme (Errington, 2013; Mercier *et al.*, 2014). Streptomycetes can also be forced to produce L-forms (Innes & Allan, 2001), and these sustain spontaneous mutations in the *mur* genes that encode components of the cell-wall precursor pathway. This again suggests that accumulation of cell-wall precursors may be lethal for streptomycetes. Metabolic analysis of SCO4393 suppressor mutants showed that they accumulate GlcN-6P (preliminary data, not shown), which would suggest that the absence of SCO4393 renders GlcN-6P accumulation non-toxic and that SCO4393 does not block GlcN-6P production but rather acts on GlcN-6P or its derivative.

Taken together, our data suggest that one or more toxic intermediates are derived from GlcN-6P but not from GlcNAc-6P, and that they relate to cell-wall precursor biosynthesis. SCO4393 is likely directly involved in the accumulation of the toxic intermediate. Structural studies indicate that SCO4393 binds a phospho-aminosugar in its linear form, structurally related to GlcNAc-6P. The latter is supported by ITC experiments that revealed that SCO4393 binds α -GlcNAc-6P. However, this is in direct conflict with the biological experiments that show that accumulation of GlcNAc-6P in cells expressing SCO4393 does not affect growth of *S. coelicolor*. Hence, we propose that the substrate of SCO4393 is a related aminosugar, with *N*-acetylgalactosamine-6P and *N*-acetylglutamate-6P as candidates, whereby *N*-acetylgalactosamine-6P is a GlcNAc-6P isomer and precursor for bacterial cell-wall components. We are currently focusing our research on elucidating the precise reaction that is catalysed by SCO4393 and the nature of the toxic intermediate.

ACKNOWLEDGEMENTS

We are grateful to Marcellus Ubbink and Vera van Noort for stimulating discussions, and to Raffaella Tassoni for help with the ITC experiments.

CHAPTER V

SUPPRESSOR MUTANTS AS A TOOL TO IDENTIFY GLCN METABOLIC GENES IN *S. COELICOLOR*

Mia Urem, Magdalena A. Świątek-Połatyńska, Roger C. A. W. van Nassau,
Christian Rückert, Jörn Kalinowski and Gilles P. van Wezel

ABSTRACT

Streptomyces are prolific producers of antibiotics, but many compounds are poorly expressed under laboratory conditions. Uncovering the control mechanisms governing the transcription of antibiotic biosynthetic genes is important for the activation and screening of cryptic antibiotics. The phosphorylated aminosugars glucosamine-6P (GlcN-6P) and *N*-acetylglucosamine (GlcNAc-6P) modulate the activity of the global antibiotic repressor DasR. While GlcNAc metabolism has been studied extensively, little is known of how GlcN is metabolised in *Streptomyces*. In an effort to define the GlcN metabolic pathway we analysed five mutants that are disturbed in GlcN metabolism, and had previously been obtained in a suppressor screen based on the lethality of GlcN to *nagB* null mutants. This identified mutations in *nagK* for the GlcNAc kinase and in *rokL6* (SCO1447) for a ROK-family protein. Deletion of either *nagK* or the GlcNAc deacetylase *nagA* in *nagB* mutants restores growth on GlcN, strongly suggesting that NagK and NagA are essential for GlcN metabolism; this suggests that after internalization, GlcN is first acetylated and phosphorylated and then follows the same metabolic route as GlcNAc-6P. Deletion of SCO1447 in *nagB* mutants relieved growth on GlcN but not on GlcNAc, identifying it as a GlcN-specific transcriptional regulatory gene.

INTRODUCTION

The emergence and rapid spread of infectious diseases involving multi-drug resistant (MDR) bacterial pathogens represents a major problem for the treatment of bacterial infections (WHO, 2014; O'Neill, 2014). One of the challenges in finding adequate novel antibiotics is replication, the rediscovery of previously identified antibiotics, while new molecules are rarely found; resulting in the extremely high cost and consequent drying up of industrial drug-discovery pipelines (Cooper & Shlaes, 2011; Kolter & van Wezel, 2016; Payne *et al.*, 2007). Multicellular, Gram-positive actinomycetes, like the streptomycetes, are producers of the majority of clinically employed antibiotics, and also a rich source of other secondary metabolites with medical and biotechnological importance, such as anticancer, antifungal and immunosuppressant drugs (Barka *et al.*, 2016; Bérdy, 2005; Hopwood, 2007). Finding the triggers and cues that activate the production of secondary metabolites is now a major challenge for novel drug discoveries, and the answers lie, among others, in the ecological context in which streptomycetes grow (Seipke *et al.*, 2012; Zhu *et al.*, 2014a).

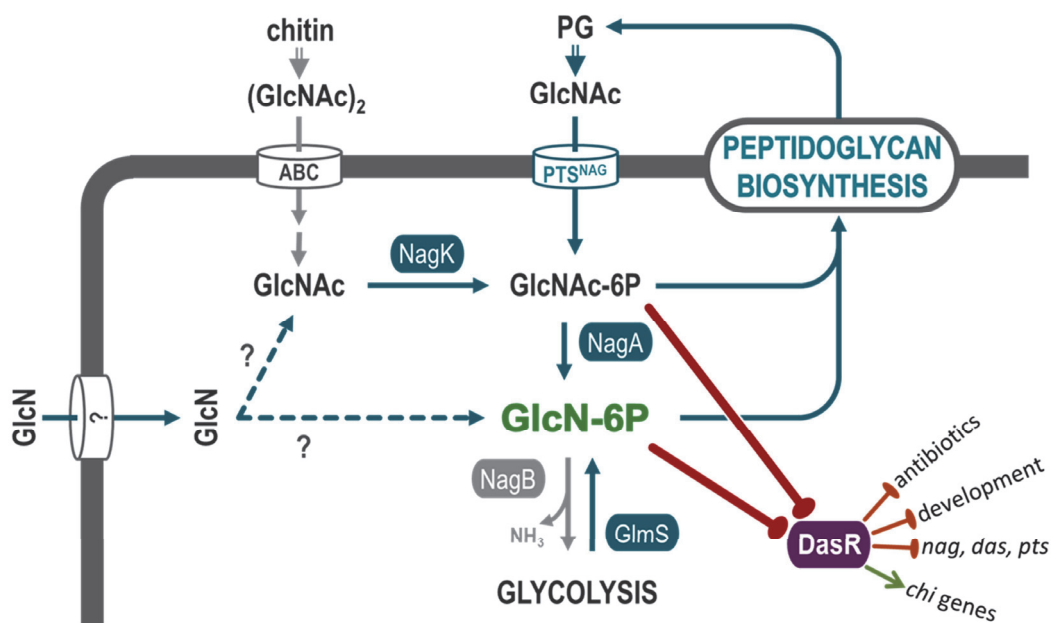


FIGURE 1. Peptidoglycan recycling and GlcN(Ac) metabolism leading to activation of the secondary metabolism in *S. coelicolor*.

Schematic representation of GlcNAc and GlcN metabolism and DasR regulation. Peptidoglycan recycling releases GlcNAc monomers which are transported into the cell and phosphorylated by the GlcNAc specific PTS. NagA deacetylates GlcNAc-6P to GlcN-6P, which is converted to Fru-6P and channelled into glycolysis. Also shown is GlcN-6P synthesis via GlmS and routes leading to cell wall synthesis. In contrast, hydrolysed chitin, in the form of GlcNAc dimers, is transported into the cell by ABC transporter DasABC, cleaved into monomers intracellularly and phosphorylated by GlcNAc kinase, NagK. The proposed pathway for GlcN metabolism is via GlcNAc metabolism by acetylation of GlcN to GlcNAc and then phosphorylation by NagK. Alternatively, and/or additionally, GlcN could be phosphorylated by an identified kinase directly to GlcN-6P. Allosteric effectors GlcNAc-6P and GlcN-6P inhibit DasR (in purple), the global, pleiotropic repressor of antibiotic production, development and GlcNAc metabolism (*nag*) and transport (*das* and *pts*) and activator of chitinolytic hydrolases (*chi*).

Inhibition is represented by red lines (with ellipses), activation by green arrows. GlcN-6P, as an important central metabolic intermediate and signalling molecule, is highlighted in green. Metabolic pathways leading to PG synthesis and recycling are highlighted in blue.

A well-studied example of an antibiotic-activating signal is *N*-acetylglucosamine (GlcNAc); its regulatory role and metabolic pathway have been extensively studied in model organism, *Streptomyces coelicolor* (Figure 1; Świątek *et al.*, 2012a; Świątek *et al.*, 2012b; Rigali *et al.*, 2008; Urem *et al.*, 2016a). When *S. coelicolor* is grown under rich growth conditions (*feast*) supplemented with GlcNAc, both morphological and chemical differentiation (including antibiotic production) are repressed in favour of growth. Conversely, under poor growth conditions (*famine*), high concentrations of GlcNAc induce development and antibiotic production; presumably, the accumulation of GlcNAc, in an otherwise nutrient-depleted environment, is interpreted as a signal that PCD has been initiated (Rigali *et al.*, 2008). A key regulator in GlcNAc sensing is the global repressor DasR, which belongs to the family of GntR regulators. In *S. coelicolor*, all pathway-specific regulatory genes for antibiotic production are controlled by DasR (Świątek-Połatyńska *et al.*, 2015). The allosteric control of DasR by GlcNAc metabolic intermediates is shown schematically in Figure 1 and reviewed in Chapter II.

The utilisation of glucosamine (GlcN), which originates from chitosan (an *N*-deacetylated derivative of chitin) and de-acetylated GlcNAc portions of PG, likely also involves complex metabolic routes, in addition to the *csnR-K* operon that encodes the machinery required for the import and utilisation of GlcN dimers and chito-oligosaccharides (Viens *et al.*, 2015; Dubeau *et al.*, 2011). A suppressor screen, making use of the lethality of GlcN and GlcNAc to *S. coelicolor nagB* mutants, directly or indirectly due to the accumulation of GlcN-6P, showed ambiguity as to how aminosugars are metabolised in streptomycetes (Świątek *et al.*, 2012a; Świątek *et al.*, 2012b). Spontaneous suppressor mutants that survive on GlcNAc include those mutated in *nagA*, which is required for the formation of GlcN-6P from GlcNAc-6P during GlcNAc metabolism (Fig. 1, Chapter II). However, GlcN toxicity is also relieved by mutations in *nagA*, suggesting that GlcN may be metabolised via the GlcNAc metabolic route (Świątek *et al.*, 2012b), rather than taking a more direct pathway toward GlcN-6P by GlcN phosphorylation.

In this work, we aimed to identify genes involved in GlcN transport and metabolism, by screening *S. coelicolor nagB* suppressor mutants isolated in the presence of high concentrations of GlcN. Genome sequencing of selected mutants revealed mutations in SCO1447 (*rokL6*), a ROK-family transcriptional regulator, as well as GlcNAc metabolic genes.

MATERIALS AND METHODS

Bacterial strains and growth media.

Bacterial strains used in this work are listed in Table S1. *E. coli* JM109 (Sambrook et al., 1989) was used as host for routine cloning, and *E. coli* ET12567 (Macneil et al. 1992) to produce non-methylated DNA for introduction into *Streptomyces* (Kieser et al., 2000). *Streptomyces coelicolor* A3(2) M145 was obtained from the John Innes Centre strain collection, and its *nagB* mutant was described previously (Świątek et al., 2012a). Cells of *E. coli* were grown in Luria-Bertani broth (LB) at 37°C. All *Streptomyces* media and routine *Streptomyces* techniques are described in the *Streptomyces* manual (Kieser et al., 2000). Yeast-extract malt extract (YEME; Kieser et al., 2000) was used to cultivate mycelia for preparing protoplasts and for genomic DNA isolation. R2YE (regeneration media with yeast extract) agar plates were used for protoplast regeneration, while SFM (soy flour mannitol) agar plates were used to prepare spore suspensions. Phenotypic characterization was done on R2YE and minimal media (MM) agar plates.

Gene replacement and knock-out mutants.

Deletion mutants of *S. coelicolor* were constructed according to a previously described method (Świątek et al., 2012a). For the deletion of SCO1447, the -1251/LR+3 (left flank) and +1200/+2565 (right flank) regions, relative to the start of the gene, were amplified by PCR using primers described in Table S2. The left and right flanks were cloned into pWHM3 (Vara et al., 1989), which is an unstable multi-copy vector that allows efficient gene disruption (van Wezel et al., 2005). The apramycin resistance cassette *aac(3)IV* flanked by *loxP* sites (*apra-loxP*) was cloned into the engineered *Xba*I sites between the flanks to create knock-out constructs pGWS948. In the same fashion, the flank regions of SCO1448 (-1422/+9 and +1221/+2603) were cloned into pWHM3 with the *apra-loxP* to create pGWS955. The plasmids were introduced into *S. coelicolor* M145 or its *nagB* mutant for gene replacements with *apra-loxP*. The apramycin resistance cassette was then excised by introduction of Cre recombinase expression plasmid, pUWLcre, to create markerless deletion mutants. The correct recombination event in each of the mutants was confirmed by PCR. *apra-loxP* gene replacement mutants were previously made for mutants *nagAB* and *nagKAB* (Świątek et al., 2012a) but the deletion mutants were created by transformation with pUWLcre here. For genetic complementation of *nagA* with its own promoter, which is located upstream of *nagK* (SCO4285), the *nagKA* operon promoter was cloned upstream of the *nagA* gene into pHJL401 (van Wezel & Kraal, 2000). The -136/-1 region (numbering relative to the translational start codon) encompassing the promoter region of *nagKA* and the +1/+1146 gene coding region of *nagA* were amplified from the *S. coelicolor* M145 chromosome using primers described (Table S2). pHJL401 is a low-copy number shuttle vector that is very well suited for genetic complementation experiments (van Wezel et al., 2000a).

Genomic DNA isolation and sequencing.

Strains were grown for 24 h in 50 mL YEME for genomic DNA isolation. Genomic DNA was isolated by phenol-chloroform extraction as described (Kieser et al., 2000) and sequenced.

RESULTS

Characterization of GlcN-derived *S. coelicolor nagB* suppressors.

The metabolic pathway of glucosamine is largely undefined in *S. coelicolor* and to identify genes involved in its metabolism and transport, the occurrence of spontaneous suppressor mutants, that relieve the toxicity of GlcN to *S. coelicolor nagB* mutants, was exploited. As GlcN is lethal to the *nagB* mutant, only strains that have sustained a second-site mutation can survive (Świątek *et al.*, 2012a; Świątek *et al.*, 2012b). It is likely that these suppressor mutants (or, suppressors) are mutated in GlcN-related genes, preventing the toxic accumulation of intermediate metabolites. For this, spores of the *nagB* mutant were plated at a high density on minimal medium (MM) agar plates with 50 mM GlcN. Over 300 spontaneous suppressor mutants, that were able to grow in the presence of GlcN, were isolated.

The suppressor mutants were grouped by phenotypic characteristics (in particular by development and pigmentation) and representatives of these groups were selected and screened for their suppressor mutations. We previously identified suppressor mutations in *nagA*, and these mutants were filtered out by genetic complementation as described (Świątek *et al.*, 2012a; Świątek *et al.*, 2012b). In brief, a plasmid expressing *nagA* was introduced into the suppressor mutants, and transformants no longer able to grow on GlcN were discarded. Following this filtration of the group representatives, two suppressor mutants were considered for further analysis (designated SMG). In an attempt to minimise the likelihood of selecting *nagA* mutated suppressors, a second set of suppressors was selected by plating transformants of *nagB* mutants harbouring an extra copy of *nagA* (on plasmid pHJL401) on MM agar plates with GlcN. From this set of suppressors, two group representatives (designated SMG+) were selected as well. The phenotypic characteristics of this selected set of GlcN suppressors (SMG38, SMG42, SMG+3 and SMG+4) to which we added one suppressor mutant (SMG1) isolated in a previous screen (Świątek *et al.*, 2012a; Świątek *et al.*, 2012b), were analysed on solid minimal media (MM) with different sugars (Fig. 2).

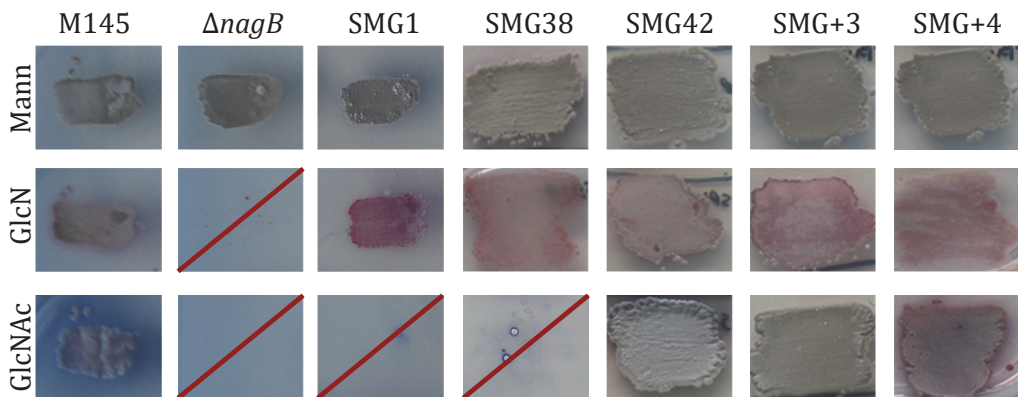


FIGURE 2. Phenotypic analysis of GlcN-derived *S. coelicolor nagB* suppressor mutants.

Spores of *S. coelicolor* wildtype M145, *nagB* deletion mutant and *nagB* suppressor mutants (SMG1, SMG38, SMG42, SMG+3 and SMG+4) were plated onto minimal medium and supplemented with 50mM of mannitol (Mann), glucosamine (GlcN) or *N*-acetylglucosamine (GlcNAC). SMG suppressor mutants are derived from *nagB* mutants on GlcN and SMG+ suppressors are derived from *nagB* harbouring a plasmid pGWS961 prior to isolation from GlcN. Mutants for which GlcN or GlcNAC was lethal are indicated with a red line. Suppressor SMG1 was first identified and described in Świątek, et al. (2012).

The five GlcN-derived *S. coelicolor nagB* suppressor mutants showed normal growth and development on MM agar with mannitol (Fig. 2). Interestingly, GlcN suppressor mutants SMG1 and SMG38 were unable to alleviate GlcNAc toxicity, which strongly suggests that mutations might have arisen in genes that are specific for the GlcN-metabolic pathway. However, growth of SMG1 and SMG38 was somewhat compromised on MM agar plates with GlcN, suggesting that the suppressor mutations could not fully alleviate the toxicity of the accumulation of GlcN-6P or (a) metabolic derivative(s) thereof. Suppressor mutants SMG42, SMG+2 and SMG+3 grew well on both sugars; however, development of all three is diminished on GlcN and altered on GlcNAc for SMG42, which is whiter in pigment, *i.e.* sporulation had been compromised. The three suppressor mutants produced antibiotics on GlcN but antibiotic production was blocked on GlcNAc for SMG42 and SMG+2 and altered for SMG+3 (loss of the production of the blue-pigmented actinorhodin). The loss of activation of antibiotic production suggests that these three suppressor mutants had, at least partially, lost their ability to sense GlcNAc under nutrient-limiting or *famine* conditions (MM agar) (Fig. 2). All five suppressor mutants had lost their ability to sense GlcNAc under rich growth conditions (*feast*; R2YE agar), given the loss of inhibition of antibiotic production in all strains and loss of inhibition of development in some (SMG42, SMG+2 and SMG+3, and somewhat in SMG38) (Fig. S1).

TABLE 1. Mutations identified in GlcN-derived *S. coelicolor nagB* suppressors.

SMG1			SMG38			Position ^d	SCO # ^e	Annotation		
Type ^a	nt ^b	aa ^c	Type ^a	nt ^b	aa ^c					
INS		fs	-	-	-	1543479i	SCO1447	transcriptional regulator (ROK family)		
-	-	-	DEL	G	fs	1544534				
-	-	-	DEL	G	fs	3850016	SCO3485	LacI family transcriptional regulator		
-	-	-	DEL	G	fs	3850017				
SNP	C>A	Q117K	-	-	-	3928899	SCO3554	putative integral membrane protein		
SNP	A>C	H182P	-	-	-	6769952	SCO6167	proline rich protein (putative membrane protein)		
-	-	-	SNP	C>G	H424Q	7265819	SCO6563	integral membrane transporter		
SMG+3			SMG+4			Position	SCO #	Annotation		
Type ^a	nt ^b	aa ^c	Type ^a	nt ^b	aa ^c					
-	-	-	-	-	-	INS +A fs	521609i	SCO0492	peptide synthetase	
-	-	-	SNP	G>C	P71R	-	1749870	SCO1635	hypothetical protein	
SNP	C>A	A315S	-	-	-	-	1760847	SCO1647	Pup deamidase/depupylase	
INS	+C	fs	-	-	-	INS +C fs	3849222i	SCO3485	LacI family transcriptional regulator	
-	-	-	DEL	-	-	DEL [#]	4692947 -	SCO4277 -	NagA, N-acetylglucosamine-6-phosphate deacetylase	
-	-	-	-	-	-		4699275	SCO4283		***
-	-	-	SNP	G>C	A354G		4699483	SCO4284		NagA, N-acetylglucosamine-6-phosphate deacetylase
SNP	T>C	K314R	SNP	T>C	K314R		4699603			
SNP	C>T	G157E	SNP	C>T	G157E		4700074			
-	-	-	DEL	-	-	4700543 -	SCO4285	NagK, N-acetylglucosamine kinase		
-	-	-	-	-	-	4701656				
-	-	-	INS	+6N	-	INS +6N -	5586261i	SCO5138	hypothetical protein	
-	-	-	SNP	C>T	A139T	SNP C>T A139T	7050737	SCO6384	integral membrane lysyl-tRNA synthetase	
-	-	-	SNP	A>C	K498Q	-	7190566	SCO6496	dehydrogenase	
-	-	-	SNP	T>G	V388G	-	7778607	SCO7004	carbohydrate kinase	

a - Type indicates whether the mutation is a SNP (single nucleotide polymorphism), deletion or insertion.
b - SNP substitutions are given as well as nucleotides that are inserted and, in case of single nucleotide deletions, the deleted nucleotide is given and strikethrough. +6N indicates the insertion of 6 nucleotides, please see Table S3 for details.
c - Amino acid substitutions are given if applicable and frameshifts are indicated by 'fs'.
d - Genomic position or range is given, 'i' indicates insertion.
e - *S. coelicolor* SCO numbers.
*** SCO4277 - putative tellurium resistance protein, SCO4278 - conserved hypothetical protein, SCO4279 - putative acetyltransferase, SCO4280 - putative reductase, SCO4281 - conserved hypothetical protein, SCO4282 - putative dimeric protein and SCO4283 - putative sugar kinase.
Region from position 4692947- 4701656 deleted in SMG42.

Identification of secondary mutations in GlcN-derived *S. coelicolor nagB* suppressors.

The genomic DNA of the five suppressor mutants was isolated from liquid-grown YEME cultures and sequenced by whole-genome sequencing. The genome of our laboratory-specific variant of *S. coelicolor* A3(2) M145 was also sequenced and used as a reference genome for detection of single nucleotide permutations (SNPs) and other mutations in the suppressor strains (Table S3). Only non-silent mutations, that were not present in the wild-type nor shared between all of the suppressor mutants, were considered (Table 1).

Analysis of the mutations identified in the suppressor mutants revealed that one of two genes, namely SCO1447 or *nagA*, were mutated or deleted in particular (Table 1). Surprisingly, despite the presence of a plasmid expressing *nagA* (SCO4284) in suppressor mutants SMG+3 and SMG+4, and the genetic complementation of SMG42 with that same plasmid, still all three were characterised by SNPs and/or deletions in *nagA* and additionally, large genomic disruptions in the *nagA* genomic context (region SCO4277-4285) were identified for SMG+4 and SMG42. This underlines the crucial role for *nagA* and potentially also its flanking genes (including *nagK*) in GlcN metabolism; the role of *nagK* (SCO4285) in GlcN metabolism is considered in more detail below. GlcN-specific suppressors SMG1 and SMG38 had single mutations in the ROK-family protein, SCO1447, in both cases resulting in a frame-shift mutation and hence an inactive gene product. Given that both strains had mutations that relieved GlcN toxicity but were unable to grow on GlcNAc, this strongly suggests that SCO1447 is a GlcN-specific transcriptional regulator and the first gene unique to GlcN metabolism and/or signalling that has been identified to date.

Other SNPs identified in the suppressor mutants were diverse and less likely to be involved in GlcN metabolism. These included genes for SCO0492, involved in the biosynthesis of the siderophore coelichelin, SCO1647, a proteasome accessory protein, SCO6384, a putative integral membrane lysyl-tRNA synthetase, SCO6496, a putative dehydrogenase, SCO6563, homolog of oxalate:format exchange protein from *Oxalobacter formigenes*, SCO7004, homolog of glycerol kinase from *Bacillus subtilis* and hypothetical genes SCO1635, SCO5138, SCO3554 and SCO6167. Considering the crucial role of *nagA* (Świątek *et al.*, 2012a; Świątek *et al.*, 2012b) and SCO1447 (see below) in relieving GlcN toxicity, none of these additional mutations were considered further.

Deletion of *nagK* suppresses toxicity of GlcN and GlcNAc to *nagB* mutants.

Closer analysis of the *nagA*-mutated suppressors revealed that the majority of the genomic region from SCO4277 to SCO4285 is absent in suppressor mutants SMG+4 and SMG42 (Table 1 and S3). This region includes *nagK* (SCO4285) and *nagA* (SCO4284), regulated from the same promoter upstream of *nagK*, and a gene for a putative acetyltransferase (SCO4279). NagK is a GlcNAc kinase, phosphorylating (chitin-derived) GlcNAc intracellularly (Plumbridge, 2009; Świątek *et al.*, 2012a). To investigate whether NagK indeed plays a key role in GlcN metabolism, *nagK* deletion mutants were created by disrupting the gene in the parental strain *S. coelicolor* M145 and its *nagB*, *nagA* and *nagAB* mutant derivatives, followed by their characterization on MM and R2YE agar plates with or without GlcN or GlcNAc (Fig. 3).

Surprisingly, deletion of *nagK* restored the ability of *nagB* mutants to grow on both GlcN and GlcNAc. The alleviation of GlcNAc toxicity strongly suggests that either a significant portion of GlcNAc is imported as GlcNAc and not as GlcNAc-6P - *i.e.* by an ABC transporter instead of by the PTS - or that GlcNAc-6P is dephosphorylated at a high rate. Given that deletion of *nagK* also rescues the lethality of *nagB* mutants on GlcN, this implies that GlcN is metabolised via NagK substrate GlcNAc. Simultaneous deletion of both *nagK* and *nagA* in

nagB mutants also restored growth on GlcN and GlcNAc, despite the disruption of the GlcNAc metabolic genes. However, disruption of the *nag* genes (individually or simultaneously) had a profound impact on GlcNAc sensing (*feast* or *famine*) in addition to affecting development and antibiotics production in general. For example, GlcNAc sensing under feast conditions is compromised in all mutants; however, GlcNAc did not inhibit the production of antibiotics of any of the mutants on R2YE, and developmental inhibition by GlcNAc was lost in *nagA* and *nagKA* null mutants.

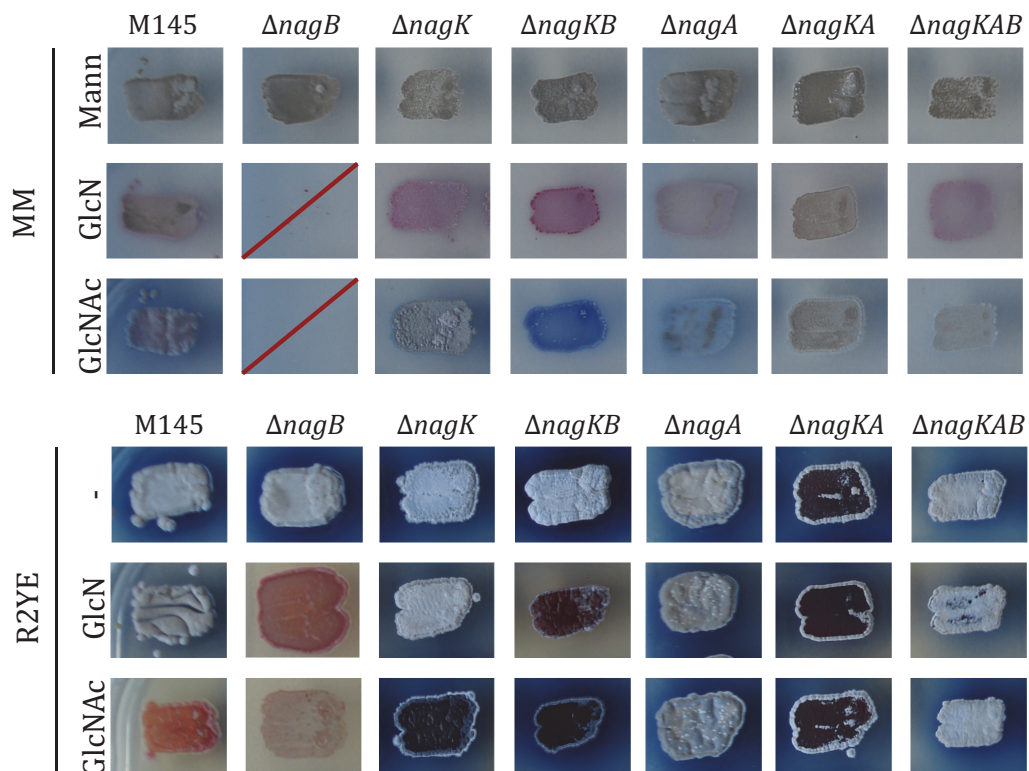


FIGURE 3. Phenotypic analysis of *S. coelicolor* *nagK* and other *nag* mutants on GlcN. Spores of *S. coelicolor* wildtype (M145) and deletion mutants *nagB*, *nagK*, *nagKB*, *nagA*, *nagKA* and *nagKAB* were plated onto minimal medium (MM) or rich glucose-containing media (R2YE) and supplemented with 50mM of mannitol (Mann), glucosamine (GlcN) or *N*-acetylglucosamine (GlcNAc) as indicated. Mutants for which GlcN or GlcNAc was lethal are indicated with a red line.

Transcriptional regulator SCO1447 (RokL6) is involved in GlcN metabolism.

Suppressor mutants SMG1 and SMG38 are of great interest due to their ability to restore growth specifically on GlcN, but not on GlcNAc (Fig. 2). Both *nagB* suppressor mutants had second-site mutations in SCO1447, which encodes a ROK-family protein. We propose the name RokL6 for the protein, based on the nomenclature for ROK-family proteins that was proposed previously (Świątek *et al.*, 2013), with the numbering based on the location of the gene on the ordered cosmid library that contains parts of the *S. coelicolor* chromosome (Redenbach *et al.*, 1996). ROK-family proteins include sugar kinases and regulators, many of which are involved in the control and the utilisation of sugars in bacteria (Titgemeyer *et al.*, 1994), and several ROK-family proteins were implicated in the control of antibiotic production in streptomycetes (Bekiesch *et al.*, 2016; Świątek *et al.*, 2013). RokL6 is a

predicted transcriptional regulator, with similarity to other ROK-family regulators such the *nag* repressor NagC from *E. coli* (Plumbridge, 1995; Plumbridge, 1991). The *rokL6* gene shares its upstream region with the divergently transcribed SCO1448, which encodes a major facilitator superfamily (MFS) transporter. To verify if either RokL6 or SCO1448 plays a role in GlcN metabolism, deletion mutants were created for either gene.

The deletion mutations were phenotypically characterized on MM agar in the presence of GlcN and GlcNAc, as shown in Figure 4. *rokL6-nagB* double mutants grew on MM with GlcN, though much as the original suppressor mutants, not on GlcNAc. Deletion of *rokL6* relieved the toxicity of GlcN to *S. coelicolor nagB* mutants (Fig. 4A), confirming its involvement in the accumulation of toxic intermediates and hence a likely role in GlcN metabolism. The *rokL6* deletion mutant could grow on both sugars, though antibiotic production was blocked by GlcNAc on minimal medium and disruption of *rokL6* in either strain did not significantly affect the phenotype on R2YE agar (Fig. S1).

Considering its genomic location next to and divergently transcribed from *rokL6*, we hypothesized that perhaps SCO1448 may play a role in the internalization of GlcN. However, deletion of the gene for this MFS transporter did not relieve the toxicity of GlcN or GlcNAc to *nagB* null mutants on MM (Fig. 4) nor did its disruption affect antibiotic production or morphology on MM or R2YE agar (Fig. S1). This suggests that, at least under the conditions tested, SCO1448 is not (solely) responsible for the internalization of GlcN.

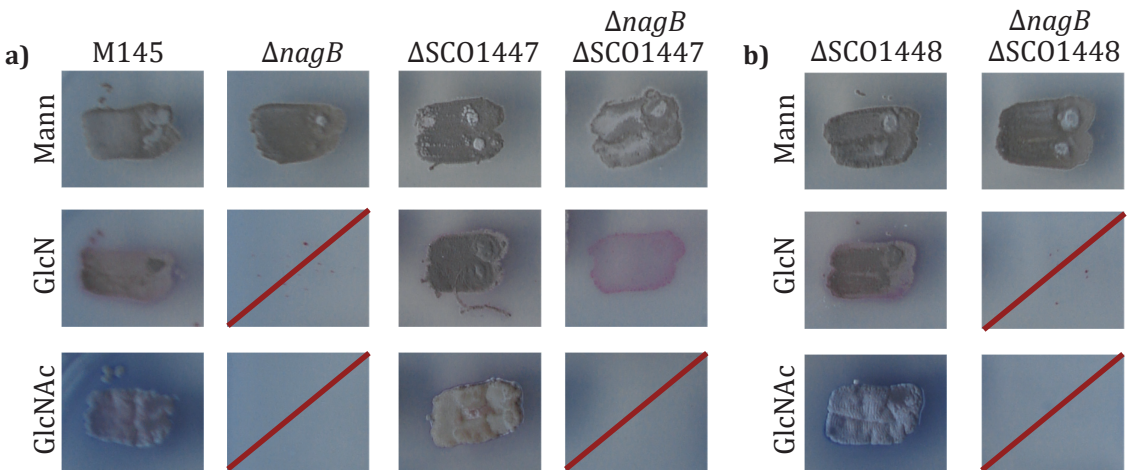


FIGURE 4. Phenotypic analysis of *S. coelicolor* SCO1447 and SCO1448 mutants.

Spores of *S. coelicolor* wildtype (M145) *nagB* and deletion mutants of SCO1447 (a) and 1448 (b) were plated onto minimal medium (MM) or rich media (R2YE) and supplemented with 50mM of mannitol (Mann), glucosamine (GlcN) or N-acetylglucosamine (GlcNAc). Mutants for which GlcN or GlcNAc was lethal are indicated with a red line.

DISCUSSION

Aminosugar metabolism plays an important role in growth and nutrient sensing of streptomycetes. GlcNAc serves as both a carbon and nitrogen source and is also involved in the signalling of various major cellular processes, including development and antibiotic production (Rigali *et al.*, 2008; Urem *et al.*, 2016a). The *S. coelicolor* genome encodes around 700 regulatory proteins in addition to a variety of transport systems and sensory proteins that coordinate the highly complex regulatory networks in this organism (Bentley *et al.*, 2002). One of these regulators is the pleiotropic antibiotic repressor DasR, which controls a large regulon including many metabolic and transport genes relating to aminosugar and polysaccharide utilisation, development and secondary metabolism (Craig *et al.*, 2012; Nazari *et al.*, 2012; Rigali *et al.*, 2006; Świątek-Połatyńska *et al.*, 2015). DasR responds to the metabolic status of the cell, in particular to metabolic intermediates of GlcNAc and GlcN metabolism (Rigali *et al.*, 2008; Tenconi *et al.*, 2015a). With this in mind, we previously investigated the potential of engineering aminosugar metabolism as a means to activate the production of antibiotics in *Streptomyces* (Świątek *et al.*, 2012b).

The GlcNAc metabolic pathway results in the formation of GlcN-6P which is then metabolised, depending on the cellular requirements, via NagB to fructose-6P for entry into glycolysis or, alternatively, via the Mur enzymes towards cell-wall synthesis. For GlcN metabolism, the most straightforward route to GlcN-6P would be the direct phosphorylation of the internalized sugar. However, the genomic analysis of GlcN-derived *nagB* suppressor mutants of *S. coelicolor* showed that NagA plays an important role in GlcN metabolism (Świątek *et al.*, 2012b). This suggested that GlcN is converted to GlcNAc-6P in order to be metabolised, which would most likely occur via acetylation to GlcNAc and subsequent phosphorylation by NagK to produce GlcNAc-6P. Indeed, our data show that NagK is involved in GlcN metabolism on minimal media. *nagKB* or *nagKAB* deletion mutants were both able to grow on in the presence of either GlcN or GlcNAc (Fig. 3). We propose that after internalization, GlcN is acetylated by a yet unidentified protein, phosphorylated by NagK and then joins the core *nag* pathway as GlcNAc-6P. This hypothesis will need to be investigated by metabolic flux analysis. Glucosamine acetylases have previously been identified in *Clostridium acetobutylicum* (Reith & Mayer, 2011) and we are currently investigating potential candidates in *S. coelicolor*, including the acetyltransferase SCO4279 that is located in the close vicinity of *nagKA*. However, we cannot rule out the possibility that multiple pathways are available for GlcN metabolism.

The suppressor screen identified a novel gene involved in GlcN-specific metabolism, namely SCO1447 (*rokL6*), which encodes the ROK-family regulator RokL6 (discussed in greater detail in Chapter VI). Disruption of this regulatory gene in the *nagB* mutant of *S. coelicolor* restored growth on GlcN, while GlcNAc remained toxic to the double mutant. This combined with the presence of a DNA binding motif implies that RokL6 is a regulatory protein that is involved in the control of GlcN metabolism and possibly controls the transporter gene SCO1448 which lies adjacent to (and is transcribed divergently from) *rokL6*. However, SCO1448-*nagB* double mutants failed to grow on GlcN, and it is therefore unlikely that SCO1448 is (solely) responsible for GlcN transport. There may be redundancy in terms of GlcN transport, with multiple transporters involved in the import of the aminosugar. Studies are currently ongoing in our laboratory that focus on the GlcN regulon and on identifying the ligand of RokL6, aimed at better understanding of GlcN metabolism and at the identification of the toxic molecule that accumulates inside the cell when *nagB* null mutants are grown on aminosugars.

In conclusion, in addition to enhancing antibiotic production by controlling metabolic

flux via *nag* gene deletions, the emergence of suppressor mutants has proven to be an indispensable tool in the discovery of new metabolic genes and the better understanding of the aminosugar metabolic pathways in *S. coelicolor*. Through the analysis of GlcN-derived *nagB* suppressors, we have been able to identify a new transcriptional regulatory gene involved in GlcN metabolism, and have obtained new insights into the GlcN metabolic route under poor growth conditions. This includes the surprising observation that NagK plays a key role in the metabolism of GlcN, while a direct route via GlcN-6P was expected. We are currently dissecting the GlcN and GlcNAc pathways to extend our knowledge of this complex system that plays such a key role in streptomycetes as nutrient and as signalling molecule for the onset of development and antibiotic production.

CHAPTER VI

THE ROK-FAMILY REGULATOR ROKL6 (SCO1447) IS INVOLVED IN THE CONTROL OF GLUCOSAMINE- SPECIFIC METABOLISM IN *S. COELICOLOR*

Mia Urem, Magdalena A. Świątek-Połatyńska, Eva J. van Rooden,
Bobby I. Florea and Gilles P. van Wezel

ABSTRACT

The aminosugar *N*-acetylglucosamine (GlcNAc) is an important pleiotropic signalling molecule for the regulation of development and antibiotic production in *Streptomyces coelicolor*. Our data suggest that the deacetylated aminosugar glucosamine (GlcN) is metabolised via the GlcNAc pathway and that the ROK-family protein RokL6 (SCO1447) is a GlcN-specific regulator. Deletion of *rokL6* relieved the toxicity of GlcN to *nagB* mutants, while the mutant still failed to grow on GlcNAc. Initial proteomic comparison of *S. coelicolor* M145 and its *rokL6* null mutant revealed strongly enhanced expression of sporulation regulator WhiB, while Red biosynthetic proteins were down-regulated. This suggests that RokL6 directly or indirectly controls expression of genes involved in development and antibiotic production. A possible autoregulatory RokL6 binding site was discovered in the intergenic region between *rokL6* and SCO1448. The latter encodes an MFS-transporter with unknown substrate, but a direct role in GlcN transport could not be ascertained. Surprisingly, the *nagB-rokL6* double mutant was resistant to the toxic glucose analogue 2-deoxyglucose (DOG), which is a glycolytic inhibitor and promising chemotherapeutic drug. Our results expose intricate links between GlcN, GlcNAc and glucose metabolism, thereby shedding new light on the regulation and pathways for (amino-)sugar metabolism in streptomycetes.

INTRODUCTION

Secondary metabolite production in the filamentous streptomycetes is closely linked to the switch from vegetative to aerial growth (Bibb, 2005; van Wezel & McDowall, 2011). At the onset of development, the vegetative mycelium is partially degraded via programmed cell death (PCD) so as to provide the building blocks necessary for aerial growth in an otherwise nutrient-depleted environment (Manteca *et al.*, 2005; Miguelez *et al.*, 1999; Park & Uehara, 2008). During cell-wall recycling, the subunits of the peptidoglycan (PG), namely *N*-acetylglucosamine (GlcNAc) and *N*-acetylmuramic acid (MurNAc) that make up the PG strands and the cross-linking amino acids, are re-imported into the cell. GlcNAc and its metabolism plays a key role in signalling during the control of development and antibiotic production in streptomycetes, as extensively described in Chapter II.

Streptomyces are saprophytic organisms that degrade many different polysaccharides, including cellulose, chitin and chitosan, which releases glucose (Glc), GlcNAc and glucosamine (GlcN), respectively. While metabolic pathways of glucose and GlcNAc have been well studied (Świątek *et al.*, 2012a; Nothaft *et al.*, 2010; Angell *et al.*, 1994; Gubbens *et al.*, 2012; van Wezel *et al.*, 2007; van Wezel *et al.*, 2005; Colson *et al.*, 2008; Xiao *et al.*, 2002), little is known of how GlcN is metabolised by streptomycetes (Chapter V). The hydrolysis of chitosan and the metabolism of chitosan-derived oligomers [(GlcN)₂₋₃] is controlled by CsnR (Dubeau *et al.*, 2011; Viens *et al.*, 2015), a repressor from the ROK (Repressors, ORFs and Kinases) family of transcriptional regulators (Titgemeyer *et al.*, 1994). (GlcN)₂₋₃ oligomers are imported via the ABC-transport complex CsnEFH-MsiK and are then presumably hydrolysed and phosphorylated by CsnH, a sugar hydrolase, and CsnK, a ROK-family kinase, respectively. However, the transporter of monomeric GlcN has not yet been identified.

In the absence of the NagB enzyme, high concentrations of GlcN or GlcNAc are toxic to *Streptomyces coelicolor* (Świątek *et al.*, 2012b; Świątek, 2012). This suggests that streptomycetes are not able to cope with high concentrations of GlcN-6P, which accumulates when NagB activity is low. Taking advantage of this system, a screen of GlcN-derived suppressor mutants was performed, resulting in the identification of genes related to GlcN metabolism (Świątek *et al.*, 2012b; Świątek, 2012; Chapter V). An unexpected discovery was that several suppressor mutations were found in the presumably GlcNAc-specific metabolic genes *nagA* and *nagK*, for GlcNAc deacetylase NagA and GlcNAc kinase NagK, respectively (Świątek *et al.*, 2012a; Chapter V). Since both genes are specific for GlcNAc, these data suggest a unique metabolic pathway for GlcN in *S. coelicolor*. GlcN is thereby converted to GlcNAc and then further metabolised via the GlcNAc pathway. This suggests the presence of a yet unidentified GlcN *N*-acetylase in *Streptomyces*. Interestingly, several independent suppressor mutations were found in the gene for the ROK-family regulator RokL6 (SCO1447). Deletion of *rokL6* specifically restored growth to *nagB* mutants in the presence of GlcN but not GlcNAc. The gene SCO1448 for a major facilitator superfamily (MFS) transporter, which is located divergently from *rokL6* on the genome, was subsequently also deleted in the *nagB* null mutant. However, this did not restore growth on either aminosugar (Świątek, 2012; Chapter V).

In this work, we investigated the role of GlcNAc-metabolic enzymes and RokL6 in GlcN metabolism. The regulatory role of RokL6 was investigated by comparing the proteomes of wild-type *S. coelicolor* and its *rokL6* deletion mutant in the absence and presence of GlcN.

MATERIALS AND METHODS

BACTERIAL STRAINS, CULTURE CONDITIONS, PLASMIDS AND OLIGONUCLEOTIDES.

The bacterial strains used in this work are listed in Table S1 of the supplemental material. *Escherichia coli* was transformed according to standard procedures (Sambrook *et al.*, 1989), whereby *E. coli* JM109 was used for routine cloning and *E. coli* ET12567 (MacNeil *et al.*, 1992) to generate non-methylated plasmid DNA. *E. coli* was grown in Luria-Bertani (LB) media at 30°C and selective antibiotics were added where required to the following final concentrations; ampicillin (100 µg/ml) and chloramphenicol (25 µg/ml).

Streptomyces coelicolor A3(2) M145 was obtained from the John Innes Centre strain collection. All *Streptomyces* media and routine techniques are described in the *Streptomyces* manual (Kieser *et al.*, 2000). To cultivate mycelia for protoplast preparation, a 1:1 mixture of yeast-extract malt extract (YEME) and tryptic soy broth (TSB) was used, and protoplasts were regenerated on R5 agar. Spores were cultivated on SFM (soy flour mannitol) agar. Phenotypic characterization was done on R5 and minimal media (MM) agar supplemented with sugars as stated. Induction experiments were performed in liquid cultures with mannitol as a non-repressive carbon source; NMM (without PEG) was used for proteomics experiments. All *Streptomyces* cultures were grown at 37°C and liquid cultures were grown in flasks containing spring coils and vigorously shaken. Where required, apramycin (50 µg/ml final concentration) and/or thiostrepton (20 µg/ml final concentration) were added as selectable markers for plasmids.

All plasmids and oligonucleotides are described in Table S1 and Table S2, respectively. *S. coelicolor* M145 genomic DNA was used as a template for PCR amplification and after cloning, PCR product inserts were checked by DNA sequencing. pWHM3, an unstable multi-copy shuttle vector, was used for gene replacement strategies as described (van Wezel *et al.*, 2005), and plasmid pUWLcre, which expresses Cre recombinase, was introduced into *Streptomyces* for genomic excision via *loxP* marked sites (see below for details; Fedoryshyn *et al.*, 2008). DNA sequencing was performed by BaseClear BV (Leiden, The Netherlands).

CREATION OF KNOCK-OUT MUTANTS.

Deletion mutants were created for SCO1447 (*rokL6*), SCO6110 and SCO6110-6114 in different *S. coelicolor* genetic backgrounds (Table S2). Deletion mutants for *nagB* and SCO1447 (*rokL6*) in wild-type *S. coelicolor* were described previously (Świątek, 2012). Gene replacement mutants, with the gene of interest replaced by an apramycin resistance cassette, were created via homologous recombination. The upstream (left) and downstream (right) flanking regions of the gene were cloned via engineered EcoRI/HindIII restriction sites into the highly unstable vector pWHM3. The left and right flanks were PCR-amplified from the *S. coelicolor* genome using primer pairs 6110LF-1198/6110LR+6 and 6110RF+927/6110RR+2197 for the amplification of the SCO6110 flanks, and primer pairs 6114LF-1306/6114LR+9 and 6110RF+927/6110RR+2197 for the SCO6110-6114 flanks. The *aac(3)IV* apramycin resistance cassette, flanked by *loxP* sites, was cloned between the gene flanks via engineered XbaI sites. This resulted in gene knock-out plasmids, pGWS953 and pGWS954, for SCO6110 and SCO6110-6114, respectively, and the previously described pGWS948 for SCO1447 (*rokL6*) knock-outs. To create SCO6110 mutants, the SCO6110 knock-out plasmid pGWS953 was transformed into *S. coelicolor* M145 and its *nagB* or SCO1447 (*rokL6*) deletion mutants generating M145 ΔSCO6110 and the double mutants M145 Δ*nagB*ΔSCO6110 and M145 Δ*rokL6*ΔSCO6110, respectively. To create SCO6110-6114 mutants, SCO6110-6114 knock-out plasmid pGWS954 was transformed into the same strains to create single mutant M145 ΔSCO6110-6114 and double mutants M145

Δ agB Δ SCO6110-6114 and M145 Δ rokL6 Δ SCO6110-6114.

In all cases, correct recombination events were checked by the appropriate antibiotics resistance and, where appropriate, confirmed by PCR (Colson et al., 2007). The apramycin resistance cassette was subsequently excised by introduction of pUWLcre, a Cre recombinase expressing plasmid, which allows for efficient removal of the cassette via the loxP recognition sites to obtain deletion mutants (Fedoryshyn et al., 2008; Khodakaramian et al., 2006). Deletion mutants were checked based on the appropriate antibiotic sensitivity (loss of apramycin resistance) and confirmed by PCR.

PROTEIN EXTRACTION AND LC-MS/MS ANALYSIS.

To analyse the proteomes of *S. coelicolor* M145 and its SCO1447 (*rokL6*) null mutant in the presence and absence of GlcN, protein extracts were prepared from liquid-grown cultures as described (Gubbens et al., 2014). Pre-cultures were grown overnight in YEME and used to inoculate 50 ml of fresh NMM media (NMMP without PEG) with 25 mM Mann to an OD₆₀₀ of around 0.1. Following 4 hours of growth, the cultures were induced with 50 mM of Mann or GlcN. Triplicate samples of 5 mL were taken 1 h after induction. For in-solution digestion of proteins with trypsin, the precipitated proteins were first resuspended in 50 μ l 50 mM ammonium bicarbonate with 0.1% (w/v) RapiGest SF Surfactant (Waters) and heated at 95°C for 5 min. Following resuspension, the protein concentrations were determined using the Bio-Rad Bradford-based assay, with BSA as a reference. DTT was added to each protein sample to a final concentration of 5 mM and incubated for 30 min at 60°C. Then iodoacetamide was added to a final concentration of 21.6 mM and incubated in the dark for 30 min. Finally, trypsin was added in a 1:100 (w/w) trypsin/protein ratio and the samples were digested overnight at 37°C. To acidify the samples, formic acid was added to a final concentration of 0.5% and incubated for 30 min at 37°C, and to remove RapiGest SF, the samples were then centrifuged (20,000 g for 10 min). For further purification of the supernatant, a total of 8 μ g of protein was loaded onto Stage Tips as previously described (Rappsilber et al., 2003). Acetonitrile was removed from the samples using a vacuum concentrator. Each sample was adjusted to a final concentration of around 80 ng/ μ L using a solution of 3% (v/v) acetonitrile and 0.1% (v/v) formic acid.

PROTEOMIC DATA ANALYSIS.

Peptides were analysed on a Waters ACQUITY UPLC system (Waters, Massachusetts, USA) hyphenated to an SYNAPT G2-Si mass spectrometer (Waters, Massachusetts, USA). PicoTip emitters (OD/ID = 360/20 μ m tip ID = 10 μ m), trap column (C18 100 Å, 5 μ M, 180 μ M x 20 mm, P/N 186006527) and analytical columns (HSS-T3 C18 1.8 μ M, 75 μ M x 250 mm) were obtained from Waters Corporation. The mobile phases [A: 0.1% (v/v) formic acid/H₂O, B: 0.1% (v/v) formic acid/acetonitrile] were made with ULC/MS grade solvents (Biosolve, Valkenswaard, the Netherlands). The emitter tip was coupled end-to-end with the analytical column via a 15 mm long TFE Teflon tubing sleeve (OD/ID 0.3 x 1.58 mm, Supelco, St Louis, MO) and installed in a stainless steel holder mounted in a nano-source base (I dex, Northbrook, IL). Not anymore. General mass spectrometric conditions were as follows: an electrospray voltage of 2.5–3.5 kV was applied to the emitter, trap collision energy 4 V, ramp transfer collision energy 20 to 45 V. Internal mass calibration was performed with [Glu1]-Fibrinopeptide B solution of 100 fmol/ μ L (m/z = 785.8427) as lock mass.

For shotgun proteomics analysis, 2 μ l of the samples was pressure loaded on the trap column with a 5 μ l min⁻¹ flow for 3 min followed by peptide separation with a gradient of 60 min 5–85% B, at a flow of 0.4 μ l min⁻¹. Full MS scan (50–2000 m/z) acquired in HDMSe

mode.

Data was transferred and analysed using Progenesis QI for proteomics 3.0 software (Waters, Massachusetts, USA). Peptide identification was set to a minimum 3 fragments per peptide, 7 fragments and 2 peptide per protein, and a maximum protein size of 2000 kDa.

BIOINFORMATICS ANALYSIS.

Motifs were predicted using InterProScan (Zdobnov & Apweiler, 2001), NCBI Conserved Domain Database (Marchler-Bauer *et al.*, 2015) and Pfam 24.0 (Finn *et al.*, 2008) and protein homology searches were performed using BLASTp (Altschul *et al.*, 2005). Schematic representations of *cis*-regulatory elements were produced using Boxshade (www.ch.embnet.org/software/box_form.html). Synttax was used for gene synteny (Oberto, 2013).

RESULTS

ROK6 (SCO1447) IS A CONSERVED ROK-FAMILY PROTEIN INVOLVED IN GLCN METABOLISM.

Putative transcriptional regulator RokL6 is characterised by an N-terminal winged helix-turn-helix DNA-binding site, found in various families of DNA-binding proteins, and a ROK-family protein domain (Fig. S1). The ROK (Repressor, ORF and Kinase) family of proteins play an important role in the (control of) sugar utilization in bacteria (Titgemeyer *et al.*, 1994). The family includes GlcNAc kinase NagK and NagC, the repressor of the *E. coli* aminosugar uptake and metabolism operon *nag* (Plumbridge, 1991); NagC also activates transcription of the *glmUS* operon, which is responsible for the synthesis of the cell-wall precursor UDP-GlcNAc (Plumbridge, 2015). In *S. coelicolor*, several ROK-family proteins have been identified that control sugar metabolism, while several also play a key role in the control of secondary metabolism (Bekiesch *et al.*, 2016; Świątek *et al.*, 2013). Disruption of *rokL6* restored growth to *S. coelicolor nagB* mutants in the presence of GlcN, strongly suggesting that RokL6 plays a key role in (the control of) GlcN metabolism (Świątek, 2012; Chapter V).

RokL6 is found in most streptomycetes, with relatively high sequence similarity between the orthologues (67-100% similarity) (Fig. S1). There is also significant gene synteny for the genomic region surrounding *rokL6* and its orthologues (Fig. 1). In particular, a gene for a major facilitator superfamily (MFS) transporter (SCO1448) often lies divergently transcribed from *rokL6*. Bioinformatic analysis using the String algorithm (Szklarczyk *et al.*, 2015) suggested a functional correlation between *rokL6* and SCO6110, a ROK-family kinase. The gene lies in an operon with genes SCO6111-6114 for an ABC transporter complex that is predicted to transport an oligopeptide.

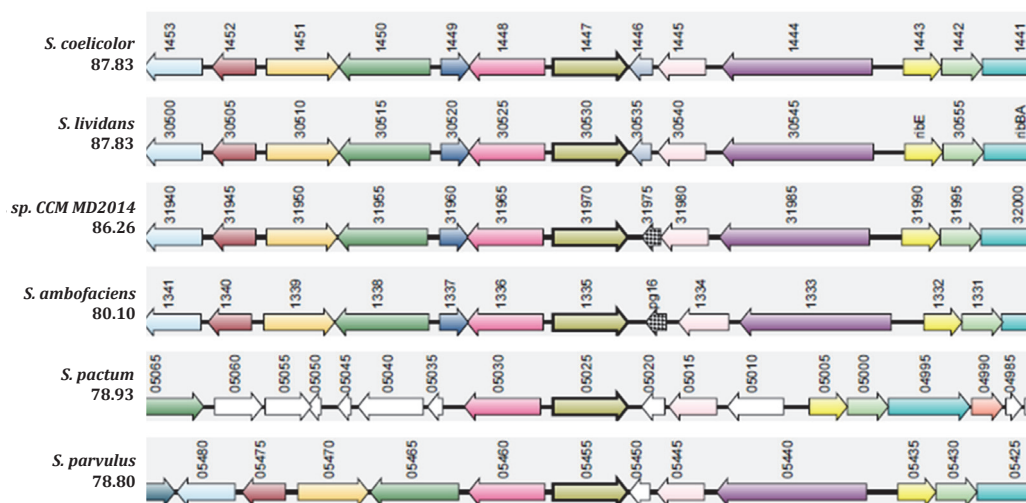


FIGURE 1. RokL6 conserved domains and gene synteny.

Gene synteny between RokL6 in *S. coelicolor* and homologs in other *Streptomyces* species. Synteny analysis performed by Synttax. Homologous genes are presented in the same colours.

MUTATIONAL ANALYSIS OF SCO6110-6114.

Deletion mutants of SCO6110 and the entire SCO6110-6114 gene cluster were created in *S. coelicolor* by replacing the entire coding regions by the *aac(3)IV* apramycin resistance cassette via homologous recombination (see Materials and Methods for details). Mutants were selected based on apramycin resistance as a marker for the deletion and sensitivity to thiostrepton for loss of the plasmid. The resistance cassette *aac(3)IV* was flanked by *loxP*

sites, which were then used to create markerless deletion mutants via genomic excision by Cre recombinase, expressed from plasmid pUWLcre. All mutants were verified by PCR. To examine whether SCO6110 or the transporter complex SCO6111-6114 may be involved in GlcN or GlcNAc metabolism, the genes were also deleted in the *nagB* deletion mutant. To analyse possible functional linkage between SCO6110 and RokL6, a SCO6110-*rokL6* double mutant was also created by deleting SCO6110 in the *rokL6* null mutant.

Mutants with gene deletions for SCO6110 or the SCO6110-6114 operon were phenotypically characterized on MM and R5 agar with or without 50 mM GlcN or GlcNAc (Fig. 2). Deletion of neither SCO6110 nor operon SCO6110-6114 significantly altered antibiotic production or development under any of these growth conditions. In line with this, deletion of SCO6110 in the *rokL6* mutant led to a phenotype highly similar to that of the single *rokL6* mutant. The inability to restore growth of the *nagB* deletion mutation on aminosugars by deleting SCO6110 or SCO6110-6114 suggests that GlcN metabolism is not fully blocked in the mutants.

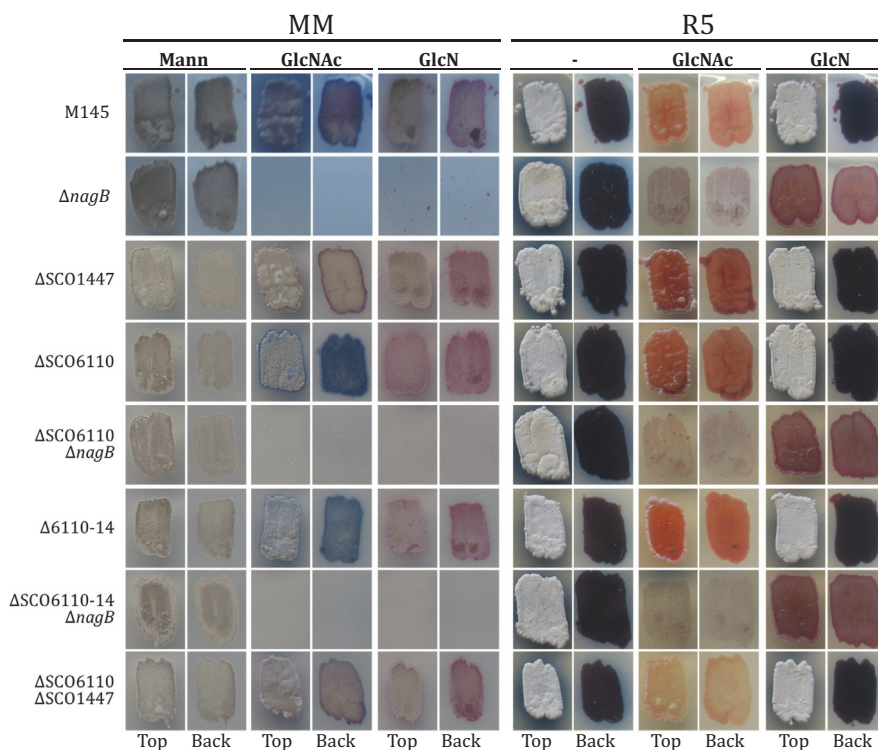


FIGURE 2. Phenotypic analysis of *S. coelicolor* mutants.

Phenotypic analysis of *S. coelicolor* wild-type (M145) and deletion mutants (Δ) as annotated on the left for each row. Spores were plated on minimal medium (MM) or rich glucose-containing media (R5) and supplemented with 50 mM mannitol (Mann), glucosamine (GlcN) or *N*-acetylglucosamine (GlcNAc) as indicated. Strains that were inhibited by GlcN or GlcNAc are indicated (red line). The top view and bottom (back) view of plates are indicated underneath.

PROTEOMIC ANALYSIS OF GLcN-SPECIFIC METABOLISM.

To assess the response of *S. coelicolor* to GlcN and potentially identify novel GlcN-metabolic enzymes, proteome analysis was done on *S. coelicolor* grown in the presence and absence of GlcN. For this, *S. coelicolor* M145 was pre-grown in YEME media, then the mycelia were washed in NMM and transferred to fresh NMM with mannitol as the sole carbon source,

to a starting OD₆₀₀ of around 0.1. After 4 h of growth in NMM, the culture was split into six subcultures and 50 mM GlcN was added to three cultures and 50 mM Mann to the other three. A sample was collected from each subculture 1 h after induction and analysed separately to obtain three replicates. The proteomes of *S. coelicolor* grown on GlcN and Mann were then compared. The same experiment was simultaneously carried out with the *S. coelicolor rokL6* deletion mutant in order to investigate the effect of RokL6 absence on the *S. coelicolor* proteome on Mann and on GlcN, as a means to examine the potential regulatory role of RokL6.

A total of 1462 proteins were identified in all four sample groups, with an average of 1475 proteins identified per sample. This means that over 99% of all proteins were identified in all samples. Differences in protein levels between samples were only considered relevant with a fold change of 2.5 or higher and a statistically significant difference determined by ANOVA analysis using a significance level of $p < 0.1$ (Table S).

GLCN INDUCTION

Despite the large number of proteins identified, addition of GlcN significantly altered the expression of only 38 proteins in the wild-type strain, many of which of unknown function (Fig. 3A). Two well-known targets stood out, namely NagE2 (5.5 fold upregulated in the presence of GlcN) and WhiB (2.7 fold upregulated). NagE2 (SCO2907) is the membrane component IIBC of the GlcNAc-specific PTS transporter (Nothhaft *et al.*, 2010) and WhiB (SCO3034) is a regulatory protein that is required for the transition from aerial growth to sporulation (Flardh & McCormick, 2017; Willemse *et al.*, 2012; Molle *et al.*, 2000). Other categories of proteins whose expression was significantly increased in the presence of GlcN included those involved in nucleotide metabolism and members of the so-called conserved (Cvn) proteins. Additionally, protein levels of three putative transport-related proteins were significantly (around 3-fold) increased in cultures containing GlcN, namely the sugar binding protein SCO3484 and the ABC-transporter components SCO2830 (likely involved in amino acid transport) and SCO4585.

EFFECT OF DELETION OF ROKL6

To establish the global changes in protein expression as the result of the absence of RokL6, the proteomes of *S. coelicolor* M145 were compared to those of its *rokL6* null mutant. Again, only a small number of proteins were differentially expressed between the two strains, namely 19 proteins in the mannitol-grown cultures and 28 when GlcN was added (Fig. 3B, Table S3). In the *rokL6* mutant both RedY and RedI, which are biosynthetic proteins involved in the production of undecylprodigiosin (Red; Cerdano *et al.*, 2001), were at least 2.5-fold decreased, suggesting that RokL6 may directly or indirectly control Red biosynthesis. Additionally, sporulation regulator WhiB again stood out, with a 4.4-fold increase in the *rokL6* mutant during growth on mannitol and 1.8-fold during growth on Mann+GlcN. Taken together, the data are consistent with induction of *whiB* by GlcN, while the gene is repressed by RokL6.

SEARCHING FOR A ROKL6 BINDING SITE AND REGULON PREDICTION.

A bioinformatic analysis was carried out on the *S. coelicolor* genome in an attempt to identify possible DNA binding sites for RokL6. This should allow correlation of predicted RokL6 binding sites to the proteomic data. We anticipated that RokL6 auto-regulates its own gene expression and therefore the SCO1447-SCO1448 intergenic region was scrutinized for potential DNA-binding motifs. For this, the intergenic and coding regions of *S. coelicolor*

a)

GlcN-Mann		SCO#	Description
WT	$\Delta 1447$		
10.1	5.4	SCO3399	Uncharacterized protein
8.1		SCO5539	Conservon CvnB2
5.5		SCO2907	PTS component NagE2
5.4		SCO4545	Uncharacterized protein
5.1		SCO0672	Anti-sigma factor antagonist
4.6		SCO1678	Putative transcriptional regulator
4.5		SCO4610	Putative integral membrane protein
4.4		SCO4096	ATP-dependent RNA helicase
4.0		SCO0719	Uncharacterized protein
4.0		SCO5563	Hydroxymethylpyrimidine/phosphomethylpyrimidine kinase ThiD
3.9		SCO1953	UvrABC system protein C
3.9		SCO3914	Putative transcriptional regulator
3.6		SCO3756	Putative two component system response regulator
3.5		SCO7631	Putative secreted protein
3.4		SCO6635	Bacteriophage (PhiC31) resistance PglY
3.4		SCO6169	Putative regulatory protein
3.3	1.5	SCO6207	Uncharacterized protein
3.3		SCO5244	Anti-sigma factor antagonist PrsH
3.2		SCO1766	Putative glycohydrolase
3.2		SCO3484	Putative secreted sugar-binding protein
3.2		SCO2830	Probable amino acid ABC transporter protein
3.1		SCO5648	Fe(3+) ions import ATP-binding protein FbpC
3.0		SCO7292	Putative threonine dehydratase
3.0		SCO4585	Putative ABC transporter protein
3.0	2.8	SCO7325	Anti-sigma factor antagonist RsbV
2.9		SCO5289	Putative two component sensor kinase CvnA5
2.9		SCO1571	Uncharacterized protein
2.8		SCO3896	Putative RNA nucleotidyltransferase
2.8		SCO2123	Putative esterase/lipase
2.7		SCO0888	Putative secreted protein
2.7		SCO5701	Uncharacterized protein
2.7		SCO5240	Transcriptional regulator WhiB
2.6		SCO5367	ATP synthase AtpB
2.6		SCO5038	Putative integral membrane protein F42a
2.5		SCO4577	Putative helicase
0.4	0.5	SCO5290	Uncharacterized protein CvnB5
0.4		SCO0679	Uncharacterized protein
0.3		SCO3302	Putative integral membrane protein

b)

$\Delta 1447$ -wt		SCO#	Description
M	G		
10.4	6.0	SCO3967	Conserved hypothetical membrane protein
5.1	2.1	SCO1602	Uncharacterized protein
4.4	1.9	SCO5240	Transcriptional regulator WhiB
3.9	3.2	SCO2444	Putative fatty acid synthase
3.7	1.6	SCO2301	conserved hypothetical protein
3.7	2.0	SCO6068	Uncharacterized protein CvnB6
3.6	4.5	SCO0868	Putative regulatory protein
3.4		SCO5652	Uncharacterized protein
2.9		SCO5563	Hydroxymethylpyrimidine/phosphomethylpyrimidine kinase ThiD
2.9	3.1	SCO4055	Putative alcohol dehydrogenase
2.8		SCO6207	Uncharacterized protein
2.6	1.9	SCO5024	Putative oxidoreductase
2.6	2.3	SCO6375	Putative secreted protein
2.5	1.5	SCO4444	Glutathione peroxidase
0.4	0.6	SCO2280	Putative transcriptional regulator
0.4	0.2	SCO5880	RedY protein
0.3	0.4	SCO5895	Putative methyltransferase RedI
0.2	0.2	SCO2256	3-methyl-2-oxobutanoate hydroxymethyltransferase PanB
0.1		SCO6804	Uncharacterized protein

Key:

5
4
3
2
1
0.9
0.8
0.7
0.6
0.5
0.4
0.3
0.2

FIGURE 3. Proteomic comparison of *S. coelicolor* M145 and its *rokL6* mutant.

Proteomic analysis was done for *S. coelicolor* M145 with or without added GlcN (a) and of *S. coelicolor* M145 and its *rokL6* deletion mutant ($\Delta 1447$) (b). Heat maps are shown of differentially expressed proteins and represent fold-changes, whereby changes of 2.5-fold or higher with a significance of $p < 0.1$ are shown. Fold changes are represented from red (0.2) to green (5.0) as shown in the colour key. See Table S3 in the supplemental material for the full data set. Strains were grown in liquid NMM media with mannitol and induced by adding of Mann or Mann + GlcN (50 mM each) for 1 h.

RokL6 and SCO1448, and eight orthologous pairs from other streptomycetes were analysed for conserved motifs using MEME. This identified a sequence of 38 nucleotides that is conserved in the intergenic region between *rokL6* and SCO1448 in *S. coelicolor* and other streptomycetes (Fig. 4A). The motif includes the inverted repeat CTATCAGG - 7 nt - CCTGATAG. The element was used to build a consensus sequence in PREDetector (Hiard *et al.*, 2007), which was then used to scan the *S. coelicolor* genome for similar motifs (Table S4). This identified three potential target sites with a medium score of 8 or higher in addition to the motif between *rokL6* and SCO1448. These putative binding sites were found in the regulatory region, upstream of gene SCO0317 encoding a putative transmembrane transport protein, SCO4114 encoding a sporulation-associated protein (Li *et al.*, 2006), and SCO2657, which encodes ROK-family transcriptional regulator CsnR. The latter is an important hit as CsnR regulates the uptake and metabolism of chitosan, the polymer of GlcN (Dubeau *et al.*, 2011; Viens *et al.*, 2015). None of the gene products of these genes were identified in the proteomic experiments so that at this stage no information on the effect on gene expression is available.

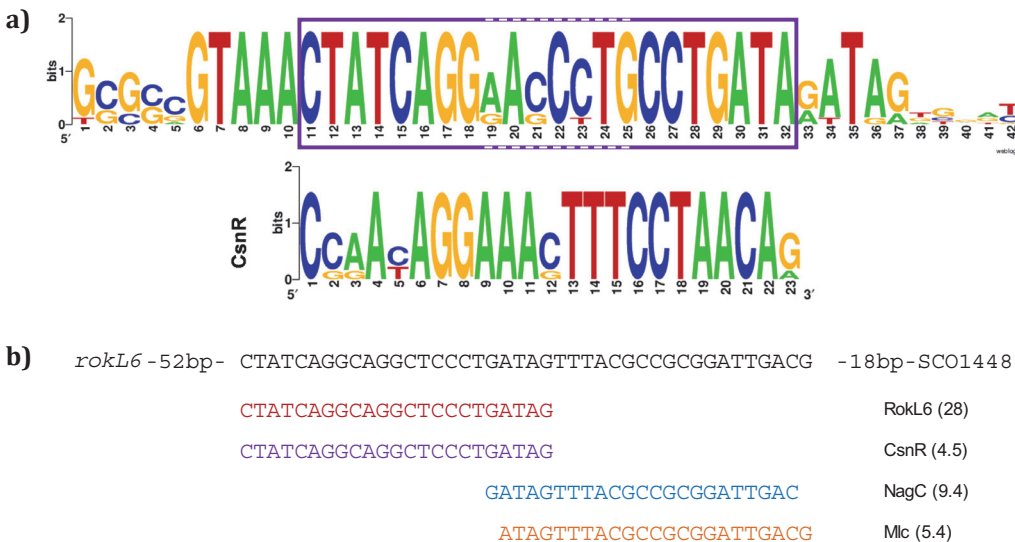


FIGURE 4. Predicted putative RokL6 binding site.

- a) Schematic representation of MEME output for conserved DNA sequences identified upstream of *rokL6*. The consensus sequence was identified in the intergenic region of *rokL6*-SCO1448 and eight homologous pairs from other *Streptomyces* species using MEME. The 23 bp inverted repeat is highlighted. Also shown is the putative CsnR binding site (Dubeau *et al.*, 2011).
- b) Putative binding sites of ROK-family regulators RokL6, CsnR, NagC and Mlc in the intergenic region between *rokL6* and SCO1448 (top sequence), predicted by PREDetector, are shown. The regulators are listed on the right and the PREDetector score is given in brackets.

Interestingly, the predicted binding site of CsnR (Dubeau *et al.*, 2011) resembles that of RokL6 (Fig. 4A) and scanning the genome with this consensus sequence also identifies the same site upstream of *rokL6* (with a score of 4.5) as a potential CsnR target. The extensively studied ROK-family regulators Mlc and NagC from *E. coli*, involved in the regulation of aminosugar and glucose utilization, respectively, also have highly similar binding sites (Brechemier-Baey *et al.*, 2015). Indeed, scanning the genome of *S. coelicolor* using the consensus binding sequences of Mlc and NagC identified a putative site upstream of *rokL6* for both regulators, 1 nt apart (Fig. 4B). This putative binding site was located just upstream

of the predicted RokL6 site with a 5 nt overlap, suggesting some level of conservation in the recognition sites of ROK-family regulators. More extensive systems biology is required to definitively determine the binding site of RokL6, any cross-regulation with CsnR and establish the full extent of the RokL6 regulon.

THE *ROKL6-NAGB* DOUBLE MUTANT IS RESISTANT TO GLCN AND DOG.

As discussed in this Chapter and elsewhere in this thesis (Chapters II, IV, V and VII), a toxic molecule accumulates in *nagB* null mutants when grown in the presence of either GlcN or GlcNAc. However, the nature of this molecule is as of yet unknown. A well-known toxic compound is 2-deoxyglucose (DOG), a non-metabolisable glucose derivative with a hydrogen in the place of its 2-hydroxyl group, that inhibits growth of prokaryotic and eukaryotic cells. In addition to applications as a glycolytic inhibitor, DOG is also being investigated as an anticancer drug (Zhang *et al.*, 2014; Bost *et al.*, 2016). In most organisms, DOG is taken up via the native glucose import system and subsequently phosphorylated to 2-deoxyglucose 6-phosphate (DOG-6P). Challenge of streptomycetes with the toxic molecule results in spontaneous *glk* mutants, lacking glucose kinase activity (Ikeda *et al.*, 1984). Though DOG-6P is responsible for the inhibition of glycolysis, by interfering with phosphoglucose isomerase (PGI) activity (Wick *et al.*, 1957), this is insufficient to cause the growth inhibition observed in the presence of DOG (Ralsler *et al.*, 2008).

Since glucose and aminosugar metabolism are closely linked, we tested whether any of the mutants created in this study might override toxicity to DOG by testing for their ability to grow on MM with 50 mM DOG (Fig. 5). As expected, growth of wild-type *S. coelicolor* was inhibited by DOG, as were mutants deleted for *nagB*, *rokL6*, SCO1448, SCO6110, *nagA* and SCO4393 (the latter two not shown). Intriguingly, the *rokL6-nagB* double mutant showed significant DOG resistance. This suggests that RokL6 may play an important role in the metabolism of DOG, and in particular in the accumulation of a toxic compound derived thereof.

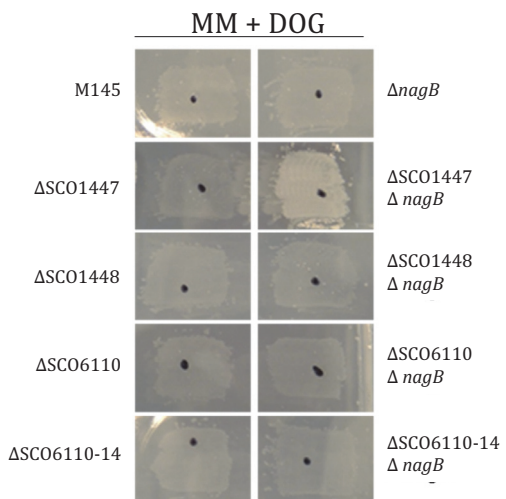


FIGURE 5. Phenotypic analysis of *S. coelicolor* mutants on 2-deoxy-D-glucose (DOG).

Phenotypic analysis of *S. coelicolor* M145 and deletion mutants (Δ) as annotated. Spores were plated onto minimal medium (MM) supplemented with 50 mM DOG.

DISCUSSION

The aminosugar *N*-acetylglucosamine (GlcNAc) is a preferred nutrient for *Streptomyces* and also acts as a signalling molecule for the nutritional status of the environment. Antibiotic production and development are activated by GlcNAc under poor growth conditions (famine), while these processes are blocked under rich conditions (feast) (Rigali *et al.*, 2008). This property of GlcNAc has been exploited to screen for novel antibiotics (Zhu *et al.*, 2014a). While GlcNAc metabolism and transport in streptomycetes are generally well understood, little was known about how the de-acetylated form, GlcN, is metabolised in these organisms. Our initial experiments suggested that GlcN may be metabolised via the GlcNAc pathway, and among others revealed the likely involvement of the ROK-family protein RokL6 (Świątek, 2012; Świątek *et al.*, 2012b; Chapter V).

The impact of GlcN induction was examined at the level of protein expression. GlcN induced the expression of PTS GlcNAc-specific membrane component NagE2 over five-fold in *S. coelicolor* (Nothaft *et al.*, 2010). GlcN-6P is the ligand for DasR, and renders its DNA-binding activity inactive (Rigali *et al.*, 2006). Therefore, the effect of GlcN on NagE2 expression may be governed indirectly, via the inhibition of DasR, which represses the transcription of *nagE2*. However, we cannot rule out that NagE2 is involved in GlcN transport, especially since many of the known DasR targets did not show elevated protein levels under the same growth conditions. The expression of SCO3484, SCO2830 and SCO4585 was also strongly increased when GlcN was added, and both are ATP-binding proteins of ABC transporters. SCO3484 is strongly repressed by DasR (Świątek-Połątyńska *et al.*, 2015), and may therefore be induced via GlcN-mediated metabolic inactivation of DasR. SCO4585 is part of an ABC-type multidrug transport system and SCO2830 is predicted to be involved in amino acid transport.

To obtain further insights into the role of RokL6 in the control of gene expression in *S. coelicolor*, the *rokL6* deletion mutant was also examined by proteome analysis. The deletion of *rokL6* did not significantly influence genes involved in aminosugar metabolism and GlcN sensing. The absence of RokL6 resulted in a significant decrease in levels of proteins related to prodigiosin production, which suggests that RokL6 is directly or indirectly involved in the control of prodiginine biosynthesis. Whether RokL6 directly regulates secondary metabolism remains to be determined through DNA binding studies. The data suggest that RokL6 could also have a role in development; the levels of sporulation regulator WhiB were strongly increased in the absence of RokL6. Additionally, a putative RokL6 binding site was predicted upstream of the gene encoding sporulation-associated protein SCO4114 (Li *et al.*, 2006).

A 23bp inverted repeat (CTATCAGG - 7 nt – CCTGATAG) was identified in the intergenic region between *rokL6* and SCO1448. Regulatory proteins often autoregulate their own gene expression, therefore this element qualifies as a potential RokL6 binding site. The element was used to scan the *S. coelicolor* genome for similar motifs using the PREDetector algorithm (Hiard *et al.*, 2007). In addition to the putative auto-regulatory site, a motif was also identified upstream of SCO0317 encoding a transporter with unknown substrate. Interestingly, a putative binding site was also identified upstream of *csnR*, which controls utilization of the GlcN polymer chitosan scanning the genome with the CsnR element identified the same 23bp inverted repeat as a potential binding site. The extensively studied ROK-family regulators Mlc and NagC from *E. coli*, involved in the regulation of aminosugar and glucose utilization, respectively, also have highly similar binding sites. However, it was shown that under native conditions the regulators bind exclusively to their own targets, demonstrating the subtlety and fine-tuning in the regulatory function of these proteins

(Brechemier-Baey *et al.*, 2015). Systems biology should reveal the binding site for RokL6 and establish the full extent of the RokL6 regulon.

A major question to answer is, what is the toxic molecule that accumulates in *nagB* mutants grown on aminosugars? An important cue may come from the fact that *rokL6-nagB* double mutants can grow on 2-deoxyglucose (DOG), while single mutants deleted for either *rokL6* or *nagB* cannot. This connects glucose and aminosugar metabolism. DOG is a toxic analogue of glucose, which is also a safe and effective chemotherapeutic agent against various cancers (Thompson & Kleinzeller, 1989; Zhang *et al.*, 2014). DOG is a known inhibitor of glycolysis; however, this does not fully explain the growth inhibition in eukaryotic cells (yeast and mammalian cells) (Ralser *et al.*, 2008; Thompson & Kleinzeller, 1989). Our data suggest that the toxicity may instead be mediated by an intermediate or end product of aminosugar metabolism and that this may directly connect to the toxicity of DOG. The surprising ability of the *rokL6-nagB* mutant to grow on DOG suggests that DOG toxicity is mediated via aminosugar metabolism. This discovery is not only relevant for the understanding of the function of RokL6, but may also provide new insights into the mode of action of the important anticancer drug 2-deoxyglucose.

Taken together, our studies on transcriptional repressor RokL6 shed new light on aminosugar metabolism in *Streptomyces*. Like for most ROK-family regulators, the ligand and regulon for RokL6 remain to be identified. Our data will help define a clearer and more concise picture of the pathways for aminosugar metabolism, specifically GlcN, as well as the intricate deviations and overlaps between GlcNAc, GlcN and potentially DOG metabolism and regulation.

ACKNOWLEDGEMENTS

We are very grateful to Chao Du for proteomics support.

CHAPTER VII

**GENERAL DISCUSSION
&
NEDERLANDSE SAMENVATTING**

GENERAL DISCUSSION

Bacteria exhibit great complexity and diversity in many aspects of their life cycle, in terms of their morphology, adaptability, primary metabolism and the diverse array of natural products they can produce. Bacteria have adapted and evolved to survive in all ecological niches, from the most extreme to the most heterologous habitats. A striking example are the filamentous actinobacteria that inhabit both terrestrial and aquatic environments; here, nutrient supplies fluctuate, and they must contend with biotic and abiotic stresses such as toxins, competing organisms, heat and cold shock and hypoxia. To correctly and efficiently coordinate and time responses to these stresses, an array of regulatory systems is in place, exemplified by the high percentage of regulatory and sugar transporter genes in the actinobacterial genomes. Extensive studies of streptomycetes unveiled antagonistic as well as cooperative actions of transcriptional regulators, and strong crosstalk between them, together leading to intricate regulatory networks controlling gene expression (Urem *et al.*, 2016a).

One of the stresses streptomycetes face is low oxygen, such as environmental hypoxia in the soil or inside mycelial pellets as a result of dense, aggregated growth. Since streptomycetes are considered strict aerobic bacteria, specific stress responses are initiated to survive hypoxia (Fischer *et al.*, 2010, Fischer *et al.*, 2014, van Keulen *et al.*, 2007). In this thesis, we characterise a novel two-component systems pair SCO0203-0204, named OsdKR (oxygen availability, stress, and development), likely to be involved in the coordination of the stress response as a result of oxygen depletion (Urem *et al.*, 2016b and Chapter III). Daigle and colleagues previously showed that *osdR* transcription is induced over 7-fold after exposure to low oxygen (Daigle *et al.*, 2015). The deletion of either response regulator (RR) gene *osdR* or sensory kinase (SK) gene *osdK* affects the ability of *S. coelicolor* spores to grow after exposure to hypoxia (our unpublished data, not shown). The OsdRK pair is also homologous to the system regulating dormancy in response to oxygen depletion in human pathogen and fellow actinomycete, *Mycobacterium tuberculosis*. This dormancy regulon is controlled by the OsdR response regulator homolog DevR (also known as DosR) and two sensory kinases, both homologous to OsdK, which sense gradual oxygen depletion. In line with these findings and the similarities between the signal recognition amino acid residues of DosT/DevS and OsdK, it is highly likely that the OsdK is responsible for the sensing of oxygen depletion in *S. coelicolor* in a similar way to DosT/DevS.

In Chapter III it is shown that OsdR regulates numerous stress response genes, many of which lie in the genomic region around *osdRK* and include genes for several universal stress proteins and Nar2, required for the anaerobic respiration during hypoxia. The direct control of genes by OsdR, including *osdR* itself, was confirmed by EMSA assays, which confirmed specific binding to the bioinformatically predicted recognition site. Specific binding by OsdR was also shown for targets lacking the predicted binding site, which could point to a larger regulon than predicted based on the consensus sequence. Regulatory control via OsdRK is likely further expanded by the orphan RR SCO3818, which like OsdR is phosphorylated by sensory kinase OsdK *in vitro* and shares high homology in its DNA binding domain (Wang *et al.*, 2009). And, much like the DevRS-DosT system in *M. tuberculosis*, an additional layer of complexity may also be provided by a second sensory kinase; a candidate is SCO3948, which has high amino acid identity to OsdK. The OsdK-based sensory system, with a potential role for SCO3948, maybe well execute the appropriate responses via both OsdR and SCO3818 under different conditions.

Nutrient depletion and hypoxia are signals that activate the developmental program, which begins with the erection of aerial hyphae and concludes with the formation of

unigenomic and stress-resistant spores. In the absence of OsdR, early development is accelerated in the mutant and sporulation is enhanced. This too is reflected in the transcriptome where a distinctive pattern of deregulated gene expression was observed for developmental genes. However, the transcriptome data also suggest that OsdR is required for a switch from early development to late developmental growth. Whole regulons were activated or silenced right at the onset of development, while this striking transcription patterning was absent in the *osdR* mutant. The pivotal role of OsdR in mediating rapid and global, though temporary, changes in gene expression requires further investigation.

Another central feature of the transition from vegetative growth to the onset of aerial mycelium formation is the autolytic process which degrades part of the vegetative hyphae via programmed cell death (PCD) (Migueluez *et al.*, 1999, Manteca *et al.*, 2005a). The PCD of the vegetative mycelium provides the recyclable building blocks for the formation of aerial hyphae, and the coinciding production of antibiotics presumably acts as a shield of the high local concentration of nutrients being released. Among the released nutrients are fragments of the peptidoglycan (PG) layer of the cell wall, which is built up of chains of alternating *N*-acetylglucosamine (GlcNAc) and *N*-acetylmuramic acid (MurNAc), crosslinked by peptides. GlcNAc and MurNAc monomers, cleaved as a result of PD degradation, can be taken up by the cells to fuel glycolysis or for the biosynthesis of new PG (Fig. 1).

GlcNAc is an important signalling molecule for streptomycetes and pleiotropically regulates development and secondary metabolism under different growth conditions (Rigali *et al.*, 2008). The presence of high concentrations of GlcNAc during growth under nutritionally poor conditions activates development and antibiotic production, while it blocks these processes and instead promotes growth if conditions are nutritionally rich. This phenomenon, known as the decision between feast and famine, is at least partially due to differential interpretation of the presence of GlcNAc; as a by-product of peptidoglycan hydrolysis, GlcNAc likely indicates PCD during famine but, in contrast, it signals abundance in a nutritionally rich environment. The complex regulatory control and decision-making involved in the differential response to GlcNAc remains to be fully elucidated. It likely involves the coordinated efforts of multiple transcriptional regulators, including DasR, AtrA, Rok7B7 and others, between which extensive crosstalk exists (Chapter II; Urem *et al.*, 2016a, Nothaft *et al.*, 2010, Świątek *et al.*, 2013). The response to GlcNAc is mediated via the pleiotropic transcriptional repressor DasR in response to GlcNAc metabolic intermediates, GlcN-6P and GlcNAc-6P (Fig. 1; Rigali *et al.*, 2006, Rigali *et al.*, 2008, Świątek-Połątyńska *et al.*, 2015, Fillenberg *et al.*, 2015, Liao *et al.*, 2015, Tenconi *et al.*, 2015b). Both metabolites allosterically induce the release of DasR from its targets, which include genes for GlcNAc transport and metabolism, antibiotic production and development.

With this in mind, *S. coelicolor nag* mutants were created for the metabolic engineering of antibiotic production by manipulating GlcNAc metabolism (Świątek *et al.*, 2012a, Świątek *et al.*, 2012b). This revealed that the *nagB* deletion mutant of *S. coelicolor*, which accumulates GlcN-6P due to its inability to convert it to Fru-6P for glycolysis (Fig. 1), was unable to grow on GlcNAc or its deacetylated derivative glucosamine (GlcN). However, the emergence of spontaneous suppressor mutants, which are able to survive due to secondary mutations, proved to be an indispensable tool for studying aminosugar metabolism and revealed novel aspects of the respective pathways and their regulation (Świątek, 2012, Świątek *et al.*, 2012b and Chapter V). This included the intriguing involvement in, and even requirement for, *nagA* GlcN metabolism (Świątek *et al.*, 2012b), and the discovery of genes for phosphosugar isomerase SCO4393 and ROK-family regulator RokL6 (SCO1447) (Chapters IV and VI).

SCO4393 is highly conserved in streptomycetes and also in some firmicutes and

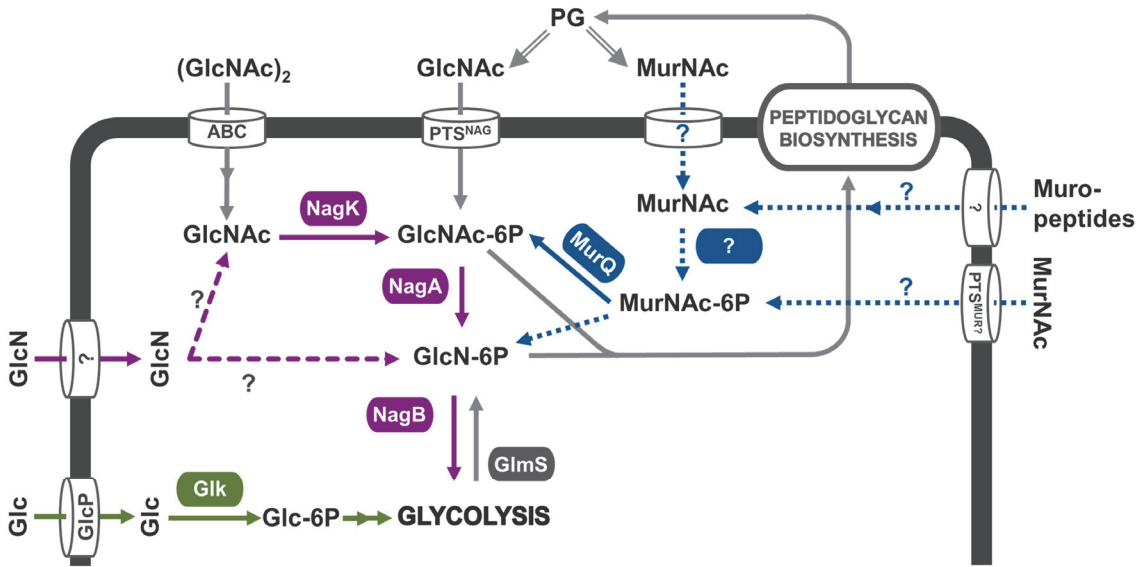


FIGURE 1. Schematic representation of aminosugar metabolism and peptidoglycan recycling in *S. coelicolor*.

Monomers of GlcNAc and MurNAc, released during peptidoglycan recycling, are taken back up by the cells. MurNAc metabolism involves transport and phosphorylation by unidentified proteins, followed by the conversion of MurNAc-6P to GlcNAc-6P by MurQ. The PTS phosphorylates monomeric GlcNAc during import to give GlcNAc-6P, which is deacetylated to GlcN-6P by NagA. NagB then converts GlcN-6P to Fru-6P for glycolysis or alternatively, GlcN-6P can be used for the biosynthesis of novel PG. In the absence of aminosugars, GlcN-6P can also be synthesised via GlmS from glycolytic products (Fru-6P). Chitin derived, dimeric (GlcNAc)₂ is imported via the ABC transporter system DasABC and cleaved to intracellular monomers of GlcNAc, which is phosphorylated by NagK. Limited information is available on GlcN transport and metabolism in *S. coelicolor* but GlcN metabolic pathway is proposed via acetylation to GlcNAc and NagK phosphorylation or GlcN could also be phosphorylated to GlcN-6P directly. Also shown is glucose (Glc) metabolism towards glycolysis, Glc is imported by MFS importer GlcP and then phosphorylated to Glc-6P by glucokinase (Glc).

Metabolic routes are represented by arrows and proposed/unknown routes by dotted arrows. For details, refer to the text.

proteobacteria. On the *S. coelicolor* genome, SCO4393 is divergently expressed from *dmdR1* (SCO4394) and gene synteny around SCO4393 is high between species, especially in relation to *dmdR1*. DmdR1 is an iron-homeostasis regulator; that also regulates the production of the siderophores coelichelin and desferrioxamine (Flores & Martin, 2004). The addition of iron to rich media containing GlcNAc (feast) was previously shown to restore antibiotic production and development in *S. coelicolor* despite the presence of GlcNAc (Lambert *et al.*, 2014). The discovery of a putative DasR binding site in the intergenic region of SCO4393 and *dmdR1* identified a link between iron and GlcNAc in *Streptomyces* (Craig *et al.*, 2012).

Given that the disruption of SCO4393 restores growth of the *nagB* mutant on both GlcNAc and GlcN (Chapter IV), this led to the assumption that SCO4393 may be involved in the formation of the metabolite responsible for growth inhibition by aminosugars to the *nagB* mutant. The structure of SCO4393 was solved to high resolution by X-ray crystallography. The structure included a ligand bound in its intermediate state, which showed that SCO4393 binds a molecule with a likely phosphate group, possibly *N*-acetylglucosamine-6P or a similar aminosugar such as GalNAc-6P (*N*-acetylgalactosamine-6P) (Chapter IV). Ligand-binding assays by ITC showed that SCO4393 specifically binds GlcNAc-6P. Indeed, both the

acetyl group and the 6-phosphate were essential as neither GlcNAc, GlcN-6P nor GlcNAc-1P could bind to SCO4393.

It is important to note that GlcNAc-6P accumulates when *nagA* mutants are grown on GlcNAc, but this is not toxic for the cells. Conversely, *nagB* mutants accumulate GlcN-6P, which is lethal. Thus, since active SCO4393 enzyme does not prevent growth of *nagA* mutants on GlcNAc, it is highly unlikely that SCO4393 is responsible for the biosynthesis of a toxic intermediate directly from GlcNAc-6P. GlcN-6P accumulation is most likely the key, somehow mediated through SCO4393. Work is on-going to unravel the exact reaction catalysed by SCO4393.

Fairly little is known about the specific pathways involved in the metabolism of GlcN in *Streptomyces coelicolor*. The most straightforward route for metabolism of GlcN would be via direct phosphorylation to GlcN-6P during or after transport, as is the case in for example *E. coli* and *B. subtilis* (Fig. 1; Plumbridge, 2015). However, the discovery that the *nagAB* mutant is able to grow on both GlcNAc and GlcN suggested that GlcN may be metabolised via the GlcNAc pathway in streptomycetes (Świątek *et al.*, 2012b). How else can we explain that mutation of *nagA* relieves toxicity of GlcN to *nagB* mutants? A screen of *nagB* suppressor mutants on GlcN, focused on identifying additional aspects of GlcN metabolism, identified several suppressors with large deletions and mutations in the adjacent *nagKA* genes despite the presence of an extra copy of *nagA* (on a plasmid) in some strains (Chapter V). This reaffirmed the importance of the GlcNAc metabolic genes for the processing of GlcN under these conditions. The discovery that also *nagK* mutations suppress the toxicity of GlcN to *nagB* deletion mutants, further supports the hypothesis that GlcN may be converted to GlcNAc for metabolism (Chapter V). The metabolism of GlcN to GlcN-6P via GlcNAc-6P, rather than via direct phosphorylation of GlcN, would require an *N*-acetyltransferase prior to phosphorylation by NagK and deacetylation by NagA to yield GlcN-6P.

Remarkably, metabolic analysis of the *nagA* mutant revealed GlcNAc-6P accumulation after induction with GlcN, which would suggest that GlcN metabolism leads to GlcNAc-6P formation through a yet undefined route (preliminary data, not shown). The double mutant *nagAB* accumulated both GlcN-6P and GlcNAc-6P when media were supplemented with GlcN, suggesting that multiple pathways may be available for GlcN metabolism. However the effect of PG recycling cannot be ruled out. Another interesting discovery was that mutants lacking the *nagK* gene produced an unknown compound with a mass of m/z 256.06 after induction with GlcN (preliminary metabolomic data, not shown). Though further investigation is needed to elucidate this unknown compound, we hypothesise that it may well be an oxidized form of GlcN-6P (m/z 258.04) which could present a novel feature of GlcN metabolism. It remains to be determined how the metabolome of these mutants responds to GlcNAc induction and how this compares to GlcN metabolism. It would also be valuable to track the metabolism of labelled aminosugars to distinguish other possible sources of the pathway metabolic intermediates, such as those generated during PG recycling. Also, more research is needed to understand how the deletion of *nagK* may relieve GlcNAc toxicity to the *nagB* mutant under conditions presumed to involve PTS transport of the sugar. This may well suggest that a portion of GlcNAc is located intracellularly, via alternative transporters or PG recycling, and that blocking its phosphorylation aids in the prevention of the toxic accumulation of GlcN-6P or related metabolites.

Mutations in SCO4393 were exclusively identified in GlcNAc-isolated suppressors while the majority of *nag(K)A* mutations were found in GlcN-isolated suppressors (Świątek, 2012, Świątek *et al.*, 2012b; Chapter V). However, these mutations were able to alleviate the toxic effects of both sugars, highlighting the overlap between the GlcN and GlcNAc pathways.

The relief of toxicity of only GlcN or GlcNAc, which would help identify features unique to the given sugar, was only seen when *rokL6* (SCO1447) was mutated (Chapters V-VI). As GlcNAc remained toxic to mutants of *rokL6-nagB*, this suggests that RokL6 is a GlcN-specific regulator. The function of RokL6 remains unknown, however it stands to reason that it may involve the regulation of the bacterium's response to the sugar and GlcN transport and/or metabolism.

To assess the potential influence of RokL6, the proteome of the *rokL6* deletion mutant was compared to that of wild-type *S. coelicolor* in the presence and absence of GlcN (chapter VI). The data suggested that GlcN sensing may be independent of RokL6, given that protein levels were not altered significantly during growth on GlcN or mannitol. The data did reveal that the level of sporulation regulator WhiB was increased in the *rokL6* mutant compared to the wild-type strain, and the levels of proteins related to prodigiosin biosynthesis were decreased in the mutant, which implicates RokL6 in the direct or indirect control of development and antibiotics production. As *rokL6* was identified as a GlcN-specific gene, we hypothesized that the divergently expressed MFS transporter SCO1448 could be an importer of GlcN. However, the double mutant SCO1448-*nagB* was also unable to grow on GlcN (Chapter V). Genes for putative MFS transporters, homologous to SCO1448, were identified divergently from genes of *rokL6* orthologues in different species of *Streptomyces*, suggesting linkage between them. Further investigation is needed to determine the role SCO1448 plays in aminosugar transport.

A motif search of the intergenic region between *rokL6* and SCO1448 identified a 23 nt putative binding sequence, which may be a target of autocontrol by RokL6. A scan of the *S. coelicolor* genome for similar motifs identified only a minimal set of targets including a site upstream of *csnR*. A ROK-family regulator itself, CsnR controls the utilization of chitosan, the polysaccharidic form of GlcN, and recognises a consensus sequence remarkably similar to the sequence predicted to be bound by RokL6 (Dubeau *et al.*, 2011, Viens *et al.*, 2015). Extensive analysis of ROK-family regulators and their binding sites has highlighted the similarity between their binding sites (Brechemier-Baey *et al.*, 2015; Conejo *et al.*, 2010); the *E. coli* ROK-family regulators Mlc and NagC, regulating the utilization of glucose and aminosugars, respectively, have high homology and recognise very similar binding sites. However, the regulators exclusively regulate their own specific targets under native conditions with cross-regulation only occurring under enhanced levels of regulator (Plumbridge, 2001). Indeed, scanning the genome of *S. coelicolor* with the AT-rich consensus sequences of either Mlc or NagC identified a site in the *rokL6*-SCO1448 intergenic region, with a 5 nt overlap with the *Streptomyces* ROK-regulator sites. Whether RokL6 is directly involved in the regulation of these predicted targets or any of the proteins affected in the proteome analysis will remain to be seen, a transcriptomic comparison of the mutant and wild-type in combination with *in vitro* and *in vivo* verification techniques should aid in the resolution of the RokL6 regulon.

Fascinatingly, *rokL6-nagB* double mutants are resistant to 2-deoxyglucose (DOG), though the single mutants are still sensitive (Chapter VI). DOG is a glucose analogue that is toxic to most cells and is known to be an inhibitor of glycolysis (Wick *et al.*, 1957). DOG is currently explored as a chemotherapeutic drug against cancer (Zhang *et al.*, 2014; Bost *et al.*, 2016). Interestingly, however, the mechanism by which DOG affects cells is unclear given that glycolytic inhibition was shown to be insufficient to explain its lethal effect on eukaryotic cells (Ralser *et al.*, 2008). Streptomyces are also unable to grow on DOG and only suppressors with mutations in genes for glucose utilization, such as the gene for glucose kinase, are able to survive on the toxic sugar (Ikeda *et al.*, 1984). Exploring the mechanism by which *rokL6-nagB* mutants escape DOG toxicity will provide novel insights

into glucose and aminosugar metabolism. At the same time, it will also provide new clues as to how DOG is metabolized to a toxic intermediate, and our data suggest this may well be via aminosugar metabolism.

Sugar sensitivity, rising from the mutation of a key enzymatic component for its metabolism and resulting in the toxic accumulation of sugar-phosphates, has long been known (Irani & Maitra, 1977; Englesberg *et al.*, 1962; Yarmolinsky *et al.*, 1959; Sabag-Daigle *et al.*, 2016). Growth inhibition by phosphosugar toxicity has been shown to be bactericidal in some cases and bacteriostatic in others. Despite extensive studies focusing on the understanding of metabolic pathways, the underlying cause of sugar-toxicity remains a mystery. There is evidence that suggests that depletion of some important down-stream intermediates, such as PEP in the case of glucose-6P (Glc-6P) accumulation, could be the responsible (Richards *et al.*, 2013; Vanderpool, 2007). However, different consequences of accumulation of intermediates can also cause the observed growth inhibition. High levels of non-metabolisable phosphosugars could create osmotic problems within cells, metabolic flux disruptions may lead to the formation of toxic metabolic products and some phosphosugars, such as Glc-6P, may act as catabolic repressors (Vanderpool, 2007; Kadner *et al.*, 1992). Indeed, a study of growth inhibition of *E. coli* by enhanced phosphosugar import identified at least two causes for the toxicity (Kadner *et al.*, 1992). Elevated levels of Glc-6P and Fru-6P resulted in the formation of methylglyoxal, a toxic side product of glycolysis, which led to growth inhibition and cell death. Conversely, neither DOG-6P nor GlcN-6P caused the formation of methylglyoxal, and the authors could not explain why GlcN-6P, which can enter glycolysis via conversion to Fru-6P by NagB, did not result in the accumulation of methylglyoxal. This suggests that aminosugar-sensitivity is not mediated through glycolysis in *E. coli*. As mentioned above, the same conclusion can be drawn for deoxyglucose.

Aminosugar sensitivity may relate to the accumulation of precursors or intermediates of cell-wall synthesis. During spore germination and early growth, when peptidoglycan synthesis is low, GlcN and GlcNAc are toxic to *nagB* mutants (Świątek *et al.*, 2012a). However, adding either aminosugar to exponentially growing *nagB* mutants does not affect growth, perhaps because cell-wall synthesis is at its maximum at this point in the life cycle, so that the aminosugars are efficiently turned over. Given that inactivation of SCO4393 relieves the toxicity of GlcN and GlcNAc, a role for SCO4393 in cell-wall precursor supply should be investigated. One molecule that has hardly been explored is MurNAc. *nagB* mutants are sensitive to MurNAc while the wild-type strain and its *nagA*, *nagK*, *rokL6* and SCO4393 mutants are not. As MurNAc-sensitivity could not be relieved by the simultaneous deletion of *nagA* and *nagB*, it is likely that MurNAc is not first phosphorylated and then converted to GlcNAc-6P (Fig. 1), but instead it might be deacetylated and converted to GlcN-6P instead.

In conclusion, this thesis has provided important new insights into (the control of) oxygen stress and primary metabolism revolving around aminosugar metabolism. Major discoveries described in this thesis are a dormancy-like regulon controlled by the OsdRK TCS, the surprisingly crucial role of RokL6 in glucosamine toxicity in *nagB* mutants and the unexpected role of SCO4393 in aminosugar metabolism. The high-resolution crystal structure of SCO4393 will thereby guide experiment to uncover the true ligands for the enzyme, while full systems biology of the RokL6 regulon will undoubtedly unveil new aspects of primary metabolic control. Unravelling the precise reaction catalysed by phospho-aminosugar isomerase SCO4393 as well as the way RokL6 controls GlcN-6P catalysis, will help us to better our understanding of central primary metabolism at the interface of glycolysis, aminosugar metabolism and cell wall synthesis.

NEDERLANDSE SAMENVATTING

Micro-organismen laten grote diversiteit en ook complexiteit zien qua levenscyclus, morfologie, adaptatie en metabolisme. Gedurende de evolutie hebben bacteriën zich aangepast om te overleven in de meest uiteenlopende ecologische niches, van de meest extreme tot de meest heterogene omgevingen. De filamenteuze actinobacteriën produceren daarbij een grote variëteit aan bioactieve natuurstoffen, zoals met antibacteriële, antischimmel-, of antitumoractiviteit (Barka *et al.*, 2016). Veel hogere organismen als planten, sponzen en insecten maken gebruik van de bioactieve verbindingen die ze produceren voor hun eigen bescherming en ze zijn daarom voor veel dieren en planten een graag geziene gast (van der Meij *et al.*, 2017). Actinobacteriën zijn overal op het land en in water te vinden, en de voorraad en aard van de voedingsstoffen fluctueert vaak. Tevens worden ze er blootgesteld aan verschillende soorten stress, zoals toxines, concurrerende organismen, honger, hitte, kou en hypoxie. Om hiermee om te kunnen gaan, moeten actinobacteriën de signalen die ze ontvangen op de juiste wijze vertalen naar een response, via vaak complexe regulatienetwerken. Studies aan streptomyceten laten een complex netwerk van antagonistische en coöperatieve regulons zien, die worden gecoördineerd door een breed scala aan transcriptiefactoren (Urem *et al.*, 2016a).

Een van de oorzaken van stress is een te laag zuurstofgehalte, bijvoorbeeld door hypoxie in hun omgeving. Aangezien streptomyceten aerobe bacteriën zijn, worden specifieke stress-responses geïnitieerd om hypoxie te overleven (Fischer *et al.*, 2010; Fischer *et al.*, 2014; van Keulen *et al.*, 2007). In dit proefschrift karakteriseren wij een nieuw two-component system gevormd door de genen SCO0203 en SCO0204, die we *osdK* en *osdR* hebben genoemd (oxygen availability, stress, and development). *OsdK* spelen een rol bij het controleren van de stress response die nodig is om onder condities van zuurstoflimitatie te overleven (Urem *et al.*, 2016 en Hoofdstuk III). Daigle en collegae hebben eerder aangetoond dat *osdR* transcriptie geïnduceerd wordt na blootstelling aan lage zuurstofspanning (Daigle *et al.*, 2015). *OsdRK* is ook homoloog aan het system die geactiveerd wordt bij zuurstoflimitatie in de humane pathogeen *Mycobacterium tuberculosis*, welke tuberculose veroorzaakt. De twee sensory kinases *DosT* en *DevS*, beide homoloog aan *OsdK*, reageren op geleidelijke daling van de zuurstof. Deze bevindingen en de overeenkomsten tussen de eiwitten *DosT/DevS* enerzijds en *OsdK* anderzijds, maken het zeer waarschijnlijk dat *OsdK* verantwoordelijk is voor het reageren op fluctuaties in de hoeveelheid zuurstof in *S. coelicolor*.

De experimenten in hoofdstuk III laten zien dat *OsdR* talrijke stress-response-genen reguleert, waarvan vele nabij *osdRK* op het chromosoom liggen, waaronder meerdere genen voor universele stress-eiwitten. De consensus sequentie voor de bindingssite die herkend wordt door response regulator *OsdR* is bepaald door middel van een combinatie van DNA-binding assays (EMSAs) en voorspelling door middel van bioinformatica. Controle van deze genen gebeurt niet alles door *OsdR* maar vermoedelijk ook door de 'orphan' regulator SCO3818, die ook *in vitro* gefosforyleerd wordt door sensory kinase *OsdK* en een nagenoeg identiek DNA-bindend domein heeft als *OsdR* (Wang *et al.*, 2009). Nutriëntlimitatie en hypoxie zijn signalen die het ontwikkelingsprogramma van streptomyceten activeren. Bij afwezigheid van *OsdR* wordt de ontwikkeling en sporulatie versneld. Dit wordt bevestigd door globale analyse van de genexpressie, met duidelijk verschil in expressie van genen die betrokken zijn bij de (controle van) sporulatie. De data suggereren echter ook dat *OsdR* nodig is voor de overgang van vroege naar late ontwikkeling. Hele sets van genen werden direct aan het begin van de ontwikkeling geactiveerd of stilgelegd, terwijl dit opvallende transcriptiepatroon niet te zien was in de *osdR* mutant. De centrale rol van *OsdR* bij de

controle van de sporulatie verdient verder onderzoek. Nog een centraal kenmerk van de overgang van vegetatieve groei naar luchtmycelium is het autolytische proces dat een deel van de vegetatieve hyfen afbreekt (Miguel et al., 1999; Manteca et al., 2005a). Dit levert herbruikbare bouwstenen voor de vorming van luchtmycelium, en hangt samen met productie van antibiotica. Antibiotica worden vermoedelijk juist op dit moment in de levenscyclus geproduceerd, omdat andere motiele bacteriën aangetrokken worden door de plotseling ontstane nutriënten via chemotaxis. Om de voedingsbron te beschermen zijn antibiotica noodzakelijk. Onder de vrijkomende voedingsstoffen zijn fragmenten van de peptidoglycan (PG) laag van de celwand, die is opgebouwd uit ketens van alternerende aminosuikers *N*-acetylglucosamine (GlcNAc) en *N*-acetylmuraminezuur (MurNAc). GlcNAc- en MurNAc-monomeren, gesplitst als gevolg van PD-afbraak, kunnen door de cellen worden opgenomen om verbruiken voor glycolyse of voor de biosynthese van nieuw PG (Figuur 1).

GlcNAc is naast een belangrijke voedingsbron ook een sleutelmolecuul in de signalering van de voedingsrijkheid van de omgeving waarin de bacterie zich bevindt. Het molecuul en zijn metabolische derivaten reguleert de ontwikkeling en het secundaire metabolisme onder verschillende groeicondities (Rigali et al., 2008). De aanwezigheid van hoge concentraties GlcNAc tijdens de groei onder arme omstandigheden activeert de ontwikkeling en de productie van antibiotica, terwijl deze processen geblokkeerd zijn als er veel hoogwaardige suikers aanwezig zijn. Dit fenomeen staat bekend als *feast and famine*. Als één van de metaboliëten die vrijkomt bij de hydrolyse van de celwand geeft GlcNAc waarschijnlijk aan dat er afbraak van vegetatieve mycelium is tijdens honger (*famine*), omdat op dat moment de enige bron van GlcNAc de celwand (en dus zelfafbraak) kan zijn. Echter, als er naast GlcNAc nog veel andere nutriënten zijn, dan wordt dit geïnterpreteerd als dat de GlcNAc van chitine komt, oftewel een voedingsrijke omgeving (*feast*). De complexe regulatie die hieraan ten grondslag ligt is nog niet geheel ontrafeld maar waarschijnlijk wordt deze gecoördineerd door meerdere transcriptionele regulatoren, waaronder DasR, AtrA en Rok7B7 (Hoofdstuk II; Urem et al., 2016a; Nothhaft et al., 2010; Świątek et al., 2013). GlcNAc wordt in de cel omgezet in GlcNAc-6P en glucosamine-6-fosfaat (GlcN-6P) en deze binden beide aan de globale repressor DasR (Figuur 1; Rigali et al., 2006; Rigali et al., 2008; Świątek-Połatyńska et al., 2015; Fillenberg et al., 2015; Liao et al., 2015; Tenconi et al., 2015b). Binding van één van deze liganden zorgt ervoor dat DasR niet meer aan DNA kan binden, met als gevolg dat de transcriptie van de genen van het DasR regulon wordt verhoogd. Dit regulon omvat genen voor afbraak van polysacchariden, transport en metabolisme van aminosuikers, antibioticumproductie en de ontwikkeling.

Met dit in gedachte zijn *S. coelicolor nag* mutanten gemaakt om antibiotica productie te beïnvloeden (Świątek et al., 2012a; Świątek et al., 2012b). Hieruit bleek dat de *nagB* deletiemutant, die GlcN-6P ophoopt (Fig. 1), niet meer kan groeien op GlcNAc of GlcN. Echter, spontane suppressormutanten werden geïsoleerd, die door een tweede mutatie wel kunnen overleven. Dit bleek een onmisbaar hulpmiddel voor het bestuderen van aminosuiker metabolisme en de regulatie ervan (Świątek, 2012; Świątek et al., 2012b; Hoofdstuk V). Dit leidde tot de ontdekking van genen voor fosfosuiker isomerase SCO4393 en ROK-familie regulator RokL6 (SCO1447) (Hoofdstukken IV en VI).

SCO4393 is aanwezig in de meeste streptomyceten en ook in sommige bacilli en proteobacteriën. Op het *S. coelicolor* genoom ligt SCO4393 divergent van *dmdR1* (SCO4394) en de link met *dmdR1* kan worden teruggevonden in veel bacteriën. *DmdR1* is een ijzer-homeostase regulator, die ook de productie van de sideroforen coelichelin en desferrioxamine regelt (Flores & Martin, 2004). Aangezien mutatie of deletie van SCO4393 de groei van de *nagB* mutant op zowel GlcNAc als GlcN herstelt (Hoofdstuk IV), is het logisch aan te nemen

dat SCO4393 betrokken is bij de vorming van de metaboliet die verantwoordelijk is voor groeiremming van de *nagB* mutant bij groei op aminosuikers. Ik heb de structuur van SCO4393 opgelost op hoge resolutie door middel van kristallografie. De structuur bevatte een ligand in open conformatie, en de structuur laat zien dat SCO4393 een molecuul bindt wat vermoedelijk een fosfaat- en een acetylgroep bevat, zoals *N*-acetylglucosamine-6P of een vergelijkbare aminosuiker (Hoofdstuk IV). Ligand-bindingsassays via ITC toonden vervolgens aan dat SCO4393 sowieso GlcNAc-6P bindt. In feite waren zowel de acetylgroep als de 6-fosfaatgroep essentieel voor binding, aangezien moleculen die deze groepen niet bevatte, zoals GlcNAc, GlcN-6P of GlcNAc-1P, niet aan SCO4393 binden.

Het is belangrijk om op te merken dat de accumulatie van GlcNAc-6P, zoals tijdens de groei van de *nagA* mutant op GlcNAc, niet toxisch is voor *S. coelicolor* terwijl de *nagB* mutant vooral GlcN-6P accumuleert, wat de groei wel remt. Aangezien *nagA* mutanten gewoon een actief SCO4393 hebben, is het niet waarschijnlijk dat SCO4393 verantwoordelijk is voor de biosynthese van een toxisch intermediair gebaseerd op GlcNAc-6P. GlcN-6P accumulatie is waarschijnlijk de sleutel, op één of andere manier gekatalyseerd door SCO4393. De exacte reactie die door SCO4393 wordt gekatalyseerd is nog onbekend.

In tegenstelling tot GlcNAc is er nog weinig bekend over het metabolisme van GlcN in *S. coelicolor*. De meest eenvoudige route zou via fosforylering van GlcN naar GlcN-6P lopen, zoals in bijvoorbeeld *E. coli* en *B. subtilis* gebeurt (Fig. 1; Plumbridge, 2015). De ontdekking dat de *nagAB* mutant op zowel GlcNAc als GlcN kan groeien, maakt het echter zeer waarschijnlijk dat er een andere route wordt gevolgd, namelijk via GlcNAc. Een screen van *nagB* suppressormutanten op GlcN identificeerde opnieuw een aantal suppressors. Vele daarvan hadden deleties en/of mutaties in *nagKA* (Hoofdstuk V). Dit bevestigde opnieuw het belang van GlcNAc metabolische enzymen voor het metabolisme van GlcN onder deze omstandigheden. De ontdekking dat ook *nagK* mutaties de toxiciteit van GlcN onderdrukken, ondersteunt verder de hypothese dat GlcN eerst wordt omgezet in GlcNAc en dan via GlcNAc-6P naar GlcN-6P (Hoofdstuk V).

Mutaties in SCO4393 werden uitsluitend geïdentificeerd in GlcNAc-geïsoleerde suppressors, terwijl de meeste *nag(K)A* mutaties in GlcN-geïsoleerde suppressors werden gevonden (Świątek, 2012; Świątek et al., 2012b; Hoofdstuk V). Deze mutaties stellen *S. coelicolor* in staat om gewoon te groeien in aanwezigheid van zowel GlcN als GlcNAc, wat de overlap tussen het metabolisme van GlcN en GlcNAc benadrukt. Mutaties die toxiciteit van slechts één van de twee opheffen zijn daarom van groot belang om verschillen tussen de twee metabole netwerken te identificeren. Een zo'n mutatie is in het gen *rokL6*: *rokL6-nagB* mutanten kunnen we groeien op GlcN maar niet op GlcNAc, hetgeen suggereert dat RokL6 een GlcN-specifieke regulator is (Hoofdstukken V-VI). De functie van RokL6 is nog niet duidelijk, maar het kan wel eens een belangrijke schakel blijken in de divergentie tussen GlcN en GlcNAc metabole routes.

Om de potentiële invloed van RokL6 te beoordelen, is het proteome van het *rokL6* deletiemutant vergeleken met die van wild-type *S. coelicolor* in aanwezigheid en afwezigheid van GlcN (Hoofdstuk VI). De gegevens suggereren dat GlcN-detectie onafhankelijk is van RokL6, aangezien er weinig verschil te zien was tussen eiwitprofielen van cellen die gegroeid waren op GlcN of mannitol. Een belangrijk verschil is dat *rokL6* mutanten veel meer WhiB (een regulator die essentieel is voor sporulatie) produceren, terwijl expressie van biosynthese-eiwitten voor het antibioticum undecylprodigiosin juist lager waren. Dit wijst op een rol van RokL6 bij de controle van ontwikkeling en productie van antibiotica. In veel streptomyceten ligt een gen voor een suikertransporter direct naast *rokL6*, waarbij de promotergebieden gedeeld worden. Omdat *rokL6* GlcN-specifiek is, veronderstelden we

dat het MFS transporteiwit SCO1448 een rol speelt bij de import van GlcN, maar bewijs hiervoor werd niet gevonden (hoofdstuk V).

Een fascinerende ontdekking was dat *rokl6-nagB* dubbelmutanten bestand zijn tegen de antitumor drug 2-deoxyglucose (DOG) (Hoofdstuk VI). DOG is een glucose-analoog welke toxisch is voor zowel bacteriële als eukaryote cellen en een remmer is van de glycolyse (Wick *et al.*, 1957). DOG wordt momenteel getest als een chemotherapeutisch geneesmiddel tegen kanker (Zhang *et al.*, 2014; Bost *et al.*, 2016). Echter, het mechanisme waarmee DOG de groei remt is nog onbekend, en het effect op de glycolyse is niet voldoende om de cytotoxiciteit van het molecuul te verklaren (Ralser *et al.*, 2008). Streptomyceten zouden hier nu wel eens belangrijke aanwijzingen voor kunnen geven. Streptomyceten kunnen niet op DOG groeien en alleen suppressors met mutaties in het gen voor glucokinase, wat glucose fosforyleert tot glucose-6P, kunnen overleven in aanwezigheid van DOG (Ikeda *et al.*, 1984). Het ontrafelen van het mechanisme waarmee *rokl6-nagB* mutanten DOG toxiciteit ontsnappen zullen nieuwe inzichten kunnen geven in glucose en aminosuiker metabolisme, en tegelijk ook aanwijzingen geven over het metabolisme en de toxiciteit van DOG.

Het onderzoek beschreven in dit proefschrift heeft daarmee belangrijke nieuwe inzichten gegeven in (de controle van) zuurstofstress en het metabolisme van aminosuikers in streptomyceten. Dit omvat een 'dormancy' regulon dat wordt gecoördineerd door de two-component system OsdRK, de verrassende rol van RokL6 bij glucosamine metabolisme en de ontdekking van SCO4393 als een nieuw enzym in het metabolisme van aminosuikers. Dit proefschrift vormt daarmee een belangrijk vertrekpunt voor nieuwe ontdekkingen. De hoge resolutie kristalstructuur van SCO4393 is de eerste grote stap om het daadwerkelijke ligand van het enzym te ontdekken, terwijl systeembioologische analyse van het RokL6 regulon nieuwe aspecten van de controle van het primaire metabolisme naar voren zal brengen. Het ontrafelen van de reactie die door fosfo-aminosuikerisomerase SCO4393 wordt gekatalyseerd, evenals de manier waarop RokL6 GlcN metabolisme reguleert, zal nieuwe inzichten verschaffen in het centrale metabolisme rond de belangrijke driehoek die glycolyse, aminosuikermetabolisme en celwandsynthese verbindt. Verder onderzoek zal moeten uitwijzen hoeveel nieuwe principes er nog te ontdekken zijn in dit reeds zeer intensief bestudeerde veld. *The truth is out there.*

REFERENCES

REFERENCES

- Agirre, J., Iglesias-Fernandez, J., Rovira, C., Davies, G.J., Wilson, K.S., and Cowtan, K.D. (2015) Privateer: software for the conformational validation of carbohydrate structures. *Nat Struct Mol Biol* **22**: 833-834.
- Al-Bassam, M.M., Bibb, M.J., Bush, M.J., Chandra, G., and Buttner, M.J. (2014) Response regulator heterodimer formation controls a key stage in *Streptomyces* development. *PLoS Genet* **10**: e1004554.
- Alice, A.F., Perez-Martinez, G., and Sanchez-Rivas, C. (2003) Phosphoenolpyruvate phosphotransferase system and *N*-acetylglucosamine metabolism in *Bacillus sphaericus*. *Microbiology* **149**: 1687-1698.
- Allenby, N.E., Laing, E., Bucca, G., Kierzek, A.M., and Smith, C.P. (2012) Diverse control of metabolism and other cellular processes in *Streptomyces coelicolor* by the PhoP transcription factor: genome-wide identification of *in vivo* targets. *Nucleic Acids Res* **40**: 9543-9556.
- Altschul, S.F., Wootton, J.C., Gertz, E.M., Agarwala, R., Morgulis, A., Schaffer, A.A., and Yu, Y.K. (2005) Protein database searches using compositionally adjusted substitution matrices. *FEBS J* **272**: 5101-5109.
- Angell, S., Lewis, C.G., Buttner, M.J., and Bibb, M.J. (1994) Glucose repression in *Streptomyces coelicolor* A3(2): a likely regulatory role for glucose kinase. *Mol Gen Genet* **244**: 135-143.
- Angell, S., Schwarz, E., and Bibb, M.J. (1992) The glucose kinase gene of *Streptomyces coelicolor* A3(2): its nucleotide sequence, transcriptional analysis and role in glucose repression. *Mol Microbiol* **6**: 2833-2844.
- Ausmees, N., Wahlstedt, H., Bagchi, S., Elliot, M.A., Buttner, M.J., and Flardh, K. (2007) SmeA, a small membrane protein with multiple functions in *Streptomyces* sporulation including targeting of a SpoIIIE/FtsK-like protein to cell division septa. *Molecular Microbiology* **65**: 1458-1473.
- Bailey, T.L., Boden, M., Buske, F.A., Frith, M., Grant, C.E., Clementi, L., Ren, J., Li, W.W., and Noble, W.S. (2009) MEME SUITE: tools for motif discovery and searching. *Nucleic Acids Res* **37**: W202-208.
- Barka, E.A., Vatsa, P., Sanchez, L., Gavaut-Vaillant, N., Jacquard, C., Klenk, H.P., Clément, C., Oudouch, Y., and van Wezel, G.P. (2016) Taxonomy, physiology, and natural products of the *Actinobacteria*. *Microbiol Mol Biol Rev* **80**: 1-43.
- Bateman, A. (1999) The SIS domain: a phosphosugar-binding domain. *Trends in biochemical sciences* **24**: 94-95.
- Bates, C.J., and Pasternak, C.A. (1965) Further Studies on the Regulation of Amino Sugar Metabolism in *Bacillus subtilis*. *Biochem J* **96**: 147-154.
- Bekiesch, P., Forchhammer, K., and Apel, A.K. (2016) Characterization of DNA Binding Sites of RokB, a ROK-Family Regulator from *Streptomyces coelicolor* Reveals the RokB Regulon. *PLoS ONE* **11**: e0153249.
- Bentley, S.D., Chater, K.F., Cerdeno-Tarraga, A.M., Challis, G.L., Thomson, N.R., James, K.D., Harris, D.E., Quail, M.A., Kieser, H., Harper, D., Bateman, A., Brown, S., Chandra, G., Chen, C.W., Collins, M., Cronin, A., Fraser, A., Goble, A., Hidalgo, J., Hornsby, T., Howarth, S., Huang, C.H., Kieser, T., Larke, L., Murphy, L., Oliver, K., O'Neil, S., Rabbinowitsch, E., Rajandream, M.A., Rutherford, K., Rutter, S., Seeger, K., Saunders, D., Sharp, S., Squares, R., Squares, S., Taylor, K., Warren, T., Wietzorrek, A., Woodward, J., Barrell, B.G., Parkhill, J., and Hopwood, D.A. (2002) Complete genome sequence of the model actinomycete *Streptomyces coelicolor* A3(2). *Nature* **417**: 141-147.
- Bérdy, J. (2005) Bioactive microbial metabolites. *J Antibiot (Tokyo)* **58**: 1-26.
- Berman, H., Henrick, K., and Nakamura, H. (2003) Announcing the worldwide Protein Data Bank. *Nat Struct Biol* **10**: 980.
- Bertram, R., Rigali, S., Wood, N., Lulko, A.T., Kuipers, O.P., and Titgemeyer, F. (2011) Regulon of the *N*-acetylglucosamine utilization regulator NagR in *Bacillus subtilis*. *J Bacteriol* **193**: 3525-3536.
- Bertram, R., Schlicht, M., Mahr, K., Nothhaft, H., Saier, M.H., and Titgemeyer, F. (2004) *In silico* and transcriptional analysis of carbohydrate uptake systems of *Streptomyces coelicolor* A3 (2). *Journal of bacteriology* **186**: 1362-1373.
- Bhatnagar, R.K., Doull, J.L., and Vining, L.C. (1988) Role of the carbon source in regulating chloramphenicol production by *Streptomyces venezuelae*: studies in batch and continuous cultures. *Can J Microbiol* **34**: 1217-1223.
- Bibb, M.J., Domonkos, A., Chandra, G., and Buttner, M.J. (2012) Expression of the chaplin and rodlin hydrophobic sheath proteins in *Streptomyces venezuelae* is controlled by sigma(BldN) and a cognate anti-sigma factor, RsbN. *Mol Microbiol* **84**: 1033-1049.
- Bibb, M.J. (2005) Regulation of secondary metabolism in streptomycetes. *Curr Opin Microbiol* **8**: 208-

- 215.
- Bibb, M.J., Molle, V., and Buttner, M.J. (2000) sigma(BldN), an extracytoplasmic function RNA polymerase sigma factor required for aerial mycelium formation in *Streptomyces coelicolor* A3(2). *J Bacteriol* **182**: 4606-4616.
- Blondelet-Rouault, M.H., Weiser, J., Lebrihi, A., Branny, P., and Pernodet, J.L. (1997) Antibiotic resistance gene cassettes derived from the omega interposon for use in *E. coli* and *Streptomyces*. *Gene* **190**: 315-317.
- Borodina, I., Siebring, J., Zhang, J., Smith, C.P., van Keulen, G., Dijkhuizen, L., and Nielsen, J. (2008) Antibiotic overproduction in *Streptomyces coelicolor* A3(2) mediated by phosphofructokinase deletion. *The Journal of biological chemistry* **283**: 25186-25199.
- Borodina I, Krabben P, Nielsen J. 2005. Genome-scale analysis of *Streptomyces coelicolor* A3(2) metabolism. *Genome Res* **15**:820-829.
- Bost, F., Decoux-Poullot, A.G., Tanti, J.F., and Clavel, S. (2016) Energy disruptors: rising stars in anticancer therapy? *Oncogenesis* **5**: e188.
- Boulanger, A., Dejean, G., Lautier, M., Glories, M., Zischek, C., Arlat, M., and Lauber, E. (2010) Identification and regulation of the *N*-acetylglucosamine utilization pathway of the plant pathogenic bacterium *Xanthomonas campestris* pv. *campestris*. *Journal of bacteriology* **192**: 1487-1497.
- Bouma, C.L., and Roseman, S. (1996) Sugar transport by the marine chitinolytic bacterium *Vibrio furnissii*. Molecular cloning and analysis of the mannose/glucose permease. *The Journal of biological chemistry* **271**: 33468-33475.
- Brechemier-Baey, D., Dominguez-Ramirez, L., Oberto, J., and Plumbridge, J. (2015) Operator recognition by the ROK transcription factor family members, NagC and Mlc. *Nucleic Acids Res* **43**: 361-372.
- Brückner, R., and Titgemeyer, F. (2002) Carbon catabolite repression in bacteria: choice of the carbon source and autoregulatory limitation of sugar utilization. *FEMS Microbiol Lett* **209**: 141-148.
- Bueno, E., Mesa, S., Bedmar, E.J., Richardson, D.J., and Delgado, M.J. (2012) Bacterial adaptation of respiration from oxic to microoxic and anoxic conditions: redox control. *Antioxid Redox Signal* **16**: 819-852.
- Butler, M.J., Deutscher, J., Postma, P.W., Wilson, T.J., Galinier, A., and Bibb, M.J. (1999) Analysis of a *ptsH* homologue from *Streptomyces coelicolor* A3(2). *FEMS Microbiol Lett* **177**: 279-288.
- Cerdeno, A.M., Bibb, M.J., and Challis, G.L. (2001) Analysis of the prodiginine biosynthesis gene cluster of *Streptomyces coelicolor* A3(2): new mechanisms for chain initiation and termination in modular multienzymes. *Chemistry & biology* **8**: 817-829.
- Chao, M.C., and Rubin, E.J. (2010) Letting sleeping dos lie: does dormancy play a role in tuberculosis? *Annu Rev Microbiol* **64**: 293-311.
- Chauhan, S., Sharma, D., Singh, A., Surolia, A., and Tyagi, J.S. (2011) Comprehensive insights into *Mycobacterium tuberculosis* DevR (DosR) regulon activation switch. *Nucleic Acids Res* **39**: 7400-7414.
- Chauhan, S., and Tyagi, J.S. (2008) Cooperative binding of phosphorylated DevR to upstream sites is necessary and sufficient for activation of the Rv3134c-devRS operon in *Mycobacterium tuberculosis*: implication in the induction of DevR target genes. *Journal of bacteriology* **190**: 4301-4312.
- Chen, V.B., Arendall, W.B., 3rd, Headd, J.J., Keedy, D.A., Immormino, R.M., Kapral, G.J., Murray, L.W., Richardson, J.S., and Richardson, D.C. (2010) MolProbity: all-atom structure validation for macromolecular crystallography. *Acta Crystallogr D Biol Crystallogr* **66**: 12-21.
- Cho, H.Y., Cho, H.J., Kim, Y.M., Oh, J.I., and Kang, B.S. (2009) Structural insight into the heme-based redox sensing by DosS from *Mycobacterium tuberculosis*. *J Biol Chem* **284**: 13057-13067.
- Chouayekh, H., and Virolle, M.J. (2002) The polyphosphate kinase plays a negative role in the control of antibiotic production in *Streptomyces lividans*. *Mol Microbiol* **43**: 919-930.
- Claessen, D., Rozen, D.E., Kuipers, O.P., Sogaard-Andersen, L., and van Wezel, G.P. (2014) Bacterial solutions to multicellularity: a tale of biofilms, filaments and fruiting bodies. *Nat Rev Microbiol* **12**: 115-124.
- Claessen, D., Rink, R., de Jong, W., Siebring, J., de Vreugd, P., Boersma, F.G., Dijkhuizen, L., and Wösten, H.A. (2003) A novel class of secreted hydrophobic proteins is involved in aerial hyphae formation in *Streptomyces coelicolor* by forming amyloid-like fibrils. *Genes Dev* **17**: 1714-1726.
- Claessen, D., Wösten, H.A., van Keulen, G., Faber, O.G., Alves, A.M., Meijer, W.G., and Dijkhuizen, L. (2002) Two novel homologous proteins of *Streptomyces coelicolor* and *Streptomyces lividans* are involved in the formation of the rodlet layer and mediate attachment to a hydrophobic

REFERENCES

- surface. *Mol Microbiol* **44**: 1483-1492.
- Colson, S., van Wezel, G.P., Craig, M., Noens, E.E., Nothaft, H., Mommaas, A.M., Titgemeyer, F., Joris, B., and Rigali, S. (2008) The chitobiose-binding protein, DasA, acts as a link between chitin utilization and morphogenesis in *Streptomyces coelicolor*. *Microbiology* **154**: 373-382.
- Colson, S., Stephan, J., Hertrich, T., Saito, A., van Wezel, G.P., Titgemeyer, F., and Rigali, S. (2007) Conserved cis-acting elements upstream of genes composing the chitinolytic system of streptomycetes are DasR-responsive elements. *J Mol Microbiol Biotechnol* **12**: 60-66.
- Conejo, M.S., Thompson, S.M., and Miller, B.G. (2010) Evolutionary bases of carbohydrate recognition and substrate discrimination in the ROK protein family. *Journal of molecular evolution* **70**: 545-556.
- Cooper, M.A., and Shlaes, D. (2011) Fix the antibiotics pipeline. *Nature* **472**: 32.
- Cortes, J., Liras, P., Castro, J.M., and Martin, J.F. (1986) Glucose regulation of cephamycin biosynthesis in *Streptomyces lactamurans* is exerted on the formation of alpha-aminoadipyl-cysteinyl-valine and deacetoxycephalosporin C synthase. *J Gen Microbiol* **132**: 1805-1814.
- Craig, M., Lambert, S., Jourdan, S., Tenconi, E., Colson, S., Maciejewska, M., Ongena, M., Martin, J.F., van Wezel, G., and Rigali, S. (2012) Unsuspected control of siderophore production by N-acetylglucosamine in streptomycetes. *Environ Microbiol Rep* **4**: 512-521.
- Crooks, G.E., Hon, G., Chandonia, J.M., and Brenner, S.E. (2004) WebLogo: A sequence logo generator. *Genome Research* **14**: 1188-1190.
- Cruz-Morales, P., Vijgenboom, E., Iruegas-Bocardo, F., Girard, G., Yanez-Guerra, L.A., Ramos-Aboites, H.E., Pernodet, J.L., Anne, J., van Wezel, G.P., and Barona-Gomez, F. (2013) The genome sequence of *Streptomyces lividans* 66 reveals a novel tRNA-dependent peptide biosynthetic system within a metal-related genomic island. *Genome Biol Evol* **5**: 1165-1175.
- Dai, Y., and Outten, F.W. (2012) The E. coli SufS-SufE sulfur transfer system is more resistant to oxidative stress than IscS-IscU. *FEBS Lett* **586**: 4016-4022.
- Daigle, F., Lerat, S., Bucca, G., Sanssouci, E., Smith, C.P., Malouin, F., and Beaulieu, C. (2015) A terD domain-encoding gene (SCO2368) is involved in calcium homeostasis and participates in calcium regulation of a DosR-like regulon in *Streptomyces coelicolor*. *J Bacteriol* **197**: 913-923.
- Demain, A.L., and Inamine, E. (1970) Biochemistry and regulation of streptomycin and mannosidostreptomycinase (alpha-D-mannosidase) formation. *Bacteriol Rev* **34**: 1-19.
- Derouaux, A., Dehareng, D., Lecocq, E., Halici, S., Nothaft, H., Giannotta, F., Moutzourelis, G., Dusart, J., Devreese, B., Titgemeyer, F., Van Beeumen, J., and Rigali, S. (2004a) Crp of *Streptomyces coelicolor* is the third transcription factor of the large CRP-FNR superfamily able to bind cAMP. *Biochem Biophys Res Commun* **325**: 983-990.
- Derouaux, A., Halici, S., Nothaft, H., Neutelings, T., Moutzourelis, G., Dusart, J., Titgemeyer, F., and Rigali, S. (2004b) Deletion of a cyclic AMP receptor protein homologue diminishes germination and affects morphological development of *Streptomyces coelicolor*. *J Bacteriol* **186**: 1893-1897.
- Deutscher, J., Kuster, E., Bergstedt, U., Charrier, V., and Hillen, W. (1995) Protein kinase-dependent HPr/CcpA interaction links glycolytic activity to carbon catabolite repression in gram-positive bacteria. *Mol Microbiol* **15**: 1049-1053.
- Di Berardo, C., Capstick, D.S., Bibb, M.J., Findlay, K.C., Buttner, M.J., and Elliot, M.A. (2008) Function and redundancy of the chaplin cell surface proteins in aerial hypha formation, rodlet assembly, and viability in *Streptomyces coelicolor*. *J Bacteriol* **190**: 5879-5889.
- Dubeau, M.P., Poulin-Laprade, D., Ghinet, M.G., and Brzezinski, R. (2011) Properties of CsnR, the transcriptional repressor of the chitosanase gene, *csnA*, of *Streptomyces lividans*. *J Bacteriol* **193**: 2441-2450.
- Durand, P., Golinelli-Pimpaneau, B., Moulleron, S., Badet, B., and Badet-Denisot, M.A. (2008) Highlights of glucosamine-6P synthase catalysis. *Arch Biochem Biophys* **474**: 302-317.
- Eisenbeis, S., Lohmiller, S., Valdebenito, M., Leicht, S., and Braun, V. (2008) NagA-dependent uptake of N-acetyl-glucosamine and N-acetyl-chitin oligosaccharides across the outer membrane of *Caulobacter crescentus*. *Journal of bacteriology* **190**: 5230-5238.
- Elliot, M.A., Buttner, M.J., and Nodwell, J.R., (2008) Multicellular Development in *Streptomyces*. In: Myxobacteria: Multicellularity and Differentiation. D.E. Whitworth (ed). Washington, D.C.: ASM Press, pp. 419-438.
- Elliot, M.A., Karoonuthaisiri, N., Huang, J., Bibb, M.J., Cohen, S.N., Kao, C.M., and Buttner, M.J. (2003) The chaplins: a family of hydrophobic cell-surface proteins involved in aerial mycelium formation in *Streptomyces coelicolor*. *Genes Dev* **17**: 1727-1740.
- Emsley, P., Lohkamp, B., Scott, W.G., and Cowtan, K. (2010) Features and development of Coot. *Acta Crystallogr D Biol Crystallogr* **66**: 486-501.

- Englesberg, E., Anderson, R.L., Weinberg, R., Lee, N., Hoffee, P., Huttenhauer, G., and Boyer, H. (1962) L-Arabinose-sensitive, L-ribulose 5-phosphate 4-epimerase-deficient mutants of *Escherichia coli*. *J Bacteriol* **84**: 137-146.
- Errington, J. (2013) L-form bacteria, cell walls and the origins of life. *Open biology* **3**: 120143.
- Escalante, L., Lopez, H., del Carmen Mateos, R., Lara, F., and Sanchez, S. (1982) Transient repression of erythromycin formation in *Streptomyces erythraeus*. *J Gen Microbiol* **128**: 2011-2015.
- Evans, P.R., and Murshudov, G.N. (2013) How good are my data and what is the resolution? *Acta Crystallogr D Biol Crystallogr* **69**: 1204-1214.
- Facey, P.D., Sevcikova, B., Novakova, R., Hitchings, M.D., Crack, J.C., Kormanec, J., Dyson, P.J., and Del Sol, R. (2011) The *dpsA* gene of *Streptomyces coelicolor*: induction of expression from a single promoter in response to environmental stress or during development. *PLoS One* **6**: e25593.
- Fedoryshyn, M., Welle, E., Bechthold, A., and Luzhetskyy, A. (2008) Functional expression of the Cre recombinase in actinomycetes. *Appl Microbiol Biotechnol* **78**: 1065-1070.
- Fillenberg, S.B., Friess, M.D., Korner, S., Bockmann, R.A., and Muller, Y.A. (2016) Crystal Structures of the Global Regulator DasR from *Streptomyces coelicolor*: Implications for the Allosteric Regulation of GntR/HutC Repressors. *PLoS ONE* **11**: e0157691.
- Fillenberg, S.B., Grau, F.C., Seidel, G., and Muller, Y.A. (2015) Structural insight into operator *dre*-sites recognition and effector binding in the GntR/HutC transcription regulator NagR. *Nucleic Acids Res* **43**: 1283-1296.
- Fink, D., Weissschuh, N., Reuther, J., Wohlleben, W., and Engels, A. (2002) Two transcriptional regulators GlnR and GlnRII are involved in regulation of nitrogen metabolism in *Streptomyces coelicolor* A3 (2). *Molecular microbiology* **46**: 331-347.
- Finn, R.D., Tate, J., Mistry, J., Coghill, P.C., Sammut, S.J., Hotz, H.R., Ceric, G., Forslund, K., Eddy, S.R., Sonnhammer, E.L., and Bateman, A. (2008) The Pfam protein families database. *Nucleic Acids Res* **36**: D281-288.
- Fischer, M., Falke, D., Pawlik, T., and Sawers, R.G. (2014) Oxygen-dependent control of respiratory nitrate reduction in mycelium of *Streptomyces coelicolor* A3(2). *J Bacteriol* **196**: 4152-4162.
- Fischer, M., Alderson, J., van Keulen, G., White, J., and Sawers, R.G. (2010) The obligate aerobic *Streptomyces coelicolor* A3(2) synthesizes three active respiratory nitrate reductases. *Microbiology* **156**: 3166-3179.
- Flardh, K., and McCormick, J.R. (2017) The Streptomyces O-B One Connection: A Force within Layered Repression of a Key Developmental Decision. *Mol Microbiol* **104**: 695-699
- Flardh, K., and Buttner, M.J. (2009) *Streptomyces* morphogenetics: dissecting differentiation in a filamentous bacterium. *Nat Rev Microbiol* **7**: 36-49.
- Flores, F.J., and Martin, J.F. (2004) Iron-regulatory proteins DmdR1 and DmdR2 of *Streptomyces coelicolor* form two different DNA-protein complexes with iron boxes. *Biochem J* **380**: 497-503.
- Floriano, B., and Bibb, M. (1996) *afsR* is a pleiotropic but conditionally required regulatory gene for antibiotic production in *Streptomyces coelicolor* A3(2). *Mol Microbiol* **21**: 385-396.
- Francis, I.M., Jourdan, S., Fanara, S., Loria, R., and Rigali, S. (2015) The cellobiose sensor CebR is the gatekeeper of *Streptomyces scabies* pathogenicity. *MBio* **6**: e02018.
- Gao, C., Hindra, Mulder, D., Yin, C., and Elliot, M.A. (2012a) Crp is a global regulator of antibiotic production in *Streptomyces*. *MBio* **3**: 00407-00412.
- Gao, Z., Li, F., Wu, G., Zhu, Y., Yu, T., and Yu, S. (2012b) Roles of hinge region, loops 3 and 4 in the activation of *Escherichia coli* cyclic AMP receptor protein. *Int J Biol Macromol* **50**: 1-6.
- Gaugué, I., Oberto, J., Putzer, H., and Plumbridge, J. (2013) The use of amino sugars by *Bacillus subtilis*: presence of a unique operon for the catabolism of glucosamine. *PLoS ONE* **8**: e63025.
- Gentleman, R.C., Carey, V.J., Bates, D.M., Bolstad, B., Dettling, M., Dudoit, S., Ellis, B., Gautier, L., Ge, Y., Gentry, J., Hornik, K., Hothorn, T., Huber, W., Iacus, S., Irizarry, R., Leisch, F., Li, C., Maechler, M., Rossini, A.J., Sawitzki, G., Smith, C., Smyth, G., Tierney, L., Yang, J.Y., and Zhang, J. (2004) Bioconductor: open software development for computational biology and bioinformatics. *Genome biology* **5**: R80.
- Gerasimova, A., Kazakov, A.E., Arkin, A.P., Dubchak, I., and Gelfand, M.S. (2011) Comparative genomics of the dormancy regulons in mycobacteria. *J Bacteriol* **193**: 3446-3452.
- Ghorbel, S., Kormanec, J., Artus, A., and Viroille, M.J. (2006a) Transcriptional studies and regulatory interactions between the *phoR-phoP* operon and the *phoU*, *mtpA*, and *ppk* genes of *Streptomyces lividans* TK24. *J Bacteriol* **188**: 677-686.
- Ghorbel, S., Smirnov, A., Chouayekh, H., Sperandio, B., Esnault, C., Kormanec, J., and Viroille, M.J. (2006b) Regulation of *ppk* expression and *in vivo* function of Ppk in *Streptomyces lividans* TK24. *J Bacteriol* **188**: 6269-6276.

REFERENCES

- Gomez-Escribano, J.P., Song, L., Fox, D.J., Yeo, V., Bibb, M.J., and Challis, G.L. (2012) Structure and biosynthesis of the unusual polyketide alkaloid coelimycin P1, a metabolic product of the *cpk* gene cluster of *Streptomyces coelicolor* M145. *Chem Sci* **3**: 2716-2720.
- Gorke, B., and Stulke, J. (2008) Carbon catabolite repression in bacteria: many ways to make the most out of nutrients. *Nat Rev Microbiol* **6**: 613-624.
- Gubbens J., Zhu H., Girard G., Song L., Florea B.I., Aston P., Ichinose K., Filippov D.V., Choi Y.H., Overkleeft H.S., Challis G.L., van Wezel G.P. (2014) Natural Product Proteomics, a Quantitative Proteomics Platform, Allows Rapid Discovery of Biosynthetic Gene Clusters for Different Classes of Natural Products. *Chemistry & biology* **21**: 707-718.
- Gubbens, J., Janus, M., Florea, B.I., Overkleeft, H.S., and van Wezel, G.P. (2012) Identification of glucose kinase dependent and independent pathways for carbon control of primary metabolism, development and antibiotic production in *Streptomyces coelicolor* by quantitative proteomics. *Mol Microbiol* **86**: 1490-1507.
- Gunnewijk, M.G., van den Bogaard, P.T., Veenhoff, L.M., Heuberger, E.H., de Vos, W.M., Kleerebezem, M., Kuipers, O.P., and Poolman, B. (2001) Hierarchical control versus autoregulation of carbohydrate utilization in bacteria. *J Mol Microbiol Biotechnol* **3**: 401-413.
- Guzman, S., Carmona, A., Escalante, L., Imriskova, I., Lopez, R., Rodriguez-Sanoja, R., Ruiz, B., Servin-Gonzalez, L., Sanchez, S., and Langley, E. (2005) Pleiotropic effect of the SCO2127 gene on the glucose uptake, glucose kinase activity and carbon catabolite repression in *Streptomyces peucetius* var. *caesius*. *Microbiology* **151**: 1717-1723.
- Hiard, S., Marée, R., Colson, S., Hoskisson, P.A., Titgemeyer, F., van Wezel, G.P., Joris, B., Wehenkel, L., and Rigali, S. (2007) PREDetector: A new tool to identify regulatory elements in bacterial genomes. *Biochemical and Biophysical Research Communications* **357**: 861-864.
- Hindle, Z., and Smith, C.P. (1994) Substrate induction and catabolite repression of the *Streptomyces coelicolor* glycerol operon are mediated through the GylR protein. *Mol Microbiol* **12**: 737-745.
- Hodgson, D.A. (2000) Primary metabolism and its control in streptomycetes: a most unusual group of bacteria. *Adv Microb Physiol* **42**: 47-238.
- Hogema, B.M., Arents, J.C., Bader, R., Eijkemans, K., Yoshida, H., Takahashi, H., Aiba, H., and Postma, P.W. (1998) Inducer exclusion in *Escherichia coli* by non-PTS substrates: the role of the PEP to pyruvate ratio in determining the phosphorylation state of enzyme IIAGlc. *Mol Microbiol* **30**: 487-498.
- Honaker, R.W., Dhiman, R.K., Narayanasamy, P., Crick, D.C., and Voskuil, M.I. (2010) DosS responds to a reduced electron transport system to induce the *Mycobacterium tuberculosis* DosR regulon. *J Bacteriol* **192**: 6447-6455.
- Honaker, R.W., Leistikow, R.L., Bartek, I.L., and Voskuil, M.I. (2009) Unique roles of DosT and DosS in DosR regulon induction and *Mycobacterium tuberculosis* dormancy. *Infect Immun* **77**: 3258-3263.
- Hong, B., Phornphisutthimas, S., Tilley, E., Baumberg, S., and McDowall, K.J. (2007) Streptomycin production by *Streptomyces griseus* can be modulated by a mechanism not associated with change in the *adpA* component of the A-factor cascade. *Biotechnol Lett* **29**: 57-64.
- Hong, F., Breitling, R., McEntee, C.W., Wittner, B.S., Nemhauser, J.L., and Chory, J. (2006) RankProd: a bioconductor package for detecting differentially expressed genes in meta-analysis. *Bioinformatics* **22**: 2825-2827.
- Hopwood, D.A., (2007) *Streptomyces in nature and medicine: the antibiotic makers*. Oxford University Press, New York.
- Hopwood, D.A. (2006) Soil to genomics: the *Streptomyces* chromosome. *Annu Rev Genet* **40**: 1-23.
- Hostalek, Z. (1980) Catabolite regulation of antibiotic biosynthesis. *Folia Microbiol (Praha)* **25**: 445-450.
- Huang, J., Lih, C.J., Pan, K.H., and Cohen, S.N. (2001) Global analysis of growth phase responsive gene expression and regulation of antibiotic biosynthetic pathways in *Streptomyces coelicolor* using DNA microarrays. *Genes Dev* **15**: 3183-3192.
- Hutchings, M.I., Hoskisson, P.A., Chandra, G., and Buttner, M.J. (2004) Sensing and responding to diverse extracellular signals? Analysis of the sensor kinases and response regulators of *Streptomyces coelicolor* A3(2). *Microbiology* **150**: 2795-2806.
- Ikeda, H., Ishikawa, J., Hanamoto, A., Shinose, M., Kikuchi, H., Shiba, T., Sakaki, Y., Hattori, M., and Omura, S. (2003) Complete genome sequence and comparative analysis of the industrial microorganism *Streptomyces avermitilis*. *Nature biotechnology* **21**: 526-531.
- Ikeda, H., Seno, E.T., Bruton, C.J., and Chater, K.F. (1984) Genetic mapping, cloning and physiological aspects of the glucose kinase gene of *Streptomyces coelicolor*. *Mol Gen Genet* **196**: 501-507.

- Innes, C.M., and Allan, E.J. (2001) Induction, growth and antibiotic production of *Streptomyces viridifaciens* L-form bacteria. *Journal of applied microbiology* **90**: 301-308.
- Irani, M.H., and Maitra, P.K. (1977) Properties of *Escherichia coli* mutants deficient in enzymes of glycolysis. *J Bacteriol* **132**: 398-410.
- Jaeger, T., and Mayer, C. (2008) N-acetylmuramic acid 6-phosphate lyases (MurNAc etherases): role in cell wall metabolism, distribution, structure, and mechanism. *Cellular and Molecular Life Sciences* **65**: 928-939.
- Jakimowicz, D., and van Wezel, G.P. (2012) Cell division and DNA segregation in *Streptomyces*: how to build a septum in the middle of nowhere? *Mol Microbiol* **85**: 393-404.
- Jault, J., Fieulaine, S., Nessler, S., Gonzalo, P., Di Pietro, A., Deutscher, J., and Galinier, A. (2000) The HPr kinase from *Bacillus subtilis* is a homo-oligomeric enzyme which exhibits strong positive cooperativity for nucleotide and fructose 1,6-bisphosphate binding. *J Biol Chem*. **275**: 1773-1780.
- Jones-Mortimer, M.C., and Kornberg, H.L. (1980) Amino-sugar transport systems of *Escherichia coli* K12. *J Gen Microbiol* **117**: 369-376.
- Jones, B.E., Dossonnet, V., Kuster, E., Hillen, W., Deutscher, J., and Klevit, R.E. (1997) Binding of the catabolite repressor protein CcpA to its DNA target is regulated by phosphorylation of its corepressor HPr. *J Biol Chem* **272**: 26530-26535.
- Jung, Y.-G., Cho, Y.-B., Kim, M.-S., Yoo, J.-S., Hong, S.-H., and Roe, J.-H. (2011) Determinants of redox sensitivity in RsrA, a zinc-containing anti-sigma factor for regulating thiol oxidative stress response. *Nucleic Acids Research* **39**: 7586-7597.
- Kadner, R.J., Murphy, G.P., and Stephens, C.M. (1992) Two mechanisms for growth inhibition by elevated transport of sugar phosphates in *Escherichia coli*. *J Gen Microbiol* **138**: 2007-2014.
- Kallifidas, D., Pascoe, B., Owen, G.A., Strain-Damerell, C.M., Hong, H.J., and Paget, M.S. (2010) The zinc-responsive regulator Zur controls expression of the coelibactin gene cluster in *Streptomyces coelicolor*. *J Bacteriol* **192**: 608-611.
- Kamionka, A., Parche, S., Nothaft, H., Siepmeyer, J., Jahreis, K., and Titgemeyer, F. (2002) The phosphotransferase system of *Streptomyces coelicolor*. *Eur J Biochem* **269**: 2143-2150.
- Kang, J.G., Paget, M.S., Seok, Y.J., Hahn, M.Y., Bae, J.B., Hahn, J.S., Kleanthous, C., Buttner, M.J., and Roe, J.H. (1999) RsrA, an anti-sigma factor regulated by redox change. *The EMBO Journal* **18**: 4292-4298.
- Keijser, B.J.F., Noens, E.E.E., Kraal, B., Koerten, H.K., and Wezel, G.P. (2003) The *Streptomyces coelicolor* *ssgB* gene is required for early stages of sporulation. *FEMS Microbiology Letters* **225**: 59-67.
- Kelemen, G.H., Brian, P., Flårdh, K., Chamberlin, L., Chater, K.F., and Buttner, M.J. (1998) Developmental regulation of transcription of *whiE*, a locus specifying the polyketide spore pigment in *Streptomyces coelicolor* A3 (2). *J Bacteriol* **180**: 2515-2521.
- Khodakaramian, G., Lissenden, S., Gust, B., Moir, L., Hoskisson, P.A., Chater, K.F., and Smith, M.C. (2006) Expression of Cre recombinase during transient phage infection permits efficient marker removal in *Streptomyces*. *Nucleic Acids Res* **34**: e20.
- Kieser, T., Bibb, M.J., Buttner, M.J., Chater, K.F., and Hopwood, D.A. (2000) Practical *Streptomyces* genetics. *The John Innes Foundation, Norwich, United Kingdom*.
- Kim, E.S., Hong, H.J., Choi, C.Y., and Cohen, S.N. (2001) Modulation of actinorhodin biosynthesis in *Streptomyces lividans* by glucose repression of *afsR2* gene transcription. *J Bacteriol* **183**: 2198-2203.
- Kim, J.N., Jeong, Y., Yoo, J.S., Roe, J.H., Cho, B.K., and Kim, B.G. (2015a) Genome-scale analysis reveals a role for NdgR in the thiol oxidative stress response in *Streptomyces coelicolor*. *BMC Genomics* **16**: 116.
- Kim, M.S., Dufour, Y.S., Yoo, J.S., Cho, Y.B., Park, J.H., Nam, G.B., Kim, H.M., Lee, K.L., Donohue, T.J., and Roe, J.H. (2012) Conservation of thiol-oxidative stress responses regulated by SigR orthologues in actinomycetes. *Mol Microbiol* **85**: 326-344.
- Kim, S.H., Traag, B.A., Hasan, A.H., McDowall, K.J., Kim, B.G., and van Wezel, G.P. (2015b) Transcriptional analysis of the cell division-related *ssg* genes in *Streptomyces coelicolor* reveals direct control of *ssgR* by AtrA. *Antonie Van Leeuwenhoek* **108**: 201-213.
- Kim, Y., Quartey, P., Ng, R., Zarembinski, T., and Joachimiak, A. (2009) Crystal structure of YfeU protein from *Haemophilus influenzae*: a predicted etherase involved in peptidoglycan recycling. *Journal of structural and functional genomics* **10**: 151-156.
- Kodani, S., Hudson, M.E., Durrant, M.C., Buttner, M.J., Nodwell, J.R., and Willey, J.M. (2004) The SapB morphogen is a lantibiotic-like peptide derived from the product of the developmental gene *ramS* in *Streptomyces coelicolor*. *Proc Natl Acad Sci U S A* **101**: 11448-11453.
- Kolter, R., and van Wezel, G.P. (2016) Goodbye to brute force in antibiotic discovery? *Nat Microbiol*

REFERENCES

- 1:15020.
- Komatsuzawa, H., Fujiwara, T., Nishi, H., Yamada, S., Ohara, M., McCallum, N., Berger-Bachi, B., and Sugai, M. (2004) The gate controlling cell wall synthesis in *Staphylococcus aureus*. *Molecular microbiology* **53**: 1221-1231.
- Labeda, D.P., Goodfellow, M., Brown, R., Ward, A.C., Lanoot, B., Vannanneyt, M., Swings, J., Kim, S.B., Liu, Z., Chun, J., Tamura, T., Oguchi, A., Kikuchi, T., Kikuchi, H., Nishii, T., Tsuji, K., Yamaguchi, Y., Tase, A., Takahashi, M., Sakane, T., Suzuki, K.I., and Hatano, K. (2012) Phylogenetic study of the species within the family Streptomycetaceae. *Antonie Van Leeuwenhoek* **101**: 73-104.
- Laing, E., and Smith, C.P. (2010) RankProdIt: A web-interactive Rank Products analysis tool. *BMC Res Notes* **3**: 221.
- Lambert, S., Traxler, M.F., Craig, M., Maciejewska, M., Ongena, M., van Wezel, G.P., Kolter, R., and Rigali, S. (2014) Altered desferrioxamine-mediated iron utilization is a common trait of bald mutants of *Streptomyces coelicolor*. *Metallomics* **6**: 1390-1399.
- Larson, J.L., and Hershberger, C.L. (1986) The minimal replicon of a streptomycete plasmid produces an ultrahigh level of plasmid DNA. *Plasmid* **15**: 199-209.
- Laub, M.T., Chen, S.L., Shapiro, L., and McAdams, H.H. (2002) Genes directly controlled by CtrA, a master regulator of the *Caulobacter* cell cycle. *Proc Natl Acad Sci U S A* **99**: 4632-4637.
- Le Marechal, P., Decottignies, P., Marchand, C.H., Degrouard, J., Jaillard, D., Dulermo, T., Froissard, M., Smirnov, A., Chapuis, V., and Virolle, M.J. (2013) Comparative proteomic analysis of *Streptomyces lividans* Wild-Type and *ppk* mutant strains reveals the importance of storage lipids for antibiotic biosynthesis. *Appl Environ Microbiol* **79**: 5907-5917.
- Lee, E.J., Karoonuthaisiri, N., Kim, H.S., Park, J.H., Cha, C.J., Kao, C.M., and Roe, J.H. (2005) A master regulator sigmaB governs osmotic and oxidative response as well as differentiation via a network of sigma factors in *Streptomyces coelicolor*. *Mol Microbiol* **57**: 1252-1264.
- Lee, H., Im, J., Lee, M., Lee, S., and ES, K. (2009) A putative secreted solute binding protein, SCO6569 is a possible AfsR2-dependent down-regulator of actinorhodin biosynthesis in *Streptomyces coelicolor*. *Process Biochemistry* **44**: 373-377.
- Lee, P.C., Umeyama, T., and Horinouchi, S. (2002) *afsS* is a target of AfsR, a transcriptional factor with ATPase activity that globally controls secondary metabolism in *Streptomyces coelicolor* A3 (2). *Molecular microbiology* **43**: 1413-1430.
- Lewis, K. (2013) Platforms for antibiotic discovery. *Nat Rev Drug Discov* **12**: 371-387.
- Lewis, R.A., Shahi, S.K., Laing, E., Bucca, G., Efthimiou, G., Bushell, M., and Smith, C.P. (2011) Genome-wide transcriptomic analysis of the response to nitrogen limitation in *Streptomyces coelicolor* A3 (2). *BMC research notes* **4**: 78.
- Li, W., Ying, X., Guo, Y., Yu, Z., Zhou, X., Deng, Z., Kieser, H., Chater, K.F., and Tao, M. (2006) Identification of a gene negatively affecting antibiotic production and morphological differentiation in *Streptomyces coelicolor* A3(2). *J Bacteriol* **188**: 8368-8375.
- Li, W., Bottrill, A.R., Bibb, M.J., Buttner, M.J., Paget, M.S., and Kleantous, C. (2003) The Role of zinc in the disulphide stress-regulated anti-sigma factor RsrA from *Streptomyces coelicolor*. *J Mol Biol* **333**: 461-472.
- Liao, C.H., Yao, L., Xu, Y., Liu, W.-B., Zhou, Y., and Ye, B.-C. (2015a) Nitrogen regulator GlnR controls uptake and utilization of non-phosphotransferase-system carbon sources in actinomycetes. *Proceedings of the National Academy of Sciences*: 201508465.
- Liao, C.H., Xu, Y., Rigali, S., and Ye, B.C. (2015b) DasR is a pleiotropic regulator required for antibiotic production, pigment biosynthesis, and morphological development in *Saccharopolyspora erythraea*. *Appl Microbiol Biotechnol* **99**: 10215-10224.
- Liao, C.H., Yao, L.-l., and Ye, B.-C. (2014a) Three genes encoding citrate synthases in *Saccharopolyspora erythraea* are regulated by the global nutrient-sensing regulators GlnR, DasR, and CRP. *Molecular Microbiology* **94**: 1065-1084.
- Liao, C.H., Rigali, S., Cassani, C.L., Marcellin, E., Nielsen, L.K., and Ye, B.C. (2014b) Control of chitin and N-acetylglucosamine utilization in *Saccharopolyspora erythraea*. *Microbiology* **160**: 1914-1928.
- Ludwig, W., Euzéby, J., Schumann, P., Busse, H.-J., Trujillo, M.E., Kämpfer, P., and Whitman, W.B., (2012) Road map of the phylum Actinobacteria. In: *Bergey's Manual of Systematic Bacteriology*. M. Goodfellow, P. Kämpfer, H.-J. Busse, M.E. Trujillo, K.-I. Suzuki, W. Ludwig & W.B. Whitman (eds). New York: Springer, pp. 1-28.
- MacNeil, D.J., Gewain, K.M., Ruby, C.L., Dezeny, G., Gibbons, P.H., and MacNeil, T. (1992) Analysis of *Streptomyces avermitilis* genes required for avermectin biosynthesis utilizing a novel integration vector. *Gene* **111**: 61-68.
- Mahr, K., van Wezel, G.P., Svensson, C., Krengel, U., Bibb, M.J., and Titgemeyer, F. (2000) Glucose kinase

- of *Streptomyces coelicolor* A3(2): large-scale purification and biochemical analysis. *Antonie Van Leeuwenhoek* **78**: 253-261.
- Manteca, A., Fernandez, M., and Sanchez, J. (2005a) A death round affecting a young compartmentalized mycelium precedes aerial mycelium dismantling in confluent surface cultures of *Streptomyces antibioticus*. *Microbiology* **151**: 3689-3697.
- Manteca, A., M. Fernandez & J. Sanchez, (2005b) Mycelium development in *Streptomyces antibioticus* ATCC11891 occurs in an orderly pattern which determines multiphase growth curves. *BMC microbiology* **5**: 51.
- Marchler-Bauer, A., Derbyshire, M.K., Gonzales, N.R., Lu, S., Chitsaz, F., Geer, L.Y., Geer, R.C., He, J., Gwadz, M., Hurwitz, D.I., Lanczycki, C.J., Lu, F., Marchler, G.H., Song, J.S., Thanki, N., Wang, Z., Yamashita, R.A., Zhang, D., Zheng, C., and Bryant, S.H. (2015) CDD: NCBI's conserved domain database. *Nucleic Acids Res* **43**: D222-226.
- Martin, J.F., Sola-Landa, A., Santos-Beneit, F., Fernández-Martínez, L.T., Prieto, C., and Rodríguez-García, A. (2011) Cross-talk of global nutritional regulators in the control of primary and secondary metabolism in *Streptomyces*. *Microbial biotechnology* **4**: 165-174.
- Martin, J.F., and Liras, P. (2010) Engineering of regulatory cascades and networks controlling antibiotic biosynthesis in *Streptomyces*. *Curr Opin Microbiol* **13**: 263-273.
- Martin, J.F. (2004) Phosphate control of the biosynthesis of antibiotics and other secondary metabolites is mediated by the PhoR-PhoP system: an unfinished story. *J Bacteriol* **186**: 5197-5201.
- Martinez, A., Kolvek, S.J., Hopke, J., Yip, C.L., and Osburne, M.S. (2005) Environmental DNA fragment conferring early and increased sporulation and antibiotic production in *Streptomyces* species. *Appl Environ Microbiol* **71**: 1638-1641.
- Martinez, J.L., and Rojo, F. (2011) Metabolic regulation of antibiotic resistance. *FEMS Microbiol Rev* **35**: 768-789.
- McCormick, J.R., and Flardh, K. (2012) Signals and regulators that govern *Streptomyces* development. *FEMS Microbiol Rev* **36**: 206-231.
- Medema, M.H., Kottmann, R., Yilmaz, P., Cummings, M., Biggins, J.B., Blin, K., de Bruijn, I., Chooi, Y.H., Claesen, J., Coates, R.C., Cruz-Morales, P., Duddela, S., Düsterhus, S., Edwards, D.J., Fewer, D.P., Garg, N., Geiger, C., Gomez-Escribano, J.P., Greule, A., Hadjithomas, M., Haines, A.S., Helfrich, E.J.N., Hillwig, M.L., Ishida, K., Jones, A.C., Jones, C.S., Jungmann, K., Kegler, C., Kim, H.U., Kötter, P., Krug, D., Masschelein, J., Melnik, A.V., Mantovani, S.M., Monroe, E.A., Moore, M., Moss, N., Nützmans, H.-W., Pan, G., Pati, A., Petras, D., Reen, F.J., Rosconi, F., Rui, Z., Tian, Z., Tobias, N.J., Tsunematsu, Y., Wiemann, P., Wyckoff, E., Yan, X., Yim, G., Yu, F., Xie, Y., Aigle, B., Apel, A.K., Balibar, C.J., Balskus, E.P., Barona-Gómez, F., Bechthold, A., Bode, H.B., Borriss, R., Brady, S.F., Brakhage, A.A., Caffrey, P., Cheng, Y.-Q., Clardy, J., Cox, R.J., De Mot, R., Donadio, S., Donia, M.S., van der Donk, W.A., Dorrestein, P.C., Doyle, S., Driessen, A.J.M., Ehling-Schulz, M., Entian, K.-D., Fischbach, M.A., Gerwick, L., Gerwick, W.H., Gross, H., Gust, B., Hertweck, C., Höfte, M., Jensen, S.E., Ju, J., Katz, L., Kayser, L., Klassen, J.L., Keller, N.P., Kormanec, J., Kuipers, O.P., Kuzuyama, T., Kyrpides, N.C., Kwon, H.-J., Lautru, S., Lavigne, R., Lee, C.Y., Linquan, B., Liu, X., Liu, W., et al. (2015) Minimum Information about a Biosynthetic Gene cluster. *Nature Chemical Biology* **11**: 625-631.
- Mercier, R., Kawai, Y., and Errington, J. (2014) General principles for the formation and proliferation of a wall-free (L-form) state in bacteria. *eLife* **3**.
- Midelfort, C.F., and Rose, I.A. (1977) Studies on the mechanism of *Escherichia coli* glucosamine-6-phosphate isomerase. *Biochemistry* **16**: 1590-1596.
- Miguel, E.M., Hardisson, C., and Manzanal, M.B. (2000) Streptomycetes: a new model to study cell death. *Int Microbiol* **3**: 153-158.
- Miguel, E.M., Hardisson, C., and Manzanal, M.B. (1999) Hyphal death during colony development in *Streptomyces antibioticus*: morphological evidence for the existence of a process of cell deletion in a multicellular prokaryote. *J Cell Biol* **145**: 515-525.
- Mijakovic, I., Poncet, S., Galinier, A., Monedero, V., Fieulaine, S., Janin, J., Nessler, S., Marquez, J.A., Scheffzek, K., Hasenbein, S., Hengstenberg, W., and Deutscher, J. (2002) Pyrophosphate-producing protein dephosphorylation by HPr kinase/phosphorylase: a relic of early life? *Proc Natl Acad Sci U S A* **99**: 13442-13447.
- Molle, V., Fujita, M., Jensen, S.T., Eichenberger, P., Gonzalez-Pastor, J.E., Liu, J.S., and Losick, R. (2003) The Spo0A regulon of *Bacillus subtilis*. *Mol Microbiol* **50**: 1683-1701.
- Molle, V., W.J. Palframan, K.C. Findlay & M.J. Buttner, (2000) WhiD and WhiB, homologous proteins required for different stages of sporulation in *Streptomyces coelicolor* A3(2). *J. Bacteriol.* **182**:1286-1295.
- Murshudov, G.N., Skubak, P., Lebedev, A.A., Pannu, N.S., Steiner, R.A., Nicholls, R.A., Winn, M.D., Long, F,

REFERENCES

- and Vagin, A.A. (2011) REFMAC5 for the refinement of macromolecular crystal structures. *Acta Crystallogr D Biol Crystallogr* **67**: 355-367.
- Nazari, B., Kobayashi, M., Saito, A., Hassaninasab, A., Miyashita, K., and Fujii, T. (2012) Chitin-induced gene expression involved in secondary metabolic pathways in *Streptomyces coelicolor* A3(2) grown in soil. *Appl Environ Microbiol* **79**: 707-713.
- Nett, M., Ikeda, H., and Moore, B.S. (2009) Genomic basis for natural product biosynthetic diversity in the actinomycetes. *Nat Prod Rep* **26**: 1362-1384.
- Nieselt, K., Battke, F., Herbig, A., Bruheim, P., Wentzel, A., Jakobsen, O.M., Sletta, H., Alam, M.T., Merlo, M.E., Moore, J., Omara, W.A., Morrissey, E.R., Juarez-Hermosillo, M.A., Rodriguez-Garcia, A., Nentwich, M., Thomas, L., Iqbal, M., Legaie, R., Gaze, W.H., Challis, G.L., Jansen, R.C., Dijkhuizen, L., Rand, D.A., Wild, D.L., Bonin, M., Reuther, J., Wohlleben, W., Smith, M.C., Burroughs, N.J., Martin, J.F., Hodgson, D.A., Takano, E., Breitling, R., Ellingsen, T.E., and Wellington, E.M. (2010) The dynamic architecture of the metabolic switch in *Streptomyces coelicolor*. *BMC Genomics* **11**: 10.
- Nothaft, H., Rigali, S., Boomsma, B., Swiatek, M., McDowall, K.J., van Wezel, G.P., and Titgemeyer, F. (2010) The permease gene *nagE2* is the key to *N*-acetylglucosamine sensing and utilization in *Streptomyces coelicolor* and is subject to multi-level control. *Mol Microbiol* **75**: 1133-1144.
- Nothaft, H., Dresel, D., Willimek, A., Mahr, K., Niederweis, M., and Titgemeyer, F. (2003a) The phosphotransferase system of *Streptomyces coelicolor* is biased for *N*-acetylglucosamine metabolism. *J Bacteriol* **185**: 7019-7023.
- Nothaft, H., Parche, S., Kamionka, A., and Titgemeyer, F. (2003b) *In vivo* analysis of HPr reveals a fructose-specific phosphotransferase system that confers high-affinity uptake in *Streptomyces coelicolor*. *J Bacteriol* **185**: 929-937.
- O'Neill, J., Antimicrobial Resistance: Tackling a Crisis for the Health and Wealth of Nations. (2014) *Review on antimicrobial resistance*.
- Oberto, J. (2013) SyntTax: a web server linking synteny to prokaryotic taxonomy. *BMC Bioinformatics* **14**: 4.
- Ohnishi, Y., Ishikawa, J., Hara, H., Suzuki, H., Ikenoya, M., Ikeda, H., Yamashita, A., Hattori, M., and Horinouchi, S. (2008) Genome sequence of the streptomycin-producing microorganism *Streptomyces griseus* IFO 13350. *J Bacteriol* **190**: 4050-4060.
- Okada, B.K., and Seyedsayamdost, M.R. (2016) Antibiotic dialogues: induction of silent biosynthetic gene clusters by exogenous small molecules. *FEMS Microbiol Rev* **41**:19-33,
- Pagels, M., Fuchs, S., Pane-Farre, J., Kohler, C., Menschner, L., Hecker, M., McNamarra, P.J., Bauer, M.C., von Wachenfeldt, C., Liebeke, M., Lalk, M., Sander, G., von Eiff, C., Proctor, R.A., and Engelmann, S. (2010) Redox sensing by a Rex-family repressor is involved in the regulation of anaerobic gene expression in *Staphylococcus aureus*. *Mol Microbiol* **76**: 1142-1161.
- Paget, M.S., Molle, V., Cohen, G., Aharonowitz, Y., and Buttner, M.J. (2001) Defining the disulphide stress response in *Streptomyces coelicolor* A3(2): identification of the sigmaR regulon. *Mol Microbiol* **42**: 1007-1020.
- Park, J.T., and Uehara, T. (2008) How bacteria consume their own exoskeletons (turnover and recycling of cell wall peptidoglycan). *Microbiol Mol Biol Rev* **72**: 211-227
- Park, S.S., Yang, Y.H., Song, E., Kim, E.J., Kim, W.S., Sohng, J.K., Lee, H.C., Liou, K.K., and Kim, B.G. (2009) Mass spectrometric screening of transcriptional regulators involved in antibiotic biosynthesis in *Streptomyces coelicolor* A3(2). *J Ind Microbiol Biotechnol* **36**: 1073-1083.
- Park, S.Y., Moon, M.W., Subhadra, B., and Lee, J.K. (2010) Functional characterization of the glxR deletion mutant of *Corynebacterium glutamicum* ATCC 13032: involvement of GlxR in acetate metabolism and carbon catabolite repression. *FEMS Microbiol Lett* **304**: 107-115.
- Perez-Redondo, R., Santamarta, I., Bovenberg, R., Martin, J.F., and Liras, P. (2010) The enigmatic lack of glucose utilization in *Streptomyces clavuligerus* is due to inefficient expression of the glucose permease gene. *Microbiology* **156**: 1527-1537.
- Piette, A., Derouaux, A., Gerkens, P., Noens, E.E., Mazzucchelli, G., Vion, S., Koerten, H.K., Titgemeyer, F., De Pauw, E., Leprince, P., van Wezel, G.P., Galleni, M., and Rigali, S. (2005) From dormant to germinating spores of *Streptomyces coelicolor* A3(2): new perspectives from the *crp* null mutant. *J Proteome Res* **4**: 1699-1708.
- Plumbridge, J. (2015) Regulation of the utilization of amino sugars by *Escherichia coli* and *Bacillus subtilis*: same genes, different control. *Journal of molecular microbiology and biotechnology* **25**: 154-167.
- Plumbridge, J. (2009) An alternative route for recycling of *N*-acetylglucosamine from peptidoglycan involves the *N*-acetylglucosamine phosphotransferase system in *Escherichia coli*. *Journal of bacteriology* **191**: 5641-5647.

- Plumbridge, J. (2001) DNA binding sites for the Mlc and NagC proteins: regulation of *nagE*, encoding the *N*-acetylglucosamine-specific transporter in *Escherichia coli*. *Nucleic Acids Res* **29**: 506-514.
- Plumbridge, J. (1995) Co-ordinated regulation of amino sugar biosynthesis and degradation: the NagC repressor acts as both an activator and a repressor for the transcription of the *glmUS* operon and requires two separated NagC binding sites. *EMBO J* **14**: 3958-3965.
- Plumbridge, J.A. (1991) Repression and induction of the *nag* regulon of *Escherichia coli* K-12: the roles of *nagC* and *nagA* in maintenance of the uninduced state. *Mol Microbiol* **5**: 2053-2062.
- Podust, L.M., Ioanoviciu, A., and Ortiz de Montellano, P.R. (2008) 2.3 Å X-ray structure of the heme-bound GAF domain of sensory histidine kinase DosT of *Mycobacterium tuberculosis*. *Biochemistry* **47**: 12523-12531.
- Postma, P.W., Lengeler, J.W., and Jacobson, G.R. (1993) Phosphoenolpyruvate:carbohydrate phosphotransferase systems of bacteria. *Microbiol Rev* **57**: 543-594.
- Pullan, S.T., Chandra, G., Bibb, M.J., and Merrick, M. (2011) Genome-wide analysis of the role of GlnR in *Streptomyces venezuelae* provides new insights into global nitrogen regulation in actinomycetes. *BMC Genomics* **12**: 175.
- Ralser, M., Wamelink, M.M., Struys, E.A., Joppich, C., Krobitsch, S., Jakobs, C., and Lehrach, H. (2008) A catabolic block does not sufficiently explain how 2-deoxy-D-glucose inhibits cell growth. *Proc Natl Acad Sci U S A* **105**: 17807-17811.
- Rappsilber, J., Ishihama, Y., and Mann, M. (2003) Stop and go extraction tips for matrix-assisted laser desorption/ionization, nanoelectrospray, and LC/MS sample pretreatment in proteomics. *Anal Chem* **75**: 663-670.
- Redenbach, M., Kieser, H.M., Denapaite, D., Eichner, A., Cullum, J., Kinashi, H., and Hopwood, D.A. (1996) A set of ordered cosmids and a detailed genetic and physical map for the 8 Mb *Streptomyces coelicolor* A3(2) chromosome. *Mol Microbiol* **21**: 77-96.
- Reith, J., and Mayer, C. (2011) Characterization of a glucosamine/glucosaminide *N*-acetyltransferase of *Clostridium acetobutylicum*. *J Bacteriol* **193**: 5393-5399.
- Reizer, J., Bachem, S., Reizer, A., Arnaud, M., Saier, M.H., Jr., and Stulke, J. (1999) Novel phosphotransferase system genes revealed by genome analysis - the complete complement of PTS proteins encoded within the genome of *Bacillus subtilis*. *Microbiology* **145**: 3419-3429.
- Reuther, J., and Wohlleben, W. (2007) Nitrogen metabolism in *Streptomyces coelicolor*: transcriptional and post-translational regulation. *Journal of molecular microbiology and biotechnology* **12**: 139-146.
- Richards, G.R., Patel, M.V., Lloyd, C.R., and Vanderpool, C.K. (2013) Depletion of glycolytic intermediates plays a key role in glucose-phosphate stress in *Escherichia coli*. *J Bacteriol* **195**: 4816-4825.
- Rigali, S., Nivelle, R., and Tocquin, P. (2015) On the necessity and biological significance of threshold-free regulon prediction outputs. *Mol Biosyst* **11**: 333-337.
- Rigali, S., Titgemeyer, F., Barends, S., Mulder, S., Thomae, A.W., Hopwood, D.A., and van Wezel, G.P. (2008) Feast or famine: the global regulator DasR links nutrient stress to antibiotic production by *Streptomyces*. *EMBO reports* **9**: 670-675.
- Rigali, S., Nothaft, H., Noens, E.E., Schlicht, M., Colson, S., Muller, M., Joris, B., Koerten, H.K., Hopwood, D.A., Titgemeyer, F., and van Wezel, G.P. (2006) The sugar phosphotransferase system of *Streptomyces coelicolor* is regulated by the GntR-family regulator DasR and links *N*-acetylglucosamine metabolism to the control of development. *Mol Microbiol* **61**: 1237-1251.
- Rodríguez-García, A., Barreiro, C., Santos-Beneit, F., Sola-Landa, A., and Martín, J.F. (2007) Genome-wide transcriptomic and proteomic analysis of the primary response to phosphate limitation in *Streptomyces coelicolor* M145 and in a Δ *phoP* mutant. *Proteomics* **7**: 2410-2429.
- Romero-Rodríguez, A., Rocha, D., Ruiz-Villafan, B., Tierrafría, V., Rodríguez-Sanoja, R., Segura-González, D., and Sánchez, S. (2016) Transcriptomic analysis of a classical model of carbon catabolite regulation in *Streptomyces coelicolor*. *BMC microbiology* **16**: 1.
- Romero, A., Ruiz, B., Sohng, J.K., Koirala, N., Rodriguez-Sanoja, R., and Sanchez, S. (2015) Functional analysis of the GlcP promoter in *Streptomyces peucetius* var. *caesius*. *Appl Biochem Biotechnol* **175**: 3207-3217.
- Rutledge, P.J., and Challis, G.L. (2015) Discovery of microbial natural products by activation of silent biosynthetic gene clusters. *Nat Rev Microbiol* **13**: 509-523.
- Sabag-Daigle, A., Blunk, H.M., Sengupta, A., Wu, J., Bogard, A.J., Ali, M.M., Stahl, C., Wysocki, V.H., Gopalan, V., Behrman, E.J., and Ahmer, B.M. (2016) A metabolic intermediate of the fructose-asparagine utilization pathway inhibits growth of a *Salmonella fraB* mutant. *Sci Rep* **6**: 28117.
- Saier, M.H., Jr., and Reizer, J. (1992) Proposed uniform nomenclature for the proteins and protein

REFERENCES

- domains of the bacterial phosphoenolpyruvate: sugar phosphotransferase system. *J Bacteriol* **174**: 1433-1438.
- Saito, A., Ebise, H., Orihara, Y., Murakami, S., Sano, Y., Kimura, A., Sugiyama, Y., Ando, A., Fujii, T., and Miyashita, K. (2013) Enzymatic and genetic characterization of the DasD protein possessing N-acetyl-beta-d-glucosaminidase activity in *Streptomyces coelicolor* A3(2). *FEMS Microbiol Lett* **340**: 33-40.
- Saito, A., Fujii, T., Shinya, T., Shibuya, N., Ando, A., and Miyashita, K. (2008) The *msiK* gene, encoding the ATP-hydrolysing component of N,N'-diacetylchitobiose ABC transporters, is essential for induction of chitinase production in *Streptomyces coelicolor* A3(2). *Microbiology* **154**: 3358-3365.
- Saito, A., and Schrepf, H. (2004) Mutational analysis of the binding affinity and transport activity for N-acetylglucosamine of the novel ABC transporter Ngc in the chitin-degrader *Streptomyces olivaceoviridis*. *Molecular Genetics and Genomics* **271**: 545-553.
- Saito, A., Shinya, T., Miyamoto, K., Yokoyama, T., Kaku, H., Minami, E., Shibuya, N., Tsujibo, H., Nagata, Y., and Ando, A. (2007) The *dasABC* gene cluster, adjacent to *dasR*, encodes a novel ABC transporter for the uptake of N, N'-diacetylchitobiose in *Streptomyces coelicolor* A3 (2). *Applied and environmental microbiology* **73**: 3000-3008.
- Saito, A., Ishizaka, M., Francisco, P.B., Jr., Fujii, T., and Miyashita, K. (2000) Transcriptional co-regulation of five chitinase genes scattered on the *Streptomyces coelicolor* A3(2) chromosome. *Microbiology* **146**: 2937-2946.
- Salerno, P., Persson, J., Bucca, G., Laing, E., Ausmees, N., Smith, C.P., and Flardh, K. (2013) Identification of new developmentally regulated genes involved in *Streptomyces coelicolor* sporulation. *BMC Microbiol* **13**: 281.
- Sambrook, J., Fritsch, E.F., and Maniatis, T., (1989) *Molecular cloning: a laboratory manual*. Cold Spring Harbor laboratory press, Cold Spring harbor, N.Y.
- Sanchez, S., Chavez, A., Forero, A., Garcia-Huante, Y., Romero, A., Sanchez, M., Rocha, D., Sanchez, B., Avalos, M., Guzman-Trampe, S., Rodriguez-Sanoja, R., Langley, E., and Ruiz, B. (2010) Carbon source regulation of antibiotic production. *J Antibiot (Tokyo)* **63**: 442-459.
- Santos-Beneit, F., Rodríguez-García, A., and Martín, J.F. (2012) Overlapping binding of PhoP and AfsR to the promoter region of *glnR* in *Streptomyces coelicolor*. *Microbiological research* **167**: 532-535.
- Santos-Beneit, F., Rodríguez-García, A., and Martín, J.F. (2011) Complex transcriptional control of the antibiotic regulator *afsS* in *Streptomyces*: PhoP and AfsR are overlapping, competitive activators. *J Bacteriol* **193**: 2242-2251.
- Santos-Beneit, F., Rodríguez-García, A., Sola-Landa, A., and Martín, J.F. (2009) Cross-talk between two global regulators in *Streptomyces*: PhoP and AfsR interact in the control of *afsS*, *pstS* and *phoRP* transcription. *Molecular microbiology* **72**: 53-68.
- Schrepf, H. (2001) Recognition and degradation of chitin by streptomycetes. *Antonie Van Leeuwenhoek* **79**: 285-289.
- Seipke, R.F., Kaltenpoth, M., and Hutchings, M.I. (2012) *Streptomyces* as symbionts: an emerging and widespread theme? *FEMS Microbiol Rev* **36**: 862-876.
- Selvaraj, S., Sambandam, V., Sardar, D., and Anishetty, S. (2012) *In silico* analysis of DosR regulon proteins of *Mycobacterium tuberculosis*. *Gene* **506**: 233-241.
- Seo, J.W., Ohnishi, Y., Hirata, A., and Horinouchi, S. (2002) ATP-binding cassette transport system involved in regulation of morphological differentiation in response to glucose in *Streptomyces griseus*. *J Bacteriol* **184**: 91-103.
- Shin, J.H., Jung, H.J., An, Y.J., Cho, Y.B., Cha, S.S., and Roe, J.H. (2011a) Graded expression of zinc-responsive genes through two regulatory zinc-binding sites in *Zur*. *Proc Natl Acad Sci U S A* **108**: 5045-5050.
- Shin, J.H., Singh, A.K., Cheon, D.J., and Roe, J.H. (2011b) Activation of the SoxR regulon in *Streptomyces coelicolor* by the extracellular form of the pigmented antibiotic actinorhodin. *J Bacteriol* **193**: 75-81.
- Smyth, G.K., and Speed, T. (2003) Normalization of cDNA microarray data. *Methods* **31**: 265-273.
- Sola-Landa, A., Rodríguez-García, A., Amin, R., Wohlleben, W., and Martín, J.F. (2013) Competition between the GlnR and PhoP regulators for the *glnA* and *amtB* promoters in *Streptomyces coelicolor*. *Nucleic acids research* **41**: 1767-1782.
- Solomons, J.T., Zimmerly, E.M., Burns, S., Krishnamurthy, N., Swan, M.K., Krings, S., Muirhead, H., Chirgwin, J., and Davies, C. (2004) The crystal structure of mouse phosphoglucose isomerase at 1.6Å resolution and its complex with glucose 6-phosphate reveals the catalytic mechanism of sugar ring opening. *J Mol Biol* **342**: 847-860.

- Stock, A.M., Robinson, V.L., and Goudreau, P.N. (2000) Two-component signal transduction. *Annu Rev Biochem* **69**: 183-215.
- Strakova, E., Bobek, J., Zikova, A., and Vohradsky, J. (2013) Global features of gene expression on the proteome and transcriptome levels in *S. coelicolor* during germination. *PLoS One* **8**: e72842.
- Świątek-Połatyńska, M.A., Bucca, G., Laing, E., Gubbens, J., Titgemeyer, F., Smith, C.P., Rigali, S., and van Wezel, G.P. (2015) Genome-wide analysis of *in vivo* binding of the master regulator DasR in *Streptomyces coelicolor* identifies novel non-canonical targets. *PLoS ONE* **10**: e0122479.
- Świątek, M.A., Gubbens, J., Bucca, G., Song, E., Yang, Y.H., Laing, E., Kim, B.G., Smith, C.P., and van Wezel, G.P. (2013) The ROK family regulator Rok7B7 pleiotropically affects xylose utilization, carbon catabolite repression, and antibiotic production in *Streptomyces coelicolor*. *J Bacteriol* **195**: 1236-1248.
- Świątek, M.A., (2012) Global control of development and antibiotic production by nutrient-responsive signalling pathways in *Streptomyces*. In: Department of Molecular Biotechnology, Leiden Institute of Chemistry (LIC), Faculty of Science, Leiden University, pp.
- Świątek, M.A., Tenconi, E., Rigali, S., and van Wezel, G.P. (2012a) Functional analysis of the *N*-acetylglucosamine metabolic genes of *Streptomyces coelicolor* and role in control of development and antibiotic production. *Journal of bacteriology* **194**: 1136-1144.
- Świątek, M.A., Urem, M., Tenconi, E., Rigali, S., and van Wezel, G.P. (2012b) Engineering of *N*-acetylglucosamine metabolism for improved antibiotic production in *Streptomyces coelicolor* A3(2) and an unsuspected role of NagA in glucosamine metabolism. *Bioengineered* **3**: 280-285.
- Szklarczyk, D., Franceschini, A., Wyder, S., Forslund, K., Heller, D., Huerta-Cepas, J., Simonovic, M., Roth, A., Santos, A., Tsafou, K.P., Kuhn, M., Bork, P., Jensen, L.J., and von Mering, C. (2015) STRING v10: protein-protein interaction networks, integrated over the tree of life. *Nucleic Acids Res* **43**: D447-452.
- Taneja, N.K., Dhingra, S., Mittal, A., Naresh, M., and Tyagi, J.S. (2010) *Mycobacterium tuberculosis* transcriptional adaptation, growth arrest and dormancy phenotype development is triggered by vitamin C. *PLoS One* **5**: 13.
- Taylor, P.L., Blakely, K.M., de Leon, G.P., Walker, J.R., McArthur, F., Evdokimova, E., Zhang, K., Valvano, M.A., Wright, G.D., and Junop, M.S. (2008) Structure and function of sedoheptulose-7-phosphate isomerase, a critical enzyme for lipopolysaccharide biosynthesis and a target for antibiotic adjuvants. *J Biol Chem* **283**: 2835-2845.
- Tenconi, E., Urem, M., Świątek-Połatyńska, M.A., Titgemeyer, F., Muller, Y.A., van Wezel, G.P., and Rigali, S., (2015) Multiple allosteric effectors control the affinity of DasR for its target sites. In: Biochemical and Biophysical Research Communications. pp. 324-329.
- Tenconi, E., Jourdan, S., Motte, P., Virolle, M.-J., and Rigali, S. (2012) Extracellular sugar phosphates are assimilated by *Streptomyces* in a PhoP-dependent manner. *Antonie van Leeuwenhoek* **102**: 425-433.
- Terrak, M., Ghosh, T.K., van Heijenoort, J., Van Beeumen, J., Lampilas, M., Aszodi, J., Ayala, J.A., Ghuysen, J.M., and Nguyen-Disteche, M. (1999) The catalytic, glycosyl transferase and acyl transferase modules of the cell wall peptidoglycan-polymerizing penicillin-binding protein 1b of *Escherichia coli*. *Mol Microbiol* **34**: 350-364.
- Thompson, K.A., and Kleinzeller, A. (1989) 2-Deoxy-D-glucose accumulation in adipocytes: apparent transport discrimination between 2-deoxy-D-glucose and 3-O-methyl-D-glucose. *Biochim Biophys Acta* **1011**: 58-60.
- Tiffert, Y., Supra, P., Wurm, R., Wohlleben, W., Wagner, R., and Reuther, J. (2008) The *Streptomyces coelicolor* GlnR regulon: identification of new GlnR targets and evidence for a central role of GlnR in nitrogen metabolism in actinomycetes. *Mol Microbiol* **67**: 861-880.
- Titgemeyer, F., Reizer, J., Reizer, A., and Saier, M.H., Jr. (1994) Evolutionary relationships between sugar kinases and transcriptional repressors in bacteria. *Microbiology* **140**: 2349-2354.
- Titgemeyer, F., Walkenhorst, J., Reizer, J., Stuver, M.H., Cui, X., and Saier, M.H., Jr. (1995) Identification and characterization of phosphoenolpyruvate:fructose phosphotransferase systems in three *Streptomyces* species. *Microbiology* **141**: 51-58.
- Traag, B.A., and van Wezel, G.P. (2008) The SsgA-like proteins in actinomycetes: small proteins up to a big task. *Antonie Van Leeuwenhoek* **94**: 85-97.
- Traxler, M.F., Seyedsayamdost, M.R., Clardy, J., and Kolter, R. (2012) Interspecies modulation of bacterial development through iron competition and siderophore piracy. *Molecular Microbiology* **86**: 628-644.
- Uguru, G.C., Stephens, K.E., Stead, J.A., Towle, J.E., Baumberg, S., and McDowall, K.J. (2005) Transcriptional activation of the pathway-specific regulator of the actinorhodin biosynthetic

REFERENCES

- genes in *Streptomyces coelicolor*. *Mol Microbiol* **58**: 131-150.
- Urem, M., Swiatek-Polatynska, M.A., Rigali, S., and van Wezel, G.P. (2016a) Intertwining nutrient-sensory networks and the control of antibiotic production in *Streptomyces*. *Mol Microbiol* **102**:183-195
- Urem, M., van Rossum, T., Bucca, G., Moolenaar, G.F., Laing, E., Swiatek-Polatynska, M.A., Willemse, J., Tenconi, E., Rigali, S., Goosen, N., Smith, C.P., and van Wezel, G.P. (2016b) OsdR of *Streptomyces coelicolor* and the Dormancy Regulator DevR of *Mycobacterium tuberculosis* Control Overlapping Regulons. *mSystems* **1**:1-21
- Vagin, A., and Teplyakov, A. (2000) An approach to multi-copy search in molecular replacement. *Acta Crystallogr D Biol Crystallogr* **56**: 1622-1624.
- van Dissel, D., Claessen, D., and van Wezel, G.P. (2014) Morphogenesis of *Streptomyces* in submerged cultures. *Advances in applied microbiology* **89**: 1-45.
- van Keulen, G., Alderson, J., White, J., and Sawers, R.G. (2007) The obligate aerobic actinomycete *Streptomyces coelicolor* A3(2) survives extended periods of anaerobic stress. *Environ Microbiol* **9**: 3143-3149.
- van der Meij, A., S.F. Worsley, M.I. Hutchings & G.P. van wezel, (2017) Chemical ecology of antibiotic production by actinomycetes. *FEMS Microbiology Reviews* **41**: 392-416.
- van Veluw, G.J., Petrus, M.L., Gubbens, J., de Graaf, R., de Jong, I.P., van Wezel, G.P., Wosten, H.A., and Claessen, D. (2012) Analysis of two distinct mycelial populations in liquid-grown *Streptomyces* cultures using a flow cytometry-based proteomics approach. *Appl Microbiol Biotechnol* **96**: 1301-1312.
- van Wezel, G.P., and McDowall, K.J. (2011) The regulation of the secondary metabolism of *Streptomyces*: new links and experimental advances. *Nat Prod Rep* **28**: 1311-1333.
- van Wezel, G.P., McKenzie, N.L., and Nodwell, J.R. (2009) Chapter 5. Applying the genetics of secondary metabolism in model actinomycetes to the discovery of new antibiotics. *Methods Enzymol* **458**: 117-141.
- van Wezel, G.P., Konig, M., Mahr, K., Nothaft, H., Thomae, A.W., Bibb, M., and Titgemeyer, F. (2007) A new piece of an old jigsaw: glucose kinase is activated posttranslationally in a glucose transport-dependent manner in *Streptomyces coelicolor* A3(2). *J Mol Microbiol Biotechnol* **12**: 67-74.
- van Wezel, G.P., Krabben, P., Traag, B.A., Keijsers, B.J., Kerste, R., Vijgenboom, E., Heijnen, J.J., and Kraal, B. (2006a) Unlocking *Streptomyces* spp. for use as sustainable industrial production platforms by morphological engineering. *Appl Environ Microbiol* **72**: 5283-5288.
- van Wezel, G.P., Titgemeyer, F., and Rigali, S., (2006b) Methods and means for metabolic engineering and improved product formation by micro-organisms. In. Patent Application WO 2007/094667, pp.
- van Wezel, G.P., Mahr, K., Konig, M., Traag, B.A., Pimentel-Schmitt, E.F., Willimek, A., and Titgemeyer, F. (2005) GlcP constitutes the major glucose uptake system of *Streptomyces coelicolor* A3(2). *Mol Microbiol* **55**: 624-636.
- van Wezel, G.P., White, J., Hoogvliet, G., and Bibb, M.J. (2000a) Application of *redd*, the transcriptional activator gene of the undecylprodigiosin biosynthetic pathway, as a reporter for transcriptional activity in *Streptomyces coelicolor* A3(2) and *Streptomyces lividans*. *J Mol Microbiol Biotechnol* **2**: 551-556.
- van Wezel, G.P., and Kraal, B. (2000b) *sgsA* Is Essential for Sporulation of *Streptomyces coelicolor* A3 (2) and Affects Hyphal Development by Stimulating septum formation.
- van Wezel, G.P., White, J., Young, P., Postma, P.W., and Bibb, M.J. (1997) Substrate induction and glucose repression of maltose utilization by *Streptomyces coelicolor* A3(2) is controlled by *malR*, a member of the *lacI-galR* family of regulatory genes. *Molecular Microbiology* **23**: 537-549.
- Vanderpool, C.K. (2007) Physiological consequences of small RNA-mediated regulation of glucose-phosphate stress. *Curr Opin Microbiol* **10**: 146-151.
- Vara, J., Lewandowska-Skarbek, M., Wang, Y.G., Donadio, S., and Hutchinson, C.R. (1989) Cloning of genes governing the deoxysugar portion of the erythromycin biosynthesis pathway in *Saccharopolyspora erythraea* (*Streptomyces erythreus*). *J Bacteriol* **171**: 5872-5881.
- Viens, P., Dubeau, M.P., Kimura, A., Desaki, Y., Shinya, T., Shibuya, N., Saito, A., and Brzezinski, R. (2015) Uptake of chitosan-derived D-glucosamine oligosaccharides in *Streptomyces coelicolor* A3(2). *FEMS Microbiol Lett* **362**.
- Wade, J.T., Reppas, N.B., Church, G.M., and Struhl, K. (2005) Genomic analysis of LexA binding reveals the permissive nature of the *Escherichia coli* genome and identifies unconventional target sites. *Genes Dev* **19**: 2619-2630.
- Wang, F., Xiao, X., Saito, A., and Schrempf, H. (2002) *Streptomyces olivaceoviridis* possesses a phosphotransferase system that mediates specific, phosphoenolpyruvate-dependent uptake

- of *N*-acetylglucosamine. *Mol Genet Genomics*. **268**: 344-351.
- Wang, J., and Zhao, G.-P. (2009) GlnR positively regulates *nasA* transcription in *Streptomyces coelicolor*. *Biochem Biophys Res Commun* **386**: 77-81.
- Wang, R., Mast, Y., Wang, J., Zhang, W., Zhao, G., Wohlleben, W., Lu, Y., and Jiang, W. (2013) Identification of two-component system AfsQ1/Q2 regulon and its cross-regulation with GlnR in *Streptomyces coelicolor*. *Mol Microbiol* **87**: 30-48.
- Wang, W., Shu, D., Chen, L., Jiang, W., and Lu, Y. (2009) Cross-talk between an orphan response regulator and a noncognate histidine kinase in *Streptomyces coelicolor*. *FEMS Microbiol Lett* **294**: 150-156.
- Whitworth, D.E., (2012) Classification and organization of two-component systems. In: Two-component systems in bacteria. R. Gross & D. Beier (eds). Poole, UK: Caister Academic Press, pp. 1-20.
- WHO, (2014) *Antimicrobial Resistance: Global Report on Surveillance*. Geneva, Switzerland.
- Wietzorrek, A., and Bibb, M. (1997) A novel family of proteins that regulates antibiotic production in streptomycetes appears to contain an OmpR-like DNA-binding fold. *Mol Microbiol* **25**: 1181-1184.
- Willemse, J., Mommaas, A.M., and van Wezel, G.P. (2012) Constitutive expression of *ftsZ* overrides the whi developmental genes to initiate sporulation of *Streptomyces coelicolor*. *Antonie van Leeuwenhoek* **101**: 619-632.
- Willemse, J., Borst, J.W., de Waal, E., Bisseling, T., and van Wezel, G.P. (2011) Positive control of cell division: FtsZ is recruited by SsgB during sporulation of *Streptomyces*. *Genes Dev* **25**: 89-99.
- Willey, J., Santamaria, R., Guijarro, J., Geistlich, M., and Losick, R. (1991) Extracellular complementation of a developmental mutation implicates a small sporulation protein in aerial mycelium formation by *S. coelicolor*. *Cell* **65**: 641-650.
- Winn, M.D., Ballard, C.C., Cowtan, K.D., Dodson, E.J., Emsley, P., Evans, P.R., Keegan, R.M., Krissinel, E.B., Leslie, A.G., McCoy, A., McNicholas, S.J., Murshudov, G.N., Pannu, N.S., Potterton, E.A., Powell, H.R., Read, R.J., Vagin, A., and Wilson, K.S. (2011) Overview of the CCP4 suite and current developments. *Acta Crystallogr D Biol Crystallogr* **67**: 235-242.
- Wisedchaisri, G., Wu, M., Rice, A.E., Roberts, D.M., Sherman, D.R., and Hol, W.G. (2005) Structures of *Mycobacterium tuberculosis* DosR and DosR-DNA complex involved in gene activation during adaptation to hypoxic latency. *J Mol Biol* **354**: 630-641.
- Xiao, X., Wang, F., Saito, A., Majka, J., Schlosser, A., and Schrempf, H. (2002) The novel *Streptomyces olivaceoviridis* ABC transporter Ngc mediates uptake of *N*-acetylglucosamine and *N,N'*-diacetylchitobiose. *Mol Genet Genomics* **267**: 429-439.
- Yamanaka, K., Oikawa, H., Ogawa, H.O., Hosono, K., Shinmachi, F., Takano, H., Sakuda, S., Beppu, T., and Ueda, K. (2005) Desferrioxamine E produced by *Streptomyces griseus* stimulates growth and development of *Streptomyces tanashiensis*. *Microbiology* **151**: 2899-2905.
- Yarmolinsky, M.B., Wiesmeyer, H., Kalckar, H.M., and Jordan, E. (1959) Hereditary Defects in Galactose Metabolism in *Escherichia coli* Mutants, II. Galactose-Induced Sensitivity. *Proc Natl Acad Sci U S A* **45**: 1786-1791.
- Zdobnov, E.M., and Apweiler, R. (2001) InterProScan - an integration platform for the signature-recognition methods in InterPro. *Bioinformatics* **17**: 847-848.
- Zhang, D., Li, J., Wang, F., Hu, J., Wang, S., and Sun, Y. (2014) 2-Deoxy-D-glucose targeting of glucose metabolism in cancer cells as a potential therapy. *Cancer Lett* **355**: 176-183.
- Zhu, H., Sandiford, S.K., and van Wezel, G.P. (2014a) Triggers and cues that activate antibiotic production by actinomycetes. *J Ind Microbiol Biotechnol* **41**: 371-386.
- Zhu, H., Swierstra, J., Wu, C., Girard, G., Choi, Y.H., van Wamel, W., Sandiford, S.K., and van Wezel, G.P. (2014b) Eliciting antibiotics active against the ESKAPE pathogens in a collection of actinomycetes isolated from mountain soils. *Microbiology* **160**: 1714-1725.
- Zuber, P. (2009) Management of oxidative stress in *Bacillus*. *Annu Rev Microbiol* **63**: 575-597.

APPENDICES

APPENDIX I **P120**

APPENDIX II **P126**

APPENDIX III **P127**

APPENDIX IV **P129**

SUPPLEMENTARY INFORMATION BELONGING TO CHAPTER III

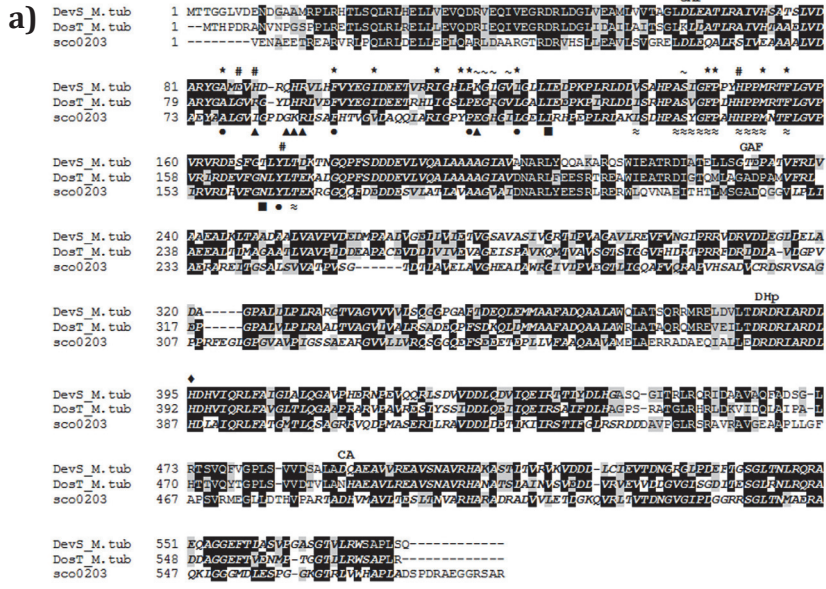


FIGURE S1: Alignment of SCO0203 (OsdK) and SCO0204 (OsdR).

Multiple alignments of OsdK with DevS and DosT of *M. tuberculosis* (A) and OsdR with DevR of *M. tuberculosis* and NarL of *P. aeruginosa* (B) are created with ClustalW (digits indicate the amino acid number). The different protein domains are indicated in italic. Amino acids conserved in at least 80% of the sequences are shaded: identical amino acids in black and amino acids with similar properties in grey. Important amino acids of DosT and DevS are indicated beneath and above the alignment, respectively. GAF, GAF domain; DHp, dimerization and histidine phosphotransfer domain; CA, C-terminal catalytic and ATP binding domain; REC, receiver domain; HTH_LuxR, helix-turn-helix-LuxR domain; ♦, phosphorylation site; ○, RR activation; #, H-bond network from iron to surface; * hydrophobic space surrounding heme; ~, contact with propionate groups heme; ●, ligand binding; ▲, surface crevice; □≈, heme binding; ■, cavity next to ligand binding pocket.

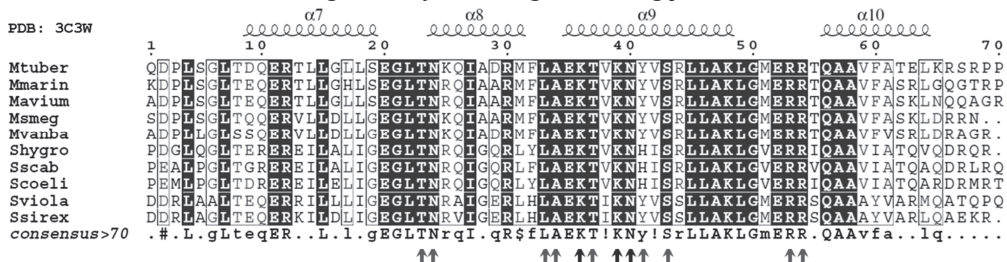


FIGURE S2. Sequence alignment of the DNA-binding domain of DevR with *Streptomyces* and *Mycobacterium* orthologues.

The secondary structure prediction was based on the crystal structure of DevR (PDB ID: 3C3W; Wisedchaisri et al., 2005), and is shown on top. Conserved residues are shown in grey, and boxes denote conservative substitutions. A symbol shows residues involved in interactions with DNA, where lighter gray arrows represent residues contacting nucleotide bases and dark gray arrows indicate residues making DNA phosphate oxygen contacts. Abbreviations (M., *Mycobacterium*; S., *Streptomyces*): Mtuber, *M. tuberculosis*; Mmarin, *M. marinum*; Mavium, *M. avium*; Msmeg, *M. smegmatis*; Mvanba, *M. vanbaalenii*; Shygro, *S. hygroscopicus*; Sscab, *S. scabies*; Scoeli, *S. coelicolor*; Sviola, *S. violaceoruber*; Ssirex, *S. sp. sirex*. For accession numbers see Methods.

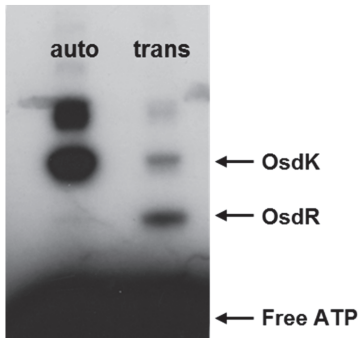


FIGURE S3. In vitro auto-phosphorylation and trans-phosphorylation of OsdRK.

OsdK was first auto-phosphorylated in the presence of unlabelled and [³²P]-radiolabelled ATP, as described previously Wang *et al.* (2009). OsdK was readily phosphorylated as shown by the large band in the lane 'auto'. Using auto-phosphorylated OsdK, OsdR was trans-phosphorylated as shown by the presence of a band of phosphorylated OsdR and OsdK in lane 'trans'. However, there was significant phosphosignal loss observed (decrease in band intensity in time). The reactions were run on 3.5% acrylamide gels in 0.5x Tris-Borate-EDTA (TBE) buffer. Gels were dried and then submitted to autoradiography for analysis.

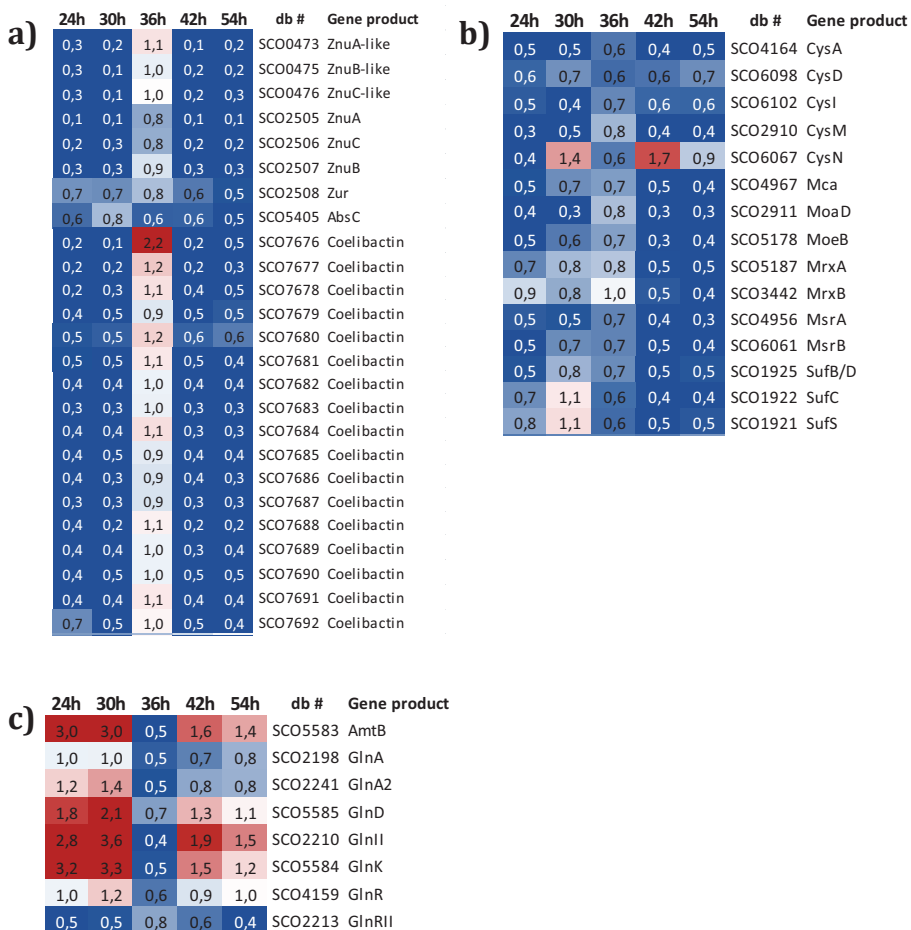


FIGURE S4. Heat maps of genes related to zinc import (A), sulphur metabolism and thiol homeostasis (B) and nitrogen metabolism (C) that are significantly differentially expressed between the *osdR* mutant and its parent *S. coelicolor* M145.

RNA was isolated from mycelium grown on MM with 1% mannitol during vegetative growth (24 h), vegetative/aerial growth (30 h), aerial growth/early sporulation (42 h) and sporulation (54 h). Only genes with a pfp value less than 0.010 and a fold change ($\Delta osdR$ expression/M145 expression) of more than 2.0 are presented. The levels of the fold changes are indicated with colours as represented by the scale bar.

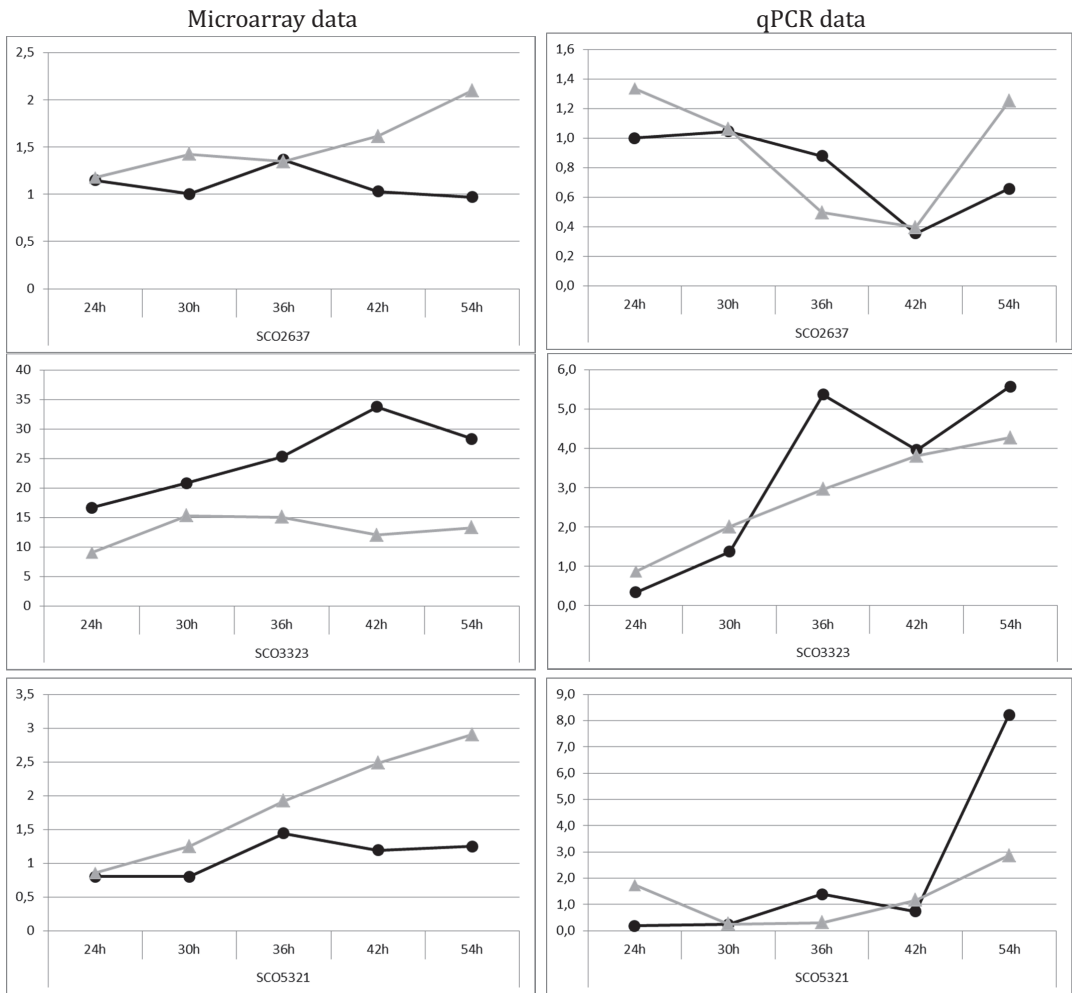


FIGURE S5. Microarray and RT-qPCR expression profiles of genes deregulated in the *osdR* mutant.

RNA was isolated, for microarray analysis (left) and RT-qPCR (right) profiling, from independent cultures grown on MM with 1% mannitol during vegetative growth (24 h), vegetative/aerial growth (30 h), aerial growth (36 h), aerial growth/early sporulation (42 h) and sporulation (54 h). The expression profiles in wild type (black, ●) and the *osdR* mutant (grey, ▲) over time were compared between the microarray data (left) and RT-qPCR (right). Genes of interest tested: SCO2637, SCO3323 (*bldN*) SCO5321 (*whiE*).

TABLE S1. Bacterial strains, plasmids and constructs.^a IFD, in-frame deletion.

Strains/plasmids	Genotype/description	Reference
Bacterial strain		
<i>S. coelicolor</i> A3(2) M145	SCP1-SCP2	(Kieser et al., 2000)
M512	M145 Δ actII-ORF4 Δ redD	(Floriano & Bibb, 1996)
GSTC1	M145 Δ SCO0203 (::aacC4)	this work
GSTC2	M145 Δ SCO0204 (::aacC4)	this work
GSTC3	M145 Δ SCO0204 (IFD ^a)	this work
GSTC4	M145 Δ SCO0203/SCO0204 (IFD ^a)	this work
GSTC6	M512 Δ SCO0204 (::aacC4)	this work
<i>E. coli</i> JM109	See reference	(Sambrook et al., 1989)
<i>E. coli</i> ET12567	See reference	(MacNeil et al., 1992)
Plasmid		
pWHM3	<i>E. coli</i> - <i>Streptomyces</i> shuttle vector (multi-copy in both hosts)	(Vara et al., 1989)
pHJL401	<i>E. coli</i> - <i>Streptomyces</i> shuttle vector with multiple copies in <i>E. coli</i> and 1-5 copies per chromosome in <i>Streptomyces</i>	(Larson & Hershberger, 1986)
pIJ2587	pHJL401 derivative with promoterless reporter gene <i>redD</i>	(van Wezel et al., 2000)
pGWS345	pIJ2587 harbouring the -395/+122 region relative to the start of <i>whiG</i>	this work
pGWS1059	pIJ2587 harbouring the -250/+38 region relative to the start of SCO0204	this work
pGWS1058	pIJ2587 harbouring the -211/+74 region relative to the start of SCO0200	this work
pGWS1060	pIJ2587 harbouring the -341/+60 region relative to the start of SCO0207	this work
pGWS376	pWHM3 with 4 kb fragment for SCO0204 replacement by <i>aacC4</i>	this work
pGWS377	pWHM3 with 3 kb fragment for SCO0204 in-frame deletion	this work
pGWS378	pWHM3 with 3.4 kb fragment for SCO0203 replacement by <i>aacC4</i>	this work
pGWS380	pWHM3 with 2.7 kb fragment for SCO0203-0204 in-frame deletion	this work
pET0203	pET28b (Novagen) protein expression vector for SCO0203	(Wang et al., 2009)
pET0204	pET28b (Novagen) protein expression vector for SCO0204	(Wang et al., 2009)

TABLE S2. Oligonucleotides*Primers for cloning and RT-qPCR reactions*

	Target *	Specification ^	Sequence(5'→3') #
Construction of mutants	SCO0203L	F-1162	GTACGAATTCGGATCAGGTACGTCTGGTGC
		R+16	CGATTGGCTGAGCTCATGAAGTTCTAGACACCTGGCCTCGCGGTCTC
	SCO0203R	F+1720	CTGCATAACCCCTGCTTCGGGGTCTAGATCCCCGACAGGGCGGAAGGC
		R+2931	GTACAAGCTTACCCGACGCCGAAAGTCCGCACC
	SCO0204L	F-1439	GTACGAATTCGCGGTATCACCTTGGTGCACGTC
		R+16	CGATTGGCTGAGCTCATGAAGTTCTAGAGCTTCCCGTGTGTGCGCCCTG
SCO0204R	F+670	CTGCATAACCCCTGCTTCGGGGTCTAGACGGGACCGGATGCGCACCGAA	
	R+2120	GTACAAGCTTAGCGGAGGCCGAAGATCGTCGAC	
Verification of mutants	SCO0203	F-1253	CGACGTCCCCATGTACCGGAAGC
		R+3037	CCGAACCACGATGCGTGGACTGG
	SCO0204	F-1529	TGGAGTACGACATCGCGGTGG
		R+2241	ACGTGCGTGTGAGCAGGCCCTC
	<i>aacC4</i>	F+783	TGCACGACATTGCACTCCAC
R+219		TCTCGAGAATGACCACGTCTG	
Promoter probing	pSCO0200	F-250	GTCAGAATTCGTATCGCGCTGGCCGCTGTCT
		R+38	GTCAGGATCCGGCGAGCCGTCGAGTCTACGGT
	pSCO0204	F-211	GTCAGAATTCGGCCAAAGTACGACGCCCTG
		R+74	GTCAGGATCCACCACCTTCGTGGTCTGTCAGGAG
	pSCO0207	F-341	GTCAGAATTCGGTGCACCAAGGTGATACCGCTC
		R+60	GTCAGGATCCACCAGAAAGTCCGGCCATGTC
RT-qPCR primers	SCO0200	F+387	CACCGAGACGCCGGTGTATCCT
		R+461	ATGCCGGTGGGGTCTTGAG
	SCO0204	F+331	GCCGGCTACGCTCTGAAGCA
		R+481	TGGCGTCCAGCAGCGACTGG
	SCO2637	F+1015	CAGGTCCGGTACTTCGGCAC
		R+1121	TTGGCACCGCGGAGTTGTA
	SCO5320	F+359	AACCGCTGGCGACCTGCGTC
		R+489	GGTGAGGGCGTGCCTACGA
	SCO5321	F+1017	CCACAACCTCGCCTGGAAGC
		R+1090	TGTCGTACGTGTCAGCAGG
	SCO1541	F+205	GAGACCGTCGAGTGGGTCTT
		R+337	GGGAGCTGAGAGCGATGCAC
	SCO3323	F+313	CTCTACGACCAGTACAGCGA
		R+407	AGAAAGTCTCGCTGGTGAG
SCO4735	F+227	ACTACTTCCCACAAGGTGC	
	R+306	GACGTCGTAGCGGTTGTCCAG	

Oligonucleotides and primers for EMSA experiments

	Target *	Location ^	Sequence(5'→3') #
50mers	pSCO0200	50F	CCCATCACCTGCGGGCAGGGACGGTCGGCCCGTCCCAGGGACCACAGGC
	wt	50R	GCCTGTGGTCCCGGGACGGGGCCGACCGTCCCTGCCCGCAGGGTGATGGG
	pSCO0200	50aF	CCCATCACCTGCGGGCAGGGACGGTCGGCACCGTCCCAGGGACCACAGGC
	50a	50aR	GCCTGTGGTCCCGGGACGGTCGGCACCGTCCCTGCCCGCAGGGTGATGGG
	pSCO0200	50bF	CCCATCACCTGCGGGCAGGGAAAGTTCGGCCCGTCCCAGGGACCACAGGC
	50b	50bR	GCCTGTGGTCCCGGGACGGGGCCGACCTTCCTGCCCGCAGGGTGATGGG
	pSCO0200	50abF	CCCATCACCTGCGGGCAGGGAAAGTTCGGCACCGTCCCAGGGACCACAGGC
	50ab	50abR	GCCTGTGGTCCCGGGACGGTCGGCACCTTCCTGCCCGCAGGGTGATGGG
<i>S. coelicolor</i> targets	pSCO0200	F-250	GTCAGAAATTCGATGGCGCTGGCCGCTGTCT
		R+38	GTCAGGATCCGGCGAGCCGTCGAGTCTACGGT
	pSCO0204	F-211	GTCAGAAATTCGCCCAAGTACGACGCCCTG
		R+74	GTCAGGATCCACCCTTCGTGGTCTCCAGGAG
	pSCO0207	F-341	GTCAGAAATTCGGTGCACCAAGGTGATACCGCTC
		R+60	GTCAGGATCCACCAGAGAAGTCCGGCCATGTC
	pSCO1541	F-355	GCCGACGACGAAAACGCCGACC
		R+98	TCGGCCGTGCTGACCCGAG
	pSCO2637	F-182	GTCAGAAATTCGTGTCCCGATGGCGCATGG
		R+36	GTCAGGATCCGCCCGGTATCGGTTCCGCT
	pSCO2967	F-218	GTCAGAAATTCACGAAGTCCCGCTCATCTGG
		R+11	GTCAGGATCCCTCCGGAACCAAGGTCAG
	pSCO5314	F-109	GCAGATGGCGTGTATCCGGGACC
		R+82	CGCTGTCGGACTCCGGAACACC
	pSCO5316	F-139	GCGCGGCTCATGGGTGCAACT
		R+68	GCGGTGCGCTTATCAGCGCCGA
	pSCO5319	F-190	TCCGTATGACGCCCTGACCGA
		R+50	TTCCGGGCGATGTCGCCGAG
	pSCO5321	F-374	CATCCGTCTGCTACGACGGGAGAG
		R+106	AGGTGACAGGCCACCAGGGAC
pSCO5979	F-293	GTCAGAAATTCGGTGTGCTCCAGCTCGGCCA	
	R+50	GTCAGGATCCAGGTGCCGCCACTCGGGGT	
pSCO6041	F-300	GTCAGAAATTCGCCGTGCTGCATCATGG	
	R+56	GTCAGTGCAGTGTCCGGTTCTCTGTTCCGGTGG	
pdasR	F+479	GCGGAAGCGGTTCCCGCCCTG	
	R+675	GTCTGGGAGTGCCGGGAGAGCATCAGCATG	
<i>M. tuberculosis</i> targets	Rv3134c	R8	CCACCCGTGCGATAGGTGAGATTC
		R9c	CTCATCGACCGCCACACAAGC
	devR	53R1	GTCAGCGCGGTTGTCCGGGAG
		R3	GACCTTTACCACCAGGGCACC
	hspX	hspXF2	TCTGAACGGCGGTTGGCAGACA
	hspXR	CGGGAAGGGTGGTGGCCATTG	

* target gene given as gene or SCO database number; nucleotide position is given relative to first nucleotide of the relevant gene.

p refers to promoter; 50mers denoted with '50'; primers for *M. tuberculosis* genes were described previously (Chauhan et al)

^ Forward (F) or reverse (R) primer; nucleotide position relative to first nucleotide of target gene.

Restriction sites underlined: GGATCC, BamHI; GAATTC, EcoRI; AAGCTT, HindIII; CTGCAG, PstI; GAGCTC, SacI; TCTAGA, XbaI.

TABLE S3. Position weight matrix for the OsdR binding site.

OsdR Position weight matrix

(Minimum score : -39.68; Maximum score : 16.45)

	1	2	3	4	5	6	7	8	9	10	11	12	13	14	15	16
A	0.91	-2.48	-2.48	-2.48	0.25	-2.48	-2.48	1.12	-0.38	-2.48	-2.48	-2.48	-2.48	-2.48	-2.48	-2.48
C	-1.16	-2.48	-2.48	-1.16	0.77	0.97	-1.16	-2.48	-0.61	0.97	-2.48	-2.48	0.97	0.97	0.97	-1.16
G	0.39	0.97	0.97	0.77	-2.48	-2.48	0.87	-0.61	-2.48	-2.48	0.97	0.87	-2.48	-2.48	-2.48	-2.48
T	-2.48	-2.48	-2.48	-0.38	-2.48	-2.48	-2.48	0.91	1.58	-2.48	-2.48	-0.38	-2.48	-2.48	-2.48	1.80

SUPPLEMENTARY INFORMATION BELONGING TO CHAPTER IV

TABLE S1. Bacterial strains and plasmids.

Bacterial strain		
Strains and genotype		Reference
<i>E. coli</i> JM109	See reference	Sambrook et al., 1989
<i>E. coli</i> ET12567	See reference	MacNeil et al., 1992
<i>E. coli</i> Rosetta(DE3)pLysS	See reference	Novagen
M145	<i>S. coelicolor</i> A3(2) M145 SCP1- SCP2- prototroph	Kieser et al., 2000
$\Delta nagB$	M145 $\Delta nagB^d$	Swiatek et al., 2012a
SMA11	M145 $\Delta nagB^{SMA11}$ suppressor	Swiatek, 2012
$\Delta SCO4393$	M145 $\Delta SCO4393^d$	This work
$\Delta SCO4393\Delta nagB$	M145 $\Delta SCO4393^d\Delta nagB^d$	This work
$\Delta nagA\Delta SCO4393$	M145 $\Delta nagA^a\Delta SCO4393^d$	This work
$\Delta SCO4393\Delta nagA$	M145 $\Delta SCO4393^a\Delta nagA^d$	This work
Plasmids		
Plasmid	Description	Reference
pHJL401	<i>E. coli - Streptomyces</i> shuttle vector, 1-5 copies per chromosome in <i>Streptomyces</i>	Larson & Hershberger, 1986
pWHM3	<i>E. coli - Streptomyces</i> shuttle vector (multi-copy in both hosts)	Vara et al., 1989
pET15b	See reference	Novagen
pUWLcre	pUWLori T derivative with <i>cre(a)</i> gene under <i>ermE*</i> promoter	Fedoryshyn et al, 2008
pGWS1051	pHJL401 harbouring SCO4393 gene under control of its own promoter	This work
pGWS1052	pWHM3 harbouring the SCO4393 flanking regions with <i>loxP-aac(3)IV-loxP</i>	This work
pGAM1	pWHM3 harbouring the <i>nagA</i> flanking regions with <i>loxP-aac(3)IV-loxP</i>	Swiatek et al., 2012a
pET4393	pET15b harbouring the SCO4393 gene	This work

^a, Apr, apramycin resistant. ^D deletion

TABLE S2. Oligonucleotides.

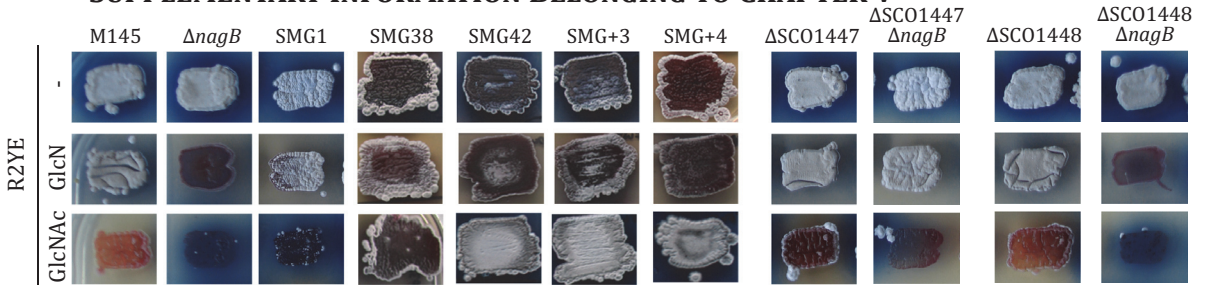
Gene*	Name^	Sequence#
SCO4393	compF-217	GTAC <u>gaaattc</u> CCCCTCGATGAGATTGCCGGAGG
	compR+762	GTC <u>Aaagctt</u> GTGCGTTCAGCGGCGGTAGAAGA
SCO4393	pETF-1	GTAC <u>gaaattc</u> catATGAGCGACCACAAGCCGGCC
	pETR-756	GTAC <u>ggatcc</u> CCGGGGCACC GGTTGCGTTCA
	LF-1438	gtcaga <u>aattc</u> acgtcgatgcccgcgccatag
SCO4393	LR+15	gaagttatccatcacct <u>ctaga</u> CTTGTGGTGCCTCATGCG
	RF+768	gaagttatcgcgcatc <u>ctaga</u> CGCCGCTGAACGCACCCGGTG
	RR+2157	gtca <u>aagctt</u> gcgacgctccattcgagcagag

* SCO database number; nucleotide position is given relative to first nucleotide of therelevant gene

^ Forward (F) or reverse (R) primer, (L and R indicate left or right flank, where applicable); nucleotide position relative to first nucleotide of target gene

Restriction sites underlined: GAATTC, EcoRI; AAGCTT, HindIII; CATATG, NdeI; CTGCAG, PstI; TCTAGA, XbaI

SUPPLEMENTARY INFORMATION BELONGING TO CHAPTER V

FIGURE S1. Phenotypic analysis of *S. coelicolor* mutants on R2YE

Spores of *S. coelicolor* wildtype (M145), suppressor mutants and deletion mutants were plated onto rich glucose-containing media (R2YE) and supplemented with glucosamine (GlcN) or N-acetylglucosamine (GlcNAc) as indicated.

TABLE S1. Bacterial strains and plasmids.

Strains/plasmids	Genotype/description	Reference
Bacterial strain		
E. coli JM109	See reference	Sambrook et al., 1989
E. coli ET12567	See reference	MacNeil et al., 1992
M145	<i>S. coelicolor</i> A3(2) M145 SCP1- SCP2-	Kieser et al., 2000
GAM4	M145 <i>nagA</i>	Swiatek et al., 2012a
GAM5	M145 <i>nagB</i>	Swiatek et al., 2012a
GAM6	M145 <i>nagK</i>	Swiatek et al., 2012a
GAM8	M145 <i>nagKA</i>	Swiatek et al., 2012a
	M145 <i>nagBA</i>	this work
	M145 <i>nagKAB</i>	this work
	M145 SCO1447	this work
	M145 SCO1447 <i>nagB</i>	this work
	M145 SCO1448	this work
	M145 SCO1448 <i>nagB</i>	this work
Plasmids		
pWHM3	E. coli - Streptomyces shuttle vector (multi-copy in both hosts)	Vara et al., 1989
pHJL401	E. coli-Streptomyces shuttle vector with multiple copies in E. coli and 1-5 copies per chromosome in Streptomyces	Larson & Hershberger, 1986
pUWLcre	pUWLori T derivative with <i>cre(a)</i> gene under <i>ermE*</i> promoter	Fedoryshyn et al., 2008
pGWS961	pHJL401 harbouring SCO4284 gene (+1/+1146) with promoter sequence (-136/-3) of the SCO4284-SCO4285 operon	this work
pGAM1	pWHM3 harbouring flanking regions of <i>S. coelicolor</i> SCO4284 with <i>apra-loxP</i> inserted between the flanks	Swiatek et al., 2012a
pGAM2	pWHM3 harbouring flanking regions of <i>S. coelicolor</i> SCO5236 with <i>apra-loxP</i> inserted between the flanks	Swiatek et al., 2012a
pGWS948	pWHM3 harbouring flanking regions of <i>S. coelicolor</i> SCO1447 with <i>apra-loxP</i> inserted between the flanks	this work
pGWS955	pWHM3 harbouring flanking regions of <i>S. coelicolor</i> SCO1448 with <i>apra-loxP</i> inserted between the flanks	this work

TABLE S2. Oligonucleotides

Gene*	Name^	Sequence#
SCO4285	F-136	gtcagaattcACCCTGACTGCTCGTTCGCGCGT
	R-1	gtcacatatgGGTGCCGCCACATCGAG
SCO4284	F+1	gtcacatATGGCCCAAGCAAGGTTCGCGC
	R+1146	gtcaaaagcttTCAGCCAGGTGGGGATCGAC
SCO1447	LF-1251	gtcagaattcACCCTCGCGAACACCACCAGGCA
	LR+3	gaagttatccatcacctctagaCATGCCGGGATCCTTCCAGAT
	RF+1200	gaagttatcgcgcacatctctagaTTCGCACCGCCGGAGCGGTAG
	RR+2565	gtcaaaagcttGCATGCCGAGGCCGTCAAGC
SCO1448	LF-1422	gtcagaattcTGCTGCCGACGGTACTCGGGTGG
	LR+9	gaagttatccatcacctctagaTGTGTTTCATGGTCCACCCCTC
	RF+1221	gaagttatcgcgcacatctctagaCCGGCAGTCTGAACGCCCTCGC
	RR+2603	gtcaaaagcttTCTCCGCGATCAGGGCGATGACG

* SCO database number; nucleotide position is given relative to first nucleotide of therelevant gene

^ Forward (F) or reverse (R) primer, (L and R indicate left or right flank, where applicable); nucleotide position relative to first nucleotide of target gene

Restriction sites underlined: GAATTC, EcoRI; AAGCTT, HindIII; CATATG, NdeI; TCTAGA, XbaI

TABLE S3. Mutations identified in GlcN-derived *S. coelicolor nagB* suppressor mutants.

Position ^d	GSM38		GSM42*		GSM+3		GSM+4		SCO # ^e	Annotation
	Type ^d	nt ^b	aa ^c	Type ^d	nt ^b	aa ^c	Type ^d	nt ^b		
5216091	C	-	-	Ins	A	-	-	-	SCO0492	peptide synthetase
1020977	G	-	-	-	-	-	SNP	T	SCO0968	hypothetical protein
1544534	G	Del	GAP	fs	-	-	-	-	SCO1447	transcriptional regulator
1749870	G	-	-	-	-	-	-	C	P71R	hypothetical protein
1760847	C	-	-	-	-	-	SNP	A	SCO1635	Pup deamidase/depupylase
3435930	G	-	-	-	-	-	SNP	A	SCO3134	two-component system response regulator
3849222i	C	-	-	Ins	C	fs	Ins	C	-	-
3850016	G	Del	GAP	fs	-	-	-	-	SCO3485	Laci family transcriptional regulator
3850017	C	Del	GAP	fs	-	-	-	-	-	-
4692947 - 46999275	-	-	-	Unc	U	-	Unc	U	SCO4277 - SCO4283	-
4699483	G	-	-	Unc	U	-	Unc	C	A354G	-
4699603	T	-	-	Unc	U	-	SNP	C	K314R	-
4700074	C	-	-	Unc	U	-	SNP	T	G157E	N-acetylglucosamine-6-phosphate deacetylase
4700217	G	-	-	Unc	U	-	SNP	A	-	-
4700588	G	-	-	Unc	U	-	SNP	A	A319V	-
4700569	C	-	-	Unc	U	-	SNP	T	A319T	-
4700571	G	-	-	Unc	U	-	SNP	T	A318D	-
4700573i	C	-	-	-	-	-	Ins	T	fs	sugar kinase
4700574	G	-	-	Unc	U	-	SNP	A	T317M	-
4700575	T	-	-	Unc	U	-	SNP	C	T317A	-
4700745	C	-	-	Unc	U	-	Unc	U	-	-
4781982	C	SNP	T	SNP	T	-	SNP	T	SCO4367	oxidoreductase
558626111	C	-	-	Ins	C	fs	Ins	C	fs	-
558626414	C	-	-	Ins	G	fs	Ins	G	fs	-
558626411	C	-	-	Ins	G	fs	Ins	G	fs	-
558626413	C	-	-	Ins	A	fs	Ins	A	fs	-
558626412	C	-	-	Ins	G	fs	Ins	G	fs	-
558626511	G	-	-	Ins	G	fs	Ins	G	fs	-
7050737	C	-	-	SNP	T	A139T	SNP	T	A139T	integral membrane lysyl-tRNA synthetase
7190566	A	-	-	-	-	-	SNP	C	K498Q	dehydrogenase
7265819	C	SNP	G	H424Q	-	-	-	-	SCO6563	integral membrane transporter
7778607	T	-	-	-	-	-	SNP	G	V388G	carbohydrate kinase
7778749	C	-	-	-	-	-	SNP	G	SCO7004	carbohydrate kinase

SUPPLEMENTARY INFORMATION BELONGING TO CHAPTER VI

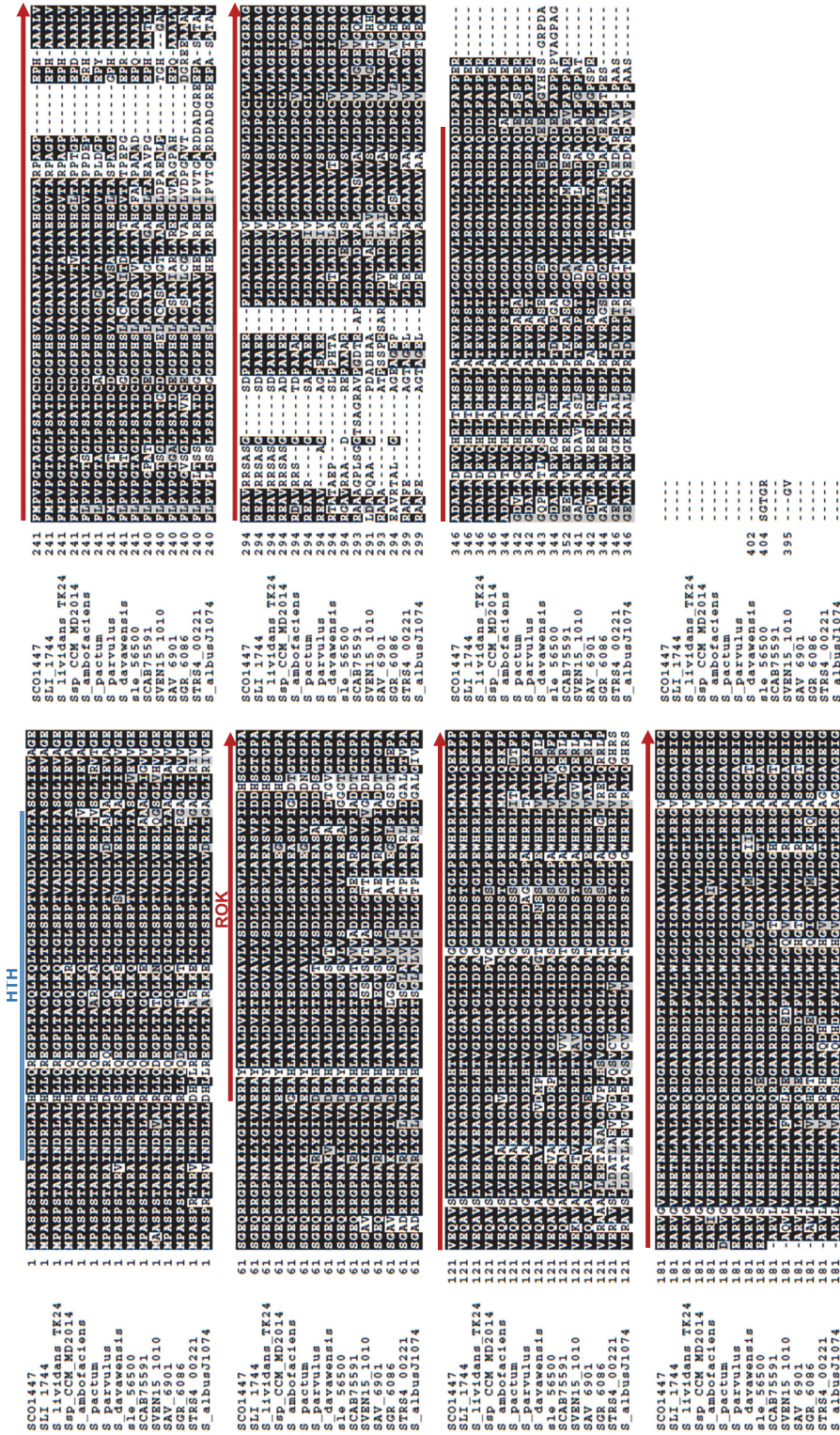


FIGURE S1. Sequence alignment of RokL6. Alignment of the RokL6 (SC01447) protein sequence with homologs from other *Streptomyces* species. Identical amino acids are shaded black and amino acids with similar properties are in grey. The HTH-domain of RokL6 is indicated as is the ROK-family domain, which begins at position 78 of RokL6. The image was generated using Boxshade.

TABLE S1. Bacterial strains and plasmids.

Bacterial strain		Reference
Strains and genotype		
<i>E. coli</i> JM109	See reference	Sambrook et al., 1989
<i>E. coli</i> ET12567	See reference	MacNeil et al., 1992
<i>E. coli</i> Rosetta(DE3)pLysS	See reference	Novagen
M145	<i>S. coelicolor</i> A3(2) M145 SCP1- SCP2- prototroph	Kieser et al., 2000
M512	M145 Δ redD Δ actII-ORF4	van Wezel et al., 2000
<i>AnagB</i>	M145 <i>AnagB</i> ^d	Swiatek et al., 2012a
GAM4	M145 <i>nagA</i>	Swiatek et al., 2012a
GAM5	M145 <i>nagB</i>	Swiatek et al., 2012a
	M145 <i>nagBA</i>	This work
	M145 SCO1447	This work
	M145 SCO1447 <i>nagB</i>	This work
	M145 SCO1448	This work
	M145 SCO1448 <i>nagB</i>	This work
Δ SCO6110	M145 Δ SCO6110	This work
Δ SCO6110 <i>AnagB</i>	M145 Δ SCO6110 ^a <i>AnagB</i> ^d	This work
Δ SCO6110 <i>ΔrokL6</i>	M145 Δ SCO6110 ^a <i>ΔrokL6</i> ^d	This work
Δ 6110-14	M145 Δ SCO6110-14	This work
Δ S6110-14 <i>AnagB</i>	M145 Δ SCO6110-14 ^a <i>AnagB</i> ^d	This work
Plasmids		
Plasmid	Description	Reference
pHJL401	<i>E. coli</i> - <i>Streptomyces</i> shuttle vector, 1-5 copies per chromosome in <i>Streptomyces</i>	Larson & Hershberger, 1986
pWHM3	<i>E. coli</i> - <i>Streptomyces</i> shuttle vector (multi-copy in both hosts)	Vara et al., 1989
pUWLcre	pUWLori T derivative with <i>cre(a)</i> gene under <i>ermE</i> * promoter	Fedoryshyn et al, 2008
pGWS948	pWHM3 harbouring flanking regions of <i>S. coelicolor</i> SCO1447 with <i>apra-loxP</i> inserted between the flanks	this work
pGWS953	pWHM3 harbouring flanking regions of <i>S. coelicolor</i> SCO6110 with <i>apra-loxP</i> inserted between the flanks	this work
pGWS954	pWHM3 harbouring flanking regions of <i>S. coelicolor</i> SCO6110-14 with <i>apra-loxP</i> inserted between the flanks	this work

^a, Aprpr, apramycin resistant. ^d deletion

TABLE S2. Oligonucleotides.

Gene*	Name [^]	Sequence#
SCO6110	6110LF-1198	<u>gtcagaattc</u> tgtgtgatcgccgacgagccac
	6110LR+6	gaagttatccatcacct <u>tctaga</u> GCTCACCCCTGCTCCTCCGTC
	6110RF+927	gaagttatcgcgcatc <u>tctaga</u> CACGAGCTGACCGCCCGCTGA
	6110RR+2197	<u>gtcaaaagcct</u> tgccaacggctatgtgcgcgaggt
SCO6110-14	6114LF-1306	<u>gtcagaattc</u> AGGACGGCTCGTTCGATGGCGAG
	6114LR+9	gaagttatccatcacct <u>tctaga</u> AGTGACATGTATCTCCTCCA
	6110RF+927	as above
	6110RR+2197	as above

* SCO database number; nucleotide position is given relative to first nucleotide of the relevant gene

[^] Forward (F) or reverse (R) primer, L and R indicate left or right flank; nucleotide position relative to first nucleotide of target gene

Restriction sites underlined: GAATTC, EcoRI; AAGCTT, HindIII; TCTAGA, XbaI

TABLE S3. Proteomic comparison of *S. coelicolor* M145 and its *rokL6* mutant.

SCO	GlcN-Mann wt	1447	Mann 1447-wt	GlcN	SCO	Description
SCO6010	1.379	1.288	1.580	1.475	SCO6010	Probable ABC-transport system ATP binding protein
SCO5869	1.389		1.796	1.273	SCO5869	Uncharacterized protein
SCO3967	1.851		10.400	6.011	SCO3967	Conserved hypothetical membrane protein
SCO5895			0.278	0.378	SCO5895	Putative methyltransferase
SCO2661	1.304	1.892	1.393	2.022	SCO2661	Putative sugar hydrolase
SCO5880			0.368	0.192	SCO5880	RedY protein
SCO5293	1.196		1.667	1.397	SCO5293	Putative oxygenase subunit
SCO5554	1.785			0.571	SCO5554	3-isopropylmalate dehydratase small subunit
SCO5113	1.305	1.071	1.419	1.165	SCO5113	BldKB_putative ABC transport system lipoprotein
SCO1245			2.186	1.968	SCO1245	Adenosylmethionine-8-amino-7-oxononanoate aminotransferase
SCO7417	1.307	0.904	2.241	1.551	SCO7417	Putative cytochrome P450-family protein
SCO3349	1.216		1.804	1.668	SCO3349	Uncharacterized protein SCO3349
SCO2280			0.445	0.601	SCO2280	Putative TetR-family transcriptional regulator
SCO2256			0.224	0.242	SCO2256	3-methyl-2-oxobutanoate hydroxymethyltransferase
SCO5259			1.827	1.509	SCO5259	Permease
SCO5512			0.489	0.300	SCO5512	Acetolactate synthase
SCO4979			2.293	1.884	SCO4979	Phosphoenolpyruvate carboxykinase [GTP]
SCO3089				0.307	SCO3089	Putative ABC transporter ATP-binding protein
SCO2620	1.406		1.754		SCO2620	Trigger factor
SCO3963			0.508	0.463	SCO3963	Uncharacterized protein
SCO6375			2.595	2.286	SCO6375	Putative secreted protein
SCO4055			2.862	3.066	SCO4055	Putative alcohol dehydrogenase
SCO1901	0.829	0.650	1.462	1.146	SCO1901	Putative zinc-binding dehydrogenase
SCO3097		1.668		0.408	SCO3097	Putative secreted protein
SCO1923			1.892	1.609	SCO1923	Putative dioxygenase ferredoxin subunit
SCO2182			0.823	0.850	SCO2182	Putative gntR-family transcriptional regulator
SCO5024			2.597	1.852	SCO5024	Putative oxidoreductase
SCO2117		0.782	1.822	1.730	SCO2117	Putative anthranilate synthase
SCO2630	1.467		0.627	0.417	SCO2630	Putative biotin synthase
SCO2225	1.717	1.559			SCO2225	Putative isomerase
SCO6540	1.471	1.191	1.242		SCO6540	Putative pterin-4-alpha-carbinolamine dehydratase
SCO3202	1.741			0.672	SCO3202	RNA polymerase principal sigma factor HrdD
SCO2780			0.726	0.667	SCO2780	Putative secreted protein
SCO1476	1.625		1.727		SCO1476	S-adenosylmethionine synthase
SCO3618			1.981	1.794	SCO3618	Recombination protein RecR
SCO0247			1.652	1.375	SCO0247	Uncharacterized protein
SCO0477	1.424	1.499		1.172	SCO0477	Uncharacterized protein
SCO1760			1.524	1.156	SCO1760	Cytidylate kinase
SCO2616		0.887	1.397	1.183	SCO2616	Putative membrane protein
SCO3731	1.443		1.448	1.219	SCO3731	Cold-shock protein
SCO1169				0.441	SCO1169	Xylose isomerase
SCO6659	1.486	1.371		0.867	SCO6659	Glucose-6-phosphate isomerase 1
SCO2164			0.759	0.590	SCO2164	Putative integral membrane efflux protein
SCO3182	1.205		1.436		SCO3182	UTP--glucose-1-phosphate uridylyltransferase
SCO1872			2.136	1.541	SCO1872	Putative IclR-family transcriptional regulator
SCO7477		0.257		5.862	SCO7477	Putative membrane protein
SCO1486	1.653		1.885		SCO1486	Dihydroorotase
SCO1406	0.857		2.354		SCO1406	Uncharacterized protein
SCO5745			1.851	1.407	SCO5745	Ribonuclease J
SCO3956			0.619	0.697	SCO3956	Putative ABC transporter ATP-binding protein
SCO3928			1.718	1.217	SCO3928	Phosphomethylpyrimidine synthase
SCO4653	1.662		1.860		SCO4653	50S ribosomal protein L7/L12
SCO5553	1.337			0.767	SCO5553	3-isopropylmalate dehydratase large subunit
SCO4472				0.442	SCO4472	Putative secreted protein
SCO2548	1.794	1.289	1.479		SCO2548	Putative Hit-family protein
SCO1666			1.610	1.252	SCO1666	Putative phosphatase
SCO6057	1.200		1.295	1.121	SCO6057	Putative ATP/GTP-binding integral membrane protein
SCO1045				1.935	SCO1045	Putative metal associated protein
SCO1773			1.501		SCO1773	Alanine dehydrogenase
SCO5472				0.434	SCO5472	Aminomethyltransferase
SCO2093	1.197	1.067	1.280	1.140	SCO2093	Carbonic anhydrase
SCO3615	1.265			0.864	SCO3615	Aspartokinase
SCO5047	0.728		0.664	0.873	SCO5047	Fructose-1_6-bisphosphatase
SCO5751	1.749	1.224	1.696		SCO5751	Putative membrane protein
SCO5290	0.439	0.498		1.968	SCO5290	Uncharacterized protein
SCO2161	1.431	1.350	1.082		SCO2161	Uncharacterized protein
SCO6804			0.147		SCO6804	Uncharacterized protein
SCO3651	1.338	1.512	0.612	0.692	SCO3651	Uncharacterized protein
SCO4661	1.351		1.480		SCO4661	Elongation factor G 1
SCO3226	1.529	1.383		1.484	SCO3226	Two component system response regulator
SCO1478	1.365		1.758	1.436	SCO1478	DNA-directed RNA polymerase subunit omega
SCO0681	1.578	1.242			SCO0681	Putative ferredoxin/ferredoxin-NADP reductase protein)
SCO4498				0.470	SCO4498	Putative proton transport protein
SCO5145			1.767	1.570	SCO5145	Uncharacterized protein
SCO3913	1.429		1.529		SCO3913	Uncharacterized protein
SCO3333		0.541		0.730	SCO3333	Putative hydrolase
SCO0923				0.494	SCO0923	Putative reductase flavoprotein subunit
SCO1116	1.600		1.894	1.358	SCO1116	Uncharacterized protein
SCO2067	2.051		2.192	1.240	SCO2067	Putative membrane protein
SCO2388			1.508	1.268	SCO2388	3-oxoacyl-[acyl-carrier-protein] synthase 3 protein 1
SCO4812				0.493	SCO4812	Putative integral membrane protein
SCO4580	0.625	0.648			SCO4580	Putative fumarylacetoacetase
SCO1870		1.671			SCO1870	Uncharacterized protein
SCO1676			1.766	1.172	SCO1676	Putative peptidase

APPENDIX IV

SCO	GlcN-Mann wt	1447	1447-wt Mann	GlcN	SCO	Description
SCO5625	1.542		2.016	1.444	SCO5625	Elongation factor Ts
SCO2322	0.783	0.656			SCO2322	Putative secreted protein
SCO2730				3.135	SCO2730	Putative regulator
SCO4242	0.472			2.290	SCO4242	Putative membrane protein
SCO4648	1.294	0.842	1.519		SCO4648	50S ribosomal protein L11
SCO6041	1.546		1.431		SCO6041	Putative protoporphyrinogen oxidase
SCO4945				0.568	SCO4945	Putative dehydrogenase
SCO5419	1.241		1.341		SCO5419	Putative thioredoxin
SCO3151	0.554	0.726			SCO3151	Uncharacterized protein
SCO5254	2.133	1.559			SCO5254	Superoxide dismutase [Ni]
SCO2619	1.622		1.392		SCO2619	ATP-dependent Clp protease proteolytic subunit 1
SCO5774		0.645		1.260	SCO5774	Glutamate permease
SCO4525	1.239		1.436		SCO4525	Uncharacterized protein
SCO5820	1.214		1.251		SCO5820	RNA polymerase principal sigma factor HrdB
SCO6123	1.912			1.479	SCO6123	Putative quinone binding protein
SCO1814			1.727	1.326	SCO1814	Enoyl-[acyl-carrier-protein] reductase [NADH]
SCO2011		0.615	2.073	1.567	SCO2011	Putative branched chain amino acid transport ATP-binding protein
SCO1480	1.322		1.431		SCO1480	Uncharacterized protein
SCO1514	1.522		1.688	1.209	SCO1514	Adenine phosphoribosyltransferase
SCO2902	1.484		1.593		SCO2902	Non-canonical purine NTP pyrophosphatase
SCO2577				1.234	SCO2577	Ribosomal silencing factor RsfS
SCO5519	1.992		1.349		SCO5519	Uncharacterized protein
SCO1461				0.667	SCO1461	Putative inosine monophosphate dehydrogenase
SCO3122	1.488				SCO3122	Bifunctional protein GlmU
SCO1942	1.475	1.312			SCO1942	Glucose-6-phosphate isomerase 2
SCO2196	1.243		1.363		SCO2196	Putative integral membrane protein
SCO2643			1.369	1.166	SCO2643	Aminopeptidase N
SCO3136	2.048	1.180			SCO3136	Galactokinase
SCO5493	1.434		1.562		SCO5493	Uncharacterized protein
SCO1560	1.331		1.289		SCO1560	Putative phosphatase
SCO1958	1.531			0.906	SCO1958	UvrABC system protein A
SCO4992			1.304	1.253	SCO4992	Uncharacterized protein
SCO6983	1.301	1.244			SCO6983	Uncharacterized protein
SCO2012			1.884	1.414	SCO2012	Putative branched chain amino acid transport ATP-binding protein
SCO1554	1.310	1.217			SCO1554	Nicotinate-nucleotide--dimethylbenzimidazole phosphoribosyltransferase
SCO1109				0.542	SCO1109	Putative oxidoreductase
SCO5592	1.166		1.332		SCO5592	UPF0109 protein SCO5592
SCO3127				1.698	SCO3127	Phosphoenolpyruvate carboxylase
SCO4173				0.437	SCO4173	Uncharacterized protein
SCO5102	0.713			1.230	SCO5102	Putative mutT-like protein
SCO1415	2.176			2.554	SCO1415	Putative membrane protein
SCO1898			1.586	1.233	SCO1898	Putative substrate binding protein
SCO0499	2.290	1.624		1.188	SCO0499	Putative formyltransferase
SCO6042	1.373				SCO6042	Uncharacterized protein
SCO4729	2.190				SCO4729	DNA-directed RNA polymerase subunit alpha
SCO1947	1.417			0.849	SCO1947	Glyceraldehyde-3-phosphate dehydrogenase
SCO5385	1.554				SCO5385	Putative 3-hydroxybutyryl-coA dehydrogenase
SCO5281	1.781			1.178	SCO5281	Putative 2-oxoglutarate dehydrogenase
SCO6310			1.183	1.281	SCO6310	Putative cytochrome P450
SCO2076			1.236		SCO2076	Isoleucine--tRNA ligase
SCO4439	1.728				SCO4439	Putative D-alanyl-D-alanine carboxypeptidase
SCO6147		1.337			SCO6147	Probable xylitol oxidase
SCO6835		1.830		1.710	SCO6835	Putative arsenate reductase
SCO4683	1.516			1.132	SCO4683	Glutamate dehydrogenase
SCO5459		0.941	1.270		SCO5459	Putative enoyl-coA hydratase
SCO2267	1.437	1.175			SCO2267	Probable heme oxygenase
SCO3156				1.375	SCO3156	Putative penicillin-binding protein
SCO5822	1.346		1.205		SCO5822	DNA topoisomerase (ATP-hydrolyzing)
SCO1646	0.745			0.640	SCO1646	Prokaryotic ubiquitin-like protein Pup
SCO5865		0.795			SCO5865	Uncharacterized protein
SCO3399	10.057	5.418			SCO3399	Uncharacterized protein
SCO6743	1.215			0.825	SCO6743	Putative transcriptional accessory protein
SCO1546				1.577	SCO1546	Putative aminotransferase
SCO1871	0.704		0.694		SCO1871	Putative aldehyde dehydrogenase
SCO2771	1.476				SCO2771	Uncharacterized phosphatase SCO2771
SCO5500	1.419				SCO5500	Putative membrane protein
SCO7443	1.942				SCO7443	Phosphoglucomutase
SCO2837		0.767		1.149	SCO2837	Putative secreted protein
SCO5470	1.682			0.704	SCO5470	Serine hydroxymethyltransferase
SCO4199	1.954				SCO4199	Uncharacterized protein
SCO1213	1.294		1.223		SCO1213	Uncharacterized protein
SCO5031	1.206	1.223			SCO5031	Alkyl hydroperoxide reductase AhpD
SCO7102		0.680		1.176	SCO7102	Uncharacterized protein
SCO1848	1.489			1.489	SCO1848	Cobyric acid synthase
SCO3063	1.196		1.243		SCO3063	Putative two-component system response regulator
SCO2162			1.345		SCO2162	Quinolinate synthase A
SCO1141	1.403		1.240	0.811	SCO1141	Uncharacterized protein
SCO4587	1.488	1.582			SCO4587	Uncharacterized protein
SCO1815				1.659	SCO1815	Probable 3-oxacyl-(Acyl-carrier-protein) reductase
SCO4584				0.685	SCO4584	Putative membrane protein
SCO0748	1.658	1.764			SCO0748	Putative hydrolase
SCO0525	1.560			1.589	SCO0525	Uncharacterized protein

SUPPLEMENTARY INFORMATION BELONGING TO CHAPTER VI

SCO	GlcN-Mann wt	1447	1447-wt Mann	GlcN	SCO	Description
SCO5170				0.512	SCO5170	Putative tetR-family transcriptional regulator
SCO6627				1.678	SCO6627	Uncharacterized protein
SCO2115	1.476				SCO2115	Phospho-2-dehydro-3-deoxyheptonate aldolase
SCO5329	1.271				SCO5329	Uncharacterized protein
SCO2778			1.297	1.120	SCO2778	Hydroxymethylglutaryl-CoA lyase
SCO1490				1.309	SCO1490	N utilization substance protein B homolog
SCO5533	2.035	1.463			SCO5533	Uncharacterized protein
SCO4152			1.764	1.565	SCO4152	Putative secreted 5'-nucleotidase
SCO5477		0.860	1.292		SCO5477	Putative oligopeptide-binding lipoprotein
SCO5260	1.903				SCO5260	Secreted protein
SCO0679	0.388				SCO0679	Uncharacterized protein
SCO3889		1.476		1.478	SCO3889	Thioredoxin-1
SCO4710	1.913			0.797	SCO4710	50S ribosomal protein L29
SCO1852	2.431			1.519	SCO1852	Hydrogenobyrinate a_c-diamide synthase
SCO4366	1.292				SCO4366	Phosphoserine aminotransferase
SCO2168				0.502	SCO2168	Uncharacterized protein
SCO3381	1.484				SCO3381	Nicotinate-nucleotide pyrophosphorylase
SCO3074				0.745	SCO3074	Putative integral membrane protein
SCO1705	1.334		1.366		SCO1705	Putative alcohol dehydrogenase (Zinc-binding)
SCO5499				1.326	SCO5499	Glutamyl-tRNA(Gln) amidotransferase subunit A
SCO3958				0.557	SCO3958	ABC transporter ATP-binding protein
SCO0740		1.442			SCO0740	Putative hydrolase
SCO4233				1.104	SCO4233	2-C-methyl-D-erythritol 4-phosphate cytidyltransferase
SCO0762	0.307			0.498	SCO0762	Subtilase-type protease inhibitor
SCO4643	1.454		1.305		SCO4643	UDP-N-acetylenolpyruvoylglucosamine reductase
SCO4832				0.000	SCO4832	Putative glycine betaine-binding lipoprotein
SCO5893	0.752			0.660	SCO5893	Oxidoreductase
SCO2597				1.443	SCO2597	50S ribosomal protein L21
SCO6076	1.957	1.398			SCO6076	Putative dipeptidase
SCO1087		0.630		0.910	SCO1087	Putative aldolase
SCO1793		0.808		0.886	SCO1793	Putative secreted protein
SCO1728		0.648	1.466		SCO1728	Putative gntR-family transcriptional regulator
SCO7523	1.353				SCO7523	Putative chaperone
SCO2387			2.035	1.892	SCO2387	Malonyl CoA:acyl carrier protein malonyltransferase
SCO6046		0.773		0.808	SCO6046	Uncharacterized protein
SCO5077				1.308	SCO5077	Uncharacterized protein
SCO3001			1.266		SCO3001	Uncharacterized protein
SCO1081	1.097		1.172		SCO1081	Putative electron transfer flavoprotein_alpha subunit
SCO7154	1.750				SCO7154	Ketol-acid reductoisomerase 2
SCO1659		0.403		0.481	SCO1659	Probable glycerol uptake facilitator protein
SCO4652	1.455				SCO4652	50S ribosomal protein L10
SCO3673	1.801			1.454	SCO3673	Putative iron-sulphur-binding reductase
SCO3897			1.321		SCO3897	Uncharacterized protein
SCO5225				1.217	SCO5225	Ribonucleoside-diphosphate reductase subunit beta
SCO5813	1.270			1.162	SCO5813	Uncharacterized protein
SCO6199		0.652			SCO6199	Secreted esterase
SCO1864				0.754	SCO1864	L-2,4-diaminobutyric acid acetyltransferase
SCO6564				1.285	SCO6564	3-oxoacyl-[acyl-carrier-protein] synthase 3 protein 4
SCO1640				0.762	SCO1640	Pup--protein ligase
SCO2169			1.395		SCO2169	Putative integral membrane protein
SCO1501				1.203	SCO1501	Alanine--tRNA ligase
SCO1404	1.349				SCO1404	Uncharacterized protein
SCO6216				1.535	SCO6216	Uncharacterized protein
SCO4636				1.167	SCO4636	UPF0336 protein SCO4636
SCO4232	1.264				SCO4232	Putative transcriptional factor regulator
SCO5806				1.387	SCO5806	Uncharacterized protein
SCO7361				1.178	SCO7361	Putative DNA-binding protein
SCO6031	1.557				SCO6031	Uroporphyrinogen decarboxylase
SCO1425	1.807			0.886	SCO1425	Putative AsnC-family transcriptional regulatory protein
SCO2669		0.569		1.222	SCO2669	Uncharacterized protein
SCO3896	2.845				SCO3896	Putative RNA nucleotidyltransferase
SCO6860			1.653	1.426	SCO6860	Uncharacterized protein
SCO1319	1.233		1.387		SCO1319	Putative membrane protein
SCO3187				1.636	SCO3187	Uncharacterized protein
SCO2147	1.306		1.498	1.302	SCO2147	Anthranilate phosphoribosyltransferase 1
SCO5232				2.426	SCO5232	Putative sugar transporter sugar binding protein
SCO1479	1.667				SCO1479	Guanylate kinase
SCO0769				0.776	SCO0769	Putative oxidoreductase
SCO4506	1.517			1.255	SCO4506	Chorismate dehydratase
SCO3977		0.698			SCO3977	Putative protease (Putative secreted protein)
SCO1900				2.255	SCO1900	Putative integral membrane sugar transport protein
SCO4078				1.351	SCO4078	Phosphoribosylformylglycinamide synthase subunit PurQ
SCO0868			3.562	4.496	SCO0868	Putative regulatory protein
SCO0719	4.043				SCO0719	Uncharacterized protein
SCO4026	0.660				SCO4026	Putative ATP binding protein
SCO3941			1.409	1.290	SCO3941	Putative serine/threonineprotein kinase
SCO1817			1.375		SCO1817	Uncharacterized protein
SCO6776		0.495			SCO6776	Uncharacterized protein
SCO2974				0.783	SCO2974	Serine/threonine-protein kinase PkaA
SCO3617			1.513		SCO3617	Uncharacterized protein
SCO1644				1.652	SCO1644	Proteasome subunit beta
SCO4637	1.532				SCO4637	Uncharacterized protein
SCO5854		1.738			SCO5854	Sulfurtransferase
SCO3884	1.129		1.123		SCO3884	Jag
SCO2075		0.666			SCO2075	Putative DNA-binding protein
SCO3899				1.347	SCO3899	Uncharacterized protein

APPENDIX IV

SCO	GlcN-Mann wt	1447	1447-wt Mann	GlcN	SCO	Description
SCO4614				1.326	SCO4614	UPF0234 protein SCO4614
SCO3137	1.401				SCO3137	UDP-glucose 4-epimerase
SCO1088		0.758		0.657	SCO1088	Putative oxidoreductase
SCO2241			0.610		SCO2241	Probable glutamine synthetase (EC 6.3.1.2)
SCO1438	0.785				SCO1438	ATP phosphoribosyltransferase
SCO3862				1.666	SCO3862	Putative membrane protein
SCO3966				1.785	SCO3966	Putative secreted protein
SCO4293				0.755	SCO4293	Putative threonine synthase
SCO3059			1.262		SCO3059	N5-carboxyaminoimidazole ribonucleotide mutase
SCO3197				1.137	SCO3197	Putative 1-phosphofruktokinase
SCO4036	1.330	1.218			SCO4036	Uncharacterized protein SCO4036
SCO4814				1.433	SCO4814	Bifunctional purine biosynthesis protein PurH
SCO1602	2.173		5.097	2.120	SCO1602	Uncharacterized protein
SCO2065	1.383				SCO2065	Uncharacterized protein
SCO0641				0.491	SCO0641	Tellurium resistance protein
SCO4493				1.182	SCO4493	Putative asnC-family transcriptional regulator
SCO4394		0.824		1.130	SCO4394	DmdR1 protein
SCO5711				1.502	SCO5711	Riboflavin biosynthesis protein
SCO3815		0.718			SCO3815	Putative dihydrolipoamide acyltransferase component
SCO2951				1.229	SCO2951	Putative malate oxidoreductase
SCO6637		0.736			SCO6637	Uncharacterized protein
SCO3950	1.856			1.150	SCO3950	Uncharacterized protein
SCO4550	1.456				SCO4550	Cyclic dehydropoxanthine futasolone synthase
SCO2008		0.623			SCO2008	Putative branched chain amino acid binding protein
SCO6723				1.144	SCO6723	Putative oxidoreductase (Putative secreted protein)
SCO3859				1.210	SCO3859	Putative DNA-binding protein
SCO5396		0.589			SCO5396	Putative cellulose-binding protein
SCO2369		1.843			SCO2369	Putative thiol-specific antioxidant protein
SCO2614	1.574				SCO2614	Folylpolyglutamate synthase
SCO4087	2.446				SCO4087	Phosphoribosylformylglycinamide cyclo-ligase
SCO6260	1.935				SCO6260	Putative sugar kinase
SCO5738		1.975			SCO5738	Uncharacterized zinc protease SCO5738
SCO3108		0.718			SCO3108	Uncharacterized protein
SCO6658				1.237	SCO6658	6-phosphogluconate dehydrogenase
SCO0736		1.396			SCO0736	Putative secreted protein
SCO6544				1.831	SCO6544	Putative membrane protein
SCO5539	8.098				SCO5539	Uncharacterized protein
SCO4261	1.746			1.073	SCO4261	Putative response regulator
SCO4894				0.374	SCO4894	Uncharacterized protein
SCO3914	3.937				SCO3914	Putative transcriptional regulator
SCO2920		0.446			SCO2920	Putative secreted protease
SCO0730				0.674	SCO0730	Uncharacterized protein
SCO0546	1.138			0.862	SCO0546	Pyruvate carboxylase
SCO4610	4.483				SCO4610	Putative integral membrane protein
SCO7319				0.378	SCO7319	Putative oxidoreductase
SCO5257				1.815	SCO5257	Methyltransferase
SCO4736	0.850		0.799		SCO4736	Phosphoglucosamine mutase
SCO2634	2.203				SCO2634	Uncharacterized protein
SCO4545	5.429				SCO4545	Uncharacterized protein
SCO1244				1.433	SCO1244	Biotin synthase
SCO1718				0.597	SCO1718	Putative regulator
SCO2908	0.833		0.845		SCO2908	Uncharacterized protein
SCO2640	1.216				SCO2640	Aspartate-semialdehyde dehydrogenase
SCO4649				1.132	SCO4649	50S ribosomal protein L1
SCO2044				0.847	SCO2044	Phosphoribosyl-AMP cyclohydrolase
SCO3957				0.550	SCO3957	Possible integral membrane protein
SCO3317				0.815	SCO3317	Putative uroporphyrin-III C-methyltransferase/ uroporphyrinogen-III synthase
SCO5151		0.480	2.143		SCO5151	Uncharacterized protein
SCO6206		2.035			SCO6206	Putative hydroxypyruvate isomerase
SCO1232	1.353				SCO1232	Urease accessory protein UreG
SCO3817				1.319	SCO3817	Putative branched-chain alpha keto acid dehydrogenase E1 alpha subunit
SCO0428		0.717			SCO0428	Putative tetR family transcriptional regulator
SCO0888	2.719			1.394	SCO0888	Putative secreted protein
SCO5136		1.197			SCO5136	Putative aminotransferase
SCO2039		1.079			SCO2039	Indole-3-glycerol phosphate synthase 1
SCO4151				1.178	SCO4151	Mycothioli acetyltransferase
SCO3871		0.282		0.557	SCO3871	Putative decarboxylase
SCO0506		1.393			SCO0506	NH(3)-dependent NAD(+) synthetase
SCO5543				1.144	SCO5543	Uncharacterized protein
SCO3484	3.178			1.661	SCO3484	Putative secreted sugar-binding protein
SCO5172	1.934				SCO5172	Putative hydrolase
SCO3401	2.064				SCO3401	Putative hydroxymethylidihydropteridine pyrophosphokinase
SCO5776		0.765			SCO5776	Glutamate binding protein
SCO5537				1.579	SCO5537	Putative ATP/GTP binding protein
SCO1008	1.725			1.168	SCO1008	Uncharacterized protein
SCO5708		0.732			SCO5708	Ribosome-binding factor A
SCO0884				1.583	SCO0884	Probable oxidoreductase
SCO5859		1.214		1.136	SCO5859	Probable ferrochelataze
SCO7072	1.561				SCO7072	Uncharacterized protein
SCO3343				0.494	SCO3343	Uncharacterized protein
SCO1343	1.226		1.310		SCO1343	Uracil-DNA glycosylase 2
SCO1138		0.750		1.304	SCO1138	Putative secreted protein
SCO1925				1.201	SCO1925	Uncharacterized protein
SCO5178	2.051				SCO5178	Putative sulfurylase

SUPPLEMENTARY INFORMATION BELONGING TO CHAPTER VI

SCO	GlcN-Mann wt	1447	1447-wt Mann	GlcN	SCO	Description
SCO5514	2.174				SCO5514	Ketol-acid reductoisomerase 1
SCO6207	3.318	1.508	2.802		SCO6207	Uncharacterized protein
SCO1556	1.245				SCO1556	Putative acetyltransferase
SCO5240	2.680		4.437	1.908	SCO5240	Transcriptional regulator WhiB
SCO4548	2.104				SCO4548	Putative integral membrane protein
SCO1201				0.555	SCO1201	Putative reductase
SCO3944	1.193			0.900	SCO3944	Putative phenylalanine aminotransferase
SCO3768		0.415	1.819		SCO3768	Putative translocase protein
SCO1706				0.531	SCO1706	Putative aldehyde dehydrogenase
SCO2884	1.990				SCO2884	Putative cytochrome P450
SCO5560	1.210		1.285		SCO5560	D-alanine--D-alanine ligase
SCO2129				1.061	SCO2129	Uncharacterized protein
SCO1598		0.734			SCO1598	50S ribosomal protein L20
SCO1553				1.611	SCO1553	Putative uroporphyrin-III methyltransferase
SCO7585		0.860		0.591	SCO7585	Putative merR-family transcriptional regulator
SCO3302	0.317				SCO3302	Putative integral membrane protein
SCO0494	1.398			0.814	SCO0494	Putative iron-siderophore binding lipoprotein
SCO1254				1.327	SCO1254	Adenylosuccinate lyase
SCO4118				0.763	SCO4118	Putative tetR-family transcriptional regulator
SCO0672	5.067				SCO0672	Anti-sigma factor antagonist
SCO0852				0.822	SCO0852	Putative aldolase
SCO5367	2.630				SCO5367	ATP synthase subunit a
SCO1630			0.592		SCO1630	Putative integral membrane protein
SCO5423	1.431			1.253	SCO5423	Pyruvate kinase
SCO7292	3.041				SCO7292	Putative threonine dehydratase
SCO5701	2.681				SCO5701	Uncharacterized protein
SCO1660				0.710	SCO1660	Glycerol kinase 2
SCO4277				0.445	SCO4277	Putative tellurium resistance protein
SCO1648				0.782	SCO1648	Proteasome-associated ATPase
SCO3669	1.314			0.792	SCO3669	Chaperone protein DnaJ 1
SCO2726	1.335				SCO2726	Methylmalonic acid semialdehyde dehydrogenase
SCO4096	4.368				SCO4096	ATP-dependent RNA helicase
SCO2769	1.974				SCO2769	Putative acetolactate synthase
SCO4734	1.333				SCO4734	50S ribosomal protein L13
SCO1699	1.769				SCO1699	Putative transcriptional regulator
SCO1571	2.873				SCO1571	Uncharacterized protein
SCO5546	1.294				SCO5546	Uncharacterized protein
SCO1639	1.329				SCO1639	Peptidyl-prolyl cis-trans isomerase
SCO3549				1.113	SCO3549	Anti-sigma-B factor antagonist
SCO7468			1.623	1.407	SCO7468	Putative flavin-binding monooxygenase
SCO4704				1.306	SCO4704	50S ribosomal protein L23
SCO6068			3.681	2.048	SCO6068	Uncharacterized protein
SCO2026				1.229	SCO2026	Putative glutamate synthase large subunit
SCO6960		1.343			SCO6960	Uncharacterized protein
SCO7699				1.376	SCO7699	Putative nucleotide-binding protein
SCO5544				1.191	SCO5544	Histidine kinase
SCO5563	4.037		2.940		SCO5563	Hydroxymethylpyrimidine/phosphomethylpyrimidine kinase
SCO0427	2.020				SCO0427	Putative hydrolase
SCO4088		0.269			SCO4088	Uncharacterized protein
SCO2582	1.248				SCO2582	Uncharacterized protein
SCO4444	1.729		2.479	1.459	SCO4444	Glutathione peroxidase
SCO5648	3.102			1.204	SCO5648	Fe(3+) ions import ATP-binding protein FbpC
SCO3619	1.567				SCO3619	Nucleoid-associated protein SCO3619
SCO1818	0.787				SCO1818	Tyrosine--tRNA ligase
SCO5140				0.631	SCO5140	Cytokinin riboside 5'-monophosphate phosphoribohydrolase
SCO4932		0.687		0.810	SCO4932	Histidine ammonia-lyase
SCO4651	0.747				SCO4651	Putative lipoprotein SCO4651
SCO3041				0.672	SCO3041	Uncharacterized protein
SCO2579	2.000				SCO2579	Probable nicotinate-nucleotide adenyltransferase
SCO2774	1.421				SCO2774	Acyl-CoA dehydrogenase
SCO3607				0.828	SCO3607	Putative secreted protein
SCO1511				0.811	SCO1511	Uncharacterized protein
SCO2793				0.784	SCO2793	Oligoribonuclease
SCO6491				2.208	SCO6491	Uncharacterized protein
SCO4585	3.008			0.322	SCO4585	Putative ABC transporter ATP-binding protein
SCO3795				1.235	SCO3795	Aspartate--tRNA ligase
SCO5044				1.167	SCO5044	Fumarate hydratase class I
SCO3060	1.191				SCO3060	N5-carboxyaminoimidazole ribonucleotide synthase
SCO6197		0.547			SCO6197	Putative secreted protein
SCO1223				0.690	SCO1223	Ornithine aminotransferase
SCO4965		0.603			SCO4965	Transcription elongation factor GreA
SCO1174	2.017			0.897	SCO1174	Probable aldehyde dehydrogenase
SCO3614				0.744	SCO3614	Aspartate-semialdehyde dehydrogenase
SCO4020				1.555	SCO4020	Putative two component system response regulator
SCO5788	1.414	0.850	1.718		SCO5788	Uncharacterized protein
SCO2600		0.778			SCO2600	Uncharacterized protein
SCO5501				1.155	SCO5501	Aspartyl/glutamyl-tRNA(Asn/Gln) amidotransferase subunit B
SCO4556				1.118	SCO4556	Demethylmenaquinone methyltransferase
SCO3009		2.024			SCO3009	Uncharacterized protein
SCO6515		1.665			SCO6515	Putative protease
SCO4708	1.353				SCO4708	30S ribosomal protein S3
SCO2444		0.374	3.884	3.222	SCO2444	Putative fatty acid synthase
SCO1766	3.200				SCO1766	Putative glycohydrolase
SCO3179				2.570	SCO3179	Molybdenum cofactor biosynthesis protein (Putative secreted protein)
SCO5651	1.525				SCO5651	Uncharacterized protein
SCO2054	2.085			1.271	SCO2054	Histidinol dehydrogenase

APPENDIX IV

SCO	GlcN-Mann wt	1447	1447-wt Mann	GlcN	SCO	Description
SCO4296			1.401		SCO4296	60 kDa chaperonin 2
SCO5655	1.301			0.750	SCO5655	Putative aminotransferase
SCO5474		3.186			SCO5474	Uncharacterized protein
SCO2900				0.743	SCO2900	Putative membrane protein
SCO2549	0.786			0.860	SCO2549	Tricorn protease homolog 1
SCO4912		0.684		0.728	SCO4912	Putative aldehyde dehydrogenase
SCO0979				1.396	SCO0979	Uncharacterized protein
SCO1506	2.034				SCO1506	Conserved ATP/GTP binding protein
SCO6456				2.626	SCO6456	Putative hydrolytic protein
SCO1594				1.345	SCO1594	Phenylalanine--tRNA ligase beta subunit
SCO1472	1.822				SCO1472	Conserved hypothetical Sun-family protein SCL6.29c
SCO2923		1.136			SCO2923	Putative membrane protein
SCO2848		0.695			SCO2848	UPF0303 protein SCO2848
SCO4919				0.782	SCO4919	Putative oxidoreductase
SCO1678	4.563				SCO1678	Putative transcriptional regulator
SCO4751				0.744	SCO4751	Putative acetyltransferase
SCO3793				0.863	SCO3793	Uncharacterized protein
SCO1824		0.675		1.197	SCO1824	Secreted subtilisin-like protease
SCO6027	1.312		1.248		SCO6027	Acetyl-coa acetyltransferase (Thiolase)
SCO3878				1.222	SCO3878	DNA polymerase III subunit beta
SCO1428		0.771			SCO1428	Acyl-CoA dehydrogenase
SCO1080				0.666	SCO1080	Uncharacterized protein
SCO4039		1.740			SCO4039	Uncharacterized protein
SCO5775				1.186	SCO5775	Glutamate permease
SCO2301			3.714	1.619	SCO2301	GTP cyclohydrolase 1 type 2 homolog
SCO4159				0.394	SCO4159	Transcriptional regulatory protein GlnR
SCO2590	1.801				SCO2590	Putative glycosyltransferase
SCO4890				3.185	SCO4890	Thymidine phosphorylase
SCO6635	3.426				SCO6635	Bacteriophage (PhiC31) resistance gene pglY
SCO3877	1.413				SCO3877	Putative 6-phosphogluconate dehydrogenase
SCO5388				1.199	SCO5388	Endonuclease NucS
SCO4886				0.720	SCO4886	Putative sugar ABC transporter ATP-binding protein
SCO5258				2.008	SCO5258	ATP-binding protein
SCO6412	1.444		1.639		SCO6412	Putative aminotransferase
SCO0563				1.246	SCO0563	Uncharacterized protein
SCO4295		1.964	0.504		SCO4295	Cold shock protein
SCO1089				0.759	SCO1089	Uncharacterized protein
SCO5583				3.787	SCO5583	Ammonium transporter
SCO5971				0.790	SCO5971	Uncharacterized protein
SCO6660	1.461			0.736	SCO6660	Uncharacterized protein
SCO2150		0.839			SCO2150	Cytochrome C heme-binding subunit
SCO2830	3.162				SCO2830	Probable amino acid ABC transporter protein_integral membrane component
SCO3049				0.782	SCO3049	Putative acyl-CoA hydrolase
SCO5420				1.456	SCO5420	Cholesterol esterase
SCO5650			0.749		SCO5650	Putative membrane protein
SCO2761				1.675	SCO2761	Putative secreted tripeptidyl aminopeptidase
SCO2266				1.418	SCO2266	Methionine aminopeptidase
SCO5360				0.820	SCO5360	Peptide chain release factor 1
SCO7695				3.516	SCO7695	Uncharacterized protein
SCO1768		0.827		0.832	SCO1768	Pseudouridine synthase
SCO1414				1.251	SCO1414	Putative ankyrin-like protein
SCO2504				1.192	SCO2504	Glycine--tRNA ligase
SCO3115				1.218	SCO3115	Uncharacterized protein
SCO2036				1.257	SCO2036	Tryptophan synthase alpha chain
SCO5038	2.614				SCO5038	F42a
SCO1013				1.141	SCO1013	Putative mut-like protein
SCO3118		1.232		1.306	SCO3118	Uncharacterized protein
SCO2113				0.636	SCO2113	Bacterioferritin
SCO1523				0.858	SCO1523	Pyridoxal 5'-phosphate synthase subunit PdxS
SCO6549	2.435				SCO6549	Uncharacterized protein
SCO4089	1.453				SCO4089	Valine dehydrogenase
SCO2367				0.764	SCO2367	Uncharacterized protein
SCO5389		0.719			SCO5389	Uncharacterized protein
SCO1681		1.290			SCO1681	Putative gluconate dehydrogenase
SCO0204				0.611	SCO0204	Putative luxR family two-component response regulator
SCO3823	1.828				SCO3823	Putative quinone oxidoreductase
SCO2275				1.204	SCO2275	Putative lipoprotein
SCO2999			0.770		SCO2999	Uncharacterized protein
SCO2461		0.526			SCO2461	Putative secreted protein
SCO1262		0.515			SCO1262	Putative gntR-family transcriptional regulator
SCO1563		0.660			SCO1563	Putative acetyltransferase
SCO5289	2.889				SCO5289	Putative two component sensor kinase
SCO1865	1.533			0.741	SCO1865	Diaminobutyrate--2-oxoglutarate transaminase
SCO6169	3.395				SCO6169	Putative regulatory protein
SCO2907	5.545				SCO2907	Putative PTS transmembrane component
SCO6218		0.831	1.351	0.877	SCO6218	Putative phosphatase
SCO4490	2.129				SCO4490	Putative decarboxylase SCD69.10
SCO4577	2.513				SCO4577	Putative helicase
SCO7631	3.538				SCO7631	Putative secreted protein
SCO3026	2.066				SCO3026	Uncharacterized protein
SCO1868				0.803	SCO1868	Uncharacterized protein
SCO1441	2.231				SCO1441	Riboflavin biosynthesis protein RibBA
SCO1945	0.740			1.152	SCO1945	Triosephosphate isomerase
SCO2131				0.791	SCO2131	Putative long chain fatty acid CoA ligase
SCO5337				1.181	SCO5337	Uncharacterized protein

SUPPLEMENTARY INFORMATION BELONGING TO CHAPTER VI

SCO	GlcN-Mann wt	1447 wt	1447-wt Mann	GlcN	SCO	Description
SCO6590		0.697			SCO6590	Putative secreted esterase
SCO1636		0.748			SCO1636	Uncharacterized protein
SCO2591				1.324	SCO2591	Putative secreted protein
SCO4800	2.358				SCO4800	Isobutyryl CoA mutase_ small subunit
SCO7324	1.151			0.896	SCO7324	Putative regulatory protein
SCO1966				0.522	SCO1966	UvrABC system protein B
SCO0302				1.317	SCO0302	Putative tetR-family transcriptional regulator
SCO7325	2.972	2.777			SCO7325	Anti-sigma factor antagonist
SCO2140	0.765				SCO2140	Putative transcriptional regulator
SCO6663				1.109	SCO6663	Transketolase B
SCO3100	1.737				SCO3100	Uncharacterized protein
SCO3123				0.787	SCO3123	Ribose-phosphate pyrophosphokinase
SCO1853				0.814	SCO1853	Precorrin-2 C20-methyltransferase (EC 2.1.1.130)
SCO3974		0.765			SCO3974	Uncharacterized protein
SCO1840		0.900		0.799	SCO1840	Putative ABC transporter ATP binding protein
SCO5528				2.297	SCO5528	Putative transcriptional regulator
SCO4702		0.712		0.765	SCO4702	50S ribosomal protein L3
SCO5244	3.266				SCO5244	Anti-sigma factor
SCO5901				1.176	SCO5901	Uncharacterized RNA methyltransferase SCO5901
SCO0596				0.707	SCO0596	DpsA
SCO0666				1.428	SCO0666	Catalase
SCO2905		1.795			SCO2905	Uncharacterized protein
SCO2562				1.128	SCO2562	Elongation factor 4
SCO5241				0.716	SCO5241	Uncharacterized protein
SCO4723				1.137	SCO4723	Adenylate kinase
SCO6008				2.106	SCO6008	Probable transcriptional repressor protein
SCO4716	1.305				SCO4716	30S ribosomal protein S8
SCO5652			3.415		SCO5652	Uncharacterized protein
SCO5265		0.647		0.774	SCO5265	Uncharacterized protein
SCO4179		0.722			SCO4179	UPF0678 fatty acid-binding protein-like protein SCO4179
SCO2123	2.837			0.704	SCO2123	Putative esterase/lipase
SCO5393				0.807	SCO5393	Putative ABC transporter ATP-binding subunit
SCO2610				0.902	SCO2610	Rod shape-determining protein
SCO5231			1.258		SCO5231	HTH-type transcriptional repressor DasR
SCO5199	1.241				SCO5199	Uncharacterized protein
SCO1405	1.414				SCO1405	Putative heat shock protein (Hsp90-family)
SCO7463				1.124	SCO7463	Putative sensor histidine kinase
SCO1559				0.639	SCO1559	Methionine import ATP-binding protein MetN
SCO2627		1.344			SCO2627	Putative sugar-phosphate isomerase
SCO2777				1.301	SCO2777	Acetyl/propionyl CoA carboxylase alpha subunit
SCO4687	2.372				SCO4687	Uncharacterized protein
SCO4813	2.186		2.208		SCO4813	Phosphoribosylglycinamide formyltransferase
SCO3960				1.253	SCO3960	Uncharacterized protein
SCO2407	2.045				SCO2407	Aldose 1-epimerase
SCO6979				1.367	SCO6979	Probable solute-binding lipoprotein
SCO6259		0.911			SCO6259	Probable ABC sugar transport ATP binding protein
SCO1758				1.129	SCO1758	GTPase Der
SCO4297	1.203				SCO4297	Putative oxidoreductase
SCO2003				0.782	SCO2003	DNA polymerase I
SCO6292	0.749				SCO6292	Putative dihydropicolinate synthase
SCO3018				0.730	SCO3018	Putative regulatory protein
SCO4958		1.676			SCO4958	Cystathionine gamma-synthase
SCO5114		0.860			SCO5114	BldKC_ putative ABC transport system integral membrane protein
SCO2859				0.378	SCO2859	Uncharacterized protein
SCO4830				0.722	SCO4830	Putative glycine betaine ABC transport system ATP-binding protein
SCO7453				1.183	SCO7453	Putative secreted protein
SCO2148		0.880			SCO2148	Ubiquinol-cytochrome c reductase cytochrome b subunit
SCO2917	0.810				SCO2917	Nicotinate phosphoribosyltransferase
SCO0304				2.498	SCO0304	Uncharacterized protein
SCO1453				0.824	SCO1453	Uncharacterized protein
SCO2126				1.099	SCO2126	Glucokinase
SCO5557				0.582	SCO5557	Uncharacterized protein
SCO2828				1.449	SCO2828	Probable amino acid ABC transporter protein_solute-binding component
SCO0436		2.291			SCO0436	50S ribosomal protein L32-2
SCO3559				1.417	SCO3559	Putative oxidoreductase
SCO2633				0.756	SCO2633	Superoxide dismutase [Fe-Zn] 1
SCO4907		0.716		0.842	SCO4907	Transcriptional regulatory protein AfsQ1
SCO6224				1.272	SCO6224	Putative secreted protein
SCO6714		1.391			SCO6714	Putative hydroxylase
SCO1938				0.833	SCO1938	Uncharacterized protein
SCO5112		0.816			SCO5112	BldKA_ putative ABC transport system integral membrane protein
SCO3951	0.865				SCO3951	Uncharacterized protein
SCO5032		1.233			SCO5032	Alkyl hydroperoxide reductase
SCO1876				0.754	SCO1876	Putative RNA polymerase sigma factor
SCO5185		0.891			SCO5185	Putative peptidase
SCO2015				2.106	SCO2015	Putative nucleotidase
SCO3658				1.549	SCO3658	Putative aspartate aminotransferase
SCO3184	1.255				SCO3184	Putative penicillin acylase (EC 3.5.1.11)
SCO1494				0.735	SCO1494	3-dehydroquininate synthase
SCO5571				1.290	SCO5571	50S ribosomal protein L32-1
SCO4645				0.842	SCO4645	Aspartate aminotransferase
SCO5292				1.274	SCO5292	Putative ATP/GTP-binding protein
SCO1965		0.763			SCO1965	Putative export associated protein
SCO6178				1.269	SCO6178	Putative deacetylase (Putative secreted protein)
SCO6195	1.237				SCO6195	Putative acetyl-coenzyme A synthetase
SCO5196		0.805		1.098	SCO5196	Uncharacterized protein

APPENDIX IV

SCO	GlcN-Mann wt	1447 wt	1447-wt Mann	GlcN	SCO	Description
SCO2180		0.810			SCO2180	Dihydrolipoyl dehydrogenase
SCO3890				0.886	SCO3890	Thioredoxin reductase
SCO2362				1.405	SCO2362	Uncharacterized protein
SCO4091				1.176	SCO4091	Putative DNA-binding protein
SCO1518				1.357	SCO1518	Holliday junction ATP-dependent DNA helicase RuvB
SCO4596				1.586	SCO4596	Putative two-component system response regulator
SCO1655				1.188	SCO1655	Putative lipoprotein oligopeptide binding protein
SCO1953	3.940				SCO1953	UvrABC system protein C
SCO1086		1.985			SCO1086	Uncharacterized protein
SCO3652		0.481	1.804		SCO3652	Putative membrane protein
SCO1827				1.182	SCO1827	Putative DNA polymerase III_ epsilon chain (EC 2.7.7.7)
SCO2396				1.465	SCO2396	Uncharacterized protein
SCO4917				0.722	SCO4917	Purine nucleoside phosphorylase
SCO4470				1.233	SCO4470	Putative phosphoglycerate mutase
SCO2855		2.459			SCO2855	Uncharacterized protein
SCO3066				1.194	SCO3066	Putative regulator of Sig15
SCO6752				1.190	SCO6752	Putative integral membrane transferase
SCO5657				1.165	SCO5657	Aldehyde dehydrogenase
SCO3756	3.634				SCO3756	Putative two component system response regulator
SCO5556				1.158	SCO5556	DNA-binding protein HU 2
SCO3373				0.891	SCO3373	Putative Clp-family ATP-binding protease
SCO4161				1.519	SCO4161	Putative molybdopterin converting factor
SCO5584				0.859	SCO5584	Nitrogen regulatory protein P-II
SCO1502				1.206	SCO1502	Putative secreted protein
SCO1378				0.765	SCO1378	Glycine dehydrogenase (decarboxylating)
SCO4163				0.849	SCO4163	Putative secreted protein
SCO7199				3.320	SCO7199	Putative membrane protein
SCO2048				1.163	SCO2048	Imidazole glycerol phosphate synthase subunit HisF
SCO1805				1.171	SCO1805	Putative membrane protein
SCO2084		0.895			SCO2084	UDP-N-acetylglucosamine--N-acetylmuramyl-(pentapeptide) pyrophosphoryl-undecaprenol N-acetylglucosamine transferase
SCO5479				1.192	SCO5479	Oligopeptide ABC transporter ATP-binding protein
SCO6060		0.892			SCO6060	UDP-N-acetylmuramate--L-alanine ligase
SCO3659				1.345	SCO3659	Uncharacterized protein
SCO1443				1.162	SCO1443	Putative riboflavin synthase
SCO6756		0.336			SCO6756	Putative glycosyltransferase
SCO6478				2.857	SCO6478	Uncharacterized protein
SCO1082				0.873	SCO1082	Putative electron transfer flavoprotein_ beta subunit
SCO7057				0.849	SCO7057	Putative esterase
SCO5520				1.176	SCO5520	Delta-1-pyrroline-5-carboxylate dehydrogenase
SCO4122				1.767	SCO4122	Putative MarR-family transcriptional regulator
SCO4901				0.600	SCO4901	Adenosine deaminase 1
SCO2034				1.041	SCO2034	Prolipoprotein diacylglycerol transferase 1
SCO1515				1.189	SCO1515	Protein translocase subunit SecF
SCO1366				0.527	SCO1366	Uncharacterized protein
SCO5595		0.791			SCO5595	50S ribosomal protein L19
SCO4654				0.763	SCO4654	DNA-directed RNA polymerase subunit beta
SCO5805		1.243		1.131	SCO5805	Vitamin B12-dependent ribonucleotide reductase
SCO1922				1.240	SCO1922	Putative ABC transporter ATP-binding subunit
SCO5783		0.846			SCO5783	Uncharacterized protein
SCO1977				0.881	SCO1977	Putative glutamate synthase small subunit
SCO5843				1.273	SCO5843	Uncharacterized protein
SCO6789				1.339	SCO6789	Putative fatty oxidation protein
SCO1210				0.836	SCO1210	Putative transcriptional regulatory protein
SCO5744				1.153	SCO5744	4-hydroxy-tetrahydrodipicolinate synthase 2
SCO6862				1.196	SCO6862	Uncharacterized protein
SCO4660		0.925			SCO4660	30S ribosomal protein S7
SCO4735		0.799			SCO4735	30S ribosomal protein S9
SCO2969				1.119	SCO2969	Cell division ATP-binding protein
SCO6767				1.245	SCO6767	4-hydroxy-3-methylbut-2-en-1-yl diphosphate synthase (flavodoxin) 1
SCO5696				1.245	SCO5696	4-hydroxy-3-methylbut-2-en-1-yl diphosphate synthase (flavodoxin) 2
SCO4719				1.095	SCO4719	30S ribosomal protein S5
SCO1651				0.801	SCO1651	Uncharacterized protein
SCO3844				0.835	SCO3844	Putative secreted protein
SCO2068		0.812			SCO2068	Putative secreted alkaline phosphatase
SCO5494				1.143	SCO5494	DNA ligase 1
SCO1643				1.234	SCO1643	Proteasome subunit alpha
SCO5837		0.939			SCO5837	Zinc protease
SCO3816				0.842	SCO3816	Putative branched-chain alpha keto acid dehydrogenase E1 beta
subunit						
SCO0741		0.900			SCO0741	Putative oxidoreductase
SCO3873				1.190	SCO3873	DNA gyrase subunit A
SCO1907				0.856	SCO1907	Uncharacterized protein
SCO6451		0.839			SCO6451	Putative substrate binding protein
SCO5552				0.915	SCO5552	Putative regulator
SCO3906				1.105	SCO3906	30S ribosomal protein S6
SCO2682		1.257			SCO2682	Putative membrane protein
SCO2363				0.907	SCO2363	Putative ATP/GTP-binding protein
SCO4429		0.853			SCO4429	FO synthase
SCO1955				1.142	SCO1955	Putative iron sulphur binding protein
SCO1508				1.072	SCO1508	Histidine--tRNA ligase
SCO5464		1.143		1.282	SCO5464	SCO5464 protein
SCO3885				0.919	SCO3885	Ribosomal RNA small subunit methyltransferase G
SCO3096				1.101	SCO3096	Enolase 1

TABLE S4. Proteomic comparison of *S. coelicolor* M145 and its *rokJ6* mutant.

SCO	Description	Sequence	Distance	Score	Region	Co-transcribed SCO
SCO1448	Uncharacterized MFS-type transporter	CTATCAGGCAGGCTCCCTGATAG	-60	28	regulatory	
SCO1447	Putative ROK-family transcriptional regulator	CTATCAGGCAGGCTCCCTGATAG	-75	28	regulatory	
SCO0317	Putative transmembrane transport protein	CTTTACAGACATGGTTCCTGATTG	-72	16.4	regulatory	
SCO4114	sporulation associated protein	TTAAGAGGCATTGTTCCGGATGG	-109	9.2	regulatory	
SCO2657	Putative ROK-family transcriptional regulator	CCAACAGGAAACTTTCCTAACAG	-127	8	regulatory	
SCO1359	Permease of the drug/metabolite transporter (DMT) superfamily	CTACGAGGACGACTGCCTCATCG	5	7.7	regulatory	
SCO7173	Transcriptional regulator	AAATCCGGAACCGTGCCGATAT	-134	6.1	regulatory	
SCO3732	ATP-dependent RNA helicase	GTATCAAGGAAGGTTCCCATGA	-19	5.8	regulatory	
Unknown_246	hypothetical protein	GTATCAAGGAAGGTTCCCATGA	-16	5.8	regulatory	
SCO3250	Integrase	CCATCAGGCAGCTCCTCGATCT	-19	5.6	regulatory	
SCO4313	Transcriptional regulator%2C AcrR family	CTCCCAGATAATGTTCTGTGATAA	-91	5.5	regulatory	SCO4314
SCO4312	hypothetical protein	CTCCCAGATAATGTTCTGTGATAA	-32	5.5	regulatory	SCO4311
SCO2089	UDP-N-acetylmuramoylanyl-D-glutamate--L-lysine ligase (EC 6.3.2.7)	TCGTCACGGATGGTTCCTGGTGG	-16	5	regulatory	
SCO2956	Integral membrane protein	CGCTCAGGCACGGGCCCGAAAG	-132	5	regulatory	
SCO2955	hypothetical protein	CGCTCAGGCACGGGCCCGAAAG	-49	5	regulatory	
SCO5864	hypothetical protein	TGATCATGCACCTGTCGAAAG	-279	4.9	regulatory	
SCO4829	Choline oxidase (EC 1.1.3.17)	CGGTACGGCAGGCTCCGTGATCG	44	4.7	regulatory	SCO4830; SCO4831;
SCO0234	Putative oxidoreductase	CTACCTGAGGCGCTGCTTATAT	-236	3.9	regulatory	
SCO0233	Putative DNA-binding protein	CTACCTGAGGCGCTGCTTATAT	-186	3.9	regulatory	
SCO5908	hypothetical protein	ATACCAGGCAGGCATCATGACCT	-24	3.9	regulatory	SCO5909; SCO5910
SCO1274	hypothetical protein	CGAACAGGCACGGCTCCGAATGG	-281	3.8	regulatory	
SCO1656	Pseudouridine-5' phosphatase (EC 3.1.3.-)	CGATCAGGCCGGTCCCACGAAG	-43	3.8	regulatory	
SCO6822	Efflux pump transporter of major facilitator superfamily (MFS)	TTAACAGTGATGACTTGTGATAG	-142	3.8	regulatory	
SCO1755	hypothetical protein	AGACCCGGAACCTCGCTTCTGG	-62	3.7	regulatory	
SCO1291	hypothetical protein	CTATCGACGACCTCCGTGCTGG	-16	3.5	regulatory	
SCO2359	Two-component system sensor histidine kinase	CGATCATGCGGTCTTCTCAGGG	-123	3.5	regulatory	SCO2358
SCO5261	NAD-dependent malic enzyme (EC 1.1.1.38)	TTGTCCGGAAGCCTGGTATGAG	-272	3.5	regulatory	
SCO5191	hypothetical protein	CTGCAGGCACCGGCTGAAGA	-108	3.4	regulatory	
Unknown_451	hypothetical protein	TGCTCAGGCAGATGCCCGATAT	5	3.4	regulatory	
SCO5210	Quaternary ammonium compound-resistance protein SugE	TGCTCAGGCTTGTTCCGGCTTG	-153	3.1	regulatory	
SCO3468	Transposase	CGAGCAGTCCCGGGCTGATGG	-130	3	regulatory	
SCO0545	putative secreted protein	CTGTGCGGAGTCTTCCGGATCG	-125	2.9	regulatory	
SCO2226	Neopullulanase (EC 3.2.1.135) / Maltodextrin glucosidase (EC 3.2.1.20)	TCTTCCGGAAGGGTCTGTAAAG	-92	2.9	regulatory	
Unknown_408	hypothetical protein	CGCTCAGGCACGCTACCTGCTGG	-282	2.9	regulatory	
SCO6806	Phage integrase	GTATTCGGCAGCTTCATGGTGG	4	2.8	regulatory	
SCO2664	putative sugar-binding protein	CGAGGAGGCAGGACCCGTGAAAG	-79	2.8	regulatory	
SCO2869	Transcriptional regulator%2C Xre family	CAGCCAGACAGCCGACTGATCG	-277	2.8	regulatory	
SCO3256	SpdA protein	CCATCAGGCTCCTTCTGTGAC	-19	2.8	regulatory	SCO3255; SCO3254;
SCO5919	hypothetical protein	CAGACGGGCGGGTTCCTGATCA	-95	2.8	regulatory	
SCO6585	Succinyl-CoA ligase [ADP-forming] beta chain (EC 6.2.1.5)	CTTTCAGTCAGGAGCCGATGAG	-160	2.8	regulatory	SCO6586; SCO6587
SCO6584	Thiamine pyrophosphate-requiring enzymes	CTTTCAGTCAGGAGCCGATGAG	-126	2.8	regulatory	SCO6583; SCO6582
SCO0083	Mobile element protein	CCATAAGAAACGACGCTAACAA	-138	2.7	regulatory	
Unknown_17	Mobile element protein	CCATAAGAAACGACGCTAACAA	-228	2.7	regulatory	
SCO0733	hypothetical protein	ATATCGGACCGGTGACTGATCA	-83	2.7	regulatory	
SCO0925	Transcriptional regulator%2C LysR family	GTTACGGGACCATGCCTCATCG	-85	2.7	regulatory	
SCO0924	Succinate dehydrogenase cytochrome b subunit	GTTACGGGACCATGCCTCATCG	-69	2.7	regulatory	SCO0923; SCO0922
SCO1675	putative small membrane protein	TTCTTGAGCATTGTTCTCTCTAG	-12	2.7	regulatory	
SCO5833	hypothetical protein	CTTATGGGCAAGGTTCTGGCAG	-33	2.7	regulatory	
SCO5690	Putative large secreted protein	CTGGGAGGACGCTTCTGAGCG	50	2.6	regulatory	
SCO2384	hypothetical protein	CTATCGGGCAGACTCGAGGAAG	-46	2.6	regulatory	
SCO6657	putative membrane protein	CCATCAGGAGGACTCTGACCC	-19	2.6	regulatory	
SCO1773	Alanine dehydrogenase (EC 1.4.1.1)	GGATCACGGTCTTGGCTCAGAG	-25	2.5	regulatory	
SCO4562	NADH ubiquinone oxidoreductase chain A (EC 1.6.5.3)	AGATCACAAAGCTTGTGAATAC	-198	2.4	regulatory	SCO4563; SCO4564;
SCO6934	putative secreted protein	CGATCAACAACCTTTCCGACAG	-23	2.3	regulatory	
SCO2788	hypothetical protein	ATATCGGGCAGGATTTTCCGCA	-52	2	regulatory	
SCO0135	hypothetical protein	CGATCATGGACCTCGTCTGTGAC	-201	1.9	regulatory	
SCO0134	hypothetical protein	CGATCATGGACCTCGTCTGTGAC	-209	1.9	regulatory	
SCO3460	Mercuric ion reductase (EC 1.16.1.1)	CCCTCGGAAACCTGCCGGGCTG	-218	1.9	regulatory	SCO3461; SCO3462;
SCO3459	type 11 methyltransferase	CCCTCGGAAACCTGCCGGGCTG	-75	1.9	regulatory	
SCO4226	hypothetical protein	GAATCGGCCATGTTCTCTCTGG	-325	1.9	regulatory	
SCO3507	putative integral membrane efflux protein	CGACCAGGAGGCGAGCCCGATTG	-119	1.8	regulatory	
SCO4616	hypothetical protein	GTATGACGCAGGTTCCGGTGTG	-133	1.8	regulatory	
SCO7490	Zinc-type alcohol dehydrogenase YcJq	GCATCAGCAACCTTCCGGAGCC	-126	1.8	regulatory	SCO7491; SCO7492;
SCO7489	ABC-type sugar transport system%2C periplasmic binding protein YcJn	GCATCAGCAACCTTCCGGAGCC	-121	1.8	regulatory	
SCO4831	Glycine betaine ABC transport system%2C permease protein OpuAB	CGATCAGGCCACGCCCCGAAAG	7	1.7	regulatory	
SCO4325	Cold shock protein of CSP family %3D> SCO4325	CTATCAAGAGCCGTTTCCGAGCA	-68	1.7	regulatory	
SCO4324	Integral membrane protein	CTATCAAGAGCCGTTTCCGAGCA	-130	1.7	regulatory	
SCO5926	Aconitate hydratase (EC 4.2.1.3)	CGATCGGGCGGGTCCCTTGAG	-61	1.7	regulatory	SCO5925

APPENDIX IV

SCO6102	Ferredoxin--sulfite reductase%2C actinobacterial type (EC 1.8.7.1)	CTCTCAGCGGCCCGACAGATGG	-218	1.7	regulatory	SCO6101; SCO6100;
SCO1094	Transcriptional regulator%2C AcrR family	TCTTGAGCGAGCCATCCAGATAG	-37	1.6	regulatory	
SCO4734	LSU ribosomal protein L13p (L13Ae)	ATGTCAGGACCACCTCACTGAAGA	-40	1.6	regulatory	SCO4735
SCO6052	putative membrane protein	ACATGGGGAACCTTCTGCTGG	-19	1.6	regulatory	
SCO2448	hypothetical protein	CTATCATGAGCGGTGCCGCTGG	-5	1.5	regulatory	
SCO0021	hypothetical protein	CTCTGAAGGACGGTCTCTGTTGG	-32	1.5	regulatory	
Unknown_6	hypothetical protein	CTCTGAAGGACGGTCTCTGTTGG	-40	1.5	regulatory	
SCO1383	hypothetical protein	GAACACATGGACCTCCCTGAAGG	-91	1.5	regulatory	
SCO7015	Putative secreted glycosyl hydrolase	CTTTCACGAGCTACGTCGGATAG	-312	1.5	regulatory	
SCO4232	CarD-like transcriptional regulator	CCATCACGGGGCCGCGTGCATCG	35	1.4	regulatory	
SCO1948	putative zinc-binding carboxypeptidase	GTTCTCATGAACCCCTAGATGG	-16	1.4	regulatory	
SCO3682	Fatty acid desaturase	TTCTCAGAGAGACGTCCTCATGA	-19	1.4	regulatory	
SCO5107	Succinate dehydrogenase flavoprotein subunit (EC 1.3.5.1)	ACATCAGAAAGCCTCACTCGTCA	-19	1.4	regulatory	
SCO6855	hypothetical protein	CCGTGATGCAGGCGCCGAGATAG	-131	1.4	regulatory	SCO6854; Unknown_441;
SCO7579	Putative DNA-binding protein	CTGTCAACAACCTGCGCAACCG	-131	1.4	regulatory	SCO7580
SCO7780	Transcriptional regulator%2C AraC family	CGATCACGTACGCTGTGGATAG	-223	1.3	regulatory	
SCO6241	hypothetical protein	TCATCTGGCTCCGTGCATGATCG	-193	1.1	regulatory	
SCO6240	hypothetical protein	TCATCTGGCTCCGTGCATGATCG	-273	1.1	regulatory	
SCO0166	Polyphosphate kinase 2 (EC 2.7.4.1)	ATCTCAGGCAAGGTGTACGAGAA	24	1	regulatory	
SCO4524	putative membrane protein	GTGGCAGGCAATTTCTGGTTG	-39	1	regulatory	SCO4525; SCO4526;
SCO7600	Alanyl-tRNA synthetase-related protein	TGATCCGGCGATGGCCCTGATCC	44	0.9	regulatory	
SCO2848	hypothetical protein	GGAGCAGGAACCGCCGCTGGTCT	41	0.8	regulatory	
SCO1845	Probable low-affinity inorganic phosphate transporter	CTGCCAGGACGCTCCGGAGAG	-156	0.8	regulatory	SCO1846
SCO1844	Ribulose-5-phosphate 4-epimerase and related epimerases and aldolases	CTGCCAGGACGCTCCGGAGAG	-239	0.8	regulatory	
SCO2527	hypothetical protein	CTTTCGGTGACCATCACAGATAT	-112	0.8	regulatory	
SCO5803	SOS-response repressor and protease LexA (EC 3.4.21.88)	CTACCGTGGCCCTGGCGGACAA	-146	0.8	regulatory	
SCO1374	putative secreted protein	CTAGCCGAAACACAGTCTGAACA	-226	0.7	regulatory	
SCO1725	putative secreted hydrolase	GTCTCATGGAACCTCCCTTAGCA	-16	0.7	regulatory	
SCO3804	Transcriptional regulator%2C AraC family	ATATGTGCGAAGGATCCTCTCAG	-47	0.7	regulatory	SCO3805
SCO3803	Mannose-6-phosphate isomerase	ATATGTGCGAAGGATCCTCTCAG	-72	0.7	regulatory	
SCO4291	putative secreted protein	CGGTCACGGAGCTTGTGTGGGAA	-82	0.7	regulatory	
SCO4290	Alpha%2Calpha-trehalose-phosphate synthase [UDP-forming] (EC	CGGTCACGGAGCTTGTGTGGGAA	-114	0.7	regulatory	
SCO5158	hypothetical protein	TTGTTTTGGAGGGTTCCCGTAG	-156	0.7	regulatory	
SCO5213	Integral membrane protein	TGTTCCGGGAGGGCTCCTCGTAC	-22	0.7	regulatory	
SCO6027	3-ketoacyl-CoA thiolase (EC 2.3.1.16)	CTCTCCCTCAGGGTGGCGGATGG	-28	0.7	regulatory	SCO6026
SCO7010	Alpha-glucosidase (EC 3.2.1.20)	CTTTCGGGAGGGTGGATCTTCG	-32	0.7	regulatory	
SCO7257	putative secreted protein	CTGGAAGGCAGGAGCCTCATGA	-43	0.7	regulatory	
SCO7256	Putative protease	CTGGAAGGCAGGAGCCTCATGA	-237	0.7	regulatory	
Unknown_157	hypothetical protein	TGAAGGAGCAGGGCTCCTGATGA	-19	0.7	regulatory	
SCO2363	Similar to citrate lyase beta subunit	TGAAGGAGCAGGGCTCCTGATGA	17	0.7	regulatory	
SCO7487	Inner membrane ABC transporter permease protein YcjP	TTGCCACTCACGCTTCTCCTGG	-12	0.6	regulatory	
SCO7790	putative secreted oxidoreductase	TTGTCCCGTTCGCTCGTGATAG	41	0.6	regulatory	SCO7789
SCO0763	Lactate 2-monooxygenase (EC 1.13.12.4)	GTTTCGGTAACCTTGGGTATTGA	-246	0.6	regulatory	
SCO1473	Methionyl-tRNA formyltransferase (EC 2.1.2.9)	CGAGCCGCAAGGTCACGGAAAG	-75	0.6	regulatory	
SCO2074	Lipoprotein signal peptidase (EC 3.4.23.36)	CCCTCAGCTAGTCTTACTGACTG	-29	0.6	regulatory	
SCO4539	hypothetical protein	TTTTCCGGAACCTTCCGGTGGTA	-193	0.6	regulatory	SCO4538
SCO4866	RNA polymerase ECF-type sigma factor	CAGTAGGAAACCCAGCCGGCAGG	-72	0.6	regulatory	SCO4867
SCO5473	ATP/GTP-binding protein	CGCCGGTAACGGTGCCTGAGAG	-265	0.6	regulatory	
SCO5472	Aminomethyltransferase (glycine cleavage system T protein) (EC	CGCCGGTAACGGTGCCTGAGAG	-184	0.6	regulatory	
SCO7337	hypothetical protein	TCAGCGCTCACGCTTCTGATCG	-96	0.6	regulatory	SCO7338
SCO7336	hypothetical protein	TCAGCGCTCACGCTTCTGATCG	-231	0.6	regulatory	
SCO2280	Transcriptional regulator%2C AcrR family	CTGCGCGGGGGTTCGTGATCG	19	0.5	regulatory	
SCO3926	Sporulation-specific cell division protein SsgA	CGTACAGGCAGAGGTCATGATGA	11	0.5	regulatory	
SCO4831	Glycine betaine ABC transport system%2C permease protein OpuAB	CCACCAGGAGCGGCTGTGATGG	-19	0.5	regulatory	
SCO6041	Protoporphyrinogen IX oxidase%2C aerobic%2C HemY (EC 1.3.3.4)	GGAAACGGAACCCGGACACGTAG	38	0.5	regulatory	SCO6042
SCO6048	Integral membrane protein	CTACCAGACCGCTCCTGCTCG	17	0.5	regulatory	
SCO2292	Endo-1%2C4-beta-xylanase (EC 3.2.1.8)	CACCTACCGTGCCTGCCGAAAAG	-202	0.5	regulatory	SCO2291
SCO2611	Rod shape-determining protein MreB	CTTTCGGCAACACTGCGGAGGG	-128	0.5	regulatory	
SCO3345	Dihydroxy-acid dehydratase (EC 4.2.1.9)	CGGTCACTCAGGGTCCGGACAG	-69	0.5	regulatory	
SCO3985	hypothetical protein	CACCTATGGAGCTGCACGGAAG	-231	0.5	regulatory	
SCO4670	putative serine protease precursor	CGTTATGGAACCCGGCTTATGG	-143	0.5	regulatory	
SCO4670	putative serine protease precursor	CGTTATGGAACCCGGCTTATGG	-158	0.5	regulatory	
SCO5190	Transcriptional regulator%2C WhiB family	CGATCAGGCCGGCCCTCAGGG	-172	0.5	regulatory	
SCO5805	Ribonucleotide reductase of class II (coenzyme B12-dependent) (EC	CGTACAGGAGCGGATGACAG	-16	0.5	regulatory	
SCO6609	putative secreted protein	CACCTCAGGAGCCCGCTGTTCG	-16	0.5	regulatory	
SCO1943	hypothetical protein	CACAGACGCAAGCCCATGATAG	-190	0.4	regulatory	
SCO2351	Integral membrane protein	CGATCACAAAGCCCTGTGAA	-131	0.4	regulatory	
SCO5930	possible NTP pyrophosphohydrolase	CTATCGGTCATGTCGCTCACGA	-54	0.4	regulatory	
SCO5929	Putative oxidoreductase	CTATCGGTCATGTCGCTCACGA	-83	0.4	regulatory	
SCO6219	Putative serine/threonine protein kinase	ACATTGTGAAGATTGCATGAGAA	-132	0.4	regulatory	
SCO6218	putative phosphoglycerate mutase family protein	ACATTGTGAAGATTGCATGAGAA	-185	0.4	regulatory	

SUPPLEMENTARY INFORMATION BELONGING TO CHAPTER VI

SCO1839	Transcriptional regulator	CCATTCGGCAAGGCTGATGAGAC	-91	0.3	regulatory	
SCO2461	Small hypothetical protein Hyp1	CGAACCCAGTAACCTGCCGGTTAA	-275	0.3	regulatory	
SCO2461	Small hypothetical protein Hyp1	CGAACCCAGTAACCTGCCGGTTAA	-197	0.3	regulatory	
SCO3644	Putative lipase/esterase	TTATCAGGCCGGTGACGTGGCGC	-93	0.3	regulatory	
SCO7514	Integral membrane protein	CTCGAAGTCAACGTTGCTGACCG	-102	0.3	regulatory	
SCO7513	putative secreted hydrolase	CTCGAAGTCAACGTTGCTGACCG	-102	0.3	regulatory	SCO7512
SCO1390	PTS system%2C N-acetylglucosamine-specific IIA component	CCATCAGACACTGTCCCTGATCC	-4834	7.8	upstream	
SCO1389	CDP-diacylglycerol-glycerol-3-phosphate 3-phosphatidyltransferase (EC	CCATCAGACACTGTCCCTGATCC	-997	7.8	upstream	
SCO3334	Tryptophanyl-tRNA synthetase (EC 6.1.1.2)	CCATCAGACACTGTCCCTGATCC	-5106	7.8	upstream	
SCO3333	Putative phosphatase YieH	CCATCAGACACTGTCCCTGATCC	-949	7.8	upstream	
SCO5746	pleiotropic regulatory protein	GGATCAGGGACAGTGTCTGATGG	-1002	7.8	upstream	
SCO5335	hypothetical protein	CTATATTGACCCCGCATGATTA	-3205	4.9	upstream	
SCO5331	Putative DNA methylase	CTATATTGACCCCGCATGATTA	-2839	4.9	upstream	
SCO0239	hypothetical protein	TGATCATGCCAGGGTCTTGAAC	-530	3.8	upstream	
SCO1273	Polyketide synthase modules and related proteins	CGAACAGGCACGGCTCCGAATGG	-448	3.8	upstream	
SCO6821	Putative transferase	TTAACAGTGATGACTGTTGATAG	-659	3.8	upstream	
SCO1756	hypothetical protein	AGACCCGGAACCTGCTCTTCTGG	-370	3.7	upstream	
SCO4632	ATP/GTP-binding protein	CTTCCAACAACCTGCCGGAAGG	-1888	3.7	upstream	
SCO7824	Transcriptional regulator%2C AcrR family	CGATCAGGCGATCTCGCTGGCAG	-1914	3.7	upstream	
SCO5260	Secreted protein	TTGTCGGGAAGCTGGCTATGAG	-390	3.5	upstream	SCO5259; SCO5258
SCO3445	putative small membrane protein	CCATCAGCAGCACGCTCGCGAA	-693	3.2	upstream	
SCO6945	hypothetical protein	ATTTGAGGGAACTTGCCCGGTAC	-1998	3.1	upstream	
SCO1390	PTS system%2C N-acetylglucosamine-specific IIA component	CCATGAGCAACCTGCGAGGACAT	-2148	2.8	upstream	
SCO1389	CDP-diacylglycerol-glycerol-3-phosphate 3-phosphatidyltransferase (EC	CCATGAGCAACCTGCGAGGACAT	-3683	2.8	upstream	
SCO3334	Tryptophanyl-tRNA synthetase (EC 6.1.1.2)	CCATGAGCAACCTGCGAGGACAT	-2414	2.8	upstream	
SCO3333	Putative phosphatase YieH	CCATGAGCAACCTGCGAGGACAT	-3641	2.8	upstream	
SCO5746	pleiotropic regulatory protein	ATGTCCTGCACGGTTGCTCATGG	-3691	2.8	upstream	
SCO5335	hypothetical protein	CAATCATGGACACAGTTGTCCAG	-819	2.6	upstream	
SCO5331	Putative DNA methylase	CAATCATGGACACAGTTGTCCAG	-5225	2.6	upstream	
SCO4632	ATP/GTP-binding protein	TGATGAGAAATGCTTCATGAAC	-4276	2.5	upstream	
SCO4561	putative NLP/P60-family protein	AGATCACAAGCTTGTAATAC	-699	2.4	upstream	
Unknown_466	hypothetical protein	CGGCAACGAATATGCTGATTG	-353	1.5	upstream	
SCO0056	Mobile element protein	GTATGAGGAAGCCGCTTCGAAA	-530	1.4	upstream	
SCO6641	Superfamily I DNA and RNA helicases and helicase subunits	CGATCAGGGAGAGTCTCGTCC	-435	1.4	upstream	
SCO7578	hypothetical protein	CTGTCAACAACCTGCGCAACCG	-386	1.4	upstream	
SCO7779	Putative oxidoreductase	CGATCAGTACGCTGTGGATAG	-473	1.3	upstream	
SCO6405	Mobile element protein	ATACAGGGCCGCTCTCTGAAAG	-823	1.1	upstream	
SCO6401	Protein of unknown function DUF664	ATACAGGGCCGCTCTCTGAAAG	-968	1.1	upstream	
SCO3585	hypothetical protein	TTAGCGGGTCCGGCCCTGAGTG	-500	1	upstream	
Unknown_300	hypothetical protein	GTGGCAGGCAATTTCTTGGTTG	-596	1	upstream	
SCO6861	hypothetical protein	CCGTGAGGAATCCGGGCTGGGAA	-1571	0.9	upstream	
SCO5804	Ribonucleotide reductase transcriptional regulator NrdR	CTACCGTGGCGCTGCGGACAA	-460	0.8	upstream	
SCO1373	hypothetical protein	CTAGCCGAAACACAGTCTGAACA	-356	0.7	upstream	
SCO5157	Magnesium and cobalt transport protein CorA	TTGTTTGGAGGGTTCCCGTAG	-390	0.7	upstream	SCO5156
SCO5335	hypothetical protein	CCATGGGAACTCAGCGAGATCA	-2419	0.7	upstream	
SCO5331	Putative DNA methylase	CCATGGGAACTCAGCGAGATCA	-3625	0.7	upstream	
SCO3981	Transcriptional regulator%2C GntR family	CACATATGGAGCCTGCACGGAAG	-778	0.5	upstream	
SCO1390	PTS system%2C N-acetylglucosamine-specific IIA component	CTCACAGTCAAGTCCCTTGTGC	-4949	0.4	upstream	
SCO1389	CDP-diacylglycerol-glycerol-3-phosphate 3-phosphatidyltransferase (EC	CTCACAGTCAAGTCCCTTGTGC	-882	0.4	upstream	
SCO3334	Tryptophanyl-tRNA synthetase (EC 6.1.1.2)	CTCACAGTCAAGTCCCTTGTGC	-5221	0.4	upstream	
SCO3333	Putative phosphatase YieH	CTCACAGTCAAGTCCCTTGTGC	-834	0.4	upstream	
Unknown_285	putative ATP-dependent DNA helicase	CAAACGTCAAGTGTGCTGATCG	-632	0.4	upstream	
SCO5746	pleiotropic regulatory protein	GCACAAGGGAGCTTACTGTGAG	-887	0.4	upstream	
SCO3468	Transposase	CTCTACGTCGGGTCTGTCAAAC	-489	0.3	upstream	
SCO7179	N-acetylmuramoyl-L-alanine amidase (EC 3.5.1.28)	CTATAGGGCAAGCTGCTGTAG	-376	0.3	upstream	

CURRICULUM VITAE & LIST OF PUBLICATIONS

CURRICULUM VITAE

Mia Urem was born on the 17th of January 1986 in Split, Croatia. She graduated from the International School Maastricht, The Netherlands, with an International Baccalaureate diploma in 2004. Starting in the autumn of that same year, she followed the joint Life Science & Technology program at Leiden University and TU Delft and obtained her Bachelor's degree in 2007. Her Bachelor's research project, focussed on DNA repair proteins in *E. coli*, was completed in the lab of Dr. Nora Goosen at the Molecular Genetics department of the Leiden Institute of Chemistry. Mia followed this up with a Master's degree, obtained in 2012, in Life Science & Technology with a specialisation in Functional Genomics. During this period, she also worked as a student assistant for Life Science & Technology practical courses and as an KNAW Academy (research) assistant on a project aimed at optimising microfluidic devices at the Chemical Engineering department of TU Delft, under the supervision of Prof. M. Kreutzer, Prof. C. Kleijn, Dr. V. van Steijn and Dr. M. Rosso. She completed her Master's research project with Prof. G. van Wezel at the Leiden Institute of Chemistry, under the supervision of Dr. L. Zhang, on the regulatory role of AfsR in streptomycetes. She also completed an internship in Leeds, in a collaboration between Dr. K. McDowall (University of Leeds) and Evocutis, on the optimisation of a novel transcriptomics method. Then, Mia began as a PhD student at the Institute of Biology Leiden in the lab of Prof. G. van Wezel at the beginning of 2012; the results of this work are presented in this thesis. During this period, she took part in the John Innes/Rudjer Bošković Summer School in Applied Molecular Microbiology (2014), held poster presentations at a number of (inter)national conferences and was selected to present at NWO CHAINS in 2015 (Veldhoven, The Netherlands) and ISBA18 in 2017 (18th International Symposium on the Biology of Actinomycetes in Jeju, South Korea). Currently, Mia is postdoctoral researcher with Prof. G. van Wezel, continuing on-going projects stemming from this thesis as well as taking up new project focussed on *Streptomyces* development and cell division.

LIST OF PUBLICATIONS

- Urem M**, Świątek-Połatyńska MA, Rigali S, van Wezel GP. (2016) Intertwining nutrient-sensory networks and the control of antibiotic production in *Streptomyces*. *Mol Microbiol.* **102**:183-195
- Urem M**, van Rossum T, Bucca G, Moolenaar GF, Laing E, Świątek-Połatyńska MA, Willemse J, Tenconi E, Rigali S, Goosen N, Smith CP, van Wezel GP. (2016) OsdR of *Streptomyces coelicolor* and the Dormancy Regulator DevR of *Mycobacterium tuberculosis* Control Overlapping Regulons. *mSystems.* **1**:1-21
- Tenconi E, **Urem M**, Świątek-Połatyńska MA, Titgemeyer F, Muller YA, van Wezel GP, Rigali S. (2015) Multiple allosteric effectors control the affinity of DasR for its target sites. *Biochem Biophys Res Commun.* **464**:324-329
- Romero DA, Hasan AH, Lin YF, Kime L, Ruiz-Larrabeiti O, **Urem M**, Bucca G, Mamanova L, Laing EE, van Wezel GP, Smith CP, Kaberdin VR, McDowall KJ. (2014) A comparison of key aspects of gene regulation in *Streptomyces coelicolor* and *Escherichia coli* using nucleotide-resolution transcription maps produced in parallel by global and differential RNA sequencing. *Mol Microbiol.* **94**:963-987
- Świątek MA, **Urem M**, Tenconi E, Rigali S, van Wezel GP. (2012) Engineering of *N*-acetylglucosamine metabolism for improved antibiotic production in *Streptomyces coelicolor* A3(2) and an unsuspected role of NagA in glucosamine metabolism. *Bioengineered.* **5**:280-285

